The impact of Beirut Rafic Hariri International Airport's activities on the air quality of Beirut & its suburbs : measurements and modelling of VOCs and NO2

Tharwat Mokalled

UNIVERSITÉ DE STRASBOURG

ÉCOLE DOCTORALE DES SCIENCES CHIMIQUE

Institut de chimie et procédés pour l'énergie, l'environnement et la santé (ICPEES)

THÈSE

EN COTUTELLE AVEC L'UNIVERSITÉ SAINT JOSEPH (Beyrouth-Liban)

présentée par:

Tharwat MOKALLED

soutenue le: **23 Septembre 2016**

pour obtenir le grade de : **Docteur de l'université de Strasbourg**

Discipline / Spécialité : CHIMIE / CHIMIE ANALYTIQUE

The Impact of Beirut Rafic Hariri International Airport's Activities on the Air Quality of Beirut & its Suburbs: Measurements and Modelling of VOCs and NO_2

THÈSE dirigée par:

M. LE CALVÉ Stéphane	Chargé de Recherche, CNRS, Université de Strasbourg (Directeur)
Mme GÉRARD Jocelyne	Professeur, Université Saint-Joseph (Directrice)
M. ABBOUD Maher	Professeur, Université Saint-Joseph (Co-directeur)

RAPPORTEURS:

M. PETITPREZ Denis	Professeur, Université de Lille 1 (Président)
M. FAOUR Ghaleb	Directeur de recherche, Centre de télédétection du CNRS libanais

AUTRES MEMBRES DU JURY:

M. MAIGNANT Gilles	Chargé de Recherche CNRS, Faculté de médecine de Nice

I **dedicate** this thesis to my precious:

Father,
Mother,
and **Brother**

For their unconditional love, uplifting support, and encouragement.

ACKNOWLEDGMENTS

This Ph.D. was realized upon the collaboration between the University of Saint Joseph-Department of Geography for the performance of Dispersion Modelling and the University of Strasbourg –ICPEES for the sampling and analysis of the VOC campaigns. This Ph.D. was funded by the Research Council at USJ, the French CNRS and ICPEES in Strasbourg, and Campus France and French CNRS which covered the trip expense.

Undertaking this Ph.D. has been a truly challenging experience for me. In fact, the support and guidance of many people was a crucial part of the completion of this research.

I would like to express my sincere gratitude to my advisors Dr. Jocelyne Adjizian Gérard, Dr. Stéphane Le Calvé, and Dr. Maher Abboud for the continuous support throughout my Ph.D. research. I want to thank Dr. Jocelyne Adjizian Gérard for teaching me how to integrate between microscale chemistry and the broader environmental and geographic phenomena, and for being more than an advisor through her strengthening positivity and extreme care; I also deeply thank Dr. Stéphane Le Calvé for his full support and guidance during the very challenging measurement campaigns and all the wise knowledge he provided me in the field of atmospheric chemistry. Moreover, I am inspired by his determination and scientific skills to solve problems. I would like to thank Dr. Maher Abboud for his dynamism and follow-up, his organization and structured way of analysis, and for his advice in the field of atmospheric chemistry.

I would like to thank the reviewers of this thesis Dr. Denis Petitprez, Professor at Lille 1 University, and Dr. Ghaleb Faour, Director of the Center for Remote Sensing (CNRS), for their time and helpful comments. I also extend my sincere appreciation to Dr. Gilles Maignant, research director at University of Nice, for graciously agreeing to be my external examiner.

I owe my deepest gratitude for the Geography Department, Mrs. Rita Zaarour being its department chef. It was a pleasure to work in such a friendly one-team environment. I am deeply grateful for the sincerely supportive Mrs. Nada Saliba who helped me with modelling and ArcInfo. I am also grateful for Mr. Pierre Charles Gérard for his kind support and for introducing me to map plotting.

The other unit, which I owe my gratitude for, is ICPEES. I am so thankful for all the help provided to me in the analysis of the most challenging samples, with all the ups and downs that we passed through. For this, I would like to thank Claire Troquet, Ruba Nassreddine, and Céline Liaud for their support, help, and humor. Special thanks to Stéphanette Englaro and Vincent Person for being amazing friends and of great support during my stays in Strasbourg.

All these campaigns wouldn't have been realized without the approval of Mr. Mohammad Chehabeddine, the Director General of Civil Aviation at Beirut Airport, who provided his full support for the occurrence of the project. I owe my deep gratitude to the very helpful airport staff who provided me with their full support. I can't but thank the Maintenance Department, the Air Traffic Control (ATC) Department and especially the "follow me" car workers who facilitated transportation in the apron. I would also like to thank the Mechanical Department at the Middle East Airports Services (MEAS).

Last but not least, I would like to thank my friends - Nehma, Aref, and Dana - for their support and positive presence.

All this work was fuelled with care and support of my family - especially my father, mother, and brother. I owe it to you.

TABLE OF CONTENTS

RÉSUMÉ

1. INTRODUCTION ET OBJECTIFS

Avec 56,6 millions d'emplois à l'échelle mondiale et un impact économique global estimé à 2,4 milliards de dollars américains (Groupe d'Action sur les Transports Aériens ATAG, 2004), l'aviation civile constitue une partie intégrante de l'économie mondiale. Son taux de croissance serait de 5% par an pour les 10-15 prochaines années (Comité sur la protection de l'environnement (CAEP) 9, 2013). Mais l'aviation, en consommant du carburant, génère des émissions impactant l'atmosphère. Cependant, contrairement à d'autres moyens de transport, les avions qui parcourent de longues distances et à diverses altitudes, émettent des polluants qui affectent le climat mondial et la qualité de l'air au niveau local et, tout particulièrement, à proximité des aéroports. Les conséquences se manifestent par des risques sur la santé publique (résidents des alentours, les travailleurs de l'aéroport et les passagers) et sur l'environnement.

En raison de la croissance continue de l'aviation commerciale et le développement résidentiel à proximité des aéroports, l'impact des activités aéroportuaires sur la qualité de l'air au niveau local se classe parmi les préoccupations les plus importantes des gouvernements locaux/régionaux, surtout que, dans de nombreuses grandes villes du monde, les émissions d'autres sources se réduisent progressivement. A cet effet, il est nécessaire de comprendre comment les activités aéroportuaires contribuent à la dégradation de la qualité de l'air, afin de prendre des mesures d'atténuation et d'évaluer les impacts potentiels de ces activités aériennes sur la santé des résidents. En fait, il n'est certes pas facile de généraliser la contribution d'un aéroport à la pollution atmosphérique locale puisqu'elle dépend des caractéristiques spécifiques de chaque aéroport et de son environnement (situation**,** topographie, aménagement, météorologie, trafic etc…). Les quelques recherches portant sur les aéroports internationaux indiquent que les teneurs en polluants sont généralement élevées au voisinage des aéroports et ce, jusqu'à une distance de 1 km. Au-delà, les valeurs diminuent significativement jusqu'à 2 à 3 km (Kim, 2015; RIDEM, 2008; Wood, 2008; Zhu *et al.*, 2011). Cependant, la plupart de ces études n'intègrent pas les émissions associées aux trajectoires des avions ou l'effet de la géographie et de la topographie sur la dispersion spatiale des polluants. Par conséquent, les contributions des aéroports pourraient avoir été **sérieusement sous-estimées** (Hudda *et al.*, 2014). Par ailleurs, il existe peu de recherches traitant de l'impact des émissions de l'aéroport sur l'air intérieur des bâtiments, sur la base de l'hypothèse que la plupart des bâtiments aéroportuaires sont bien ventilés et que les sources d'émission intérieure sont limitées.

Au **Liban**, l'Aéroport International de Beyrouth – Rafic Hariri (RHIA) se situe au sein d'une zone peuplée et se trouve à 6 km au sud de la capitale libanaise. Par conséquent,

compte tenu des vents dominants de direction SW, il est probable que la pollution issue des activités aéroportuaires n'atteigne Beyrouth et sa banlieue. Ce fait a été soutenu par des observations, résultats d'une étude préalable menée par Chelala (2008), et qui indique que 34% des concentrations totales de dioxyde d'azote mesurées sur un site de référence (la Forêt des Pins) provenait de la direction sud-ouest, où se situe l'aéroport. De plus, la trajectoire de l'atterrissage d'une grande partie des avions (Figure 1) longeant la côte ouest de la capitale, pourrait être à l'origine d'une source d'émissions de polluants.

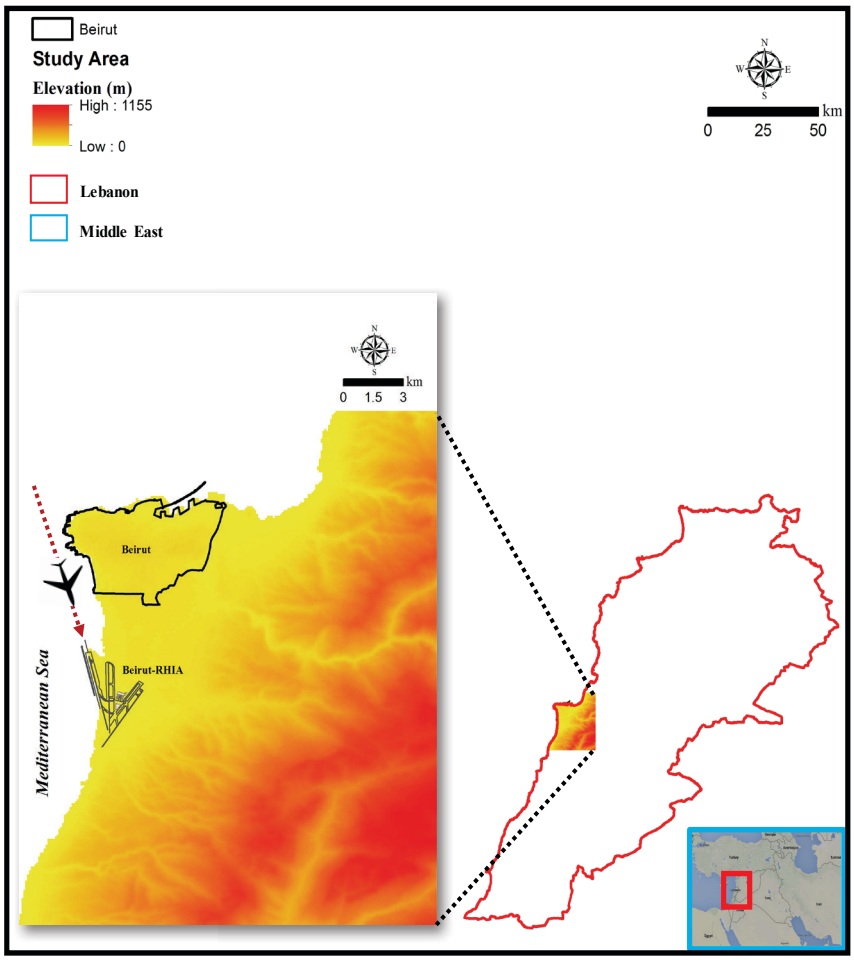

Figure 1: Zone d'étude (l'aéroport international Rafic Hariri de Beyrouth)

En outre, la topographie aux alentours de l'aéroport ainsi que la direction et la vitesse du vent qui sont variables dans le temps peuvent avoir un impact important sur la dispersion des émissions de l'aviation. Il est important de noter que l'extension urbaine de la banlieue a interpénétré le périmètre de l'Aéroport International de Beyrouth – Rafic Hariri.

Par ailleurs, les employés de l'aéroport se plaignant de symptômes respiratoires (Yaman, 2001), les ouvertures directes entre le couloir de navigation et le terminal des arrivées constituant une voie permettant à l'air contaminé de pénétrer aux bâtiments de l'aéroport,

sont des raisons qui poussent à l'évaluation de la qualité de l'air à l'intérieur de ces bâtiments.

A Beyrouth, nombreuses sont les études qui mettent l'accent sur le transport routier et son impact sur la qualité de l'air (Chelala *et al.*, 2006; Chelala ; 2008 ; Daher *et al.*; 2013). Par contre, aucune étude n'a été menée pour appréhender l'impact des activités de l'aéroport sur la qualité de l'air. Aussi, quel serait l'impact de l'Aéroport de Beyrouth sur la qualité de l'air ambiant de la capitale libanaise et de ses banlieues ? Y a-t-il un lien direct entre l'activité des avions et la pollution intérieure ?

Cette étude pourra servir de guide aux opérateurs aéroportuaires et aux compagnies aériennes pour comprendre l'impact environnemental du transport aérien, pour prendre des mesures d'atténuation en vue de réduire l'exposition du personnel travaillant à l'aéroport et des voyageurs et pour éviter les impacts négatifs sur la qualité de l'air des quartiers voisins.

Pour répondre à cette problématique, deux approches complémentaires ont été adoptées : l'une est expérimentale et l'autre est la modélisation. Pour ce faire, les objectifs spécifiques furent les suivants :

- Identifier expérimentalement l'impact des activités aéroportuaires à partir de traceurs. Par conséquent, il a fallu identifier, parmi un ensemble d'espèces de COV, des signatures caractéristiques des émissions des différentes sources aéroportuaires.
- Utiliser lesdits marqueurs pour délimiter spatialement l'impact des activités de l'aéroport.
- Modéliser la dispersion atmosphérique grâce au logiciel ADMS-Airport.
- Evaluer l'impact de l'aéroport sur sa qualité de l'air intérieur.

La présente recherche doctorale met l'accent sur les effets du dioxyde d'azote (NO_2) et des composés organiques volatils (COVs). En effet, le dioxyde d'azote (NO_2) est le polluant le plus important émis par l'aviation. De plus, sa teneur annuelle mesurée à Beyrouth est de 53 $\mu g\ m^{-3}$ dépassant les recommandations de l'Organisation Mondiale de la Santé (OMS) et présentant un risque sanitaire certain sur la population. En ce qui concerne les COVs qui sont très nombreux et possèdent des caractéristiques physico-chimiques très différentes, il s'agit d'identifier ceux qui peut être considérer comme des traceurs spécifiques aux émissions issues de l'aéroport. En outre, parmi les COVs, il existe des Polluants Atmosphériques Dangereux très nocifs pour la santé (causant une altération des voies respiratoires, cancer, décès) (Wood, 2008).

2. APPROCHE EXPERIMENTALE

2.1 Matériels et methods

Une première recherche bibliographique a permis de déterminer les principaux COVs liés aux aéronefs (AirPACA, 2004; EPA, 2009a; Lelievre, 2009; Schürmann *et al.*, 2007; Wood, 2008). Le choix des espèces de COVs a été basé sur une campagne préliminaire de signatures. 50 espèces de COVs retenus dans notre étude (tableau 1), sont divisées en familles suivantes : alcanes légers (C_2-C_7), alcanes lourds (C_8-C_{14}), alcènes (C_2-C_6), alcènes chlorés, aldéhydes légers, cétones (C_3-C_6), aldéhydes lourds (C_9 à C_{10}), d-limonène et composés monoaromatiques.

Tableau 1: Liste des COV ciblés pour les mesures

Familles de COV	Compound	Familles de COV	Compound
Alcanes légers (C_2-C_7)	Ethane[b] Propane[b] Isobutane[b] n-Butane[b]+cis-2-Butane[b] Isopentane[b] n-Pentane[b]+cis-2-Pentane[b] n-Hexane[a,b] n-Heptane[b]	**Alcènes chlorés**	Trichloroéthène Tétrachloroéthène
		Terpènes	D-Limonène
Alcanes lourds (nC_8-nC_{14})	n-Octane[b] n-Nonane n-Décane n-Undécane n-Dodécane n-Tridécane n-Tétradécane	**Aldéhydes et Cétones légers (C_3-C_6)**	Acroléine[a] Propanal[a] Butanal Pentanal Hexanal Acétone 2-Butanone
		Aldéhydes lourds (C_9-C_{10})	Nonanal Décanal
Alcynes/Alcènes (C_2-C_6)	Ethène[b] +Acetylène[b] Propène[b] 1-Butène[b] 1,3-Butadiène[a,b] Trans-2-butène[b] 1-Pentène[b] Isoprène[b] Trans-2-pentène 1-Hexène	**Composés monoaromatiques**	Benzène[a,b] Toluène[a,b] Ethylbenzène[a,b] m,p-Xylène[a,b] o-Xylène[a,b] Styrène[a] 1,2,4-Trimethylbenzène[b] 1,4-Dichlorobenzène Butylbenzène Propylbenzène

[a]Identifié comme COV émis par les aéronefs et le matériel au sol pour aéronefs

[b]Recommandé par la directive 2002/3/CE

2.1.1 Échantillonnage et analyse des COV

Des échantillons d'air ont été prélevés à l'intérieur de tubes en acier inoxydable dont les adsorbants ont été élaborés au laboratoire de l'Institut de Chimie et Procédés pour l'Energie, l'Environnement et la Santé (ICPEES) -Groupe de physico-chimie de l'atmosphère à l'Université de Strasbourg et CNRS (Liaud, 2014; Environmental protection Agency des États-Unis, 1999).

Ces adsorbants sont appropriés pour le piégeage des COV contenant 2 à 12 atomes de carbone (C_2-C_{12}). Ils sont composés de Carbosieve S-III (piège les COV de C_2 à C_5) et de Carbopack^{TM} B (piège les COV de C_5-C_{12}) (Jochmann *et al.*, 2014).

Deux types d'échantillonnages ont été utilisés: actifs et passifs. Les échantillons actifs ont été prélevés à l'aide de deux dispositifs conçus au laboratoire ICPEES. Leur principe de fonctionnement est similaire: ils sont composés d'une pompe située en aval d'un régulateur de débit massique. Au cours de toutes les campagnes, un échantillonneur automatique avec une seule voie a été employé. Grâce à ses dimensions pratiques, à sa commande à distance et à son autonomie en énergie, cet échantillonneur a facilité les prélèvements. Par ailleurs, les campagnes de mesures de la qualité de l'air intérieur ont été effectuées en utilisant un échantillonneur automatique programmable à 8 voies.

Pour évaluer l'impact spatial des activités aéroportuaires sur la qualité de l'air de Beyrouth et sa banlieue, un échantillonnage par tubes passifs de mesures de COVs à différents endroits à l'intérieur et à l'extérieur de l'aéroport a été mené.

La gamme totale de COVs cibles (à l'exception des aldéhydes lourds) a été analysée par GC-FID utilisant une technique mise au point par Liaud (2014), et qui consiste en une double colonne permettant la séparation d'un large éventail de COVs en un seul passage, contrairement au cas de la GC-MS où il n'a pas été possible de séparer les COVs légers. La GC-MS a quant à elle été utilisée pour quantifier le benzène (en raison de sa co-élution), les aldéhydes lourds. Par conséquent, les deux systèmes étaient nécessaires et complémentaires.

Des courbes d'étalonnage réalisées par GC-FID ont montré une très bonne linéarité, avec un coefficient de détermination (R^2) égal à 0,99 pour tous les composés organiques volatils à l'exception du propanal (0,98) et de l'acétone (0,98), tandis que les valeurs de LOD variaient entre 0,1 ng (acétone) et 0,8 ng (hexanal) pour la plupart des composés. Les courbes d'étalonnage liquides effectuées par GC-MS ont montré également une très bonne linéarité. En général, les valeurs de R^2 étaient supérieures à 0,97 pour tous les COV à l'exception du n-undécane (0,9100), le n-dodécane (0,9121) et le n-tétradécane (0,9400). Les valeurs de LOD variaient de 0,05 ng pour le benzène, l'éthylbenzène, le propyl benzène et augmenté pour les alcanes lourds (4,1 ng pour le tétradécane et 4,2 ng pour l'octane).

2.1.2 Échantillonnage et analyse des NO_2

Afin d'appréhender la variabilité spatiale de la teneur en NO_2 en air extérieur et intérieur, des sites ont été équipés d'un réseau de tubes de diffusion passive de type Passam. Ces tubes ont été ensuite analysés par spectrophotométrie selon la méthode bien établie de Saltzman (Saltzman, 1954).

2.2 Campagnes de mesures

2.2.1 Identification des traceurs

L'approche expérimentale utilisée était basée sur l'identification des traceurs liés aux émissions de gaz d'échappement des avions au cours d'opérations réelles. En fait, cette étude est la première à effectuer plusieurs mesures de gaz d'échappement des avions en fonctionnement réel, lors de différents modes opératoires. Plus de 100 prélèvements de panaches d'avions en activités ont ainsi été prélevés.

Les mesures de COVs ont concerné 3 types de sources :

- Les émissions typiques liées aux activités des avions opérant dans des conditions réelles ("approche", "Atterrissage ou Touchdown", "Taxi", "APU", "Décollage ou Take-off", "Réservoirs de carburant"). Les résultats obtenus concernent les émissions moyennes de plusieurs appareils fonctionnant avec un réglage de poussée similaire. Les mesures ont été faites pour les émissions d'échappement des avions pendant les différentes phases du cycle LTO (c.-à-ralenti à 7% de poussée, approche à 30% de poussée, le décollage à 85-100% de poussée), l'APU et les émissions de kérosène (voir Figure 2). L'échantillonnage a été effectué à la distance minimale autorisée par les autorités de l'aéroport (8-32 m, sauf pour le "Take-off" à 120-190 m).
- Les émissions des véhicules. L'accent a été mis sur les émissions de gaz d'échappement d'essence, choisis pour représenter les rejets des véhicules à Beyrouth.
- La concentration ambiante de l'aéroport (mesures sur le toit des bâtiments, au centre du tarmac entre les pistes Est et Ouest)

4 campagnes de mesures de COVs ont eu lieu en : Juin 2014 (2 semaines), Octobre 2014 (2 semaines), Mai / Juin 2015 (3 semaines), et Octobre 2015 (2 semaines). Seuls les résultats de 2 campagnes de mesures sont présentés ici.

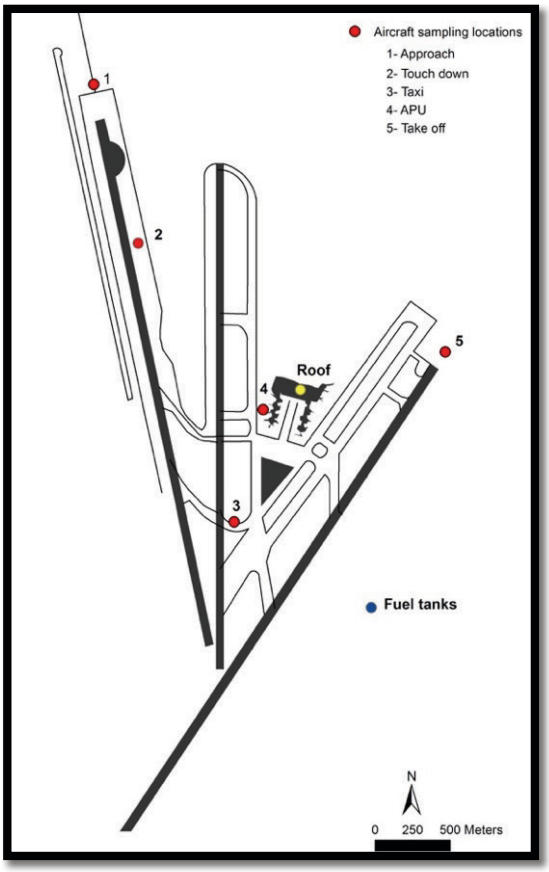

Figure 2: Localisation des sites de mesure pour les campagnes de signatures effectuées à l'aéroport de Beyrouth (Octobre 2014 et Juin 2015)

2.2.2 Campagnes de mesures le long de transects

Quatre campagnes de mesures le long de transects, allant de l'aéroport jusqu'à Beyrouth et sa banlieue, ont été entreprises pour étudier l'impact des activités de l'aéroport sur la qualité de l'air de la capitale. Cependant, en raison de problèmes techniques, seuls les résultats de deux campagnes sont présentés.

La première campagne menée en Octobre 2014 a utilisé des échantillonneurs passifs. Tous les sites (Figure 3), mesurant tout particulièrement la pollution de fond, ont été choisis de manière à être peu affectés par la circulation des véhicules et par les sources d'émissions directes. Le premier transect, situé le long du bord de mer, a été choisi pour estimer l'impact des émissions des aéronefs sur la qualité de l'air qui longent la côte ouest de la capitale à une altitude de 200 à 500m avant leur atterrissage.

Les autres transects concernent des sites bien exposés aux vents dominants du Sud-Ouest (SW).

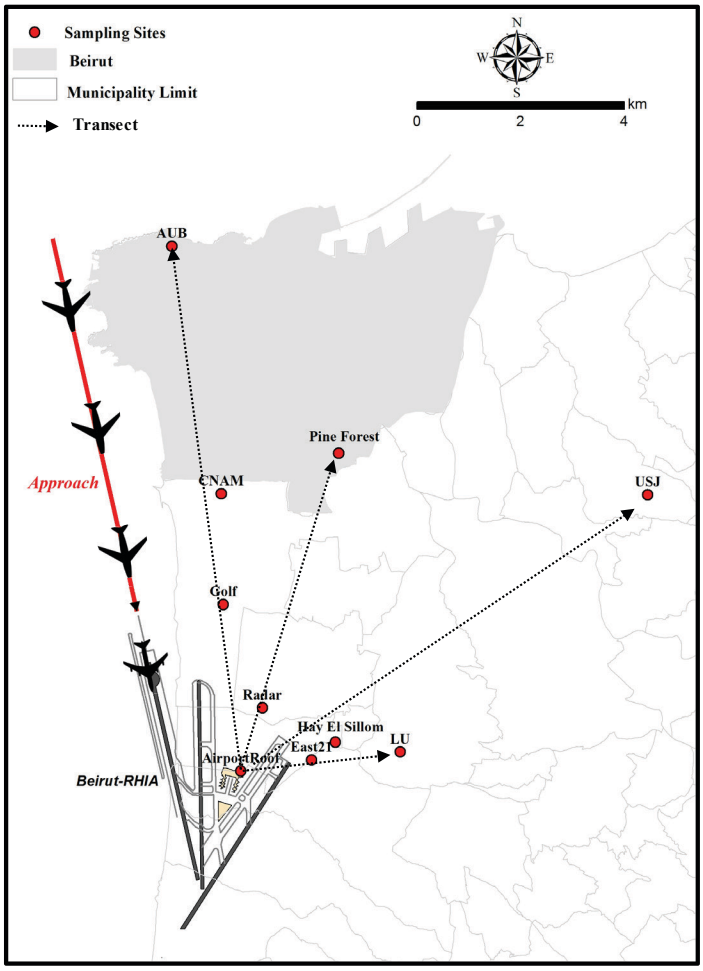

Figure 3: Localisation des sites d'échantillonnage (transect campagne, 20-22 Oct-2014).

La deuxième campagne, menée en Juillet 2015, a utilisé des prélèvements actifs. 3 échantillons ont ainsi été prélevés pour chaque site (voir la Figure 4). Cette campagne a dû être interrompue en raison d'une crise de déchets qui a secoué le Liban. L'accumulation des déchets sur les routes et les zones en friche pouvant biaiser les résultats obtenus.

Pour vérifier l'impact des émissions d'atterrissage, des prélèvements en mode actif ont été effectués au bord de la mer (Coral, 4 km du centre de l'aéroport), sur un site intérieur (CNAM, à 4 km du centre de l'aéroport) à des fins de comparaison. Pour déterminer si les zones du sud-est sont affectées par les émissions de l'aéroport, des mesures ont été prises dans la région sud-est (Khalde) à 4 km du centre de l'aéroport. Un autre site, Barouk, situé en zone montagneuse à 20 km au sud-est l'aéroport a quant à lui été choisi pour représenter un air non affecté par les émissions de l'aéroport de Beyrouth.

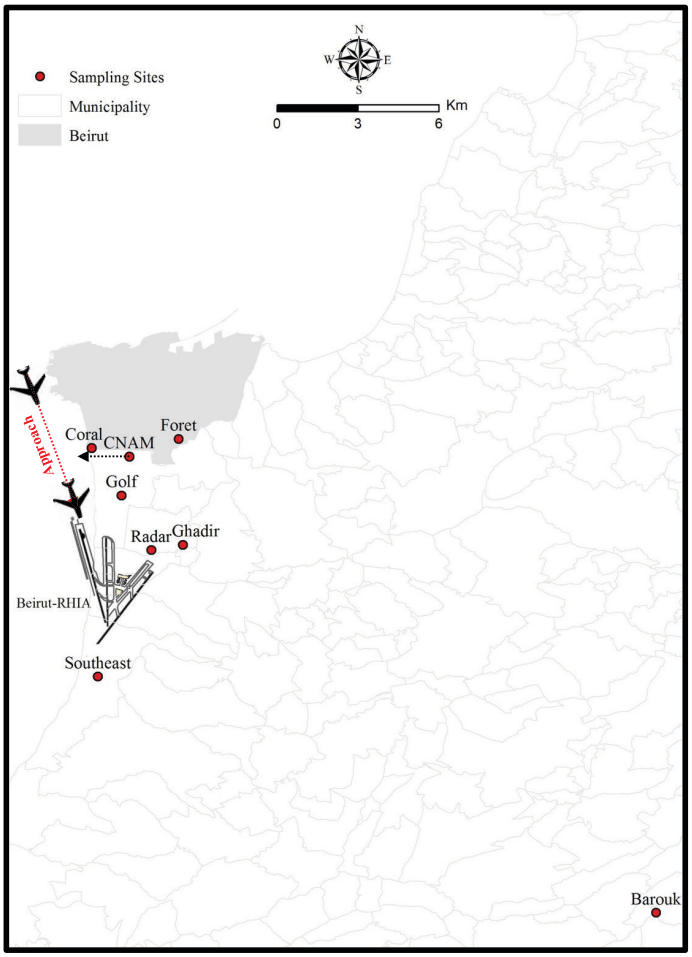

Figure 4: Localisation des sites d'échantillonnage (Campagne transect, 13-21 Juillet 2015). La ligne en pointillé rouge reflète la principale trajectoire de l'atterrissage à l'aéroport de Beyrouth.

2.2.3 Campagnes de mesures de NO_2

Le but de cette campagne était d'évaluer les niveaux de NO_2 de l'aéroport et de ses environs. Les résultats ont servi à valider le modèle ADMS-Airport. Des échantillons de NO_2 ont été collectés sur 9 sites choisis à l'intérieur de l'aéroport et sélectionnés en fonction de lignes directrices recommandées par le Manuel Qualité de l'air Aéroport d'orientation de l'OACI (OACI, 2011). Trois campagnes d'une durée de 1 semaine ont ainsi été organisées.

2.2.4 Campagnes de mesures de l'air intérieur de l'aéroport

Une partie de cette recherche a été consacrée à la pollution de l'air intérieur de l'aéroport. C'est la première étude au Liban qui concerne l'estimation des COV en air intérieur. Les

mesures ont concerné 47 espèces de COV. Cet aspect, important, permet d'identifier les polluants auxquels les employés sont exposés quotidiennement pendant 12 à 24 heures par jour.

Les mesures ont eu lieu à l'intérieur du bureau de maintenance (impact sur les employés de l'aéroport) et dans le hall des arrivées (impact sur les passagers et les employés).

Dans le bureau de maintenance, l'échantillonnage a été effectué en Juillet 2014, en utilisant l'échantillonneur automatique à 8 voies et en Novembre 2014 en utilisant l'échantillonneur à une voie. Au total, 27 échantillons d'air ont ainsi été collectés.

Dans le hall des arrivées, l'échantillonnage a été effectué en Juillet 2014 en utilisant l'échantillonneur automatique à 8 voies, en Octobre 2014 et en Novembre 2014 en utilisant l'échantillonneur à une voie. Au total, 22 échantillons d'air ont ainsi été collectés.

Pour les deux sites, les périodes d'échantillonnage ont été choisis pour couvrir différents niveaux d'activité de l'aéroport.

3. RESULTATS ET DISCUSSION

3.1 Campagnes Signature

Grâce à ces campagnes de mesures, 48 COVs ont ainsi été identifiés. Les résultats sont présentés sous forme de pourcentages en raison de la différence des conditions d'échantillonnage.

Les résultats ont montré que les échantillons d'avion pris en utilisant la technique des 30 s × 6 avaient une concentration en TVOC élevée (88 μg m^{-3}). Ils se sont avérés plus représentatifs des émissions de signature de l'aéronef que ceux pris par la technique des 30 min (15 μg m^{-3}), dont les teneurs sont plus proches de celles obtenues sur le toit de l'aéroport (représentant les concentrations ambiantes d'aéroport). Par conséquent, les résultats des 30 s × 6 ont été choisis pour discuter de la spéciation des émissions des avions à différents réglages de poussée.

La figure 5 (a) montre que les alcanes lourds et les aldéhydes sont les principaux COVs provenant des avions et apparaissent comme les traceurs les plus significatifs comparativement aux émissions des véhicules à essence. La contribution du n-octane au n-tridécane était de 51 à 64% environ de la masse totale des COVs lourds émis par les avions. Les aldéhydes lourds (nonanal et décanal), bien qu'en moindre quantité, peuvent également être considérés comme liés aux émissions des avions. D'autre part, la concentration totale des alcanes lourds dans l'air ambiant de l'aéroport constituait 48% de la masse totale des COVs lourds mesurés. Lors de l'évaluation de la spéciation des alcanes lourds et des aldéhydes (voir Figure 5- (b)), il a été démontré que le n-nonane et le n-décane a dominé la spéciation dans le profil "aviation" (30 s × 6) et "aéroport". Le profil de la source de l'air ambiant (tel que mesuré sur le toit) était comparable à celui des

échantillons prélevés avec la technique d'échantillonnage 30 s × 6. Ceci permet de conclure qu'il serait possible de déterminer des spéciations de COVs à partir d'une simple mesure sur le toit. Par ailleurs, les prélèvements, dont la durée est de 30 mn, présentait une spéciation en COVs différente où les C_9-C_{13} ont contribué de manière équivalente à la spéciation totale.

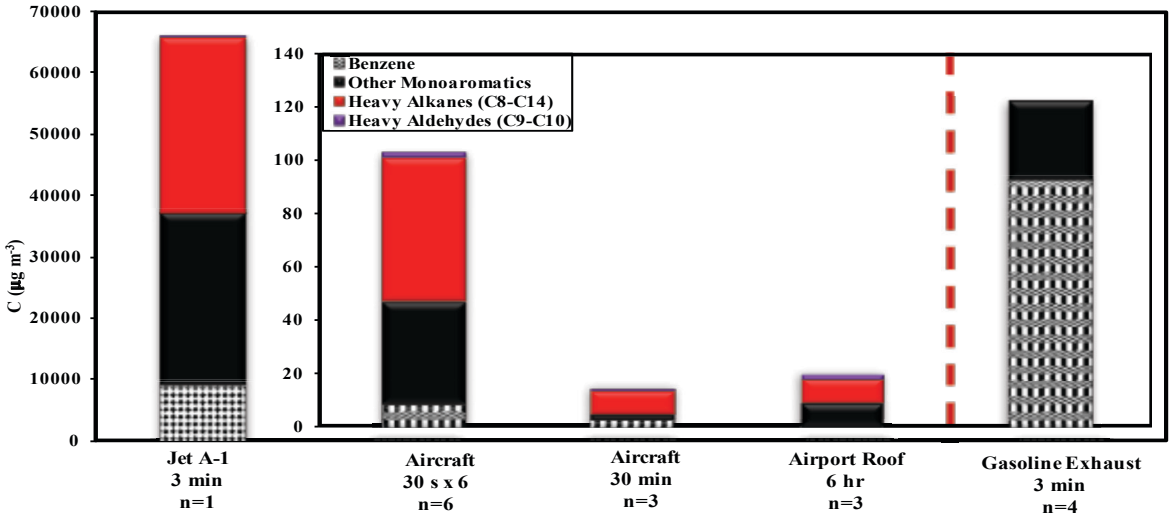

(a)

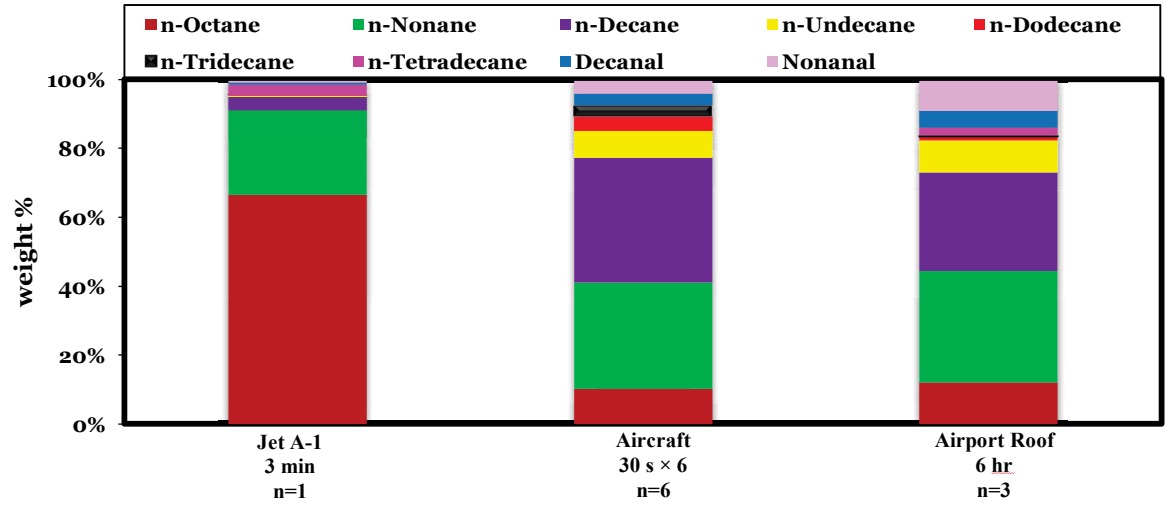

(b)

Figure 5: (a) Des groupes de COV lourd, (b) la spéciation des alcanes lourds et aldéhydes

La spéciation d'alcanes lourds dans les vapeurs de kérosène était la suivante: n-octane (67%), le n-nonane (26%), le n-décane (4%) et d'autres (<1%). Ceci explique la présence

de ces alcanes élevés dans les émissions des avions et des autres activités de l'aéroport, car ils sont des composants de carburant.

Lors de l'évaluation de la spéciation des COV totaux (voir Figure 6), le profil moyen des avions, obtenu avec la technique de 30 secondes × 6, a été dominé par les aldéhydes et les cétones légers (48% des COVT) suivis par les alcènes (16% de TVOC), les composés monoaromatiques (14.5 % de TVOC) et les alcanes légers (14,5% de TVOC) (voir figure 5). Les aldéhydes légers et les alcènes sont des composés secondaires issus de la combustion des hydrocarbures dans les réacteurs (EPA, 2009a) et qui contiennent des éléments classés comme polluants atmosphériques dangereux (PAD) par l'US EPA.

Le profil du toit a été principalement dominé par les monoaromatiques (38,5%), les alcanes légers (29%), les aldéhydes et les cétones (16,5%) et les alcanes lourds (9%). La domination des monoaromatiques et des alcanes légers est probablement renforcée par les émissions des véhicules et de l'équipement de soutien au sol (GSE) à proximité du toit de l'aéroport. Encore une fois, il a été déduit que la technique basée sur 6 échantillonnages de 30 s (notée 30 s × 6) est plus représentative des émissions des avions que celle consistant à prendre un seul échantillon de 30 min qui était quant à elle plus proche de la concentration de l'air ambiant de l'aéroport (82,61 µg m^{-3}).

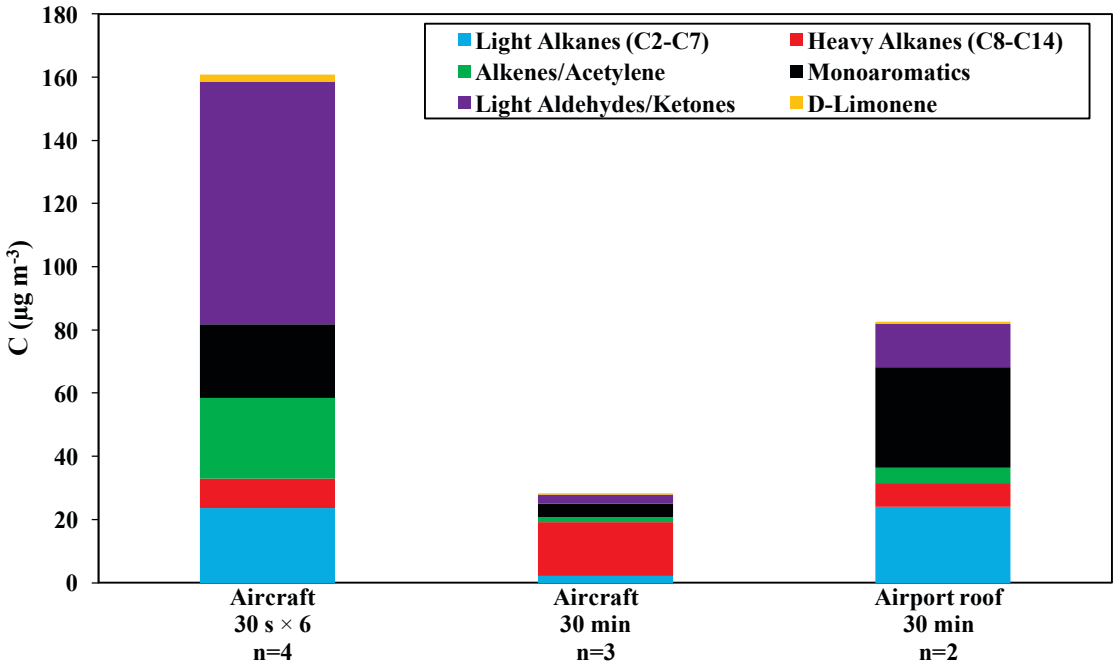

Figure 6: Distribution de COV par classe de composé déterminé à partir de mesures effectuées en Octobre 2014 (GC-FID)

3.2 Campagnes de transects

Après avoir identifié les traceurs issus des avions, l'impact des activités de l'aéroport a été évalué grâce aux campagnes le long de transects. Il a été observé que l'impact de l'aéroport est maximal dans les environs immédiats de l'aéroport. Cela est en conformité avec les résultats de la littérature. Cependant, grâce à ces campagnes de mesures, on a obtenu des résultats plus marquants et originaux.

Dans la première campagne (Figure 7) un traceur issu des émissions des avions a été retrouvé le long du transect du bord de mer, signifiant ainsi l'impact des émissions lors de la trajectoire de l'atterrissage. En effet, une étude récente a conclu que les zones touchées par les émissions du panache des avions pourraient avoir été sous-estimés. Hudda et al. (2014) a relevé des niveaux de PM2,5 élevés, émis par les jets lors de leurs trajectoires d'approche à l'aéroport international de Los Angeles.

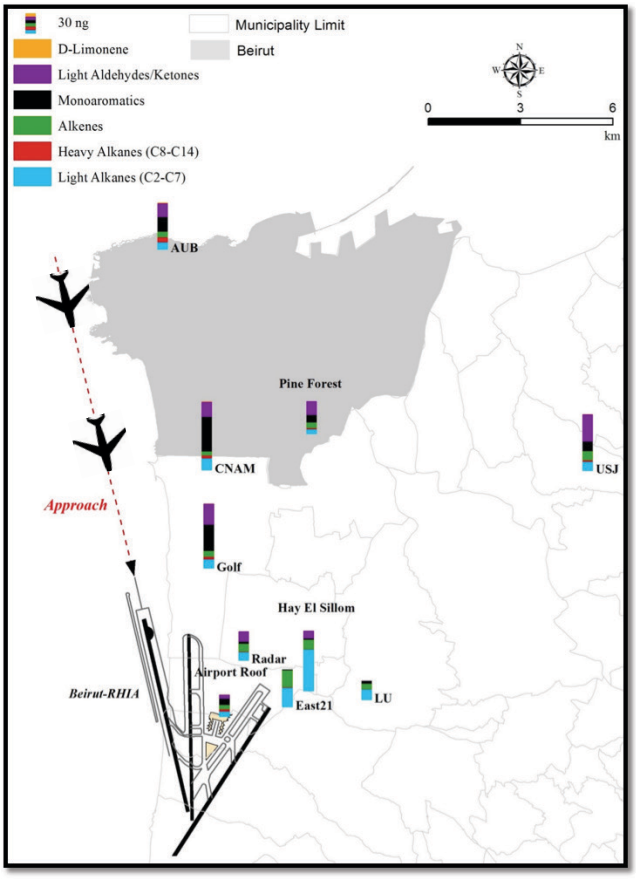

Figure 7: Distributions en masses (ng) par famille de COV pour la campagne de transect menée pendant la période du 20 au 22 Octobre 2014 (GC-FID). La ligne en pointillé rouge reflète la principale trajectoire de jet utilisée pour l'atterrissage à l'aéroport de Beyrouth

Un autre résultat important est la détection de traceurs dans une région montagneuse (USJ Mansourieh, à 8 km aéroport nord-est à 200-500 m ASL). Ceci pose de nombreuses questions concernant l'interaction complexe entre la dispersion des émissions lors de l'atterrissage, le vent et la topographie montagneuse caractéristique des environs de la capitale.

La deuxième campagne (technique active) (Figure 8) a confirmé les observations de la première campagne (passive). Tout d'abord, l'impact des émissions d'atterrissage de jet sur les zones de bord de mer a été confirmé par la présence des traceurs (alcanes lourds) exactement au bord de la mer (Coral), et leur absence à partir du site intérieur (CNAM), pourtant tous deux situés à une même distance de l'aéroport. La présence d'aldéhydes lourds (produits d'oxydation des gaz d'échappement de jet) au CNAM a confirmé que les COVs avec une plus lente cinétique de photooxydation atteignent des sites intérieurs tels que CNAM. En second lieu, la dispersion probable de l'aéroport et d'atterrissage des émissions dans les zones montagneuses a atteint le site du Barouk, région montagneuse située à environ 20 km de l'aéroport : des traceurs issus des avions y ont été relevés.

3.3 Campagnes de mesures passives du dioxyde d'azote NO_2

Les teneurs en NO_2 obtenues durant les trois campagnes présentaient des valeurs similaires. Les concentrations moyennes en NO_2 les plus faibles à savoir 27,6 $\mu g\ m^{-3}$ ont été mesurées au niveau de la phase d'approche des avions avant l'atterrissage tandis que les concentrations moyennes les plus élevées (57 $\mu g\ m^{-3}$) sont obtenues au niveau des sites de décollage correspondant au régime maximal de combustion par les moteurs d'avions ainsi qu'au niveau de la porte 12 où l'on attribue ces émissions aux avions et aux véhicules.

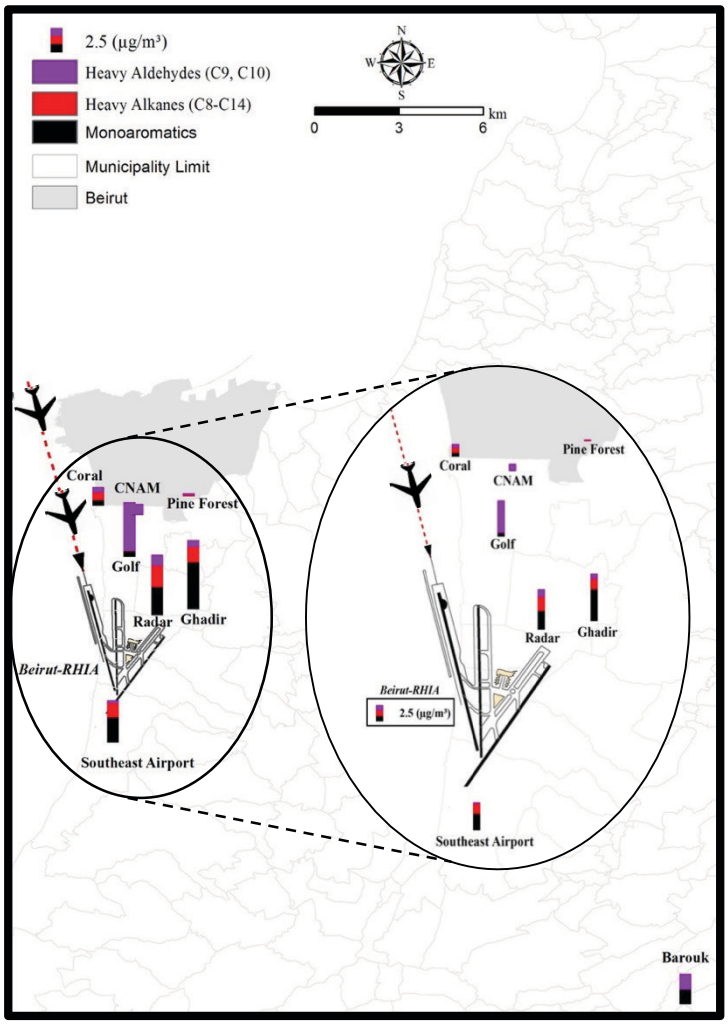

Figure 8: Concentrations (µg m^{-3}) des familles de COV lourds pour la campagne de transect menée du 13 au 21 Juillet 2015 (GC-MS).

3.4 Campagnes des mesures de l'air intérieur

Dans une étude préliminaire, les concentrations mesurées des 47 COV à l'intérieur des bâtiments de l'aéroport à savoir auprès de la salle de maintenance et dans le hall d'arrivée, présentaient des valeurs faibles, inférieures aux recommandations de l'INRS.

Par ailleurs, la concentration moyenne des COVT avait atteint une valeur de 123 µg m^{-3} durant la campagne d'été alors qu'elle est passée à plus de 250 µg m^{-3} pendant la campagne automne/hiver. Les plus faibles teneurs mesurées en été, pourraient s'expliquer par la dégradation photochimique des COVs accentuée pendant la période estivale comme rapporté par Atkinson (Atkinson, 2000).

Aussi, une corrélation entre le nombre d'avions en mouvement et les teneurs des aldéhydes légers et des cétones a été identifiée. Ces derniers sont connus d'être des

traceurs spécifiques des avions et présentent une dégradation photochimique plus lente que les autres COVs, lesquels sont moins bien corrélés avec le nombre des avions.

Lorsqu'on examine les teneurs mesurées au niveau du hall d'arrivée, il a été constaté que la concentration moyenne des COV totaux a diminué de 35% entre la période d'été et celle d'automne/hiver passant de 98 µg m^{-3} à 64 µg m^{-3} et ce, dans des conditions normales de ventilation. Dans ces mêmes conditions, les concentrations d'alcanes lourds ont varié de de 1 (activités aériennes minimales) à 52 µg m^{-3} (en heure de pointe). Ces valeurs présentaient des teneurs bien plus élevées que celles mesurées dans ces mêmes conditions dans la salle de maintenance. Il est à signaler qu'un incident exceptionnel s'est produit à l'aéroport. De manière générale, pour assurer une aération au sein des bâtiments, le pourcentage d'air pompé de l'extérieur est fixé typiquement à 20%. Suite à un problème technique, l'air pompé a été augmenté pour atteindre 50%, ce qui a certainement eu comme conséquence une augmentation notable de la concentration d'alcanes lourds (provenant de l'air extérieur) atteignant ainsi une moyenne de 407 µg m^{-3}, soit environ 40 fois supérieure à celle des 2 autres campagnes (voir la Figure 9 (a)). Une contamination directe de l'air intérieur par l'air extérieur est alors clairement identifiée. Cette contamination se produit, *via* une connexion entre le tarmac et le hall d'arrivée depuis une ouverture directe. Ainsi, suite à cette identification, une corrélation directe a pu être identifiée entre le nombre des avions en mouvements et les teneurs des alcanes lourds, ce qui conforte l'idée que ces derniers proviennent bel et bien des émissions des avions.

Par ailleurs, les concentrations en NO_2 mesurées dans le hall d'arrivée variaient entre 36 et 48 µg m^{-3} se situant autour voir au-dessus de la teneur annuelle maximale admise par l'OMS (fixée à 40 µg m^{-3}), ce qui pourrait présenter une atteinte quant à la santé des employés de l'aéroport. Ces concentrations élevées de dioxyde d'azote, résultent certainement de la contamination par l'air extérieur de teneurs en NO_2 variant de 49.0 à 64.2 µg m^{-3} et ce, suite au système de ventilation adopté dans les aéroports, constituant ainsi, fort probablement la raison pour laquelle les employés de l'aéroport souffrent de maladies pulmonaires (Yaman, 2001).

Quant aux valeurs de NO_2 mesurées dans la salle de maintenance, elles ne dépassaient guère la teneur annuelle maximale admise et variaient entre 7.2 et 10.8 µg m^{-3}.

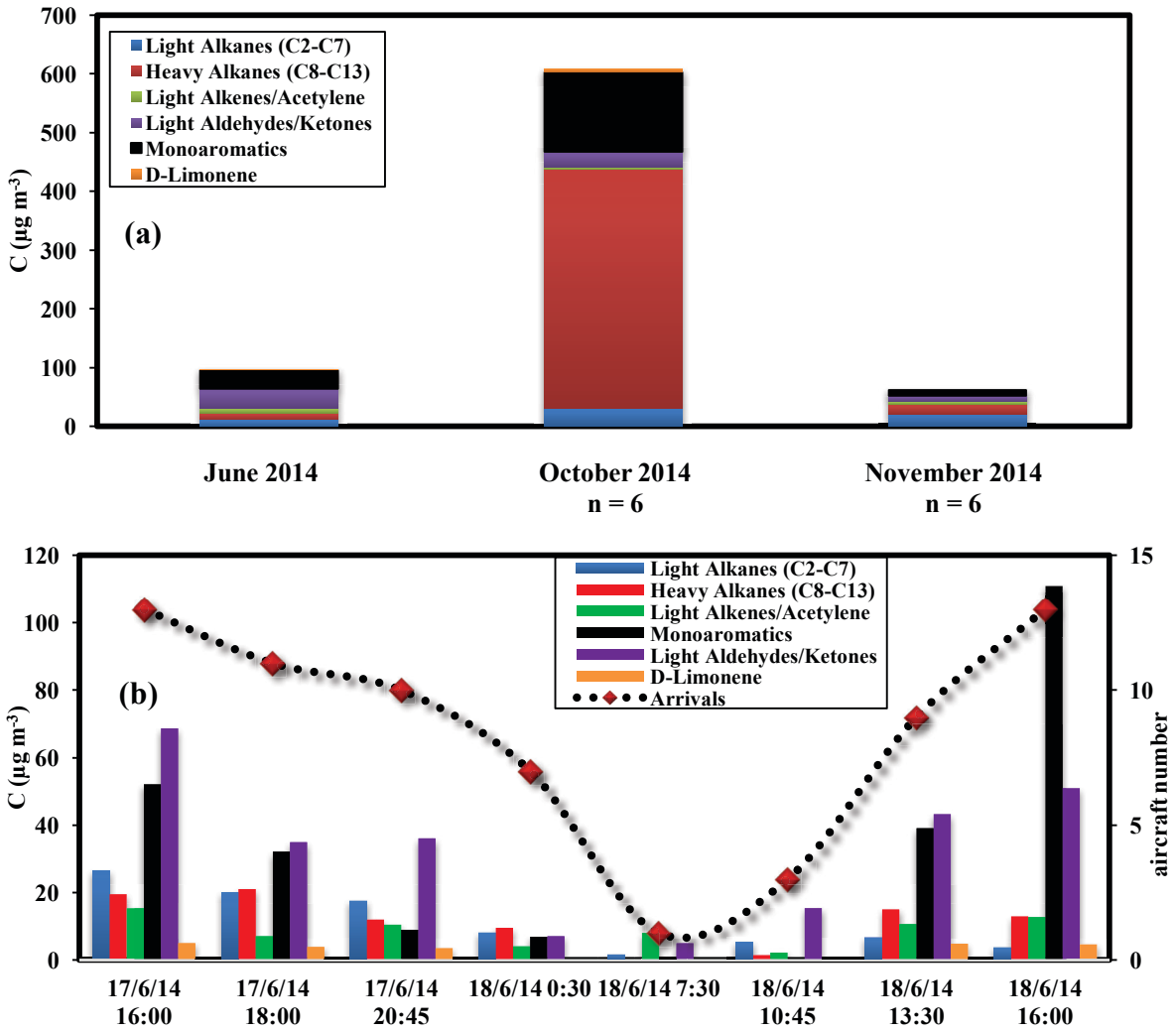

Figure 9: (a) Variation des concentrations de COV (µg m^{-3}) entre les 3 campagnes intérieures menées dans le hall des arrivées (aéroport de Beyrouth, 2014) (b) variation temporelle des groupes de COVs dans le hall des arrivées au cours de la campagne menée en Juin 2014

4. MODÉLISATION AVEC ADMS-AIRPORT

ADMS-Airport, recommandé par le Département des Transports (Dft) londonien, est l'un des 3 modèles de dispersion des polluants atmosphériques approuvés par l'Organisation de l'Aviation Civile International (OACI). Dans le cadre de cette recherche doctorale, il a été appliqué pour la première fois dans une région du Moyen-Orient. Ce modèle requiert, en premier lieu, un inventaire extrêment précis des Emissions (EMIT). Cette étape, en l'absence d'une base de données, a nécessité un travail exhaustif de recensement des émissions de toutes les sources de pollution issues de l'aéroport et de ses activités. Cet inventaire, qui a pris plus d'un an de travail, a tenu compte des détails opérationnels pour

environ 63000 mouvements d'avions durant l'année 2012 : caractéristiques des différents moteurs, nombre annuel de cycles liés à l'atterrissage et au décollage, modèles du groupe électrogène auxiliaire, temps de fonctionnement,…. D'autres sources d'émissions ont aussi été répertoriées comme l'équipement de soutien au sol (types, durée de fonctionnement annuelle, caractéristiques physiques, localisation). Les véhicules circulant sur le tarmac ont été recensés (flux, type de véhicule (moto/léger/lourd),…). Les sources fixes de l'aéroport, incluant les générateurs (diamètre et hauteur de la cheminée, etc...), les réservoirs de carburant (dimensions du réservoir, condition de la peinture, type, rayon et taille du toit, etc…) ont fait l'objet de cet inventaire. Les voitures (flux, types) pénétrant dans l'enceinte de l'aéroport ont été aussi intégrées dans le cadastre des émissions. Celui-ci, obtenu grâce à EMIT, a été exporté vers le système ADMS-Airport.

De plus, la modélisation a nécessité des paramètres météorologiques, notamment, la direction et la vitesse du vent de surface, la couverture nuageuse, la température, etc….

Les teneurs en pollution obtenues par modélisation, ont été validées par des mesures in situ. Le coefficient de corrélation (r) égal à 0,86 (entre les données modélisées et mesurées), nous conforte dans la qualité des résultats spatialisés issus de la modélisation.

Le modèle ADMS – Airport a permis de cartographier la variabilité spatiale des teneurs modélisées en NO_2 et COVs pour l'année 2012 : les concentrations en NO_2 (Figure 10) varient de 39 $\mu g\ m^{-3}$ (au sud et sud-est de l'aéroport) à 111 $\mu g\ m^{-3}$ (au centre de l'aéroport, aux portes). On relève dans la zone urbanisée, à proximité immédiate de l'aéroport, une teneur de 90 $\mu g\ m^{-3}$. Celle-ci diminue progressivement au fur et à mesure que l'on s'éloigne de l'aéroport. En raison de la direction dominante sud-ouest du vent, les régions situées au sud de l'aéroport de Beyrouth sont peu affectées. À Beyrouth, les niveaux du NO_2 varient entre 40 et 50 $\mu g\ m^{-3}$ nous laissant conclure que les émissions issues des activités aéroportuaires auraient une contribution d'environ 15 à 24% de la teneur en pollution de Beyrouth. Ces premiers résultats nous permettent de déduire que l'aéroport de Beyrouth contribue, non seulement à la dégradation de la qualité de l'air de son voisinage immédiat, mais aussi de celle de la capitale libanaise située au nord de l'aéroport. Il est à noter que la partie ouest de Beyrouth (zone en bord de la mer) semble être la plus affectée par la trajectoire des atterrissages, confirmant ainsi les observations expérimentales.

Quant aux émissions des composés organiques volatils (COVs), les valeurs maximales se situent principalement au voisinage de l'aéroport (1-23 $\mu g\ m^{-3}$) et ce, jusqu'à environ 0,5 km de distance. Les valeurs diminuent au fur et à mesure que l'on s'éloigne du site pour atteindre des teneurs de l'ordre de 0,003 à 1 $\mu g\ m^{-3}$ à Beyrouth.

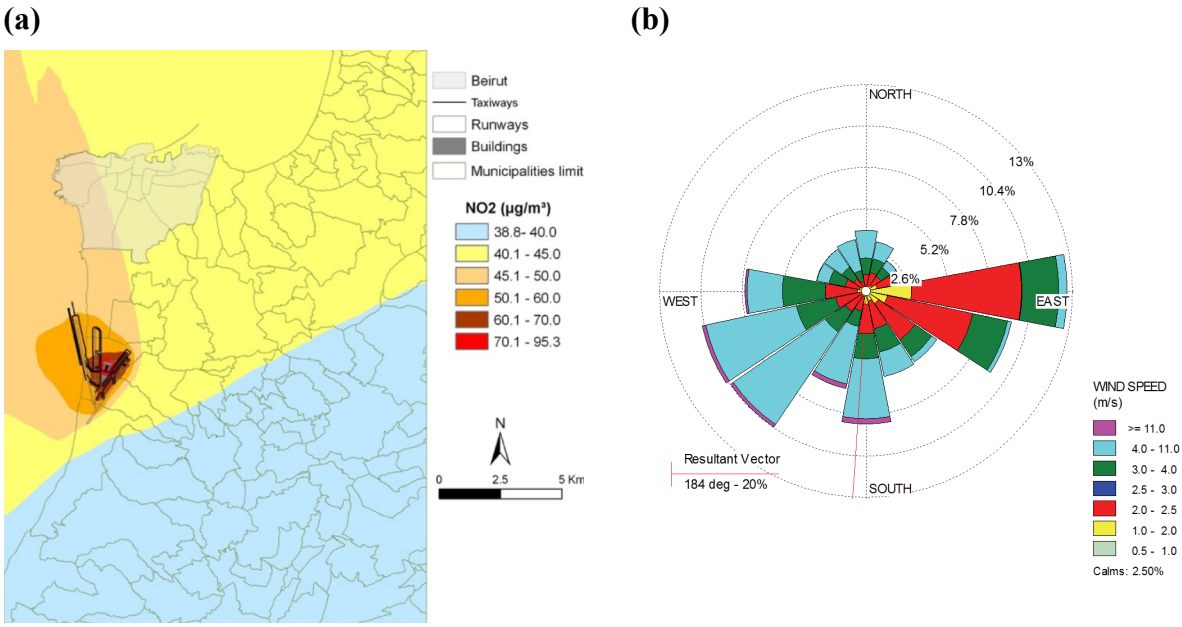

Figure 10: (a) Concentrations moyennes annuelles de NO_2 (µg m^{-3}) estimées par ADMS-Airport pour 2012 (z = 2 m), b) rose des vents pour 2012 (station aéroport de Beyrouth)

5. CONCLUSIONS ET IMPLICATIONS

Cette thèse visait en premier lieu l'identification de l'impact des activités de l'aéroport de Beyrouth sur la qualité de l'air de la ville de Beyrouth et de ses banlieues. Les deux approches adoptées, que soit l'expérimentale ou par modélisation, ont permis d'atteindre l'objectif de la thèse : les activités aéroportuaires affectent Beyrouth et sa banlieue que ce soit par les émissions de l'aéroport lui-même ou par le biais des émissions issues des atterrissages des avions. En effet, la zone côtière, à l'ouest de Beyrouth, semble la plus contaminée par les rejets des avions. Ce résultat pourrait s'expliquer par la trajectoire de l'atterrissage des avions qui survolent toute cette région à une altitude de 300 m environ (soit en-dessous de la couche limite).

Quant à l'air intérieur de l'aéroport, les résultats révèlent une relation intéressante entre l'intensité du trafic aérien (nombre d'avions) et les concentrations de COVs mesurées à l'intérieur des bâtiments.

Un résultat plus surprenant encore, les traceurs issus des avions ont été retrouvés sur deux sites localisés en zone montagneuse : à 215 m pour le premier et à 1100 m d'altitude pour le second. La topographie montagneuse et son effet sur les phénomènes aérodynamiques devraient jouer un rôle important dans la dispersion des polluants de l'aéroport.

Caractère Novateur

Le caractère novateur de cette thèse est dans sa pluridisciplinarité : connaissances dans les disciplines géographiques, chimiques et dans le domaine de l'aviation. En fait, cette recherche a permis, pour la première fois, d'identifier les signatures des émissions issues des avions (qui rappelons le étaient en mode opératoire réel) et qui sont : des alcanes lourds et des aldéhydes lourds. Les résultats des mesures le long de transects ont permis de constater que l'aéroport impacte non seulement la zone avoisinant l'aéroport mais aussi la capitale située à 8 km de distance. De même, à notre connaissance, ce travail constitue la première étude qui démontre l'impact des émissions sur la qualité de l'air lors de la phase d'atterrissage.

De plus, des mesures ont permis d'évaluer la concentration en COVs dans le hall d'arrivée et dans la salle de maintenance. Cette étude a pu démontrer, pour la première fois, une relation entre le nombre des avions et les teneurs des COVs mesurées à l'intérieur du hall des arrivées à cause d'une ouverture directe sur le tarmac.

Au niveau régional, c'est la première recherche qui utilise ADMS –Airport. Cette modélisation a permis de cartographier la répartition spatiale du NO_2 et des COVs, visualisant ainsi le rayon d'impact des activités aéroportuaires.

Ampleur et Implications

Cette étude fournit une méthodologie expérimentale pour évaluer l'extension spatiale des COVs et des NO_2 émis par les activités de l'aéroport. Ce travail s'est basé sur le suivi de traceurs spécifiques aux émissions issues des avions (alcanes lourds et aldéhydes lourds). En outre, l'identification des signatures lors de « situations opératoires réelles » peut fournir des informations sur les facteurs d'émission susceptibles d'être utilisés ultérieurement dans la modélisation. L'effet des rejets des avions lors de la trajectoire d'atterrissage démontre que l'impact n'est pas principalement localisé aux environs de l'aéroport mais que des zones plus lointaines pourraient être touchées et que de tels cas pourraient être observés exister dans des villes ayant le même contexte géographique que celui de l'aéroport de Beyrouth.

Cette recherche a fourni le premier inventaire d'émissions pour l'aéroport de Beyrouth. Ces données de base ont permis d'appliquer le modèle ADMS-Airport. Les résultats obtenus pourraient être utilisées par les décideurs lors de simulations de stratégies d'atténuation (taxi vert, réduction des heures de fonctionnement des groupes électrogènes auxiliaires à l'Aéroport International de Beyrouth – Rafic Hariri, etc…) et dans l'évaluation des impacts sur la santé.

Enfin, cette étude fournit une preuve de l'impact des activités des avions sur l'air intérieur de l'aéroport international de Beyrouth – Rafic Hariri. Des aménagements adéquats pourraient probablement améliorer la qualité de l'air intérieur.

Perspectives Futures

Cependant, Cette thèse, grâce à ses principales conclusions, ouvre de nouvelles perspectives de recherche. En effet, cette étude s'est limitée aux COVs et aux NO_2, qu'en est-il des autres polluants comme les particules ? Comment se dispersent-ils ? pourquoi relève-t-on des traceurs en zone montagneuse ?

La relation entre les teneurs en polluants intérieurs et les activités des avions peut-elle être confirmée ? Des mesures simultanées et continues de COVs et du nombre des avions en activité, pourraient en outre confirmer nos premiers résultats.

Finalement, dans cette thèse, compte tenu des données disponibles, il n'a été possible que d'appliquer une approche « intermédiaire » d'ADMS –Airport. Aussi, serait-il souhaitable d'appliquer la méthode la plus performante afin d'affiner les modèles de dispersion.

6. REFERENCES BIBLOGRAPHIQUES

AirPACA, 2004. Etude de la qualité de l'air sur l'aéroport « Nice Côte d'âzur » [WWW Document]. URL http://www.airpaca.org/sites/paca/files/publications_import/files/041200_AirPACA_etude_aeroport_Nice_net.pdf (accessed 2.28.16).

ATAG, 2014. Aviation Benefits Beyond Borders.

CAEP 9, 2013. Committee on Aviation Environmental Protection Ninth Meeting.

Daher, N., Saliba, N.A., Shihadeh, A.L., Jaafar, M., Baalbaki, R., Sioutas, C., 2013. Chemical composition of size-resolved particulate matter at near-freeway and urban background sites in the greater Beirut area. Atmos. Environ. 80, 96–106. doi:10.1016/j.atmosenv.2013.08.004

EPA, 2009. Aircraft Engine Speciated Organic Gases: Speciation of Unburned Organic Gases in Aircraft Exhaust [WWW Document]. URL https://www3.epa.gov/otaq/regs/nonroad/aviation/420r09902.pdf (accessed 2.28.16).

Hudda, N., Gould, T., Hartin, K., Larson, T.V., Fruin, S.A., 2014. Emissions from an International Airport Increase Particle Number Concentrations 4-fold at 10 km Downwind. Environ. Sci. Technol. 48, 6628–6635. doi:10.1021/es5001566

ICAO, 2011. Airport Air Quality Manual (Doc 9889).

Jochmann, M.A., Laaks, J., Schmidt, T.C., 2014. Solvent-Free Extraction and Injection Techniques, in: Dettmer-Wilde, K., Engewald, W. (Eds.), Practical Gas Chromatography. Springer Berlin Heidelberg, pp. 371–412. doi:10.1007/978-3-642-54640-2_11

Kim, B.Y., 2015. Understanding Airport Air Quality and Public Health Studies Related to Airports. Transportation Research Board.

Lelievre, C.P., 2009. La qualité de l'air en milieu aéroportuaire : étude sur l'aéroport Paris-Charles-De-Gaulle (phdthesis). Université Paris-Est.

Liaud, C., 2014. Développement de méthodes d'échantillonnage rapides et d'analyses différées au laboratoire : détermination de l'évolution temporelle des

concentrations des COVs et COSVs et compréhension des processus physico-chimiques en air intérieur (phdthesis). Université de Strasbourg.

RIDEM, 2008. Characterization of Ambient Air Toxics in Neighborhoods Abutting T.F. Green Airport and Comparison Sites: Final Report. Rhode Island Department of Environmental Management.

Saltzman, B.E., 1954. Colorimetric Microdetermination of Nitrogen Dioxide in Atmosphere. Anal. Chem. 26, 1949–1955. doi:10.1021/ac60096a025

Schürmann, G., Schäfer, K., Jahn, C., Hoffmann, H., Bauerfeind, M., Fleuti, E., Rappenglück, B., 2007. The impact of NOx, CO and VOC emissions on the air quality of Zurich airport. Atmos. Environ. 41, 103–118. doi:10.1016/j.atmosenv.2006.07.030

U.S. Environmental Protection Agency, 1999. Compendium Method TO-17 - Compendium of Methods for the Determination of Toxic Organic Compounds in Ambient Air. Determination of Volatile Organic Compounds in Ambient Air Using Active Sampling Onto Sorbent Tubes [WWW Document]. URL https://www3.epa.gov/ttnamti1/files/ambient/airtox/to-17r.pdf (accessed 3.8.16).

Wood, E., 2008. Aircraft and Airport-related Hazardous Air Pollutants: Research Needs and Analysis. Transportation Research Board.

Yaman, S.H., 2001. Aircraft and vehicle induced emissions at the Beirut International Airport a characterization and exposure assessment - by Sarah Hassan Yaman (Thesis).

Zhu, Y., Fanning, E., Yu, R.C., Zhang, Q., Froines, J.R., 2011. Aircraft emissions and local air quality impacts from takeoff activities at a large International Airport. Atmos. Environ. 45, 6526–6533. doi:10.1016/j.atmosenv.2011.08.062

List of Figures

List of Tables

List of Annexes

List of Acronyms

ADMS	Atmospheric Dispersion Modelling System
AIP	Aeronautical Information Publication
APEX	Aircraft Particle Emissions Experiment
APU	Auxiliary Power Unit
Beirut-RHIA	Beirut-Rafic Hariri International Airport
BTEX	Benzene, Toluene, Ethylbenzene, Xylenes
CAEP	Council for Aviation Environmental Protection
CERC	Cambridge Environmental Research Consultants
DGCA	Directorate General of Civil Aviation
EASA	European Aviation Safety Agency
EF	Emission Factor
EI	Emission Index
EMIT	Emissions Inventory Toolkit
EXCAVATE	EXperiment to Characterize Aircraft Volatile Aerosol and Trace Species Emissions
FAA	Federal Aviation Administration
GC-FID	Gas Chromatography-Flame Ionization Detector
GC-MS	Gas Chromatography-Mass Spectrometry
GIS	Geographical Information System
GRS	Generic Reaction Set
GSE	Ground Support Equipment
HAPs	Hazardous Air Pollutants
ICAO	International Civil Aviation Organization
IPCC	Intergovernmental Panel on Climate Change
LAQ	Local Air Quality
LTO-Cycle	Landing/Take-off-Cycle
NED	N-(1-naphthyl) ethylenediamine
NMHCs	Non-Methane Hydrocarbons
NO_2	Nitrogen Dioxide
NO_x	Nitrogen Oxides
PDTs	Passive Diffusion Tubes

SID	Standard Instrument Departure
STAR	Standard Instrument Arrival Route
TIM	Time-in-mode
UHCs	Unburned Hydrocarbons
US EPA	United States Environmental Protection Agency
VOCs	Volatile Organic Compounds

INTRODUCTION

Civil aviation is an integral part of the world economy providing 56.6 million jobs worldwide and its economic impact is estimated at $2.4 trillion, equivalent to 3.4% of world gross domestic product (GDP) (ATAG, 2014). To support our economic productivity, quality of life, and our national security, typical projected growth rates for commercial aviation activity is predicted to be 5% per year over the next 10–15 years (CAEP 9, 2013). Like other transportation modes, aviation relies on fuel combustion producing emissions. However, unlike other transportation modes aircraft travel great distances at a variety of altitudes, generating emissions that have the potential to have an impact on both the global climate and local air quality (LAQ) near airports presenting risks to public health (nearby residents, airport workers, and passengers) and the environment.

The effect of airports on local air quality is of growing concern. Due to the increasing amount of residential development surrounding airports and the continued growth of commercial air travel, the impact of airport activities on local air quality has become a significant concern for local/regional governments, especially that in many great cities of the world, emissions from automobiles, power plants, refineries, and other major sources are being steadily reduced. The constant rate of increase in aviation will be accompanied with an increase in aviation emissions if mitigation measures were not taken. Conscious of this problem, national and international air quality programs and standards are requiring governments and airport authorities to address air quality issues in the vicinity of airports and imposing mitigation measures through aircraft and engine technologies, government policies, air traffic management and operational procedures, and alternative fuel to balance environmental and economic interests. To implement mitigation measures, and to assess the potential health impacts of these aviation activities on the residents, understanding the contribution of airport operations to pollutant concentrations is necessary, which can be achieved *via* measurements and/or modelling.

Many reports were published to help better understand the contributions of airport activities to the degradation of LAQ (Kim, 2015, 2012). In fact, it is not easy to generalize an airport's contribution to the degradation of LAQ as it is dependent on each airport's own characteristics like **location**, surrounding **geography and topography, airport layout, meteorology,** traffic, etc. Despite this, the majority of the evidence indicated that pollutant concentrations were generally elevated in the vicinity of airports and that aircraft contributions were significant up to 1 km and relatively smaller 2-3 km away (Kim, 2015;

RIDEM, 2008; Wood, 2008; Zhu *et al.*, 2011). However, most of these studies focused on assessments in the vicinity of airports and did not account for emissions associated with aircraft trajectories or the effect of geography and topography on the spatial dispersion of pollutants. This can indicate that the areas affected by aircraft exhaust, as identified in these studies, might have been **seriously underestimated** (Hudda *et al.*, 2014).

As for airport indoor air, limited studies have been dedicated to assess the impact of airport emissions on indoor air of airport buildings, based on the assumption that most airport buildings are well ventilated and indoor emission sources are limited.

In **Lebanon**, the steady growth of aircraft movement at **Beirut-RHIA** (Beirut-Rafic Hariri International Airport) makes sense from the geographic perspective. Beirut-RHIA is in the middle of a populated area and upwind of the capital Beirut. Hence, the pollution from the airport is expected to blow over the capital and its suburbs. This was supported by observations found in a previous study conducted by Chelala (2008), which reported that 34% of the total nitrogen dioxide concentrations at a measurement site located at the eastern part of Beirut (Pine Forest), was coming from the southwest direction (where the airport is located). Moreover, the airport's location and layout is such that the approach jet trajectory is above the seashore area, which presents a significant emission source up to distances greater than 8 km away from the airport. Also, the topography surrounding the airport as well as time-varying wind direction and speed, can have a substantial influence on the dispersion of aviation emissions. It is important to note that in our study, inhabitants and residential apartments surrounding Beirut Rafic Hariri International Airport are much closer to it than the population surrounding other airports.

On the other hand, airport employees, who stay at least 12 h inside Beirut airport's buildings complain from respiratory symptoms (Yaman, 2001). Even more, direct openings exist between the apron and the arrivals hall providing a pathway for very contaminated air to enter the buildings. These reasons triggered the need to assess indoor air.

In Beirut, many studies have focused on road transport and its impact on air quality (Chelala *et al.*, 2006, Chelala, 2008, Daher *et al.*, 2013). Up till now, no study was conducted to assess the impact of Beirut Rafic Hariri Airport on the air quality of Beirut and its suburbs nor on the airport indoor air. We address the following questions: What is the impact of Beirut Airport's activities on the air quality of Beirut and its suburbs? How

can the potential air mass penetration into Beirut influence air quality in the city? In other words, to what extent will air quality in Beirut depend on pollutant emissions related to the operations of the Beirut Rafic Hariri airport? Is there a direct relationship between indoor pollutant levels and aircraft activity?

Objectives and Specific Aims

We hypothesized that emissions from Beirut Airport activities affected longer distances than previously observed in studies that focused mainly on the airport vicinity and that airport indoor air is affected by outdoor airport activities.

The main goal of this doctoral research is to assess the impact of Beirut-Rafic Hariri International Airport (Beirut-RHIA) activities on the air quality of Beirut and its suburbs in an attempt to understand its impact on air quality affecting the citizens in the surrounding area. A secondary goal is to assess the impact of these activities on indoor air quality affecting employees and passengers who spend time inside the airport. This study will help airport operators and airlines to understand the airport's environmental impact and accordingly undertake mitigation measures in order to minimize exposure for the personnel working at the airport, the travelling public, and avoid adverse impacts on the air quality of nearby neighbourhoods.

To address the questions of the main goal, two main pathways were followed, measurements and modelling. The combination of both approaches helps to verify the observations and fills the gaps related to each of the used approaches. To achieve this, our specific aims were:

- To experimentally identify the impact of the airport activities based on fingerprints, we had to identify special VOC fingerprints and markers, characteristic of aircraft emissions (Sections 5.1 and 6.1) by taking samples from aircraft exhaust under real aircraft operations in 4 measurement campaigns.
- Using these markers, the impact of the airport activities was tracked, as preliminary investigations (sections 5.2 and 6.2) in 4 measurement campaigns, mainly at downwind locations. It was not possible to track the impact of the airport activities using NO_2 as it is emitted from several other sources.
- Another approach to assess this impact was *via* modelling with an advanced Atmospheric Dispersion Modelling System (ADMS-Airport), which required prior

validation through NO_2 passive campaigns (sections 5.3 and 6.3) to gain confidence in utilizing this model (chapters 8 and 9). The two approaches will be compared to determine the main goal of this research.

- To assess the airport's impact on its indoor air, measurements were undertaken in 2 locations, the maintenance room to assess the impact on air quality affecting the employees, and the arrivals hall to assess the impact on passengers/employees (sections 5.4 and 6.4).

This doctoral research has focused, in particular, on the effects of nitrogen dioxide (NO_2) and Volatile organic compounds (VOCs), key ozone and PM precursors emitted from aircraft exhaust. Nitrogen dioxide (NO_2) is the most significant local air quality pollutant emitted from aircraft and presents a health risk in the Lebanese capital with annual average values of 53 $\mu g\ m^{-3}$ exceeding the World Health Organization (WHO) recommendations. VOCs, such as Hazardous Air Pollutants (HAPs), are harmful pollutants for health (alteration of the airways, cancer, and death) (Wood, 2008).

Organization

- Part I: Introductory Concepts

Chapter 1 highlights the increase in civil aviation which results in combustion products i.e. emissions. The fate of these emissions is described starting with their formation in the engine combustor, to the several chemical transformation processes (focusing on ozone formation), to wet and dry deposition, and finally their geographical transport. This geographical transport leads to the vertical and geographical distribution of emissions which is described at the end of chapter 1. This geographical and vertical distribution takes us to chapter 2 where the impacts of aviation as a result of emissions at different scales is described i.e. global and local while emphasizing on the local scale since it affects the health of citizens and personnel. Chapter 3 provides a description of the study area, signifying the reasons for making this study essential, and introduces the objectives of this thesis justifying the choice of the pollutants of concern.

✈ Part II: Experimental Approach

Part II describes all the experimental measurements done in this thesis. Chapter 5 presents all the sampling and laboratory techniques used to sample and analyse the air samples. Chapter 6 presents all the sampling methodologies adapted. This includes the signature campaigns, transect campaigns, NO_2 campaigns for model validation, and indoor campaigns. Chapter 7 presents the results obtained for these measurement campaigns.

✈ Part III: Modelling

Part III describes the advanced dispersion model used in this dissertation (ADMS-Airport), the methodology for building an emissions inventory, and the main findings. Chapter 7 provides a description of the model and its special features, which were the reasons it was adapted in this research. Chapter 8 describes the methodology adapted to apply ADMS-Airport to RHIA. Finally, chapter 9 discusses the airport's impacts on air quality, both on the vicinity and on Beirut and its suburbs.

Part I: General Contexts

The title of this doctoral thesis clearly states its objective, to assess the impact of Beirut Airport activities on air quality, which came as a result of several reasons. Literature review, along with the airport's special characteristics will be presented in Part I to justify the choice of this research.

Chapter 1 : Aviation Emissions

Like all transportation modes, aviation works on fuel combustion which leads to the production of aviation emissions, namely air pollutants which affect air quality and the global climate. The formation and transformation, evolution and geographical transport, and the resulting vertical and geographical distributions of these aviation emissions will be discussed in this chapter.

1.1 Evolution of Air Transport

"Aviation is the real world wide web, a network of airlines, airports, and air traffic control organizations that link the major cities and small communities of the world 24 hours a day with very advanced aircraft" (ATAG, 2016). Aviation has grown in a century to be the lifeblood of a globalized economy (IATA, 2013), facilitating the growth of international trade, tourism, and international investment, and connecting people across continents. In effect, the air transport industry provides 56.6 million jobs worldwide with an estimated economic impact at $2.4 trillion, equivalent to 3.4% of world gross domestic product (GDP) (ATAG, 2014).

Air transport facilitates world trade and is indispensable for tourism. The share of air transport (Figure 1-1) as a preferred mode of tourist transport is gradually increasing at a faster pace than surface transport; slightly over half of all the tourist travellers arrived to their destination by air in 2012 (52%) and 2014 (54%) while the remainder travelled by surface transport (UNWTO, 2015, 2013).

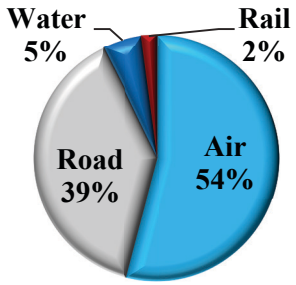

Figure 1-1: Inbound tourism by mode of transport, 2014.
Source: (UNWTO, 2015)

In 1903, the year of the Wright brothers' first flight, the earth's population was 1.6 billion (FAA, 2005); today, over 3 billion people use the world's airlines. It is acknowledged that aviation industry is experiencing the quickest growth compared with other transport modes (Kahn Ribeiro *et al.*, 2007). Civil aviation is one of the fastest growing sectors of the world economy, at consistent annual rate increases between 5 and 9% (Penner, 1999). To support our economic productivity, quality of life, and our national security, typical projected growth rates for commercial aviation activity (passenger and cargo traffic), expressed in revenue tonne-kilometres, is predicted to be 5% per year over the next 10–15 years (CAEP 9, 2013) and 4.2 to 3.7% over the extension periods 2030-2040 and 2040-2050 respectively (Figure 1-2 (a)). However, this will be accompanied with an increase in fuel consumption (Figure 1-2 (b)); it is projected that by 2040 fuel consumption will have increased by between 2.8 and 3.9 times the value in 2010 (ca. 142 million metric tonnes) and by four to six times the 2010 value by 2050 (ICAO, 2013).

While the benefits of this growth will be substantial, however, these benefits would come at a cost, most notably a significant increase in pollutant emissions (nitrogen dioxides, volatile organic compounds, carbon dioxide, etc.) from aviation activity are expected to grow by factors of 1.6 to 10, depending on the fuel use scenario (Penner, 1999). For example, NO_x aircraft emissions at the local scale (below 3,000 feet AGL) are estimated to increase from about 0.25 million metric tonnes (10^9 kg) for the year 2006 to 0.52-0.72 Mt for the year 2036 by factors of 2-3 (Figure 1-2 (c)). These emissions have aviation-related environmental impacts on two major separate levels: (i) the local level which involves ground level ozone (O_3) and acid rain; and (ii) the global level which involves climate change and ozone depletion (Macintosh and Wallace, 2009; Penner, 1999). These impacts will be discussed in chapter 2.

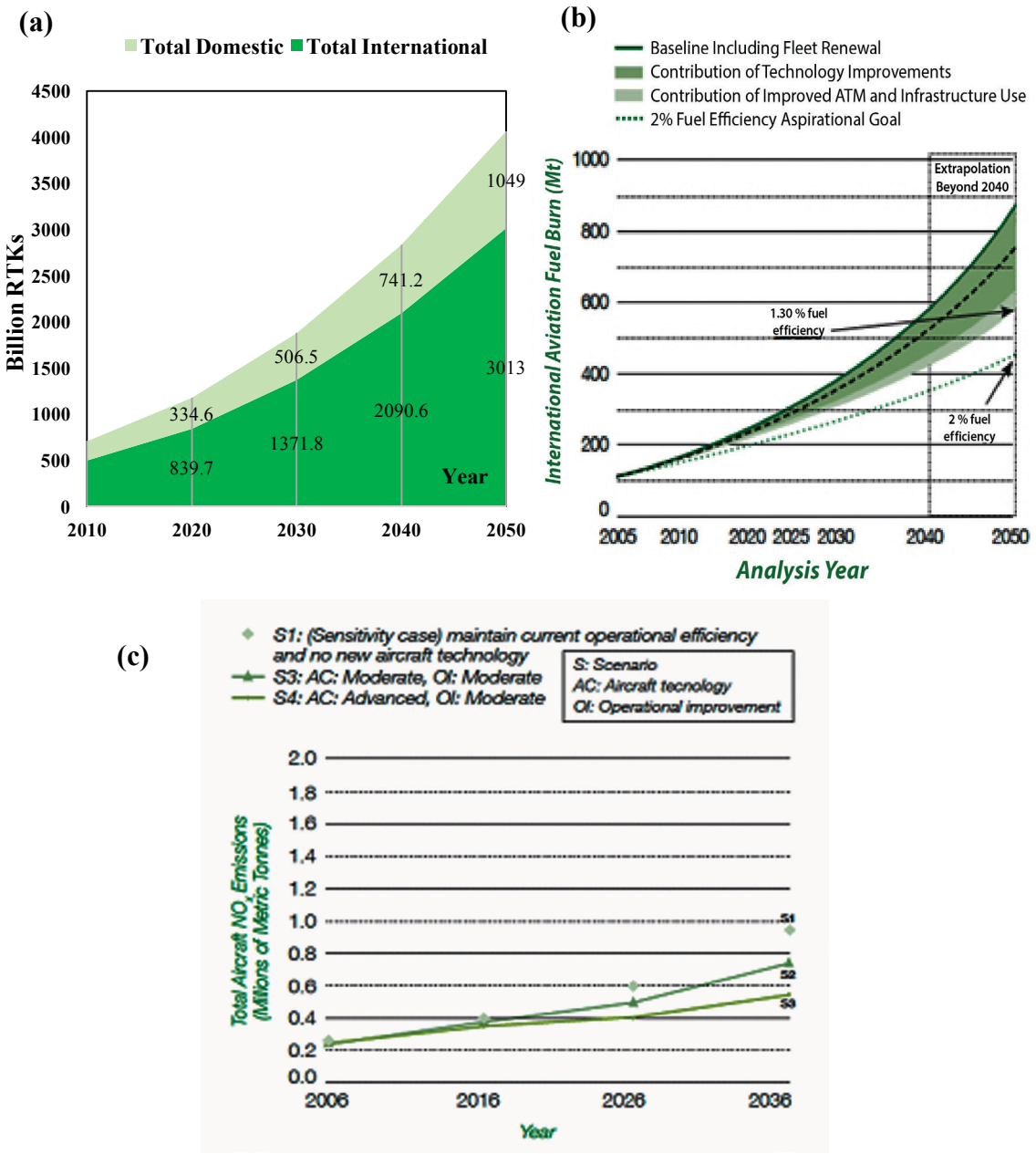

Figure 1-2: (a) CAEP/9 Combined passenger and cargo traffic forecast (Most Likely Scenario, Central Forecast) (b) ICAO/CAEP Fuel burn trends from international aviation, 2005 to 2050. Source: (ICAO, 2013) (c) Total global aircraft NO_x below 3000 ft AGL, taken from ICAO (2013)

1.2 Aircraft Exhaust and Other Airport-Related Emissions

Aircraft engine emissions, the dominant emissions at airports, have been the focus of the large majority of studies (Anderson *et al.*, 2006; Herndon, 2012; Knighton *et al.*, 2007; Wood, 2008). An aircraft exhaust plume contains combustion products (emitted species), species formed in the plume from emitted species, and atmospheric species carried into the plume. The exhaust from an aircraft gas turbine is composed of carbon dioxide (CO_2),

water vapor (H_2O), nitrogen oxides (NO_x), carbon monoxide (CO), sulphur oxides (SO_x), unburned hydrocarbons (UHC) or volatile organic compounds (VOCs), particulate matter (PM) or soot, and excess atmospheric oxygen and nitrogen. A small subset of VOCs and particulates are considered hazardous air pollutants (HAPs) which are either cancerous or have hazardous health effects. In fact, a prioritized list of gas-phase HAPs emitted by airport emission sources has been constructed based on the product of the compounds' toxicities and emission rates. This list consists of acrolein (propenal), formaldehyde, 1,3-butadiene, naphthalene, benzene, acetaldehyde, ethylbenzene, and propanal (propionaldehyde). Glyoxal, methylglyoxal, and crotonaldehyde (butenal), although not officially hazardous air pollutants, may be comparable in importance to the compounds listed above (Wood, 2008).

Figure 1-3 (b) reports a detailed breakdown of combustion products; approximately 72% of combustion emissions are CO_2 emissions; H_2O makes up 27.6% while the rest of the pollutant species amount to less than 0.4% of the total emissions (Lewis *et al.*, 1999). CO_2 and H_2O emissions are directly relevant as greenhouse gases (GHG). Thus, the remaining 0.4% plays an important role in local air quality. In this context, nitrogen oxides, which are ozone precursors, constitute 84% of the local air quality emissions implying that NO_x are the most significant local air quality pollutants related to aviation. VOC and carbon monoxide emissions from aircraft are of relevance to air quality, mainly near airports (Lee *et al.*, 2010).

1.2.1 FORMATION OF AVIATION EMISSIONS

The majority of the emitted species (gases and soot particles) are products of kerosene combustion with ambient air in the combustion chamber of the engine (Lee *et al.*, 2010) (Figure 1-3 (a)). Kerosene is the mostly used fuel in civil aviation. A number of types of kerosene are in common usage, the most commonly used fuel in commercial aviation is Jet A-1with a maximum freezing point of -47°C and a mean C/H ratio of $C_{12}H_{23}$. Jet A is in common usage in the US and has a maximum freezing point of -40°C (Lewis *et al.*, 1999). ASTM specification D1655 is recommended for both fuel types.

The combustion of kerosene primarily produces carbon dioxide and water (Anderson *et al.*, 2006; Lee *et al.*, 2010). The oxidation of atmospheric nitrogen at the very high temperatures in engine combustors drives the formation of nitrogen oxides, while the

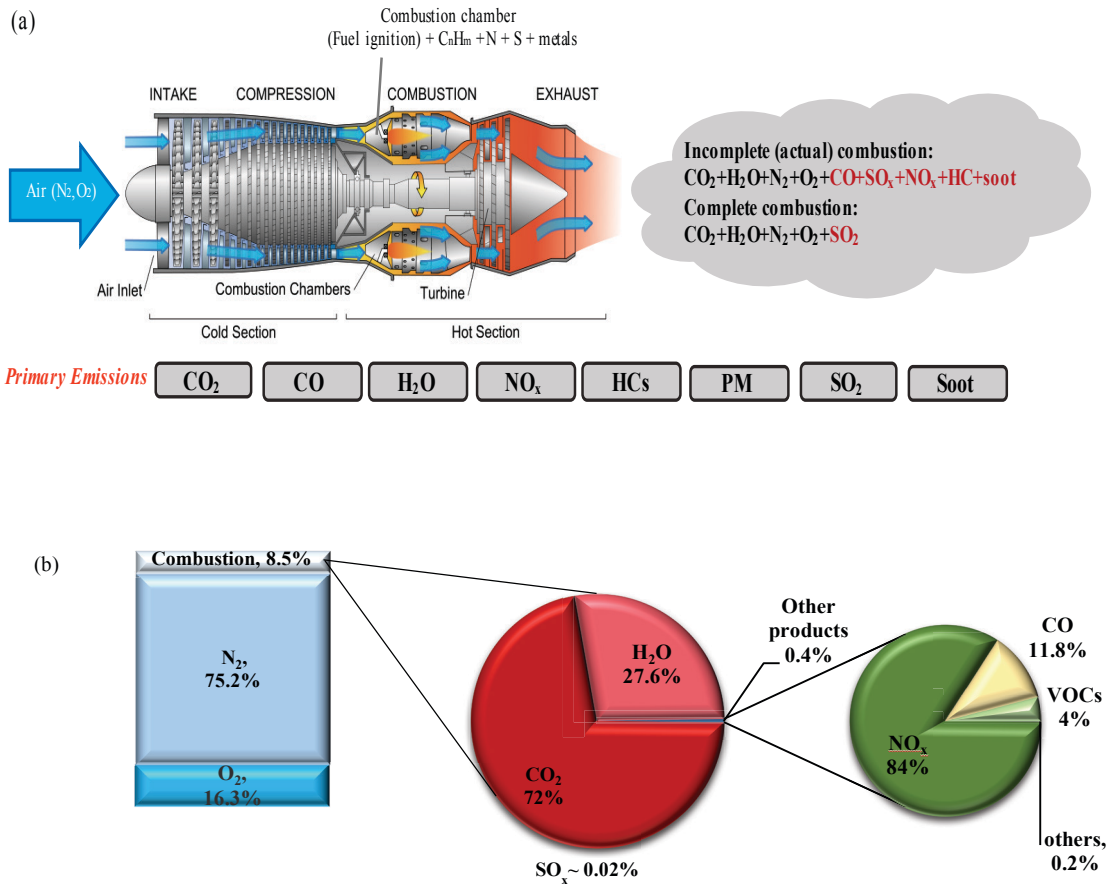

Figure 1-3: (a) Simplified diagram of a turbojet engine and products of complete and incomplete combustion, adapted from Masiol *et al.* (2014) (b) Division of the combustion products of an aircraft engine, adapted from Lewis *et al.* (1999)

presence of trace amounts of sulphur, nitrogen, and some metals (e.g., Fe, Cu, Zn) in fuels (Lewis *et al.*, 1999) and non-ideal combustion conditions within engines may lead to the production of by-products, including sulphur oxides, additional nitrogen oxides, unburned hydrocarbons and particulate soot. In addition, exhausts can also contain species from the combustion and release of lubricant oils (Dakhel *et al.*, 2007) and from the erosion of metal parts (Demirdjian *et al.*, 2006). A realistic, but simplified, combustion scheme in aircraft engines can be summarized as (Lee *et al.*, 2009; Mahashabde *et al.*, 2011):

$$C_nH_m + S + N_2 + O_2 \rightarrow CO_2 + N_2 + H_2O + O_2 + CO + SO_x + NO_x + HC + soot \qquad (1\text{-}1)$$

Aircraft main engines are not the only source of airport emissions. Airport access and ground support vehicles typically burn fossil fuels and produce similar emissions. Other emission sources at the airport include auxiliary power units (APU) providing electricity and air conditioning to aircraft parked at airport terminal gates, traffic to and from the

airport, shuttle buses and vans serving passengers, and ground support equipment (GSE) that service aircraft, stationary airport power sources, and construction equipment operating on the airport (FAA, 2015). These sources will be discussed in section 2.5.

1.2.2 EMISSION TRANSFORMATION

Airport emissions include primary and secondary emissions. Pollutants, which are present in the engine exhaust as it leaves the aircraft (or other airport sources), are primary pollutants. These pollutants include NO_x, VOCs, CO, PM, SO_x, CO_2, and H_2O. Many of these pollutants transform when they are emitted to the atmosphere to form secondary emissions (National Research Council (U.S.), 2002).

In fact, aircraft pollutants generally transform in three different zones: i) immediately after exiting the combustor within the engine, ii) downstream from the engine in the hot exhaust plume, and iii) after emissions have cooled and mixed with the ambient atmosphere (FAA, 2015). Examples of secondary emissions are ozone (O_3), nitric acid (HNO_3), sulfuric acid (H_2SO_4), PAN (peroxyacetylnitrate), aldehydes, aerosols, and some types of particulates (Lelievre, 2009). Likewise, gaseous and particle emissions from cars, trucks, and ground vehicles that have exhaust pipes transform in the exhaust plume after mixing with the ambient atmosphere.

In the ambient atmosphere, chemical reactions involve both molecules emitted from the aircraft and vehicle engines as well as molecules already in the air. For example, ozone is formed by the reaction of VOCs and NO_x in the presence of heat and sunlight (explained in section 1.3.1 below). Also, complex chemical reactions and/or particle nucleation processes can produce new particles or add to pre-existing particles. These particles are much greater in magnitude than primary particles (Jathar *et al.*, 2012). Other examples are the conversion of nitrogen dioxide (NO_2) from the plume to nitric acid (HNO_3) vapor that interacts with ammonia in the atmosphere and forms ammonium nitrate (NH_4NO_3) particles and oxidation reactions involving gaseous hydrocarbons from the plume, yielding condensable organic compounds that form organic aerosol particles (FAA, 2015).

1.3 Evolution of Pollutants (Fate of pollutants)

After a given pollutant is emitted, its behavior and fate (lifetime) in the atmosphere are determined by its (i) transformation reactions (e.g. ozone formation by NO_x and VOCs),

(ii) removal pathways (photolysis, wet or dry deposition), and (iii) geographical transport (Atkinson *et al.*, 2006).

1.3.1 ROLE OF VOCS AND NO_X IN OZONE FORMATION

Ozone is formed exclusively in the atmosphere by the reaction of atomic oxygen (O) and O_2; it is not emitted from any other source. In the troposphere, the principle source of atomic oxygen is the photochemical cycle involving NO, NO_2 and sunlight (Seinfeld, 1995). The oxygen atoms are produced from photolysis of NO_2 by the ultraviolet portion (wavelength = 290 – 430 nm) of solar radiation (h**ν**) (California Environmental Protection Agency, 2005):

$$NO_2 + h\nu \rightarrow NO + O(^3P) \ (290 < \lambda < 430 \text{ nm}) \quad (1\text{-}2)$$

$$O + O_2 + M \rightarrow O_3 + M \quad (1\text{-}3)$$

$$O_3 + NO \rightarrow O_2 + NO_2 \quad (1\text{-}4)$$

$O(^3P)$ is an oxygen atom that has been electronically excited to the $O(^3P)$ state, and M represents any other molecule, usually N_2 or O_2, whose role is to absorb the energy lost by $O(^3P)$. The only reaction actually producing ozone is reaction (1-3), whereas reaction (1-4) converts ozone back to oxygen and NO back to NO_2 completing the "nitrogen cycle". Reactions (1-3) and (1-4) are comparatively fast, which renders the slower photolysis reaction (1-2) as the rate-limiting reaction for the nitrogen cycle and the reason why ozone is not formed appreciably at night. It is also one of the reasons why ozone concentrations are high during the summer months at elevated temperatures and intense solar radiations. The nitrogen cycle operates fast enough to maintain a close approximation to the following photostationary-state equation derived from the above reactions. $[O_3]_{\text{photostationary-state}} = (k_{(1\text{-}2)}/k_{(1\text{-}4)}) \times [NO_2]/[NO]$. The ratio of the rate constants for reactions 1-2 and 1-4, $(k_{(1\text{-}2)}/k_{(1\text{-}4)})$, is about 1:100. Assuming equilibrium is reached at typical urban pollution concentrations, then a NO_2 to NO ratio of 10:1 would be needed to generate about 0.1 ppm of ozone. In contrast, the NO_2 to NO emission ratio is approximately 1:10; therefore, the nitrogen cycle by itself does not generate the high ozone concentrations observed in urban areas. The net effect of the nitrogen cycle is neither to generate nor destroy ozone molecules. Therefore, for ozone to accumulate according to the photostationary - state equation, an additional pathway is needed to convert NO to NO_2, one that will not destroy ozone. In the case of polluted tropospheric conditions, the photochemical oxidation of

VOCs, such as hydrocarbons and aldehydes, provides that pathway (California Environmental Protection Agency, 2005). Thus, the accumulation of ozone takes place in a polluted environment when the concentration of both precursors, namely VOCs and NO_x, are high.

- Oxidation of VOCs

The major chemical reaction pathways involved in the photo-oxidation of VOCs and the formation of summer smog are summarized in Figure 2-4 (Camredon and Aumont, 2007). The most important sink for VOCs in the atmosphere is the photo-oxidation initiated by hydroxyl radical (HO•), which is almost exclusively diurnal. The final products of this oxidation are CO_2 and water which makes atmospheric oxidation similar to combustion (Koppmann, 2008). To a lesser extent is the oxidation of VOCs by ozone O_3 (diurnal and nocturnal), and nitrate radicals (NO_3•) (exclusively nocturnal) (Atkinson *et al.*, 1984). The products of these reactions are numerous; the principle is ozone (O_3), CO_2, PeroxyAcetylNitrate (PAN), hydrogen peroxide (H_2O_2), etc. In the following paragraphs, the photo-oxidation of VOCs by OH will be discussed since it is the most important loss process.

The photo-oxidation of VOCs (RH) is a chain reaction process including radical initiation (e.g. formation of HO•), radical propagation, and radical termination steps. The degradation (radical propagation) of atmospheric hydrocarbons is initiated largely by OH radical attack, predominately H-atom abstraction from alkanes, and by radical addition to alkenes and aromatics. H-atom abstraction leaves an alkyl radical that rapidly adds O_2 to produce the alkyl peroxy radical, RO_2•. Likewise, OH• addition to alkenes and aromatics leads to a hydroxyl alkyl radical that also adds O_2 rapidly to give an RO_2 radical. Propagation is divided into 4 stages (Seinfeld, 1995; Semadeni, 1994):

-Formation of an organic radical upon the reaction with HO•. In general, the major reaction pathway is *via* H atom abstraction from the secondary C-H bonds (Atkinson *et al.*, 1982):

$$RH\ (VOC) + HO\bullet \rightarrow R\bullet + H_2O \qquad (1\text{-}5)$$

- The alkyl radicals formed are quickly oxidized by O_2 to form an alkylperoxy radical $RO_2^{\bullet}$:

$$R\bullet + O_2 + M \rightarrow RO_2\bullet + M \qquad (1\text{-}6)$$

-Reduction of the peroxy radical by NO:

$$RO_2\bullet + NO \rightarrow RO\bullet + NO_2 \text{ or } RONO_2 \text{ (alkyl nitrates)} \quad (1\text{-}7)$$

It is important to note that in environments with low NO_x concentrations, $RO_2\bullet$ reacts with $HO_2\bullet$ (derived from the oxidation of formaldehydes) to produce hydroperoxides (ROOH):

$$RO_2\bullet + HO_2\bullet \rightarrow ROOH + O_2 \quad (1\text{-}8)$$

- Degradation of RO• formed in reaction (1-7) takes place either by hydrogen abstraction by O_2 to yield aldehydes and ketones (reaction (1-9)), thermal decomposition (reaction (1-10)), or isomerization ($nC \geq 4$) (reaction (1-11)):

$$RO\bullet + O_2 \rightarrow R'CHO + HO_2\bullet \text{ or } R'C(O)R'' + HO_2\bullet \quad (1\text{-}9)$$

$$RO\bullet \rightarrow R'\bullet + R''CHO \text{ or } R'\bullet + R''C(O)R''' \quad (1\text{-}10)$$

$$RO\bullet \rightarrow R'OH \quad (1\text{-}11)$$

The chain reaction is terminated when free radicals are converted to stable products, for example through the formation of nitric acid.

$$OH\bullet + NO_2 \rightarrow HNO_3 \quad (1\text{-}12)$$

$$HO_2\bullet + NO \rightarrow OH + NO_2 \quad (1\text{-}13)$$

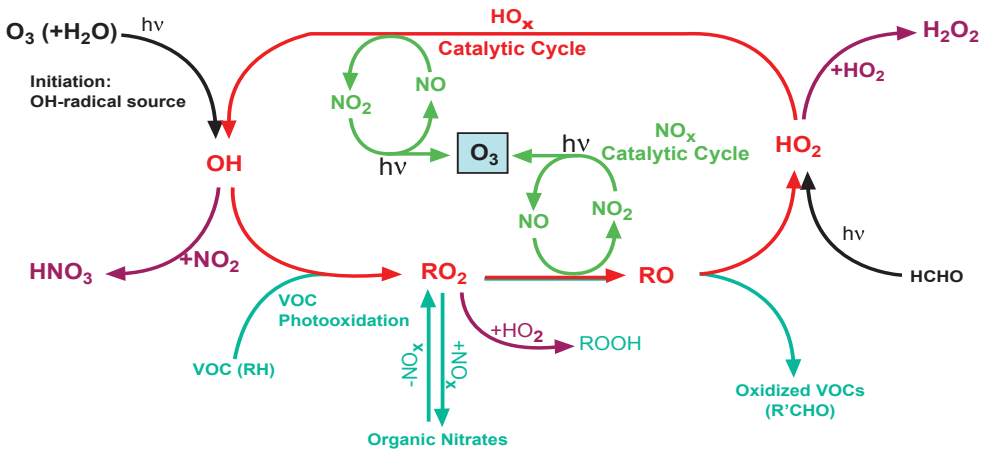

Figure 1-4: Major chemical reaction pathways involved in the photo-oxidation of VOCs and the formation of summer smog, adapted from Camredon and Aumont (2007)

1.3.2 Wet and Dry Deposition

Deposition can occur in two forms: (i) wet deposition when pollutants are trapped into water droplets and consequently into rain, clouds, or fog or (ii) dry deposition when pollutants are adsorbed on surfaces such as vegetation or aerosols. Dry deposition is expected to play a minor role in the removal of VOCs while wet deposition can be important for highly water soluble VOCs (alcohols, aldehydes, dicarbonyls and

hydroperoxides). Most primary emitted VOCs are non-polar and insoluble in water and rain. However, rainout becomes significant as VOCs are oxidized, thus becoming more polar (Julia, 2014).

1.3.3 GEOGRAPHICAL TRANSPORT

After being emitted, pollutants are dispersed by atmospheric transport processes while undergoing chemical transformation (removal process) (Figure 1-5). Atmospheric transport occurs at 4 scales: micro with a typical scale of 2 m, meso (or local) with a typical scale of 20 km, and macroscale i.e. synoptic (typical scale of 2000 km) at the regional scale and global (typical scale of 5000 km) at the intercontinental scale (Ahrens, 2009). The term "long-range transport" refers to transport on the synoptic or global scales.

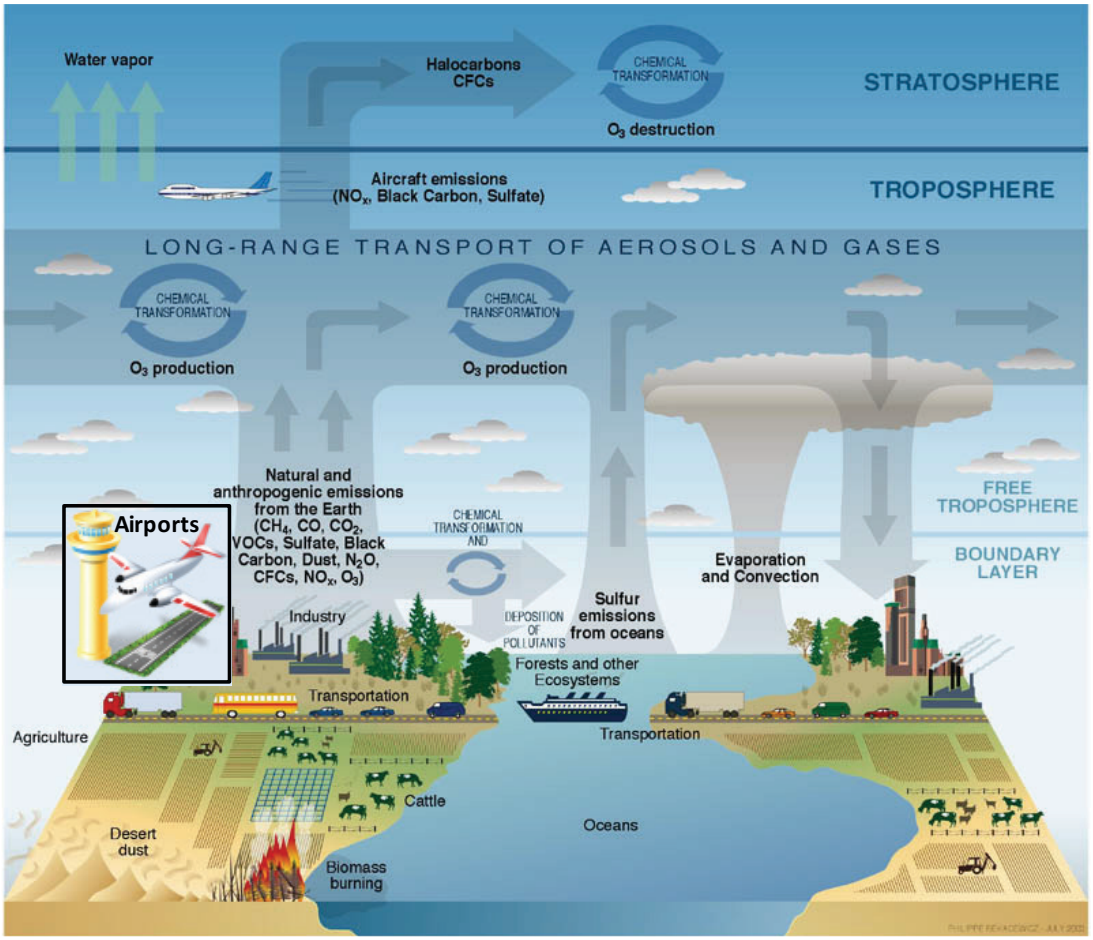

Figure 1-5: Schematic of chemical and transport processes that determine the fate of pollutants in the atmosphere, adapted from Climate Change Science Program and the Subcommittee on Global Change Research (2003)

In the next sections, I will focus on microscale and to a larger extent mesoscale winds since mesoscale winds play a big role in the dispersion of pollutants from Beirut airport (see chapter 3). This relates to the fact that Lebanon has a stable climate, which makes local climatology play an important role in pollutant dispersion. These mesoscale (local) winds are signified by the special geography and topography surrounding Beirut Airport i.e. the sea and the mountains.

- Winds and the Atmospheric/Planetary Boundary Layer

Dispersion occurs in the portion of atmosphere that extends to 1 or 2 km above ground level, called atmospheric boundary layer. The dispersion of air pollutants depends on meteorological processes, such as advection and convection of air masses. Advection refers to the horizontal movement of air masses, most often related to wind. Convection processes define the vertical movements of air masses. These movements are due to the rise of thermals of warm air as a result of solar heating.

Transport of pollutants at the local scale is physically bound by the planetary boundary layer within which pollutants are usually emitted. The planetary boundary layer or atmospheric boundary layer is "that part of the troposphere that is directly influenced by the presence of the earth's surface, and responds to surface forcings with a time scale of an hour or less" (Stull, 1988). Frictional drag, evaporation, heat transfer, pollutant emission, and terrain induced flow modification are examples of surface forcings. The three major components of the boundary layer are the mixed layer, the residual layer, and the stable boundary layer (Figure 1-6). In the mixed layer (ML), turbulence is usually caused by thermal convection (vertical transport) and to a lesser extent by wind shear. Thermal convection occurs during the day when the heated ground surface, under the effect of solar heating, creates thermals of warm air arising from the ground. Thus, a turbulent ML begins to grow in depth about half an hour after sunrise and reaches its maximum depth in the late afternoon. The resulting turbulence tends to effectively mix and dilute pollutants emitted; also, the formation of a stable layer at the top of the ML (called the entrainment zone) acts as a lid to the rising thermals, thus physically bounding the vertical dispersion of pollutants (Stull, 1988). Trapping of pollutants within the entrainment zone, also denoted as the inversion layer, is common in high-pressure regions and sometimes leads to pollution alerts in large communities. The mixing layer typically undergoes a diurnal cycle rising to heights of 1-2 km in the day and lowering to 100-300 m at night (Committee on

Atmospheric Transport and Chemical Transformation in Acid Precipitation, 1983). At night, when thermals stop to form and turbulence decays, the top of the mixing layer lowers down to form the base of the stable (nocturnal) boundary layer. The top of the stable boundary layer is defined as the height where turbulence intensity is a small fraction of its surface value. Limited vertical mixing takes place within the nocturnal boundary layer, which leads to increased pollutant concentrations (e.g. NO) thus influencing the initial chemical conditions for photochemistry, including NO_x and ozone concentrations, during the second day (Pisano *et al.*, 1997).

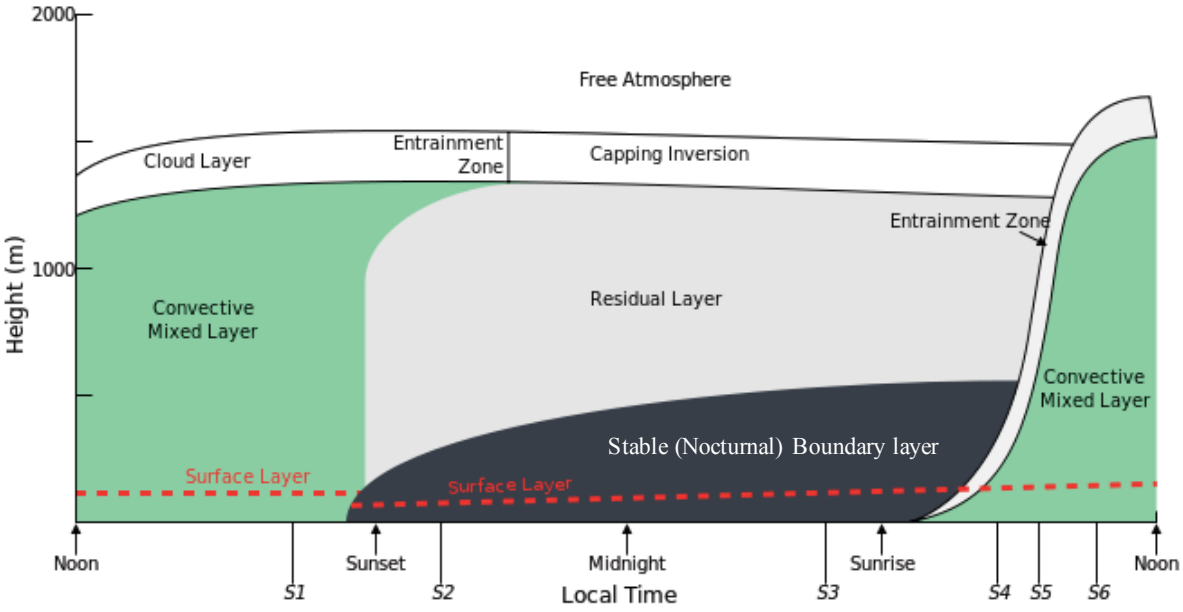

Figure 1-6: Planetary boundary layer, adapted from Stull (1998)

- Local winds: Sea breeze/ Land breeze and Valley/Mountain breeze

Physical geography can play a significant role in local air pollutant dispersion. Mountain ranges can define their own weather and channel air sheds to form distinct wind patterns. Also, valleys do not allow airport emissions to disperse as rapidly in comparison to emissions at airports in open terrain that experiences no major geographical hindrance to dispersion. For example, Los Angeles and LAX sit in a bowl surrounded by mountains to the north and east that trap pollutants in an urban basin. To add to this, in warm weather, a cool sea breeze is drawn onshore at ground level creating a temperature inversion that further prevents pollutants from dispersing, which can result in photochemical smog. Likewise, Mexico City's MEX Airport is located at over 7,000 feet above mean sea level

(AMSL) in a basin constrained by mountains with intense solar radiation, which causes air quality problems related to both primary and secondary pollutants (Kim, 2015).

Similarly, Lebanon has a special geography, with its narrow coastal plane and two parallel north/south mountains at its eastern part that makes it subject to local winds (sea breeze/land breeze and valley/mountain breeze). These local winds form as a result of thermally driven circulations, caused by uneven heating of the earth's atmosphere in local areas.

Before describing mesoscale winds, it is important to keep in mind that wind, the horizontal movement of air, is a result of the movement of air from higher pressures toward lower pressures (Ahrens, 2009). Consequently, high winds occur as a result of steep pressure gradients, whereas light winds occur as a result of weak pressure gradients.

A sea breeze (Figure 1-7) is a local wind that blows onshore (from sea to land) during daytime. It occurs as a result of the uneven heating of land and water which creates a pressure difference in the air above. During the day, the land heats more rapidly than the adjacent sea water, which leads to intensive heating of the air above it creating a pressure difference. This causes the cooler and denser air over the water to move toward the low-pressure land area. Since the strongest pressure and temperature gradients exist near the land-water boundary, the strongest winds normally occur right near the beach and decrease inland. Also, due to the fact that the greatest temperature gradient between land and sea water normally takes place during the afternoon hours, sea breezes are strongest at this time. The reverse of this phenomenon takes place at night, when the land breeze forms in response to the cooling of the land surface relative to the sea. Consequently, the air above the land becomes cooler than the air over the water, producing a pressure distribution as the one shown in Figure 2-9, with higher surface pressure now over the land. This leads to the formation of land breeze, a breeze that flows from the land toward the water. Normally, land breezes are weaker than sea breezes since temperature contrasts between land and water are much smaller at night (Ahrens, 2009). These phenomena (sea/land breeze) affect air quality. The sea/land breeze can limit vertical mixing since it is a relatively cool layer close to the earth's surface and is therefore a stable layer. Sea breeze can spread polluted air inland from emission sources (e.g. emissions from aircraft and other sources related to Beirut Airport, located adjacent to the sea). In some cases, pollutants dispersed under the effect of sea breeze can return back during the night (land breeze) but with more dangerous chemical products (Simpson, 1994).

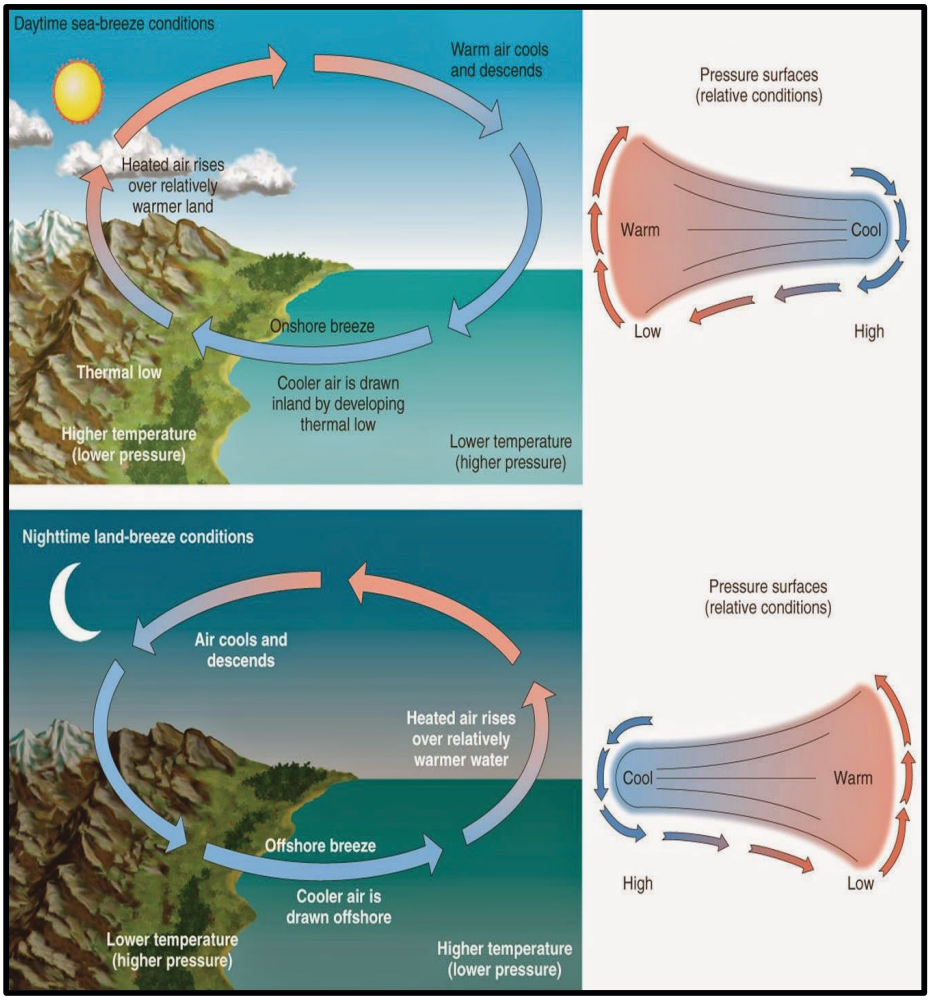

Figure 1-7: Schematic of sea breeze and land breeze, taken from Nullet (2016)

In a similar behaviour to land and sea breezes, mountains and surrounding valleys also have breezes called mountain and valley breezes (Figure 1-8). Mountain and valley breezes constitute a local wind system of a mountain valley that blows downhill (mountain breeze) at night and uphill (valley breeze) during the day (Ahrens and Henson, 2015). During daytime, the sun heats up the valley walls or mountain slopes rapidly, which in turn warms the air in contact with them. Convection causes air it to rise and expand, which creates a small low pressure system on mountain slopes, drawing in air from the valley upslope to the mountains, causing a valley breeze.

At night, this process is reversed. Mountain air cools rapidly at night creating a high pressure system. Thus, wind blows down the mountain, causing a mountain breeze. These breezes occur mostly during calm and clear weather (Ahrens, 2009). It is important to note that the vertical ascent of both breezes is limited by the presence of a temperature inversion that forces the air to begin moving horizontally, thus completing the circulation system cycle. Similar to the previously described sea/land breezes, these breezes also

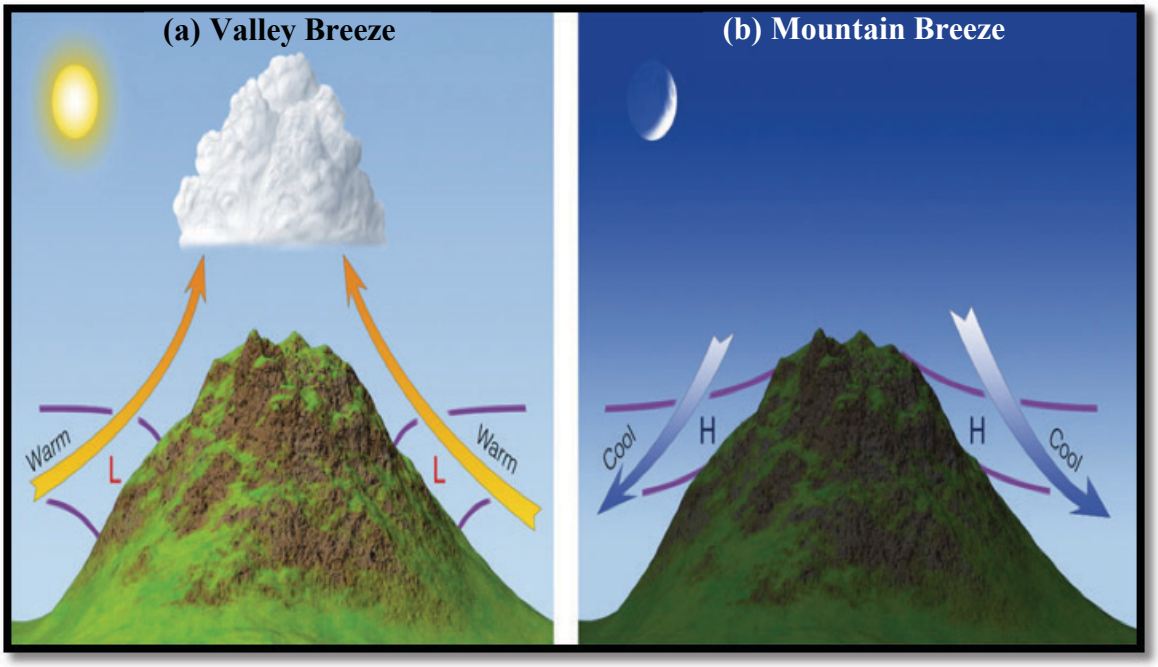

Figure 1-8: Schematic of (a) Valley breeze blowing uphill during daytime and (b) Mountain breeze blowing downhill at night, taken from Ahrens (2009). (The L's and H's represent pressure, whereas the purple lines represent surfaces of constant pressure.)

affect air quality. Air pollution is carried out to the mountains during the day thus polluting the mountainous areas, while a mountain breeze causes pollution to return to the valley at night causing elevated levels of pollution, as seen in a previous study conducted in the Kathmandu Valley-Nepal (Hildebrandt *et al.*, 2002).

1.4 Geographical and Vertical Distributions of Emissions

A series of studies were conducted to assess the geographical and vertical distributions of fuel consumption based on the main air traffic routes, in order to understand the relative aviation emissions (Kim *et al.*, 2007; Olsen *et al.*, 2013; Simone *et al.*, 2013; Wilkerson *et al.*, 2010). According to Kim *et al.* (2007), fuel consumed by international flights were dominated by Asia, North America and the Caribbean, Western Europe and the Middle East region in the 2000s, affected by the distribution of civil aviation (Figure 1-9 (a)). In fact, 92% of fuel burn took place in the northern hemisphere, with 67% of global fuel burn taking place in the northern mid-latitudes between 30°N and 60°N. Only 0.06% of fuel burn occurred lower than 45°S resulting in negligible emissions. The largest peak occurs between 40 and 41°N due to the presence of three of the US's busiest airports (John F. Kennedy, Newark, and LaGuardia) in this latitude range (Simone *et al.*, 2013). The geographical distribution of NO_x aircraft emissions at the perturbation level 11.4 km

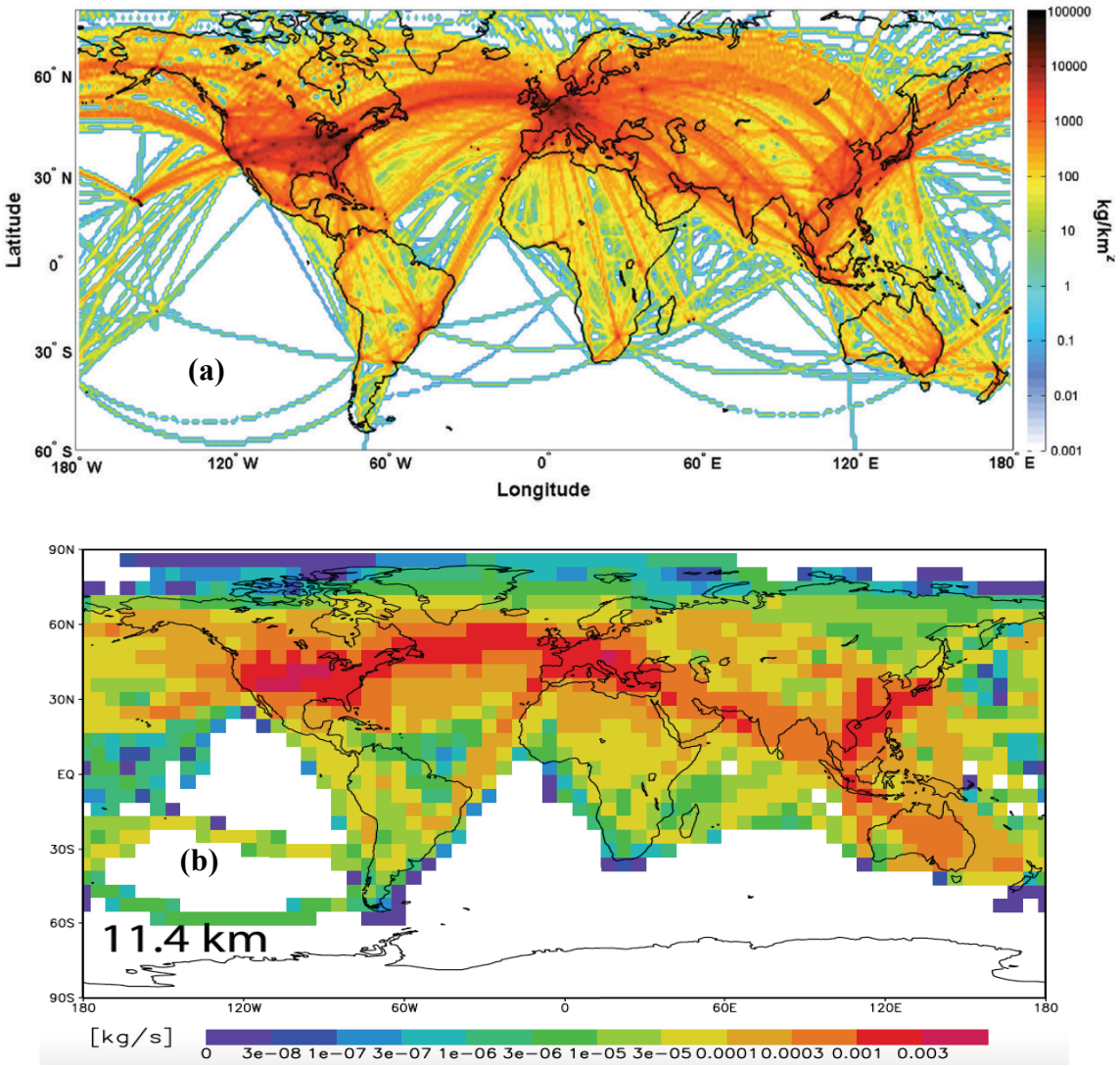

Figure 1-9: (a) Global fuel burn from scheduled civil aviation in 2005, taken from Simone *et al.* (2013) (b) Geographical distribution of NO_x emission perturbations at 11.4 km using the 3D chemistry transport model p-TOMCAT, taken from Köhler *et al.* (2008)

(Figure 1-9 (b)), expressed as a percentage of the global horizontal model domain, shows that NO_x emissions are concentrated at the northern hemisphere similar to the fuel burn (Kohler *et al.,* 2008; Olsen *et al.*, 2013). The CO and HC latitudinal distributions (not shown) exhibit more variability but are still quite similar to the fuel burn (Olsen *et al.*, 2013).

Generally, about 10 percent of aircraft pollutant emissions are emitted close to the surface of the earth (less than 3000 feet above ground level), whereas the remaining 90 percent of aircraft emissions are emitted at altitudes above 3000 feet. The pollutants CO and HCs are exceptions to this rule as they are produced when aircraft engines are operating at their lowest combustion efficiency (while wheels are on the ground), which makes their split

about 30 percent below 3000 feet, and 70 percent above 3000 feet (Masiol *et al.*, 2014). Figure 1-10 shows the distribution of aircraft emissions and fuel burn as a function of altitude, for the year 2000. Kim *et al.* (2007) indicated that the highest fuel burn and aircraft emissions are between 9 and 12 km as a result of the frequent use of these altitudes for the cruise flight segment (using the System for assessing Aviation's Global Emissions (SAGE) model). The relatively high levels of HC and CO in the 0 to 1 km band (i.e., below 3000 ft) are due to the higher emission rates per unit fuel burn for those pollutants at lower aircraft power settings (e.g., during taxiing, idle, and approach conditions). Generally, most studies also reported that about 5-10% of total jet fuel is consumed within 1 km above ground level during airport operations (Masiol *et al.*, 2014). Despite these observations, aircraft operations at ground proximity within airports may further increase fuel consumption (Masiol *et al.*, 2014) as a result of engine emissions during airport congestion (Nikoleris *et al.*, 2011) or the unaccounted use of fuel for APUs (Ratliff and Sequeira, 2009).

Due to this heterogeneity in aircraft emissions, aircraft affect the environment at the local, regional, and global levels as will be discussed in chapter 2.

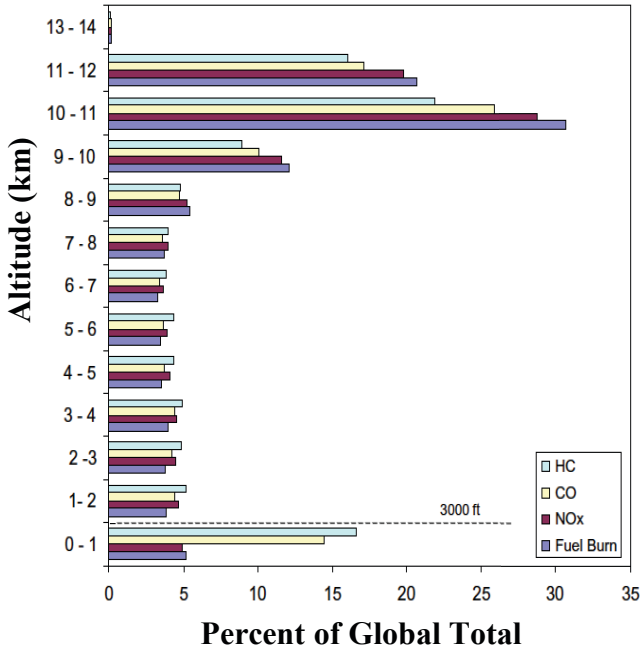

Figure 1-10: Distribution of aircraft emissions and fuel burn as a function of altitude for the year 2000, taken from Kim *et al.* (2007)

Conclusion

This chapter briefly presented all the aviation-related emissions. According to literature, NO_x is the most significant local air quality pollutant with predicted growth rates in 2036 between 2 and 3 times that of 2006. On the other hand, it has also been reported that due to their health hazards, a prioritized list of HAPs (mainly comprised of VOCs) has been classified for assessment. Another important aspect that has been underlined is the effect of geography and topology on the dispersion of air pollutants, which is an important factor to be taken into consideration.

Chapter 2 : Aviation and Local Air Quality

With the increasing growth of aviation and its emissions (NO_x, VOCs, PM, etc.), the environmental impacts of aviation are getting more pronounced. Depending on whether they occur near the ground or at high altitude, these emissions can affect local air quality or the global climate. This chapter provides an overview of the impacts of aviation activities on the environment and the significance of studying these impacts, with special emphasis on local air quality, due to its direct effects on the residents near airports as well as passengers and airport employees (indoor air).

2.1 Environmental Impacts of Aviation

Aircraft emissions produce air contaminants (chapter 1) such as NO_x, VOCs, and fine particulate matter (PM), which in turn can involve broader environmental issues related to ground level ozone (O_3), acid rain, and climate change that present potential risks relating to public health and the environment (Table 2-1). Unlike most transportation modes, aircraft travel great distances at a variety of altitudes, generating emissions that have the potential to impact air quality in the local, regional and global environments (ICAO, 2011) (Figure 2-1).

Table 2-1: Environmental impacts of primary emissions, information taken from FAA (2015); Mahashabde *et al.* (2011); National Research Council (U.S.) (2002)

Emission	Local Effects	Regional Effects	Global Effects (Climate Change)
Oxides of Nitrogen (NO_x): Nitric oxide (NO) and nitrogen dioxide (NO_2) together are referred to as NO_x. Both are produced when air passes through high pressures and temperatures in jet engines, primarily in the combustor. NO_x contribute to ozone and secondary particulate matter formation.	They contribute to the formation of photochemical smog and/or ozone in the lower atmosphere and to ambient particulate matter (PM) formation. They also have adverse health effects. According to US EPA, there is a positive association between short-term exposure to gaseous NO_2 and respiratory morbidity.	NO_x emissions can also produce regional variations in ozone**.** Ozone resulting from aircraft emissions of NO_x is concentrated in the Northern Hemisphere and along major flight routes.	NO_x lead to ozone production (UT/LS) and destruction (stratosphere). In the UT/LS, NO_X emissions from subsonic aircraft have warming effects from ozone production and cooling from the destruction of methane.
VOCs: VOCs are emitted due to incomplete fuel combustion or as a result of vaporization of liquid fuel from spills, venting of fuel tanks, or engine start-up.	Unburned HCs are precursors to photochemical smog and/or ozone. Some of them are toxic and hazardous air pollutants (HAPs).	Unburned HCs are precursors to photochemical smog and/or ozone.	The global effects of HC emissions are similar to those of CO, and their effects are estimated to be negligible.
Particulate Matter (non-volatile) and Aerosols: The most prevalent particulates are carbon particles (soot). The highest level occurs during take-off and climb out, when fuel flows and pressures are at their highest. As the atmosphere cools aircraft exhaust, particulates, water vapour, and other constituents in the exhaust of hydrocarbon-fuelled engines can form liquid aerosols.	Visible smoke emissions contribute to the formation of photochemical smog and may be a health hazard. Some particulates can block some air passages in the lungs. In addition, aerosol droplets contain combustion by-products in a much more concentrated form than the exhaust gases from which they are formed, which may pose a health risk if they are ingested into the lungs.	Particulates and aerosols can contribute to changes in atmospheric visibility and ozone on a regional scale, but this has not been observed as a significant problem with regard to aircraft emissions.	Sulphate aerosols reflect sunlight with a cooling effect; black carbon or soot on the other hand absorbs sunlight and has a warming effect. Both have a residence time lasting from days to weeks. Aerosol emissions from aircraft may also serve as cloud condensation nuclei or alter the microphysical properties of cirrus clouds thereby modifying their radiative impact
Carbon Monoxide (CO): CO is the result of incomplete combustion of carbon in fuel and are produced primarily at taxi and engine idle conditions on the ground.	Early investigations showed low levels of CO near airport terminals, with ground support vehicles being the major contributor. Subsequent improvements in the combustion efficiency of aircraft and ground support vehicles have essentially eliminated CO as a concern.	None	CO results in higher concentrations of ozone and methane and thus acts as an indirect greenhouse gas, but the CO in aircraft emissions is a very small fraction of all anthropogenic CO thus has a negligible impact on tropospheric ozone chemistry.

Table 2-1 (Continued): Environmental impacts of primary emissions, information taken from FAA (2015); Mahashabde *et al.* (2011); National Research Council (U.S.) (2002)

Emission	Local Effects	Regional Effects	Global Effects (Climate Change)
Sulfur Oxides (SO_x): Combustion of sulfur containing fossil fuels leads to the formation of sulfur dioxide (SO_2), sulfur trioxide (SO_3), and gas - phase sulfuric acid (H_2SO_4), which are referred to as sulfur oxides or SO_X. SO_2 is the dominant species and can also be transformed into secondary sulfate particles depending on atmospheric conditions thereby leading to PM formation.	It leads to the formation of particulates and aerosols and increased mortality and morbidity.	It leads to the formation of particulates and aerosols.	Indirect: Formation of Aerosol (+Radiative Forcing)
Carbon dioxide (CO_2): CO_2 is the product of complete combustion of fossil fuels. Carbon in fuel combines with oxygen in the air to produce CO_2.	CO contributes to the formation of ozone, leading to adverse health effects.	None	CO_2 is a greenhouse gas thus has a net warming effect with a positive radiative forcing.
Water vapor (H_2O): H_2O is the other product of complete combustion formed when hydrogen in the fuel combines with oxygen in the air to produce H_2O. This is the source of water in condensation trails (contrails).	None	Even if the effects of contrails and aviation-induced cirrus clouds are small when averaged globally, they may have significant climatological effects in some regions.	H_2O is a greenhouse gas. The emission of water vapor from aircraft in the troposphere is not significant except in the UT/LS, where it can lead to the formation of contrails and cirrus clouds. For supersonic aircraft, which fly in the stratosphere, H_2O can be a significant greenhouse gas.

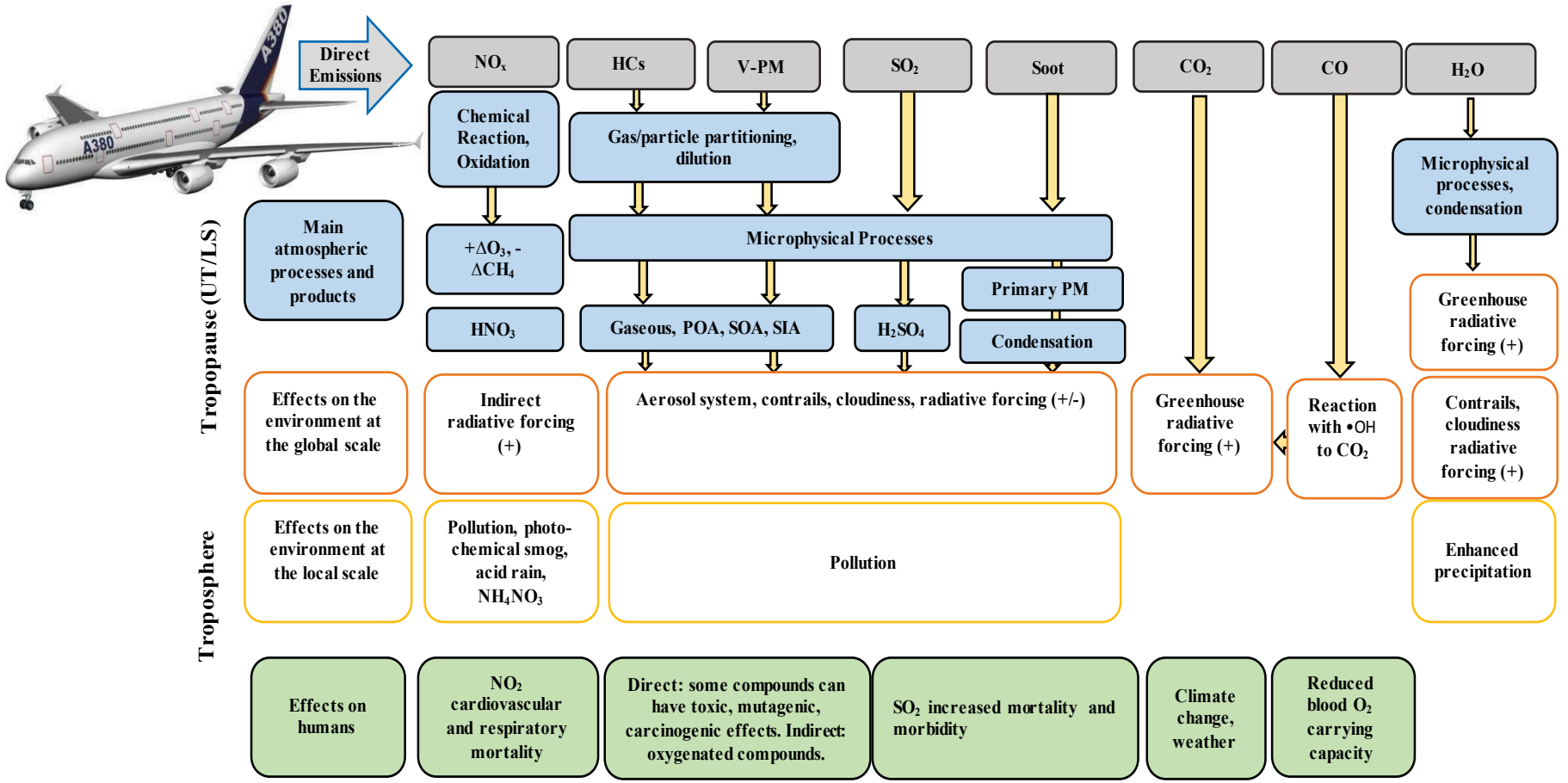

Figure 2-1: Environmental and health impacts of aviation emissions, adapted from Lee *et al.* (2009); Masiol *et al.* (2014)

2.1.1 GLOBAL SCALE – CLIMATE IMPACTS

Aircraft emit gases and particles at cruise altitudes, mainly the upper troposphere and lower stratosphere (UT/LS), altering the atmospheric composition (gases and aerosols), hence affecting the radiative forcing and climate. The Intergovernmental Panel on Climate Change (IPCC) has published a comprehensive report on the climate impacts of aviation identifying the main pathways through which aviation perturbs the planetary radiative balance (Penner, 1999). According to the report, atmospheric changes from aircraft are due to 3 different processes: (i) direct emission of radiatively active substances (e.g. CO_2 or water vapor); (ii) emission of chemical species that alter the concentration of radiatively active substances (e.g. NO_x, which modifies O_3 concentration); and (iii) emission of substances that cause the generation of aerosol particles or lead to changes in natural clouds (e.g. contrails).

Studies reported that NO_x is the most important emission with respect to ozone production (UT/LS) and destruction (stratosphere) processes. In the UT/LS, NO_x emissions from subsonic aircraft lead to the increase in ozone levels, estimated to range between 5.5 and 16.4 Tg-O_3/Tg-N (Lee *et al.*, 2010), with the largest impact occurring in the main flight corridors in the Northern Hemisphere at cruise altitude (Köhler *et al.*, 2013; Myhre *et al.*, 2011). On the other hand, NO_x emissions of supersonic aircraft at the higher altitudes (18 km or above) tend to deplete ozone (Penner, 1999) although the decrease in concentration of this species remains low, about 5 ppb/ year (Köhler *et al.*, 2008). In the UT/LS, NO_x emissions result in a radiative forcing (RF); NO_x has two indirect effects—warming (positive radiative forcing) from ozone production and cooling (negative radiative forcing) from the destruction of methane. The destruction of methane, due to the increased oxidizing capacity of the troposphere, does not offset the O_3 forming effect of NO_x emissions (Lee *et al.*, 2010; Myhre *et al.*, 2011). According to Lee *et al.* (2010), the net RF from aircraft NO_x emissions for the year 2005 is the second largest (13.8 mW m^{-2}) after that from CO_2 (28 mW m^{-2}). Further impacts from NO_x emissions are the formation of nitrate particles (Kärcher, 1996) and indirectly a more effective conversion of SO_2 to sulphuric acid due to an increase in OH and the subsequent formation of sulphate aerosol (Pitari *et al.*, 2002).

Aviation CO_2 emissions have the same climate change impacts as CO_2 emissions from any other sources given that CO_2 is a long-lived, well-mixed greenhouse gas with a net

warming effect i.e. a positive radiative forcing. H_2O is a greenhouse gas (positive radiative forcing); however, its emissions in the troposphere is not significant except in the UT/LS, where it can lead to the formation of contrails and cirrus clouds. For supersonic aircraft, which fly in the stratosphere, H_2O can be a significant green house gas.

Similar to the global effects of CO, the global effects of HC emissions are estimated to be negligible. Sulfate aerosols from aircraft reflect sunlight with a cooling effect; on the other hand, PM (black carbon or soot) absorbs sunlight and has a warming effect. Both have a residence time lasting from days to weeks (Mahashabde *et al.*, 2011). The soot particles at cruise altitudes interact with other chemicals (sulfuric acid and nitric acid) to form small particles that act as nucleating sites for condensation of water vapor present in the upper atmosphere under certain conditions to produce larger particles leading to the formation of condensation trails or contrails, for short. These contrails are visible along flight tracks with a short lifetime around a few hours. At times, under the right meteorological conditions, these contrails expand perpendicular to the flight tracks to form contrail-induced cirrus clouds that also interact with shortwave and long wave radiation, thus affecting the climate. Atmospheric and climate system interactions (e.g. chemical, microphysical, dynamical and radiative) of aircraft emissions remain poorly understood and require more research (FAA, 2015).

The more recent IPCC Fourth Assessment Report (Solomon *et al.*, 2007) defines radiative forcing (RF) as a "measure of the influence that a factor has in altering the balance of incoming and outgoing energy in the Earth–atmosphere system". A positive RF implies a warming effect, while a negative RF indicates a cooling effect. Aviation emissions impact radiative forcing in positive (warming) and negative (cooling) ways with a total aviation radiative forcing of 47.8 mW/m^2 for 2000, excluding cirrus cloud enhancement. **However, it was estimated that subsonic aviation in 2005 was responsible for only 3% of total radiative forcing generated by human activities** (Solomon et al., 2007).

2.1.2 REGIONAL IMPACTS

A Eulerian model (CHIMERA) was used to study the impact of emissions from airliners on photochemical air pollution in the region Ile de France (Pison and Menut, 2004). The results of this work indicated that aviation contributes to increased

concentrations of NO_x and VOCs in the field of study (Ile-de-France), respectively 15.3% and 2.1%. This work however showed a decrease in ozone concentration in the vicinity of the airport due to its consumption by NO emitted by aircraft. Moussiopoulos *et al.* (1997) evaluated the influence of aircraft operations on the air quality of the city of Athens with a Eulerian model (EUMAC Zooming Model, EZM). This work showed an increase in the concentration of NO_x in the vicinity of the airport. **However, the impact of airport emissions on air quality at the regional level has proven to be limited.**

2.1.3 LOCAL IMPACTS

The local impacts of aviation are mainly associated with noise nuisance and gaseous emissions of NO_x, VOCs, smoke, CO, and SO_x in the vicinity of airports. Aviation noise is the most readily perceived environmental impact of aviation activity, and has historically been one of the most significant sources for community complaints about airports, leading to vigorous objections to most airport expansion projects (Mahashabde *et al.*, 2011). It was the first area to be regulated in the 1960s by the International Civil Aviation Organization (ICAO). ICAO published Annex 16: Environmental Protection, Volume I—International Noise Standards in 1971 with subsequent increases in stringency since that time (ICAO, 2005). **However, with the increasing amount of residential development around airports, greater concern has been given to emissions and air quality.**

Local impacts include the formation of photochemical smog and/or ozone (VOCs and NO_x) in the lower atmosphere and ambient particulate matter (PM), which have adverse health effects. Also, according to US EPA, there is a positive association between short-term exposure to gaseous NO_2 and respiratory morbidity. Moreover, VOCs have hazardous health impacts, especially those classified as HAPs that can lead to cancer and death. Visible smoke emissions contribute to the formation of photochemical smog and may be a health hazard, while some particulates can block some air passages in the lungs. In addition, aerosol droplets contain combustion by-products in a much more concentrated form than the exhaust gases from which they are formed, which may pose a health risk if they are ingested into the lungs. As for SO_x, it can lead to the formation of particulates and aerosols causing increased

mortality and morbidity. CO leads to the formation of ozone which has adverse health impacts.

2.2 Significance of Studying the Impacts of Airports on LAQ

Airport-related sources of emissions have the ability to emit pollutants that can contribute to the degradation of air quality of their nearby communities and consequently affect human health and the environment. The steady growth of commercial air travel and the increased public awareness of health impacts, along with the increasing amount of residential development surrounding airports, have made local air quality a significant concern for local/regional governments (ICAO, 2016) and urged the need for airport operators to more fully assess the potential for health impacts and acquire better information and methods to share with the public. To support airport operators, studies were done to assess airport air quality and public health to help better understand and respond to concerns over airport-related air quality and health concerns. Local air quality concerns concentrate on effects created during the landing and take-off (LTO) cycle (emissions are released below 3,000 feet (915 m)) and releases from airport sources (such as airport traffic, ground service equipment, and de-icing).

2.2.1 HEALTH IMPACTS

While aircraft operations at cruise altitudes affect the global climate, LTO operations lead to the degradation of local air quality which constitutes a real public health hazard and contribute to premature mortality (Barrett *et al.*, 2013; Levy *et al.*, 2012; Ratliff and Sequeira, 2009; Yim *et al.*, 2013). Jet kerosene-based fuels have the potential to cause acute or persistent neurotoxic effects (Ritchie *et al.*, 2001).

The exposure groups that are usually affected by jet fuel vapor and its combustion products are the workers and operators inside the airport (Cavallo *et al.*, 2006; Tunnicliffe *et al.*, 1999), aircraft crew (Schindler *et al.*, 2013), passengers in transit (Liyasova *et al.*, 2011), and the nearby residents in the vicinity of the airports (Jung *et al.*, 2011).

Several studies have been conducted to assess the health impact of aviation-related emissions. In the U.S., it was estimated that aviation LTO emissions caused about 190 early deaths and was predicted to increase up to around 350 deaths in 2018 (Ashok *et*

al., 2013). On the other hand, residents living within five miles of Rochester and La Guardia airports are more at risk of hospital admission, respectively by factors of 1.47 and 1.38 compared to residents living farther away (Lin *et al.*, 2008). Also, it was shown that concentrations of BTEX (cancerous VOCs) in the vicinity of Teterboro airport (Jung *et al.,* 2011) were close to those measured at the airport runways and higher than background locations.

2.2.2 AMBIENT AIR QUALITY STANDARDS AND REGULATIONS

ICAO has been working on initiatives to improve local air quality, as well as on proposing mitigation measures. This is manifested in the implementation of ICAO's Standards and Recommended Practices (SARPs) for aircraft emissions in the 1980s to improve air quality in the vicinity of airports. Moreover, ICAO has set emission standards that are summarized in Annex 16: Environmental Protection, Volume II-Aircraft Engine Emissions for nitrogen oxides (NO_x), hydrocarbons (HC), carbon monoxide (CO), and smoke (ICAO, 2008).

In the United States, the National Environmental Policy Act (NEPA) was authorized to serve as a national policy on protecting the environment—demanding environmental evaluations for federal actions with significant impacts on the environment. In compliance with this, the FAA is required to provide an estimation of emissions projected to occur from aircraft and other airport-related emission sources when seeking to expand or improve operations. As part of the NEPA process, FAA is required to assess all potential environmental impacts caused by an action at an airport by comparing build and alternative cases with those of the corresponding no-build (baseline) case (Kim *et al.*, 2015). Moreover, under the Clean Air Act (CAA), ambient air concentration limits of six criteria pollutants having adverse human health and environmental effects were established by the EPA as the National Ambient Air Quality Standards (NAAQS).

In Europe, the pressure of increasing aviation emissions translates into additional constraints on airport capacity with mandatory air quality limits such as EU Directive 1999/30/EC which came into force in 2010 (Eurocontrol, 2005).

In compliance with all these regulations, a first step to limit or reduce the impact of airport emissions is by evaluating airport emissions through either ambient air

monitoring or computer modelling (or a combination of both for increased accuracy). (Note that ICAO's Airport Air Quality Guidance Manual (ICAO, 2011) contains advice for the assessment of airport-related air quality).

2.3 Assessment of Airport-Related Air Quality (Previous Studies)

Aviation emissions at airports initiated interest many years ago (Daley, 1978), but only recently was there an increasing awareness of the effects of aircraft emissions at ground level, or at least within the planetary boundary layer (Masiol *et al.*, 2014). Airport emissions were assessed either *via* understanding the contribution of airport activities to the degradation of LAQ or via measuring the exhaust emissions (e.g. VOC speciation) as described in the subsections below.

2.3.1 AIRPORT CONTRIBUTIONS TO LOCAL AIR QUALITY

Many reports were published to help better understand the impact of airports on LAQ (ICAO, 2011; Kim *et al.*, 2015, 2012). Since all airports are different, it is difficult to make general statements about airport contributions to air quality as they depend on many different factors including airport source characteristics (e.g., pollutant emission rates), source types (e.g. aircraft fleet mixes), source operations, airport layout and location, surrounding geography, and meteorology. For example, one airport which produces more NO_x than another might seem to contribute less to ozone formation, if its corresponding weather conditions and geography are less favourable to ozone formation (Kim *et al.*, 2015).

Despite this complexity, the majority of the evidence appears to indicate the concentrations of pollutants (depending on the pollutant) are generally elevated in the vicinity of airports, and that aircraft contributions are significant up to 1 km and relatively smaller 2-3 km away (ICAO, 2006; Wood, 2008; RIDEM 2008; Zhu *et al.* 2011; Kim 2015) despite the fact that some studies have indicated that pollutant concentration levels near an airport are similar to urban levels (KM Chng, 1999; McGulley, Frick and Gilman, 1995; Tesseraux, 2004). Table 2-2 presents the main results and characteristics of the studies done on the vicinity airports.

The impact of airport activity on VOC concentrations was evaluated at Chicago O'Hare International airport upon undertaking fingerprinting analysis techniques (KM Chng, 1999). Results indicated that soot deposition in communities surrounding O'Hare is more the result of contamination from regional background pollution rather than aircraft fuel or engine exhaust. In another study conducted at O'Hare (City of Park Ridge, 2000), increased levels of 78 VOCs were found downwind at the fence line of O'Hare International Airport and attributed to airport activities; they consequently contribute to the overall air pollution for communities located downwind from the airport. These VOCs included alkanes (C_3-C_5 and C_7-C_{14} straight chain alkanes, etc.), aldehydes (acrolein, butanal, propanal, hexanal, heptanal, octanal, and nonanal), ketones (acetone, 2-butanone, etc.), monoaromatics (benzene, toluene, xylenes, 1,2,4-trimethyl benzene), etc.

Dispersion models were used to evaluate the local impact of airport activity. A study on Manchester Airport with ADMS (Atmospheric Dispersion Modelling System)-Urban (Peace *et al.*, 2006) showed that NO_x are emitted mainly by traffic associated with airport activity. The model results also showed that beyond 200 m altitude, the contribution of emissions from aircraft is a minority. The model ADMS has also been used to quantify the temporal and spatial contributions of NO_x due to aircraft and road traffic around Heathrow airport (Farias *et al.*, 2006). Results showed also that NO_x emissions related to road traffic around the airport are in majority with respect to those of air traffic, although a relevant percentage of local traffic is caused by the airport operations.

Using measured data near London-Heathrow, Carslaw *et al.* (2006) found that although the airport is an important source of NO_x emissions, concentrations observed near the airport are mainly attributed to road traffic. At the airport boundary, the airport contribution to the annual mean NO_2 concentrations was estimated to be 27%. Up to 1 to 1.5 km distance, the contribution of airport activity to NO_x is from 12 to 14%. NO_x emissions related to air traffic can be detected at least till 2.6 km from the airport. At background locations 2–3 km downwind of the airport, the upper limit of the airport contribution was estimated to be less than 15% (10 $\mu g\ m^{-3}$). This study considered that due to the proximity of other sources such as road traffic, the estimations made in the airport vicinity, are probably overestimated.

Based on data collected at the LAX blast fence (downwind sites up to 600 m from a runway and upwind of a major runway), Zhu *et al.* (2011) found that concentrations of $PM_{2.5}$ and two carbonyl compounds (formaldehyde and acrolein) were elevated compared to background levels.

The study conducted by Yu *et al.* (2004) examined hourly concentrations of CO, NO_x, SO_2, and respirable suspended particles (RSP) taken in the vicinity of Hong Kong International Airport (HKIA) and Los Angeles International Airport (LAX). The signature of emissions from aircraft was also highlighted by interpretation of the observed concentrations of SO_2 according to the direction and speed of wind. At LAX, CO and NO_x were dominated by emissions from ground vehicles going in and out of the airport. However, near HKIA, aircraft were an important contributor to CO and RSP (Yu *et al.*, 2004).

Westerdahl *et al.*, studying the effect of emissions of Los Angeles International Airport, has shown that the airport and ground activities, where landing and take-off of aircraft take place, influence concentration levels observed near the airport (Westerdahl *et al.*, 2008).

Measurements were performed around the airports: Paris-CDG, Paris-Orly, and Paris-Le Bourget (AIRPARIF, 2003, 2004). Measurements made near Paris-CDG indicated an increase of hourly NO_2 concentration of up to 60% in the immediate vicinity of the platform (within 300 m distance). This impact of airport NO_2 did not exceed 4 km beyond the platform. Moreover, concentrations of benzene (the only hydrocarbon measured) were not found to be associated with airport activity. Studies in Paris Orly have estimated that the average contribution of all airport activities to NO_2 levels was 6% during the measurement period (Table 2-2) (AIRPARIF, 2003).

The studies presented above have demonstrated an impact of airport activities on air quality within and around the airport. The results are quite contrasting and seem to depend on each airport's own characteristics (size, location and distance of the closest town) as well as geographic and climatic aspects (Lelievre, 2009). For example when the airport is located in a remote area with low population density and moderate industrial development, airport sources contribute to a larger extent to the total emissions (Longhurst *et al.*, 1996). It is important to note that exposure (and therefore human health risk) depends on several factors such as meteorology and the relative

location of emission sources and exposure groups. Such studies will help airport operators to minimize the health risk presented by the various emission sources present at an airport.

Table 2-2: Previous studies assessing the impacts of airports on air quality

Airport (Reference)	Sampling Period	Compounds Measured	Sampling Techniques and sites	Model Used	Objective
Paris-CDG (AIRPARIF 2003)	Winter and Spring-summer 2002 (2 months)	NO_x, SO_2, CO, benzene, PM_{10}	Continuous analysers, passive samplers	None	To quantify the influence of airport emissions.
Paris Orly (AIRPARIF 2004)	Winter-spring 2003 (2 months)	NO_x, CO, SO_2, benzene, PM10	Continuous analysers, passive samplers	None	To assess the impact related to takeoff
Los Angeles Airport (Yu et al., 2004)	2000-2001 (24 months)	CO, NO_x, SO_2 (used as tracer)	Continuous analysers: a site near Los Angeles Int'l Airport (LAX) and a monitoring station	Nonparametric regression	To assess the contribution of different airport operations
T.F. Green Airport in Warwick, Rhode Island (Adamkiewicz *et al.*, 2010)	4 days in October 2007, 7 days in both March 2008 and June 2008	NO_2	Palmes diffusion tube samplers	Regression modelling	To understand the relative contributions of local traffic and airport activities
Los Angeles airport (Westerdahl al. 2008)	Afternoon 19, 21, 23, 24 Apr 2003 Particle counts on Aug 5 2004	Ultrafine particles, Black carbon, NOx, polycyclic aromatic hydrocarbons	NO_x chemiluminiscence analysers; Various sites in and around the airport.	None	To analyse the spatial extent of Los Angeles International Airport emissions on downwind ambient air in a mixed use neighbourhood that includes residences.
Chicago O'Hare International Airport (KM Chng, 1999)	C_{10}-C_{40} saturated HCs, PAHs	Polycyclic aromatic hydrocarbons (PAHs) in soot samples	Soot samplers, Advanced Chemical Fingerprinting (ACF) GC/FID and GC/MS	None	To analyse the major sources of deposited soot near the vicinity of O'Hare Airport.
Airport of Chicago O'Hare (City of Park Ridge, 2000)	Summer-winter 2000	Benzene, toluene, and a large number of VOCs	Canisters, active tubes:	Atmospheric Dispersion Modelling *via* the USEPA Industrial Source Complex (ISCST3) model	To assess the impact of hydrocarbons emitted by airport activity
Airport of Athens (Moussiopoulos *et al.*, 1997)	-	NO_x (NO and NO_2), Ozone	None	Eulerian model (EUMAC Zooming Model, EZM)	To evaluate the influence of air operations on air quality of Athens (see breeze effect)

Table 2-2 (Continued): Previous studies assessing the impacts of airports on air quality

Airport (Reference)	Sampling Period	Compounds Measured	Sampling Techniques and sites	Model Used	Objective
Manchester Airport (Peace *et al*., 2006)	Year 1999	NO_2, NO_x	Continuous analyser, chemiluminescence, 1 monitoring station close to airport	ADMS Urban	To assess the impact of a regional airport's sources (traffic and aircraft, and the effect of modelling the above ground aircraft emissions sources.
London Heathrow Airport (Carslaw *et al*., 2006)	Summer 2001-winter 2004 (3.5 yrs.)	NO_x, NO_2	Chemiluminescent techniques, 8 monitoring sites	Graphical technique	To detect and quantify the airport contribution to NO_x. Before building of a third runway.
Heathrow airport (Farias *et al*., 2006)	Year 1998	NO_x	Continuous analyser Monitoring station	ADMS Urban	To quantify the temporal and spatial contribution of NO_x due to aircraft and road traffic around Heathrow airport
Region Ile de France (Pison et Menut, 2004).	-	NO_x, VOC	None	Eulerian model (CHIMERE)	To study the impact of emissions from airliners on photochemical air pollution in the region Ile de France

2.3.2 VOC SPECIATION FROM AIRCRAFT EXHAUST

To have a better conception about the impact of aircraft operations on local air quality in the vicinity of airports, the speciation of a wide range of VOCs within turbine engine exhaust plumes has been the focus of several studies (Table 2-3). Based on these studies, the majority of our target VOCs were selected (chapter 4). Comprehensive organic speciation measurements of aircraft exhaust emissions have resulted in a detailed species profile of these emissions, especially at low-power engine operation (EPA, 2009a, 2009b; Lieuwen *et al.*, 2013). Previous studies were conducted either during engine tests where one or few engines where studied (Anderson *et al.*, 2006; Beyersdorf *et al.*, 2012; Spicer, 1984; Knighton *et al.*, 2007; Slemr *et al.*, 2001, 1998, Spicer *et al.*, 1994, 1992; Yelvington *et al.*, 2007) or during real aircraft operations (Herndon *et al.*, 2006; Schürmann *et al.*, 2007; Lelievre, 2009; Zhu *et al.*, 2011). Despite these studies, no compound was found that could serve as a tracer for engine exhaust (Tesseraux, 2004).

- Engine Tests

Several studies have determined NMHC (nonmethane hydrocarbon) speciation within turbine engine exhaust plumes during engine tests. Spicer *et al.* investigated the gas-phase emissions of both military (GE F101 and F110) (Spicer *et al.*, 1992) and commercial engines (TF-39 and CFM-56-3) (Spicer *et al.*, 1994). At low engine power (idle power), they found that emissions were dominated by cracking products, unburned fuel, and products of incomplete combustion; with ethene, propene, acetylene, and formaldehyde comprising 30–40% of the total VOC budget. At higher engine powers, relative NMHC emissions dropped by a factor of 20–50, under the effect of combustion, unburned fuel components disappeared, and heavy alkanes dominated. Both Slemr *et al.* (Slemr *et al.*, 2001, 1998) and Spicer *et al.* (1992, 1994) note that NMHC emissions are likely dependent upon engine type, use, and maintenance history as well as fuel composition. A more recent series of measurements have focused on commercial engines. During the EXCAVATE campaign (EXperiment to Characterize Aircraft Volatile Aerosol and Trace-Species Emissions), Anderson *et al.* (2006) measured the speciated organic gas emissions from a Rolls-Royce RB21131 535-E4 engine (another high bypass turbofan engine) for two different fuel sulfur levels. Samples were collected at 10 m behind the engine exit.

Results were consistent with previous observations and indicated that turbine engines emit considerable amounts of light hydrocarbon species at idle (ethene, propene, acetylene, and formaldehyde), but significantly lesser amounts at higher engine powers. Anderson *et al.* (2006) reported that VOCs with a higher number of carbon atoms (nC ≥ 4) dominated (Figure 2-1 (a)) at this regime, upon studying the emissions of a commercial engine (RB211-535-E4). They also reported that the emissions of alkenes and alkynes are favoured at low speed, whereas the emissions of alkanes and aromatics are favoured at high speed (Figure 2-1 (b)). Afterwards, a set of studies initiated by NASA, called Aircraft Particle Emissions Experiment (APEX) (APEX was the collaborative research effort of NASA, EPA, DoD, and the FAA) dedicated engine tests, measurements were made at both the engine exit plane and in the plume at a downstream location (technically 30 m for an intermediate engine size such as a CFM56) using a wide range of analytical techniques. Some of these techniques employed in APEX (1-3) overlap with earlier tests, but with some more advanced techniques (faster response time/higher sensitivity) used during APEX (EPA, 2009a).

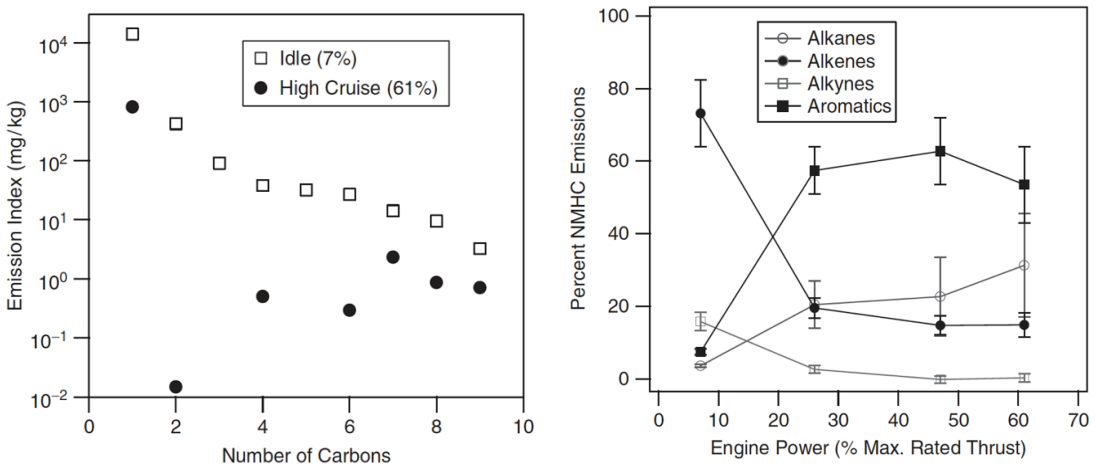

Figure 2-1: (a) VOC emissions at idle and high cruise power (i.e. 7% and 61% of the maximum rate thrust respectively) (b) Averaged hydrocarbon emissions, by family, from the RB211-535E4 engine (Source: Anderson et al., 2006)

Table 2-3: Literature studies assessing EIs from engine tests or during real aircraft operation

Reference	Airframe/Engine	Target Compounds*	Sampling system	Analytical methods	Tested Regimes, (fuel type)
		Engine Tests			
Spicer *et al.*, (1984, 1994)	TF-39 (Military TF of Lockheed C-5) and CFM-56 (TF)	Total HCs, C_2 to C_{17} organics, aldehydes	Sampling rake 0.3-0.6 behind the engine. Experimental: non-dispersive infrared instruments, chemiluminescence, FID, polymeric adsorbent (XAD) and DNPH cartridges	[GC/MS, GC/FID], On-Line Cryogenic Trap/GC, canister [GC/MS], Total HC Analyser	Idle, 30%, 80%; [JP-4; JP-5; JP-8]
Spicer *et al.*, (1992)	2 Engines: F101, used on the B-1B aircraft, and the F110, used on the F-16C and F-16D aircraft.	Total HCs, individual organic species	Samples collected from each engine using a probe positioned just behind the exhaust	-	4 power settings from idle to intermediate power
EXCAVATE: Anderson *et al.* (2006)	NASA Boeing 757; Engine: Rolls Royce RB-211-535E4 (TF)	Gaseous carbon species	10 m behind the engine exit plane.	Canister, GC/MS	4-7%; 26%; 47%; 61%; [JP-5 low and high S]
APEX-3: Knighton *et al.* (2007); Kinsey (2009); Timko *et al.* (2010)	B737-300, ERJ-145, A300, B775, plus Learjet Model 25. Engines: CFM56-3B1, AE3007A1E, plus others	CO_2, HC, $PM_{2.5}$	Sampling: 30 m downstream of the engines Experimental: continuous and time-integrated instruments: IR	PTR-MS	4%, 7%, 15%, 30%, 45%, 65%, 85%, 100%, Jet A
Eichkoff (1998)	CF6-50C2/E2, CFM56-3B1	103 organic compounds	30 m	GC-MS	Average load
		Real Aircraft Operation			
Herndon *et al.* (2006)	Regional jets, B737s, MD88s, and B757s	Formaldehyde, acetaldehyde, benzene, and toluene	Continuous analysis through a sample port located on the front of the truck.	PTR-MS	Idle, taxi, approach (or landing), and take-off
Schürmann *et al.* (2007)	Engines from 3 aircraft	VOCs	50-100 m behind an aircraft, at a height of 1 m	Canister/GC-FID	Taxi, ignition
Zhu *et al.* (2011)	-	VOCs: butadiene, benzene, acrolein, Formaldehyde,	At blast fence (140 m from the take-off)	Canister	Take-off
Lelievre (2009)	B757- 200, B777-200	VOCs	200 m below the flow reactor	Canister, ATD-GC-FID	Taxi

All of the studies indicate that a wide range of combustion-related emissions are present in aircraft exhaust and that 15-20 species represent most (95% or more) of the emissions at idle power on the basis of concentration (EPA, 2009a).These species, in descending order of magnitude, are: ethylene, formaldehyde, acetylene, propene, acetaldehyde, acrolein, 1-butene, glyoxal, 1,3-butadiene, benzene, methyl glyoxal, ethane, butanal, propanal, 1-pentene, 1-hexene, toluene, acetone. A greater number of species are present at a fraction of a percent or smaller of the total concentration.

A number of the identified species can be considered as hazardous air pollutants (HAPs). A prioritized list of gas-phase HAPs emitted by airport emission sources has been constructed based on the product of the compounds' toxicities and emission rates. This list consists of acrolein (propenal), formaldehyde, 1,3-butadiene, naphthalene, benzene, acetaldehyde, ethylbenzene, and propanal (propionaldehyde). Glyoxal, methylglyoxal, and crotonaldehyde (butenal), although not officially hazardous air pollutants, may be comparable in importance to the compounds listed above (Wood, 2008).

It is important to note that no instrument can measure all the VOC species emissions. For example, the fast time response instrument (Proton Transfer Reaction Mass Spectrometer: PTR-MS) used for HC measurements in APEX was not capable of measuring alkanes, acetylene, formaldehyde, and ethylene (Formaldehyde and ethylene were measured separately using IR techniques, e.g. Tunable Infrared Laser Absorption Spectroscopy: (TILDAS)). In the Spicer studies, a wide range of techniques was utilized, but no measurement of methanol was attempted, and none of the trimethylbenzenes nor several of C_9-C_{11} aromatic species were identified with the techniques employed therein. In many of the studies, a Flame Ionization Detector (FID) was used to quantify the total "unburned hydrocarbons" (UHCs), but this gives an imperfect estimation of the total emissions due to the FID's nonuniform response to different carbon-containing compounds. GC-FID (used in ICAO's certification measurements) is a very sensitive method for detecting many types of hydrocarbons species; however, it is neither selective nor universal and its response is diminished for several oxygenated compounds emitted by aircraft (EPA, 2009a).

- Real Aircraft Operations

Limited studies have reported on VOC measurements during real aircraft operation (see Table 2-3). Herndon *et al.* (2006) have conducted measurements on selected speciated organic gas emissions by analysing wind advected plumes at Boston Logan International Airport. In another study, Schürmann *et al.* (2007) have measured 55 VOCs in diluted gas exhaust at aircraft parking lots and exhaust aircraft plumes (3 different engines) at Zurich-Kloten airport, Switzerland. VOCs were measured using canister sampling of diluted exhaust in an operational taxiway area, where they found that nearby fuelling activity considerably altered the profile of hydrocarbons. These real-world measurements have shown higher emissions than the International Council Aviation Organization (ICAO) values for some engines, but slightly lower values for others. Large amounts of ethene and propene were detected. Lelievre *et al.* (2009) have conducted measurements, at 200 m below the flow reactor, on 2 individual aircraft (B757- 200 and one B777-200) during taxi at Paris Charles de Gaulle Airport. Results have shown that the concentrations of alkanes and monoaromatics measured in the plumes were similar, but the difference in hydrocarbon concentrations in the two plumes was due to the unsaturated aliphatic compounds.

2.4 Impact of Airport Activities on Airport Indoor Air

Since most buildings are well ventilated and there are no significant indoor sources, indoor air is normally not the main focus in airports (Kim *et al.*, 2015). However, airport indoor air pollution can impact both airport personnel and the public/passengers (Witten *et al.*, 2011) and should be considered. Indoor sources include combustion sources, smoking, cleaning solutions, building materials, and furniture (e.g., formaldehyde released from pressed-wood products). In addition to these sources, indoor air pollution can intensify if inadequate ventilation exists and insufficient outdoor air is allowed to mix with the indoor air (Kim *et al.*, 2015) or if improper filtration systems are utilized.

Some studies have measured concentration levels inside airport buildings. Measurements of aldehydes in an airport in Strasbourg, France found that the airport hall has a relatively clean environment, with formaldehyde and acetaldehyde levels not exceeding 20 and 10 $\mu g\ m^{-3}$, respectively (Marchand *et al.*, 2006). Measurements of polycyclic aromatic hydrocarbon (PAH) levels inside an Italian airport showed that benzo [b+j+k] fluoranthene

and benzo [a]-pyrene concentrations are of concern (Iavicoli *et al.*, 2006). To assess the relative exposures to JP-8 fuel (military jet fuel) vapor, a study was conducted by Pleil *et al.* (2000). Air samples from indoor Air Force base shops (break rooms, office areas, etc.) were taken using a battery-operated machine to measure the concentrations of nC_6-nC_{12} as well as monoaromatic concentrations, all of which are the main constituents of JP-8 fuel. Indoor air concentrations inside the Air Force base shops were similar to the outdoor levels in Los Angeles (used as an indicator of urban exposure) except for an obvious elevation of the JP-8 fingerprint compounds n-nonane, n-decane, and n-undecane. On the other hand, indoor levels were 5-10 times lower than the corresponding ambient air concentrations. Other measurements conducted inside the Control Tower of Athens International Airport focused on carbon monoxide, formaldehyde, volatile organic compounds and benzene. Results have shown that despite the fact that concentrations never exceeded the established limits for indoor environments, all pollutant concentrations determined were significantly higher than those outdoors (Tsakas and Siskos, 2011). This emphasizes the contributions from indoor sources such as smoking, carpets, furniture and human emanations including breathing and body odor. In fact, smoking activity increased total VOCs (TVOCs) concentrations by 2.5 times compared to concentrations measured during a non-smoking period.

2.5 Airport Emission Sources

Local air quality concerns focus on both emissions during the landing and take-off (LTO) cycle (since these emissions are released below 3,000 feet (average boundary layer height)) and on emissions from other airport activities. A large number of emission sources are found at the airport, with aircraft being the dominant source. These sources (ICAO, 2011), aircraft or ground-based, can be divided into 4 subgroups (Table 2-4):

Aircraft sources:

a) LTO cycle and Auxiliary Power Unit (APU)

Ground-based sources:

b) Aircraft handling emissions,

c) Stationary sources, and

d) Vehicle traffic sources

2.5.1 AIRCRAFT SOURCES (LTO CYCLE AND AUXILIARY POWER UNIT)

- Landing/Take-off (LTO) Cycle

In reference to the International Civil Aviation Organization (ICAO), annex 16 Vol II, it is important to differentiate between landing and take-off (LTO) and non-LTO emissions (Figure 2-2). Non-LTO emissions are emissions starting with 1 km (~3000 ft.) and above having impacts on global climate. LTO emissions (below 3000 ft.) are emissions occurring during the landing and take-off cycle and are associated with local pollutants (ICAO, 2008a).

The International Civil Aviation Organization has defined a specific reference LTO cycle for engine test certifications. The LTO cycle covers operations at the local level and below the mixing height, assumed to be 3000 ft. above ground level (AGL), although the true mixing height varies seasonally and from airport to airport (ICAO, 2011). This cycle is comprised of four modal phases that represent approach, taxi/idle, take-off, and climb (Figure 2-3). Each phase has a duration or time-in-mode and thrust settings as assigned by ICAO (Table 2-5).

In fact, this is a much simplified version of the operational flight cycle (ICAO, 2011). This is because the emissions certification LTO cycle was designed as a reference cycle for the purpose of technology comparison while not capturing the detail and variations that occur in actual operations such as aircraft weight or pilot operating procedures (e.g. noise trajectories or derated thrust). The variability of aircraft operations as a function of aircraft, airport, or airline is not considered in the ICAO reference LTO cycle. An example of its simplification is that the ICAO LTO take-off mode defines 100% rated thrust (maximum thrust available for take-off). However, in real-world conditions most take-offs take place at reduced or derated thrust to reduce engine wear and tear, if the conditions permit (runway length and condition, take-off weight, meteorology, etc.). The reduced/derated take-off is usually determined by the aircraft's actual take-off weight, runway length, and prevailing meteorological factors (ICAO, 2011). Carslaw *et al.* (2008) have reported that aircraft operational factors such as take-off weight and aircraft thrust setting have a measurable and important effect on concentrations of NO_x, where NO_x concentrations can differ by up to 41% for aircraft using the same airframe and engine type. Since the emissions of some pollutants increase with thrust (e.g., NO_x), this could lead to an overestimation of emissions from airports. Other limitations in the use of the standard LTO-cycle includes lower thrust at idle/taxi mode and acceleration and deceleration of the

engines as a result of congestion on taxiways, and use of reverse thrust during landing (Nikoleris *et al.*, 2011). Times-in-mode also differ depending on the characteristics of the airport, but it is possible to determine more detailed times-in-mode to allow for more precise results (Unique, 2004).

In addition to the LTO cycle, aircraft emission sources include Auxiliary Power Unit (APU), which is a small engine installed in the rear of the aircraft providing electrical/pneumatic power when the aircraft is taxiing or parked at the gate and no alternative is available (ICAO, 2011). APU requires jet fuel to operate.

Conventionally, air quality impact analysis for aviation has been focused on LTO cycle. The ICAO-CAEP (Council for Aviation Environmental Protection) emissions certification standards are for LTO emissions owing to air quality concerns around airports. This cycle will be the main focus of our study because it dominates impacts on local air quality and consequently involves hazards to the health of population and nearby inhabitants and leads to visibility impairment. The other emissions sources assessed in this thesis are presented in the following subsection.

Table 2-4: Airport-related emission sources. Information taken from ICAO (2011)

	EMISSION SOURCES
AIRCRAFT	Aircraft main engines: LTO cycle
	Aircraft Auxiliary Power Unit (APU)
AIRCRAFT HANDLING	Aircraft Ground Support Equipment (GSE): Ground power units, air climate units, aircraft tugs (tow bar), conveyer belts (baggage handling belt), passenger stairs, forklifts, tractors, cargo loaders, etc.
	Route traffic in the airport (airside traffic): Service vehicle and machinery traffic (sweepers, trucks (catering, fuel, sewage) cars, vans, buses, etc.) within the airport perimeter fence (usually restricted area) that circulate on service roads.
	Aircraft refuelling: Fuel tanks (vents), fuel trucks or pipeline systems during refuelling.
	Aircraft de-icing
STATIONARY SOURCES	Airport Parking
	Power/heat generating plant and facilities that produce energy for the airport's infrastructure: boiler house, heating/cooling plants, co-generators
	Airport fuel farm (evaporation) and vehicle fuel stations.
	Airport maintenance: All activities for the maintenance of airport facilities (cleaning agents, building maintenance, repairs, greenland maintenance) and machinery (vehicle maintenance, paint shop).
	Aircraft maintenance: All activities and facilities for the maintenance of aircraft, i.e. washing, cleaning, paint shop, engine test beds.
	Fire training activities
	Construction activities: All construction activities associated with airport operation and development.
	Emergency power generator: Diesel generators for emergency operations (e.g. for buildings or for runway lights).
	Surface de-icing. Emissions of de-icing and anti-icing substances applied to aircraft moving areas and service and access roads.
LANDSIDE TRAFFIC	Vehicle traffic (cars, vans, trucks, buses, etc.) and motor coaches associated with the airport as well as parking lots.

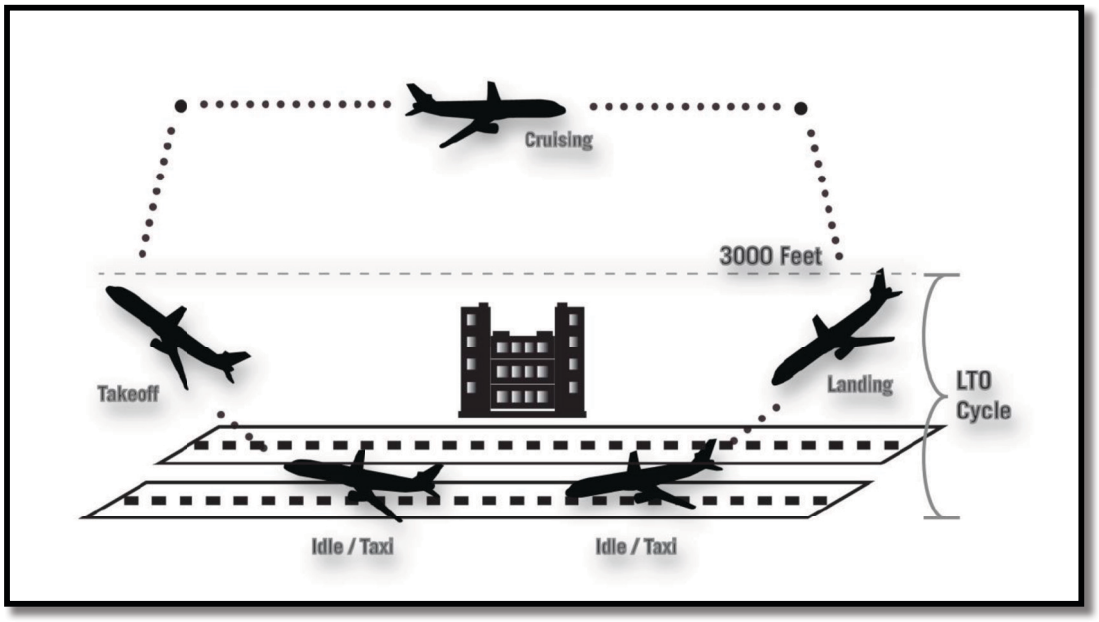

Figure 2-2: Aircraft Operations: Standard ICAO LTO cycle and non-LTO cycle, taken from Norton (2014).

Table 2-5: Reference emissions LTO cycle

Operating phase	Time-in-mode (min)	Thrust setting (% of rated thrust)
Approach	4.0	30
Taxi and Ground idle	26.0 (7.0 for taxi-in and 19.0 for taxi-out)	7
Take-off	0.7	100
Climb-out	2.3	85

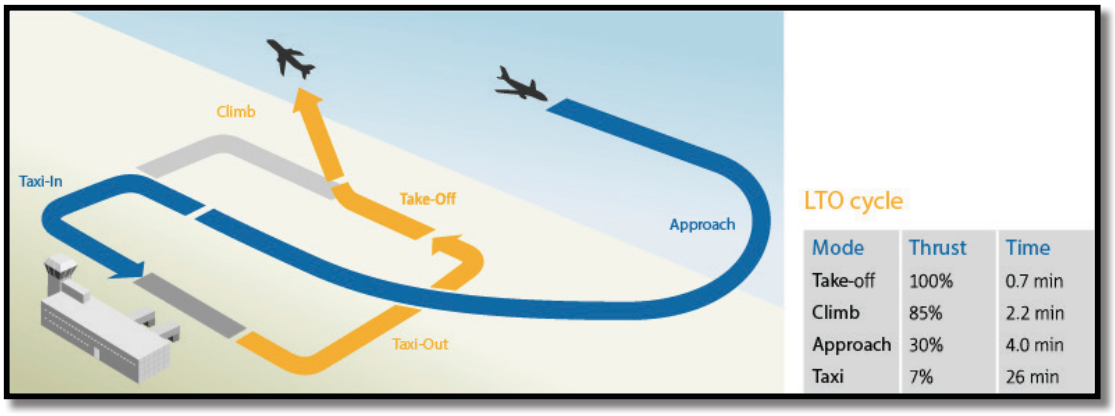

Figure 2-3: Reference ICAO Landing/Take-off Cycle (EASA, 2016)

2.5.2 LAND-BASED EMISSIONS

Aircraft handling emissions include emissions from Ground Support Equipment (GSE) necessary to serve the aircraft between flights. They also include emissions from airside traffic, which are vehicles that circulate within the airport fence; aircraft refueling emissions that result from fuel evaporation through aircraft fuel tanks (vents); and from fuel trucks or pipeline systems during refuelling. In some airports, the application of de-icing and anti-icing substances to aircraft during winter operations leads to increased emissions (ICAO, 2011).

Stationary- or infrastructure-related source categories of emissions are comprised of emissions from power/heat generating plants, emergency power generators, boilers, airport parking, fuel storage in fuel farms and vehicle fuel stations, fire training, etc. (ICAO, 2011).

Landside traffic emission sources consist of vehicle traffic (motor bikes, cars, vans, trucks, buses) associated with the airport on access roads and parking lots.

2.5.3 SOURCE EMISSIONS CONTRIBUTIONS

All of these main subgroups emit VOCs, NO_x, CO, SO_x, and PM but with different source contributions. Figure 2-4 summarizes the emissions of NO_x, VOCs, and CO by the major sources at Paris-Charles-De-Gaulle (CDG) airport in 2006. The aircraft are the

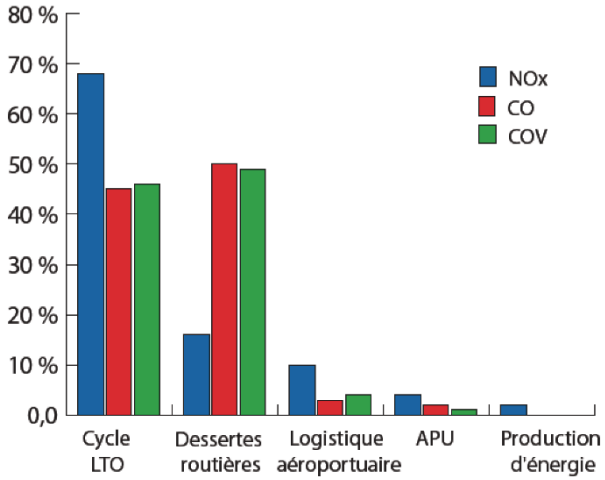

Figure 2-4: Source apportionment for airport emission sources at Paris-CDG, taken from AIRFRANCE in Lelievre (2009)

major sources of NO_x constituting 68% of the airport emissions at Paris–CDG. Road traffic accounts for 28%. However, VOC and CO emissions from road traffic are comparable to those from airplanes. Emissions from APU and energy production are minority (Lelievre, 2009).

A report done by the Transportation Research Board - Washington (Kim *et al.*, 2015) states that the major source contributors at airports are mobile sources (aircraft and vehicles). For NO_x, the major source contributors are aircraft operations. For VOCs, the 2 major contributors are aircraft and road traffic on the airport landside and on the airport road network.

It is important to note that emissions from these sources exhibit variations that are diurnal (e.g. more flights occur during the day than the night), weekly (business flights are more common on week days), and seasonal (e.g. charter flights are busier at holidays).

Conclusion

This chapter provided an overview of the significance of assessing the local impacts of airport activities, as imposed by government authorities, in order to assess and mitigate impacts on human health and the environments. Although the majority of evidence indicated that concentrations of pollutants are generally elevated in the vicinity of airports and that aircraft contribution are significant up to 1 km and relatively smaller 2-3 km away; however, these studies were contradictory and showed that the impact of the airport on LAQ is affected by the airport's own characteristics (geography, location, meteorology). On the other hand, indoor air studies were limited especially in airports, based on the assumption that proper filtration and ventilations are present. However, indoor air should be assessed to understand the impact on airport employees and passengers. These conclusions opened the door for the subject of my dissertation, to be presented in chapter 3.

Chapter 3 : Presentation of the Study

As mentioned in chapter 1, civil aviation has recorded consistent annual rate increases between 5 and 9%, and is expected to grow at an average annual growth rate of 5% over the forecast period 2010-2013 (CAEP 9, 2013; Penner, 1999). This increase in air traffic, and eventually airport-related traffic, was accompanied with increased emissions and the consequent degradation of local air quality, as evidenced by several previous studies (Carslaw *et al.*, 2006; City of Park Ridge, 2000; Peace *et al.*, 2006; Westerdahl *et al.*, 2008). Similarly, in **Lebanon**, **Beirut-RHIA** (Beirut-Rafic Hariri International Airport) experienced an average yearly increase in air traffic of 5% for the years 2013-2015 with an average number of aircraft movements equals to 65500 flights[1] (32742 arrivals and 32758 departure flights) per year. This air traffic has carried an average of 6.7 million passengers[3]/year (2013-2015) with an average yearly increase of 7.5% (Figure 3-1). Similar to the previous studies (chapter 1), this increase is expected to be accompanied with an increase in aircraft and airport-related emissions contributing to the degradation of local air quality near Beirut-RHIA. However, this contribution is expected to be **intensified** due to the airport's **layout** and **location**, **meteorology**, and the special **geography** and **topography** surrounding Beirut Airport, as will be discussed in the following paragraphs.

3.1 Study Area: Beirut-RHIA

The airport of study is Beirut Rafic Hariri International Airport, the only operational commercial airport in Lebanon. It is a midsize commercial and military airport located at 33.82N 035.49E, in the Khaldeh suburb about 8 km south of the capital's (Beirut) city center (Figure 3-2). The airport is surrounded to the west by the Mediterranean Sea making it affected by a Mediterranean climate with hot, dry and humid summers, and mild, rainy winters. To the east of the airport, the urbanized Aley district is located at only 160 m away from the main departure runway (runway 21). Most of the cities and villages of Aley district are located on the slopes of Mount Lebanon which is a mountain range sloping up to 2500 m. Excluding its western side, Beirut Airport is embedded in a very urbanized

[1] www.beirutairport.gov.lb

area, as shown in Figure 3-3 (urban areas and informal settlements). Also, its eastern side is in close proximity to an industrial zone (see Figure 3-3).

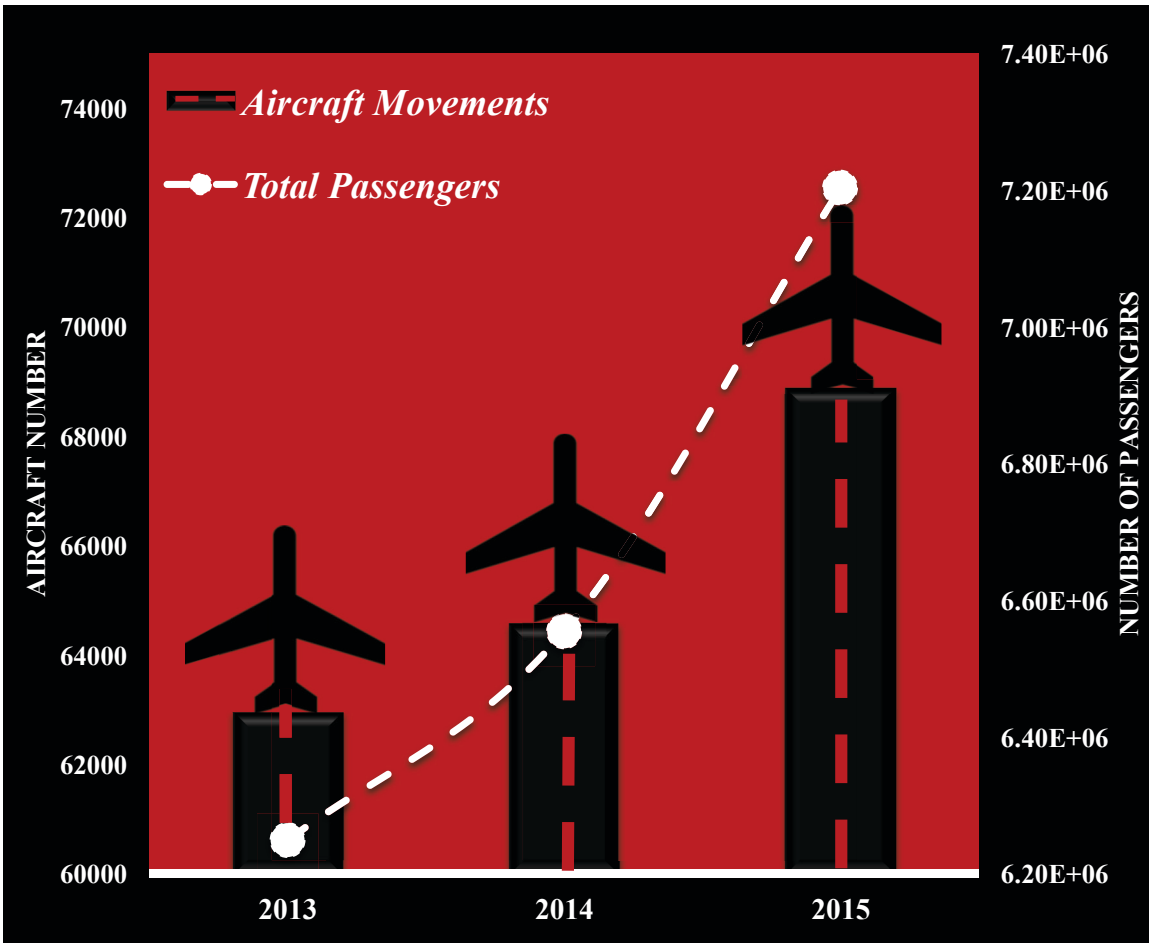

Figure 3-1: The growth rate in the number of aircraft movement (arrivals and departures) and number of passengers at Beirut Rafic Hariri International Airport (2013-2015)

The airport code number is 2E. Beirut-RHIA handles a wide range of flights including international passenger, airfreight, military, and domestic air traffic, and is primarily utilized by the Middle East Airlines (around 50% of the total fleet). The aircraft using the airport during our experimental measurements were mainly Airbus (A320, A321, A330), Boeing (B738, 757, 763, 767), McDonnel Douglas (MD), etc. Beirut airport has three runways and 14 taxiways (Figure 3-4). The runways are named according to their magnetic heading; and are runways 03/21, 16/34, and 17/35. Runway 21, located to the east of the airport center, is the main departure runway due to the prevalence of southwest wind conditions. It extends to 3800 m and is 45 m wide[2], making it well equipped to accommodate a variety of aircraft. Runway 16 is the main landing runway due to the

[2] Aeronautical Information Publication, 2010. Directorate General of Civil Aviation-Lebanon.

prevalence of wind conditions; while runway 17/35 is mainly used for landing and take-off for private and military jets. The prevailing southwest wind throughout most of the year (Chelala, 2008) with light wind up to 5-knots, makes Beirut Airport operate southerly (take-off) and northerly (landing).

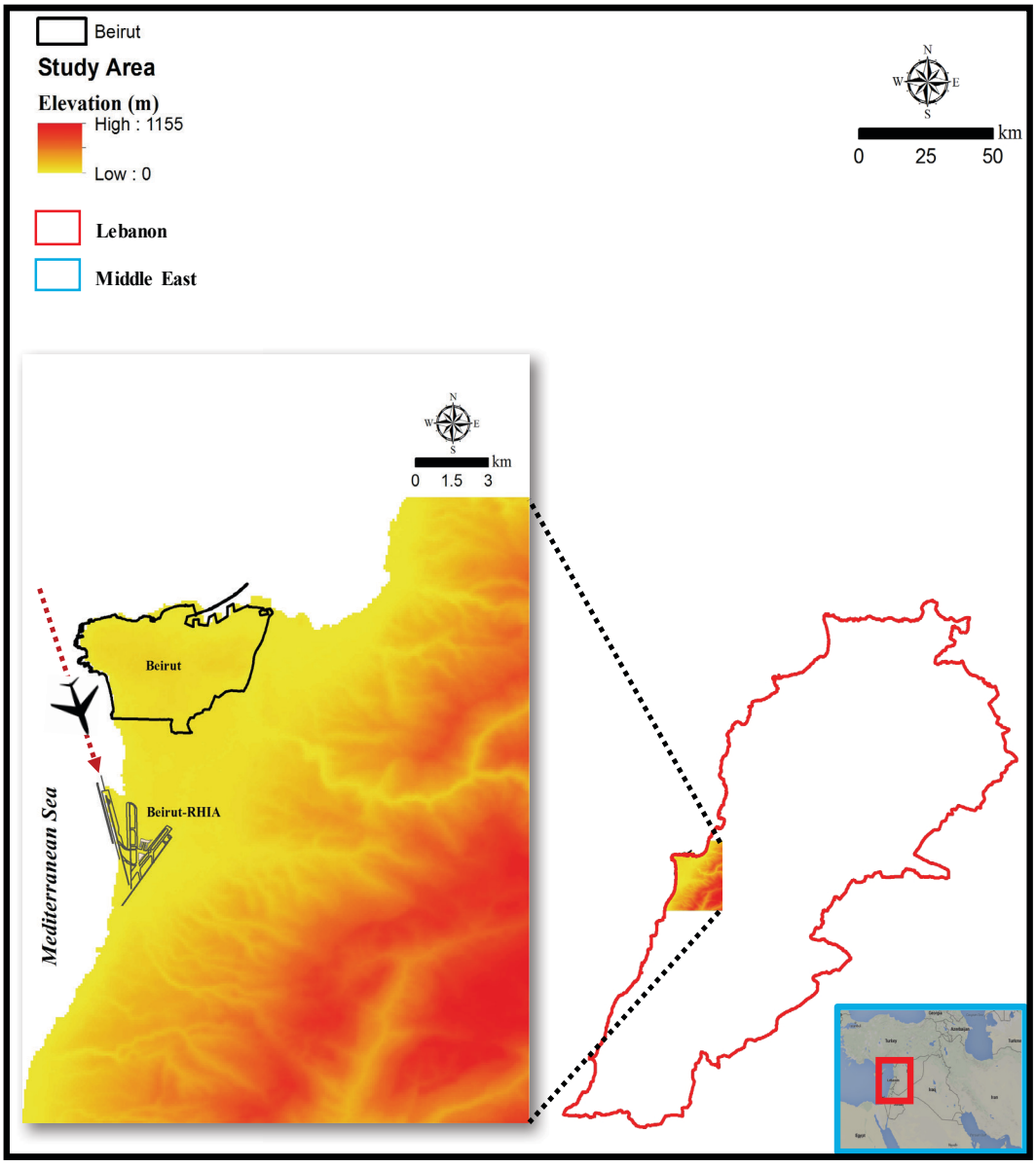

Figure 3-2: Study Area (Beirut Rafic Hariri International Airport)
The red dotted line reflects the main jet trajectory used for landing in Beirut-RHIA.

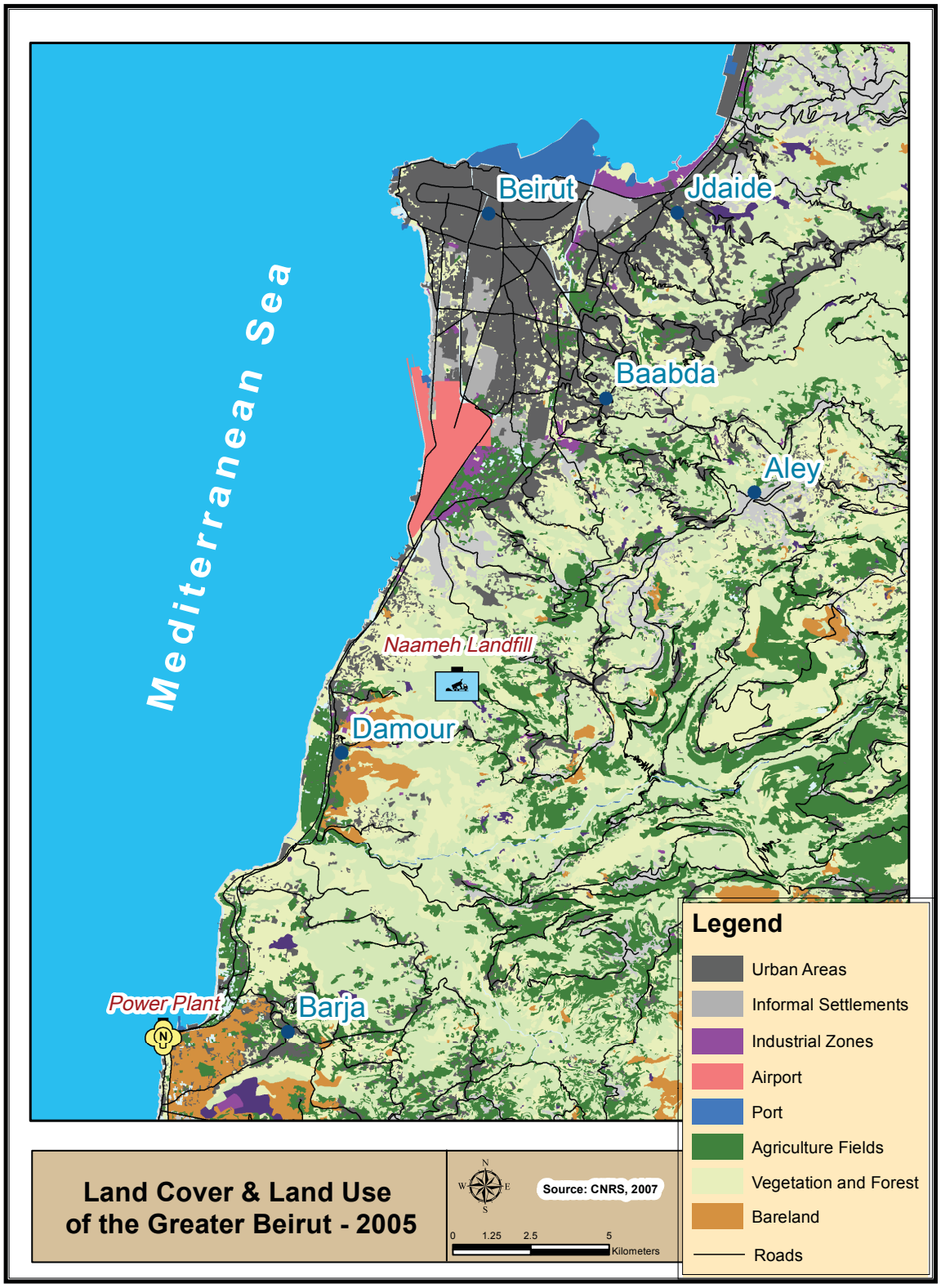

Figure 3-3[3]: Land use/land cover map of the area surrounding Beirut Airport, based on high spatial resolution (1 m) images taken in 2005

[3] This map was provided by the Lebanese CNRS - Center for Remote Sensing.

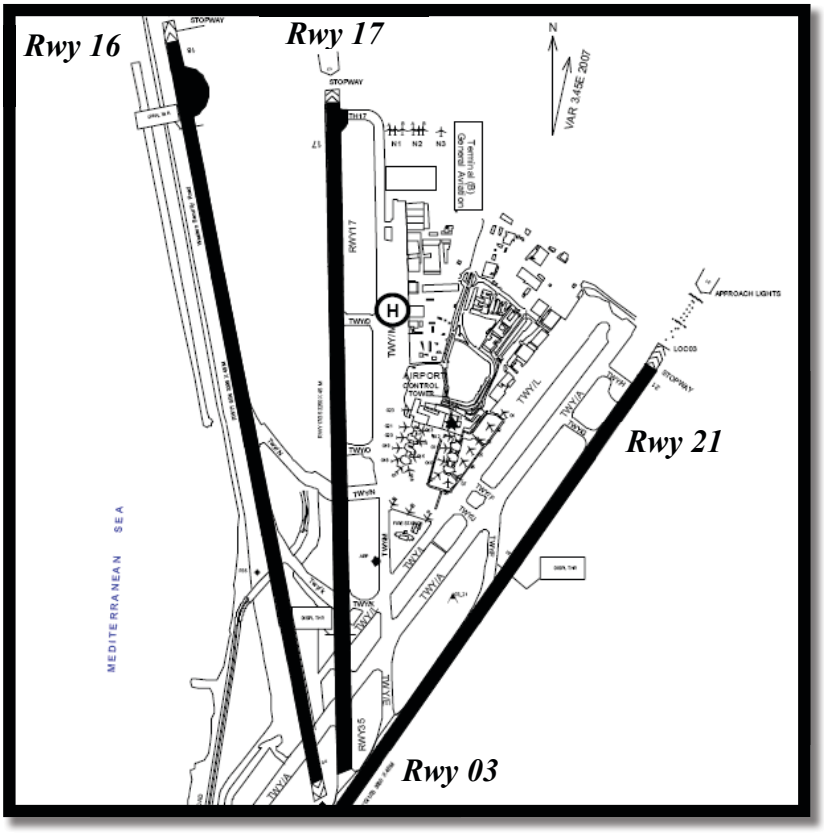

Figure 3-4: Top view of Beirut Rafic Hariri International Airport (Aeronautical Information Publication, 2010) (Rwy: runway)

3.2 Significance of the Study

It is very important to assess the impact of Beirut Airport's activities on ambient and indoor air quality for several reasons.

3.2.1 LOCAL AIR QUALITY

In addition to the constant annual growth rate of air traffic (5%), Beirut airport's impact on air quality is expected to be affected, to a large extent, by the airport's own characteristics i.e. its **location and layout**, surrounding **geography** and **topography**, and **meteorology**:

(i) The airport's **location** in a very urbanized area makes its impacts more pronounced and increases the number of nearby residents affected by its emissions. Because of the airport's **layout** and location, aircraft fly over Beirut at an altitude of 300-500 m above the seashore during inbound before landing on its main landing runway (runway 16) (Figures 3-2 and 3-5(a)). In few other cases, aircraft fly with the same altitude above several areas located in the western part of Beirut before landing at the second landing runway (17). On the other

hand, aircraft take-off at around 160 m away from the civil inhabitants at the main departure runway (21) as shown in Figure 3-5(b).

(ii) The **special geography** and **topography** surrounding the airport plays a very significant role in drawing the airport emissions to larger distances. During daytime, the airport emissions are drawn into the land by means of **sea breeze** and then driven even further upslope to the mountains by means of the **valley breeze** (Figures 3-6 and 1-8) in a very complex wind-topography interaction.

(iii) **Meteorology**: The prevailing wind direction is normally southwest throughout most of the year which increases the probability of the dispersion of air pollutants from the airport towards Beirut (Figure 3-2). This was supported by observations found in a previous study conducted by Chelala (2008) who reported that 34% of the total nitrogen dioxide concentrations at a measurement site located east of Beirut (Pine Forest), was coming from the southwest direction (where the airport is located). Even more, all the aforementioned aircraft and airport emissions are entrapped within the boundary layer which is normally between 400-900 m (Figure 3-7).

All these special geographical, topographical, and meteorological factors raise questions regarding the significance of their effect on the dispersion of the pollutants emitted from Beirut airport's activities and consequently what the impact of these activities will be. It is important to note that in most countries the effect of airport emissions is expected to be less pronounced than the emissions due to our airport because the inhabitants and residential apartments surrounding Beirut Rafic Hariri International Airport are much closer than population surrounding other airports.

Figure 3-5: Photographs showing (a) aircraft flying over Beirut at an altitude of 300-500 m during inbound (rwy 16) above the seashore and (b) aircraft take-off taking place about 150 m away from civil inhabitants

Figure 3-6: The interaction between sea breeze and valley breeze, expected to carry pollutants from Beirut Airport inwards towards the citizens and upslope towards the mountainous areas

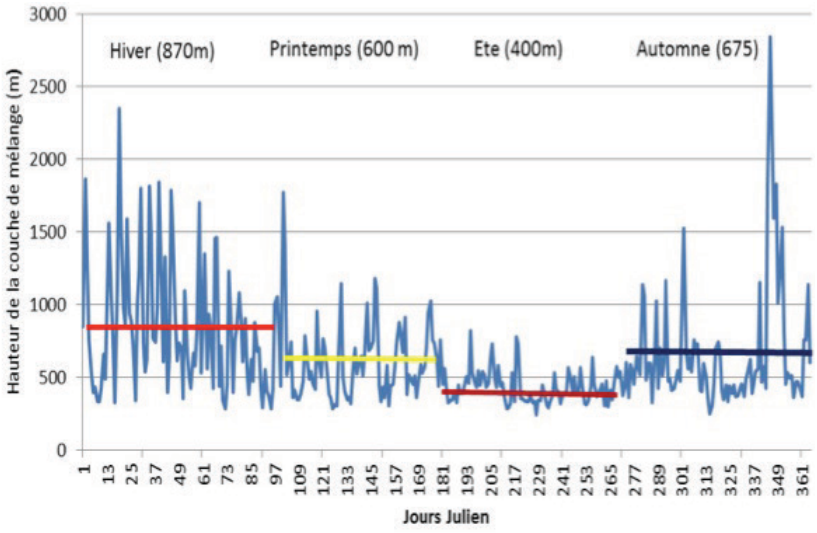

Figure 3-7[4]: Mixing layer height for Beirut for the year 2012

3.2.2 INDOOR AIR

Indoor air should be assessed since Beirut airport employees, who stay at least 12 h inside the airport buildings, suffer from dizziness (Yaman, 2001). Moreover, there are several openings which provide direct pathways for contaminated air in the apron to enter the airport buildings, which lack windows, and which might have improper ventilation and filtration systems.

In Beirut, many studies have focused on road transport and their impact on air quality (Badaro-Saliba *et al.*, 2013; Daher *et al.*, 2013). Up to now, there are no studies on the assessment of the effect of Beirut Rafic Hariri Airport on the air quality of Beirut or on the airport's indoor air quality.

3.3 Research Objectives and Approach

In this context, the main goal of this doctoral research is to assess the impact of Beirut-Rafic Hariri International Airport (Beirut-RHIA) activities on the air quality of Beirut and its suburbs in an attempt to understand its impact on air quality affecting the citizens in the surrounding area. A secondary goal is to assess the impact of these activities on indoor air quality affecting employees and passengers inside the airport. The focus will be on species that are considered key indicators of atmospheric pollution: NO_2 and VOCs.

[4] This plot was simulated by Dr. Jocelyne Gérard.

3.3.1 POLLUTANTS OF CONCERN

The pollutants of concern are nitrogen dioxide (NO_2) (one of the nitrogen oxides (NO_x)) and VOCs. In our study, we focused on NO_2 due to its toxicity, contrary to NO which is much less toxic. Moreover, NO_2 was feasible to measure. In the justifications below, both NO_2 and NO_x will be used.

Nitrogen Oxides (NO_x)

NO_x is the collective name given to the oxides of nitrogen; these being nitric oxide (NO) and nitrogen dioxide (NO_2). Nitrogen oxides can be produced from biogenic sources or anthropogenic sources. Biogenic sources of nitrogen oxides include lightning, forest fires, grass fires, trees, bushes, grasses, and yeasts (EPA, 1999). Most airborne NO_x comes from combustion-related anthropogenic emissions, which include automobiles, trucks and various non-road vehicles (e.g., aviation, construction equipment, boats, etc.) as well as industrial sources such as power plants, industrial boilers, and fossil fuel combustion.

Formation

One of the fastest growing anthropogenic source of NO_x emissions is aviation. Inside aircraft turbine engines, nitrogen dioxide is produced when air passes through high temperature/high pressure combustion in presence of air i.e. nitrogen and oxygen, which combine to form NO_x (NO and NO_2) (FAA, 2015). NO_x which leaves the engine are almost all NO with only a few percent NO_2 that is rapidly oxidized to NO_2 in the atmosphere. In combustion systems, thermal NO mechanism involves the attack of molecular nitrogen (N_2) and atomic nitrogen (N) by oxygen (O_2) and oxygen containing radicals (O, OH) which can occur in oxygen rich mixtures. The formation of thermal NO is determined by highly temperature dependent chemical reactions (reactions 3-1 to 3-3) known as the extended Zeldovich mechanism (Zeldovich, 1946), described as follows:

$$N_2 + O \rightarrow NO + N \quad (3\text{-}1)$$

$$N + O_2 \rightarrow NO + O \quad (3\text{-}2)$$

$$N + OH \rightarrow NO + H \quad (3\text{-}3)$$

Nitric oxide production is predicted by these reactions coupled with reactions describing the oxidation of species containing carbon and hydrogen to produce O and OH. Nitrogen

dioxide is formed by the reversible reactions of NO with HO_2, OH, O and O_2 *via* (Carvalho, 2002):

$$NO + HO_2 \rightarrow NO_2 + OH \quad (3\text{-}4)$$

$$NO + OH \rightarrow NO_2 + H \quad (3\text{-}5)$$

$$NO + O_2 \rightarrow NO_2 + O \quad (3\text{-}6)$$

$$NO + O + M \rightarrow NO_2 + M \quad (3\text{-}7)$$

NO_x has a local lifetime of < 1 day in the lower troposphere (IPCC, 2001).

Environmental and Health Impacts

We have chosen to assess NO_2 because:

- In the Lebanese capital (Beirut), its annual average concentration reach 53 μg m^{-3} exposing 93% of the population (around 358,459 people) to a yearly average exceeding the WHO annual guideline (40 μg m^{-3}) resulting in severe health effects (pulmonary, increased risk of lung cancer, etc.) (Badaro-Saliba *et al.*, 2013; Nakhle *et al.*, 2013).
- It is the most significant local air quality pollutant emitted from aircraft and is highly ranked against other aircraft pollutants as a contributor to adverse environmental impacts (ICAO, 2008b) due to the contribution of nitrogen oxides to: (i) two of the largest air quality concerns, tropospheric ozone and secondary PM by forming nitrate aerosols (WHO, 2005); (ii) acid rain which can damage forests and lakes. Thus, local authorities are mainly concerned with NO_2 exceedances as it is one of the main pollutants of concern associated with aviation (Peace *et al.*, 2006).
- Moreover, NO_x is linked both directly and indirectly to adverse effects on human health (EEA, 2016). Personal exposure to NO_2 affects lung function, especially on children, the elderly, and the asthmatics. Based on both epidemiological studies and human and animal clinical studies, the recent United States Environmental Protection Agency (US EPA) assessment concluded that there is a positive association between short-term exposure to gaseous NO_2 and respiratory morbidity (Mahashabde *et al.*, 2011). The indirect health effect is related to the formation of secondary PM and tropospheric ozone (O_3) in the atmosphere (chapter 1) which are both of adverse impacts on human health. PM can cause respiratory and cardiovascular effects while ozone can lead to severe respiratory problems (US

EPA, 2016). The current guideline values for NO_2 are 40 µg m^{-3} for annual mean (long-term exposure) and 200 µg m^{-3} for 1-hour mean (short-term exposure) (WHO, 2005).

- As mentioned in chapter 1 (Figure 1-1 (c)), NO_x aircraft emissions at the local scale (below 3,000 feet (ca. 900 m) AGL) are estimated to increase from about 0.25 million metric tonnes (10^9 kg) for the year 2006 to 0.52-0.72 Mt for the year 2036 by factors of 2-3. This future increase in NO_x emissions is expected; it comes as a result of the direct relationship with traffic growth, which is predicted to increase (chapter 1, Figure 1-1 (a)). This direct relationship between NO_x emissions and traffic growth has been reported by Kim *et al.* (2007) as seen in Figure 3-8. However, the increase in emissions is more moderate than that of air travel due to the enhancement of engine technology (Brasseur *et al.*, 1998).

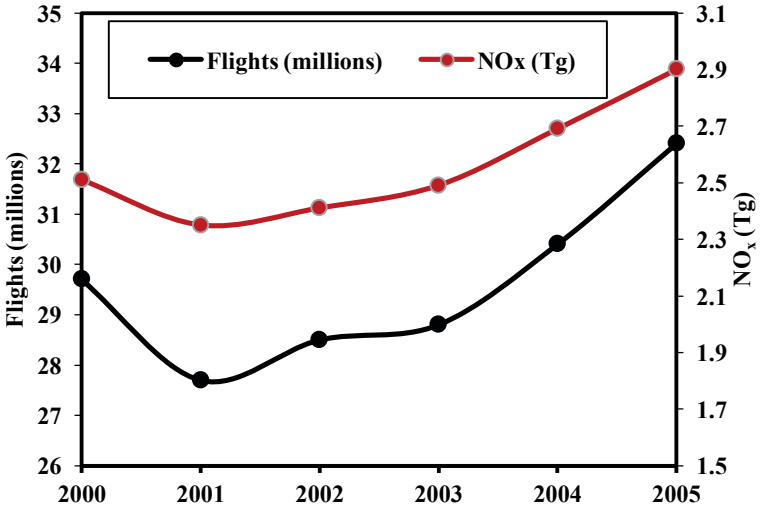

Figure 3-8: Annual change in the number of flights and emissions for nitrogen oxides at the global level

This expected increase with traffic growth, coupled with the adverse environmental and health impacts of nitrogen oxides led the ICAO in CAEP 7 to focus on NO_x and put significant pressure for further reductions of NO_x produced during the LTO cycle for the future (CAEP 7).

Volatile Organic Compounds (VOCs)

Definition and Sources

Volatile organic compounds (VOCs) are composed of a large group of carbon-based compounds with relatively high vapor pressures. The European Union (EU) directive

1999/13/EC defines a VOC as "any organic compound that has, at 293.15º K, a vapor pressure of 0.01 kPa or more. In addition, EU directive 2002/42/EC defines a VOC as any organic compound having an initial boiling point less than or equal to 250ºC measured at a standard pressure of 101.3 kPa. The U.S. Environmental Protection Agency (U.S. EPA) defines a VOC as “any compound of carbon, excluding carbon monoxide, carbon dioxide, carbonic acid, metallic carbides or carbonates, and ammonium carbonate, which participates in atmospheric photochemical reactions” with the exception of few organic compounds (e.g. methane, methylene chloride, chlorofluromethane, etc.) which have been determined to have negligible photochemical reactivity (Code of Federal Regulations, 2016).

VOCs include non-methane hydrocarbons (NMHCs) like alkanes, alkenes, alkynes and oxygenated NMHC like alcohols, aldehydes and organic acids. They have both anthropogenic or biogenic origins. Anthropogenic sources include transport (road transport, aviation, etc.), industrial sources (paint application, perfumes, etc.), and emissions from the residential/tertiary sector (household products, dry-cleaning, etc.). The major sources of VOCs are dominated by the exploitation of fossil fuels (coal, oil, and gas) (Koppmann, 2008). As for indoor VOC concentrations, they are usually up to 10 times higher than outdoor concentrations.

In airports, VOCs are emitted due to incomplete fuel combustion or as a result of vaporization of liquid fuel from spills, venting of fuel tanks, or engine start-up. Many studies have been conducted to assess the speciation of aircraft and airport-related VOCs (Anderson *et al.*, 2006; Lelievre, 2009; Spicer *et al.*, 1994, 1992; Yelvington *et al.*, 2007). These studies have shown that at idle power, C_2-C_3 unsaturated hydrocarbons constitute a big portion of the VOC mass and that the emissions tend to decrease as the power settings of the engine increase (see chapter 2).

Tropospheric Lifetime

The lifetime of a VOC, τ, is the time required for the concentration of the VOC to decrease to 1/e (37%) of its original concentration. VOCs in the troposphere are removed or transformed by reactive species (principally OH radicals, NO_3 radicals and O_3), photolysis, and the physical removal processes of wet and dry deposition. For the reaction of a VOC with OH radicals, NO_3 radicals and O_3, the lifetime is given by $\tau = 1/(k_x[X])$, where k_x is

the rate constant for reaction of species X with the VOC, and [X] is the average ambient atmospheric concentration of species X (X = OH, NO_3 or O_3) (Atkinson *et al.*, 2006).

Based on the fact that the OH radical reaction is the rate determining step in the photo-oxidative degradation of VOCs (Atkinson, 1986), the tropospheric lifetimes of several organic compounds have been estimated (Table 3-1). They vary from around an hour for isoprene to few days for benzene. It is important to note that the tropospheric lifetimes of VOCs based on OH reactions are 20 times shorter in summer than in winter when OH concentrations are significantly higher (Hellén, 2006).

Table 3-1: Atmospheric life times of several target VOCs
(Atkinson, 2000; Atkinson *et al.*, 2006; Atkinson and Arey, 2002)

VOC	OH* Radical
n-Octane	1.3 d
n-Decane	1 d
Benzene	9.4 d
Toluene	1.9 d
m, p-Xylene	5.9 h
1,2,4-TMB	4.3 h
Styrene	2.4 h
Acrolein	6.9 h
Pantanal	5.9 h
Acetone	53 d
2-Butanone	10 d
D-Limonene	50 min
Ethane	47 d
Propane	10 d
n-Butane	5 d
Ethene	1.4 d
Propene	5.3 h
1,3-Butadiene	2.1 h
Trans-2-butene	2.2 h
Isoprene	1.4 h

*For a 12-h daytime average OH radical concentration of 2.0×10^6 molecule cm^{-3}

Environmental and Health Impacts

VOCs were chosen in this study because:

- The greatest health risks i.e. cancer and morbidity associated with airport emissions seem to be posed by Hazardous Air Pollutants (HAPs) (along with $PM_{2.5}$) (Kim *et al.*, 2015). The prioritized list of airport-related pollutants based on emission rates and/or toxicity developed from Airport Cooperative Research Program (ACRP) Report 7, those from an FAA 2003 analysis and the ORD 2005 airport modernization

environmental impact statement (EIS) were majorly composed of VOCs (Kim *et al.*, 2015). In fact, increased interest is arising in regard to specific hydrocarbons owing to their potential as Hazardous Air Pollutants (HAPs) (ICAO, 2006). HAPs are generally defined as those pollutants that are known or suspected of being able to cause serious health effects such as cancer, birth defects, etc. (Kim *et al.*, 2015). The U.S. EPA has listed 14 HAPs related to aircraft exhaust and/or their ground support equipment (GSE). Ten individual HAPs comprise the vast majority of HAPs (FAA, 2003; Wood, 2008): Formaldehyde, Acetaldehyde, Benzene, Toluene, 1,3-Butadiene, Xylene, Naphthalene, Acrolein, Propionaldehyde (propanal). Formaldehyde is the most prevalent HAP in aircraft exhaust followed by acetaldehyde, benzene, and toluene. HAPs have adverse health effects; for example, benzene exposure causes illness and death in chronically exposed workers and is directly linked to the occurrence of leukemia (Ritchie *et al.*, 2003b). In general, their health effects depend on the specific species as well as exposure duration, but some short-term effects may include headaches, nausea, sore throat/eyes/nose while long-term effects may lead to depressions of the central nervous system and cancer (Kim *et al.*, 2015).

- On the other hand, VOCs have a great influence on tropospheric chemistry; they affect ozone formation and they or their reaction products are able to take part in secondary organic aerosol formation (IPCC, 2007).
- Besides this, VOCs were chosen since they are composed of a large number of compounds which increases the probability of finding specific aircraft VOC tracers (chapter 6.1).

In the European Union, the European Directive 2000/69/EC has set target values for benzene not exceeding annual concentrations of 5 μg m^{-3} in ambient air (United Nations, 2007). Acute toxicity criteria for airport-related HAPs are reported in Table 3-2.

Figure 3-9 presents the annual evolution of flight and hydrocarbon emissions from aviation for the years 2000-2005. Unlike NO_x emissions, VOC emissions are not directly related to the number of flights because they are more sensitive to changes in the combustion process within the reactor, including those related to engine power settings (Kim *et al.*, 2007). Indeed, VOC emissions is more or less stable since 2001 despite the significant increase in flight number.

Table 3-2: Acute toxicity criteria for airport-related hazardous air pollutants, adapted from Wood (2008)

HAP	Toxicity Criterion (ppm)			
	REL[a] 1-6 Hours	AEGL-1 1 Hour	AEGL-1 8 Hour	MRL 1-14 Days
Acetaldehyde		45	45	
Acetone		200	200	26
Acrolein	0.00008	0.03	0.03	0.003
Benzene	0.4	52	9	0.009
1,3-Butadiene		45	45	
Formaldehyde	0.08	0.9	0.9	0.04
Methanol		530	270	
Phenol	1.5	15	6.3	0.02
Propane		5500	5500	
Styrene	5	20	20	
Toluene	10	200	200	1
Xylenes	5	130	130	2

ppm: parts per million
HAP: hazardous air pollutant
REL: reference exposure level
AEGL: acute exposure guideline
MRL: minimum risk level
[a]Benzene REL is for a 6-hr exposure period, all other RELs are for a 1-hr exposure period.

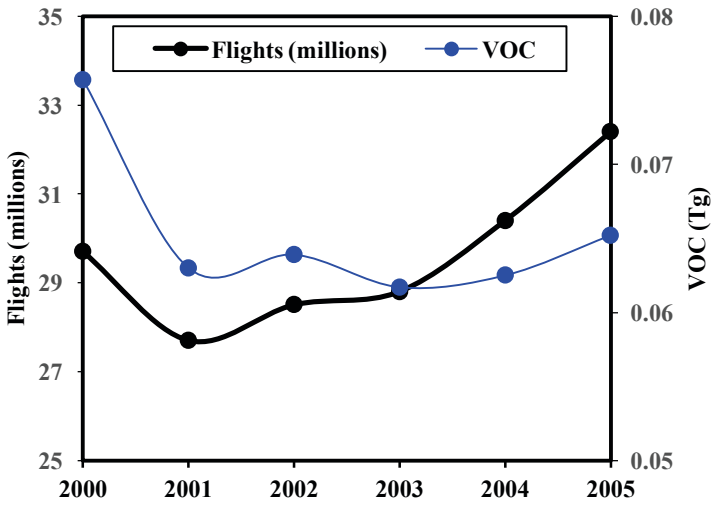

Figure 3-9: Annual change in the number of flights and emissions for hydrocarbons at the global level (Kim et al., 2007)

3.3.2 VARIABILITY OF EMISSION FACTORS

Emissions of NO_x and VOCs depend mainly on the engine speed or thrust settings (determining the temperature and pressure within the combustor), and the engine model, technology and age, as well as fuel composition (Slemr *et al.*, 2001, 1998, Spicer *et al.*, 1994, 1992).

At low engine speeds (e.g. idle), the combustion temperature is low (680°K-1700°K) (Dagaut *et al.*, 2006; Tsague *et al.*, 2006) does not guarantee optimum combustion (Heland and Schäfer, 1998). The emission of HCs is maxima (Figure 3-10). However, at high speed (e.g. during take-off), the temperature within the combustion chamber is higher (around 2300°K) (Dagaut *et al.*, 2006). This leads directly to increase in the emission of NO_x (Figure 3-10) (Heland *et al.*, 1998; Tsague *et al.*, 2006). (The emissions during reference LTO cycles are reported as emission indices (EIs) expressed as mass of pollutant emitted per unit mass of fuel burned (Masiol *et al.*, 2014)).

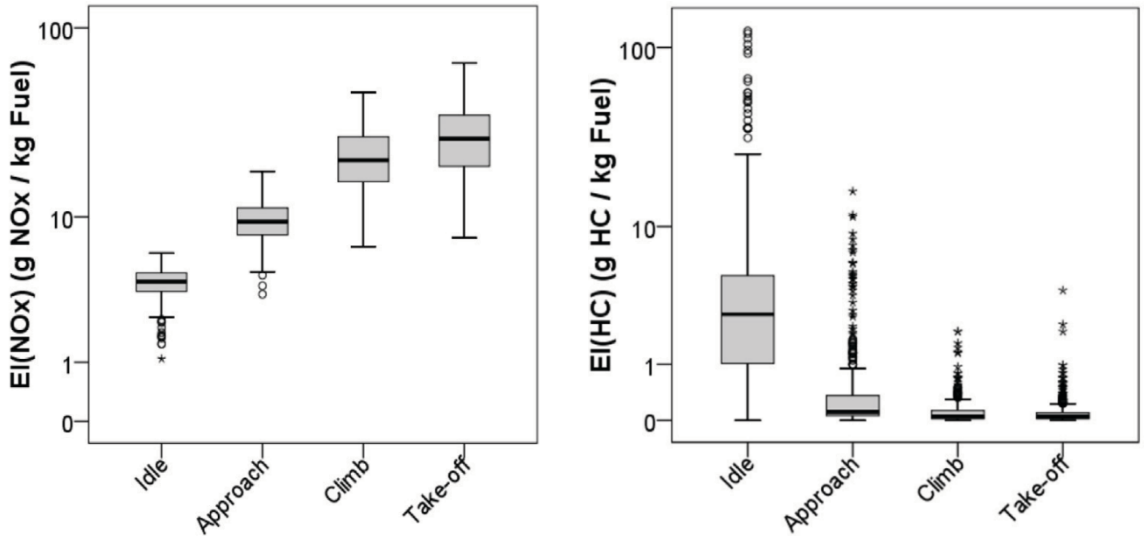

Figure 3-10: EIs provided by the ICAO databank, taken from Masiol *et al.* (2014). All in-use engines certified from 1976 to April 2013 are included.

Emissions also vary by the type of engine (age and the fuel consumption). This variability in emissions is observed in the ICAO database which lists all commercial engines in-use. The aircraft emission inventory takes into account the differences of the engine type as well as the different aircraft modes established at each phase of the LTO Cycle. However, it was shown that this database is not always representative to emissions generated by air traffic due to operational conditions in airports which can be extremely variable. Thus, it is important to evaluate this methodology by comparison with "real" operational conditions. To support this, measurements of NO_x, CO and hydrocarbons were carried out directly under the flow reactors (Schürmann *et al.*, 2007, Wood *et al.*, 2008; Heland and Schäfer, 1998; Schäfer *et al.*, 2000, 2003, Herndon *et al.*, 2004, 2006. 2009). The results of these studies confirm that emissions of pollutants are closely related to the operational mode and

engine characteristics, whereas the emission factors obtained were variable and dependent on operational conditions specific for each study.

In conclusion, the operational conditions, specifically engine speed, determine the emissions of aircraft. These emissions are listed in the ICAO emission database. However, it was shown that this database is not always representative to emissions generated by air traffic due to operational conditions at airports, which can be extremely variable (Lelievre, 2009).

3.3.3 STUDY APPROACH

For the main goal, two main pathways were followed, measurements and modelling. To experimentally identify the impact of the airport activities, I had to identify special VOC fingerprints and markers, characteristic of aircraft emissions (Sections 5.1 and 6.2) by taking samples from aircraft exhaust under real aircraft operations. Using these markers, the impact of the airport activities was tracked, as preliminary investigations (sections 5.2 and 6.2). It was not possible to track the impact of the airport activities using NO_2 as it is emitted from several other sources. Besides this, another approach to assess this impact was *via* modelling with an advanced Atmospheric Dispersion Modelling System (ADMS-Airport), which required prior validation through NO_2 passive campaigns (sections 5.3 and 6.3) to gain confidence in utilizing this model (chapters 7, 8, and 9). The two approaches will be compared to determine the main goal of my thesis.

To assess the airport's impact on indoor air, measurements were undertaken in 2 locations, the maintenance room to assess the impact on air quality affecting the employees, and the arrivals hall to assess the impact on passengers/employees (sections 5.4 and 6.4).

The motivation of this study is understanding the impact of Beirut Airport on air quality to help airport managers and airlines to minimize emissions and undertake mitigation measures to protect the health of personnel working at the airport, minimize exposure for the travelling public, and avoid adverse impacts on the air quality of nearby neighbourhoods. Such a project will also allow us, in the future, to estimate the contribution of emissions from air transport compared to that from road traffic.

Conclusion

This chapter has provided a description of the study area, Beirut-RHIA, along with its special characteristics (growth in air traffic, urbanization, location and layout, surrounding geography, meteorology) which makes the assessment of the impact of its activities significant and crucial. Moreover, the fact that nitrogen oxide is the most significant aviation-related local air quality pollutant and exceeds the WHO recommendation in the Lebanese capital, and the fact that VOCs have hazardous health effects and enable identification of special markers by means of their large number, made them the pollutants of concern in this thesis.

Conclusion - Part I

To conclude, airport emissions have adverse impacts on air quality affecting public health and the environment, as revealed by the literature reviewed in the previous chapters (FAA, 2015; Kim, 2015; Mahashabde *et al.*, 2011; Wood, 2008). In order to understand and mitigate these impacts, assessments should be done to understand the contribution of an airport's activities to the degradation of local air quality. While the extent and intensity of these impacts depend on each airport's characteristics, previous studies concluded that airport activities lead to the degradation of air quality up to 3 km (Carslaw *et al.*, 2006; Kim, 2015; Moussiopoulos *et al.*, 1997; Yu *et al.*, 2004). However, most of these studies did not really account for aircraft trajectories above the citizens nor other geographical and topographical factors that might intensify the total airport contribution. These considerations will be taken into account in this study to investigate the different impacts of Beirut Airport's activities. Of special interest are (i) nitrogen dioxide, the most significant local air quality pollutant related to aviation (chapters 1 and 2) and the most significant local air quality pollutant in the Lebanese capital, and (ii) VOCs chosen due to their hazardous health impacts (chapter 2) i.e. cancer and death (HAPs) and since their large number of species enabled us to search for special aircraft markers.

Airport indoor air was not of great interest due to the existence of proper ventilation in most of the airports, however, in the case of Beirut Airport, (i) the occurrence of several cases of pulmonary diseases affecting the airport's employees, as well as (ii) the presence of direct opening between the apron and the arrivals hall, triggered the study of airport indoor air.

Part II: EXPERIMENTAL APPROACH

The experimental methodology to identify the impact of Beirut Airport on air quality as well as the main findings will be presented in part II. It starts with the description of the materials and methods used for sampling and analysis. Next, it presents the detailed sampling methodology for campaigns conducted within or outside the airport, followed by our main experimental findings.

Chapter 4 : Materials and Methods

This chapter discusses the sampling and analysis techniques implemented for the measurement of the concentrations of our target VOCs (Table 4-1) and NO_2. The first part (section 4.1) elaborates on the sampling of VOCs into home-made adsorbent tubes, followed by the description of the analytical instrumentation used, i.e. Automated Thermal Desorption-Gas Chromatography-Flame Detector (ATD-GC-FID) and Automated Thermal Desorption-Gas Chromatograph-Mass Spectrometer (ATD-GC-MS). The second part (section 4.2) focuses on NO_2 passive sampling using Passam tubes and the subsequent laboratory analysis techniques using spectrophotometry.

4.1 Sampling and Analysis of VOCs

4.1.1 SAMPLING INSTRUMENTATION

The choice of the target VOCs was mainly based on extensive bibliographic research (Chapter 2) to determine the major aircraft-related VOCs (AirPACA, 2004; EPA, 2009a; Lelievre, 2009; Schürmann *et al.*, 2007; Wood, 2008). The target VOCs assessed in our study were 50 species (Table 4-1) divided into light alkanes (C_2-C_7), straight chain heavy alkanes (C_8-C_{14}), alkenes (C_2-C_6) and acetylene, chlorinated alkenes, light aldehydes and ketones (C_3-C_6), heavy aldehydes (C_9-C_{10}), d-Limonene, and monoaromatics. It is important to note that heavy alkanes and heavy aldehydes were assessed based on previous bibliographic results, but most importantly after being found as VOCs with highest peak intensities during the primary signature campaign, as well as the indoor campaign analysed by GC-MS. It is worth mentioning that nine of these VOCs are included in the list of 14 Hazardous Air Pollutants (HAPs) present in the exhaust of aircraft according to the US EPA Clean Air Act (FAA, 2003)**,** and twenty five of them are ozone precursors recommended for measurement by the Directive 2002/3/EC (European Environment Agency, 2002).

Air samples of diluted exhaust gases, ambient air, indoor air, and background air were collected inside stainless steel adsorbent tubes using both active and passive sampling techniques. All the adsorbent tubes were fabricated and analyzed at the laboratory of

Institute for Chemistry and Processes for Energy, the Environment and Health (ICPEES)-Group of Atmospheric Physical-Chemistry at the University of Strasbourg and CNRS.

Table 4-1: List of the target VOCs measured

VOC Family	Compound	VOC Family	Compound
Light Alkanes (C_2-C_7)	Ethane[b] Propane[b] Isobutane[b] n-Butane[b]+cis-2-Butene[b] Isopentane[b] n-Pentane[b]+cis-2-Pentene[b] n-Hexane[a, b] n-Heptane[b]	**Chlorinated Alkenes**	Trichloroethene Tetrachloroethene
		Terpene	D-Limonene
Heavy Alkanes (nC_8-nC_{14})	n-Octane[b] n-Nonane n-Decane n-Undecane n-Dodecane n-Tridecane n-Tetradecane	**Light Aldehydes and Ketones (C_3-C_6)**	Acrolein[a] Propanal[a] Butanal Pentanal Hexanal Acetone 2-Butanone
		Heavy Aldehydes (C_9-C_{10})	Nonanal Decanal
Alkynes/Alkenes (C_2-C_6)	Ethene[b] +Acetylene[b] Propene[b] 1-Butene[b] 1,3-Butadiene[a, b] Trans-2-butene[b] 1-Pentene[b] Isoprene[b] Trans-2-pentene 1-Hexene	**Monoaromatics**	Benzene[a, b] Toluene[a, b] Ethylbenzene[a, b] m, p-Xylene[a, b] o-Xylene[a, b] Styrene[a] 1,2,4-Trimethylbenzene[b] 1,4-Dichlorobenzene Butylbenzene Propylbenzene

[a]Identified as HAP related to aircraft and GSE
[b]Recommended by Directive 2002/3/EC

- Adsorbent Tubes

Air samples were collected using home-made multi-bed stainless steel thermal desorption tubes suitable for trapping C_2-C_{12} VOCs, to be later analyzed using gas chromatographic methods. To provide a large number of samples for the field campaigns with a minimum cost, 120 empty stainless steel tubes, purchased from Sigma Aldrich, were packed with two adsorbent columns according to the model "category 2" of the method TO-17 of the US-EPA, using a press (Figure 4-1) found in the laboratory at the University of Strasbourg

(Liaud, 2014; U.S. Environmental Protection Agency, 1999). Accordingly, the aforementioned tubes were filled with 10 mm Carbosieve S-III (60/80 mesh, 100 mg) designed to trap light VOCs from C_2 to C_5; and 35 mm Carbopack^{TM} B column (20/40 mesh, 160 mg) designed to trap heavier C_5-C_{12} VOCs (Jochmann *et al.*, 2014). The choice of these adsorbents was based on their characteristics (specific surface area, hydrophobicity, number of trappable carbon equivalent, etc.) (Woolfenden, 2010a) and was justified by Liaud (2014). The use of these adsorbents together is widespread and commercially found under the name "Air Toxics" (Supelco). These tubes are compatible with Perkin Elmer thermal desorption systems present in the laboratory, and possess similar trapping performance to that of "Air Toxics". Both seem not at all suitable to trap ethane, ethene, and acetylene at room temperature (Liaud, 2014). In addition, these tubes are not most suitable for n-tridecane and n-tetradecane regarding the recommendations given for carbopack^{TM} B, even if these two compounds were not tested by Liaud (2014). However, due to the sticky nature of the aforementioned heavy VOCs, we assumed that these tubes can still be used to adsorb them. Note that tubes were sealed with Swagelok end caps fitted with PTFE ferrules.

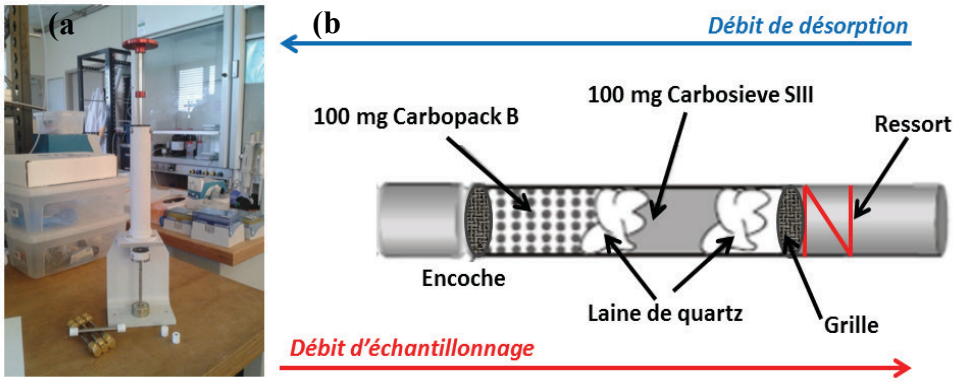

Figure 4-1: (a) Press, (b) Schema of "Air Toxics" adsorbent tube, taken from Liaud (2014)

Conditioning (Before the measurement campaign)

Once manufactured, tubes were conditioned by thermal cleaning before the beginning of every campaign to reduce the presence of residues and maintain low blank values. The adsorbent tubes are usually conditioned at 350°C under a helium flow rate of 50 mL min^{-1} for a time range of 1-3 hours by using the function "conditioning" of the automated thermal desorber (section 4.1.3). However, such conditioning was proven to be time

consuming with limited effectiveness (Kim *et al.*, 2012; Liaud, 2014), where residue was still found after conditioning. Hence, to correct for the presence of residues, adsorbent tubes were grouped into series of 10, according to the day of manufacture and group of adsorbent. After conditioning, a tube of each series (blank tube) was randomly chosen to represent the series and was analyzed under the conditions of the analytical method developed, to be later taken into account during calculations.

Our tubes were finally conditioned for 60 min prior to the first indoor campaign performed in June 2014, and for 120 min before the rest of the campaigns. This increase in duration of conditioning was to ensure a better desorption of residues. After conditioning, tubes were stored in proper isolated boxes.

Transport and Storage after Sampling

According to the recommendations (U.S. Environmental Protection Agency, 1999), sealed tubes with Swagelok® brass caps (Supelco) and Teflon ferrules were stored in the refrigerator at T < 4°C and transported to the University of Strasbourg in a suitable well-sealed multi-tube container wrapped in a storage bag, to prevent any contamination of the samples and loss of VOCs during transport. Most of the tubes were analyzed within 30 days after sampling. Due to technical reasons, part of the tubes sampled in the active transect campaign (performed in July 2015) was analyzed within 70-90 days after sampling after being stored in the refrigerator.

- Sampling Techniques

Active Sampling

Active samples were taken using two kinds of sampling devices, a one-channel autosampler and an 8-channel programmable device (Figure 4-2), designed in ICPEES laboratory. The two devices have a similar principle of operation; they are composed of a pump located downstream of a flow controller. The adsorbent tube is connected to the pump outlet. The devices use a mass flow controller to collect a constant flow of air into the empty adsorbent tube. By the very low pressure drop of the low-ΔP-flow mass flow controller (Bronkhorst), these machines are totally adapted to air sampling at atmospheric conditions with a full range of 500 mL min^{-1} and uncertainty of 1% of the full range.

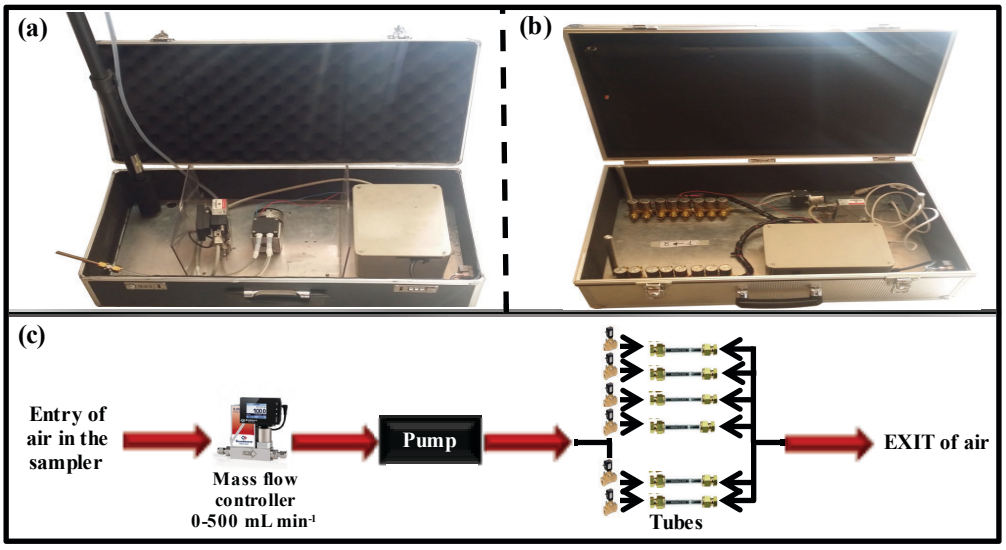

Figure 4-2: Air sampling devices: (a) One-channel autosampler (b) Programmable sampler with 8 channels, (c) Schematic description of the devices

A one-channel portable battery-operated autosampler (width: 61 cm, height: 32 cm, depth: 20 cm, weight: 4 kg)

Most of the air samples were taken using a one-channel portable autosampler, which can be powered by a battery (in addition to electricity). This advantage facilitated sampling at any site in the airfield, as well as inside or away from the airport without being constrained with the necessity of electrical supply. Moreover, its small size enabled it to be placed at sites where it is forbidden to install larger machines due to safety reasons. Furthermore, its configuration can be operated unmanned with the remote control option, which made it possible to control the machine without having to access unsafe sites close to aircraft. This machine was mostly positioned at ground level, except for transect campaigns where it was placed on the rooftops (chapter 5).

An 8-channel programmable device (width: 58 cm, height: 21 cm, depth: 42 cm, weight: 5 kg)

Unlike the one-channel autosampler, this sampler is programmable in duration and flow rate through an easy software interface, which allowed the measurement of the temporal variations of airport indoor VOC concentrations.

Literature data recommend to sample between 1 and 5 L of air with a flow rate ranging from 50 to 200 mL min^{-1} (U.S. Environmental Protection Agency, 1999; Woolfenden,

2010b). Optimization was performed by Liaud (2014); the most suitable sampling conditions for a quantitative trapping of the majority of the target VOCs in a 3L sample was sampling at 100 mL min^{-1} for 30 minutes.

It is important to note that optimization of sampling made by Liaud (2014) was based on indoor concentrations and did not include heavy alkanes and heavy aldehydes. However, some of our samples contained higher atmospheric concentrations than those tested by Liaud (2014). According to the optimization conducted by Liaud (2014), we adapted a flow rate of 100 mL min^{-1} for most of the samplings. However, the sampling duration varied depending on the site and objective of the sampling. To determine the most representative sampling approach for aircraft signature emissions, two sampling techniques were adapted: (i) "30 s × 6" i.e. sampling for 30 s repeated 6 times with a total volume of 0.3 L and (ii) 30 minutes i.e. sampling continuously for 30 min with a total volume of 3 L. For indoor and transect measurements, sampling durations were 30 minutes with a total volume of 3 L (chapter 5).

Passive Sampling

Passive/diffusive sampling relies on the unassisted molecular diffusion of analyte molecules through a diffusive surface onto an adsorbent from the sampled medium to a collecting medium, according to Fick's first law of diffusion. Unlike active (pumped) sampling, passive samplers require no pumps (electricity), have no moving parts, and are simple to use (no pump operation or calibration). The most important advantage of passive sampling is that its low cost allows the simultaneous measurement of ambient air at different locations and with minimum cost. Another benefit is that it significantly reduces the analysis costs, where only a few analyses are necessary to indicate the average concentrations over monitoring periods of 8 hours to several weeks (Namieśnik *et al.*, 2004; Sigma-Aldrich, 2016).

To assess the spatial impact of the airport activities on the air quality of Beirut and its suburbs, simultaneous passive sampling of VOCs at different locations, within or outside the airport, was achieved by means of passive tubes. As a result, tubes affected by similar meteorological conditions at different sites were collected.

Adsorbent tubes were installed in polyethylene cages by means of pen clips (purchased from Supelco) attached to the top of the tube (Figure 4-3). To allow the flow of air in the

correct direction, the lower part of the adsorbent tube was closed by means of Swagelok caps for stainless steel tubes, while the upper part was left open. Cages provided support and shelter in order to protect the samplers from wind when exposed in the field. In our field campaigns, the sampling duration was around 2 days. For cost reasons, the selected passive tubes (see Figure 4-3 (a)) were the same as those used for active sampling, even if the uptake rates of the gaseous species of interest were not known for this tube. This implies that the results will be given in collected mass and not in terms of concentrations.

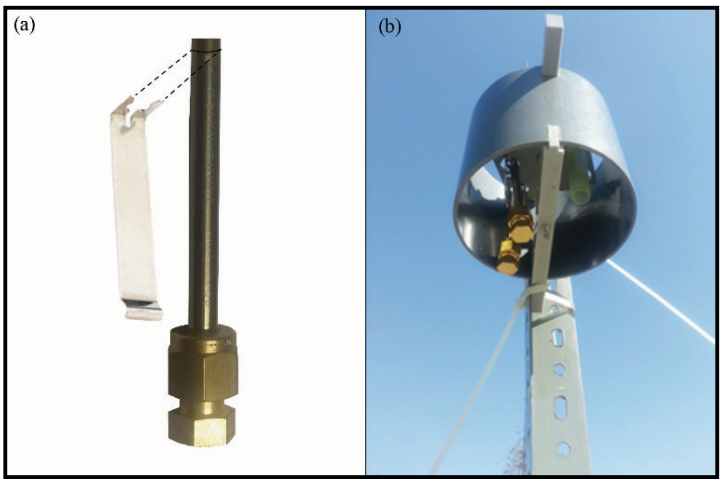

Figure 4-3: (a) Pen clips attached to the top of the adsorbent tube, (b) Adsorbent tubes installed in a polyethylene cage

4.1.2 ANALYTICAL METHOD

- Chemicals and Materials

To prepare liquid calibration curves, by spiking of adsorbent tubes, several reference compounds were purchased from Sigma Aldrich or Fluka with purity ranging mostly between 98 and 100%. Propanal, acrolein, pentanal, nonanal, d-limonene, and n-hexane have a purity ranging from 90 to 97%. A liquid standard mixture (D3710) containing heavy alkanes and 4 monoaromatics was purchased from Supelco (Bellefonte, PA, USA) (see Annex 4-1). A 100 mg L^{-1} liquid standard mixture of BTEX was purchased from Ultra Scientific (North Kingstown, USA). High purity LC-MS methanol (purity > 99.9%), purchased from Fluka, was used to prepare the diluted solutions.

Liquid calibration curves were performed with Perkin Elmer stainless steel cartridges (5 mm I.D., 6.35 mm O.D., 88.9 mm long) obtained from Supelco (Bellefonte, PA, USA) and packed with Carbopack™B (60/80 mesh, 200 mg). The choice of such adsorbent was

already explained by Liaud (2014) and was motivated by the fact that carbopack^{TM}B does not retain methanol.

Online calibration was performed with a gas standard mixture composed of light alkanes, alkenes, and one alkyne at 100 ppb (±20%) supplied by the company Air Liquide (Domdidier, Switzerland). This standard gas cylinder was associated with a dilution bench using nitrogen (99.999% purity) obtained from Messer (Puteaux, France). To complete the dilution bench, mass flow controllers were obtained from Bronkhorst (Montigny les Cormeille, France).

Helium (99.9995%) and air (99.999%) used for gas chromatography and detectors were also obtained from Messer. Hydrogen was produced by a hydrogen generator HyGen 200 from CLAIND (Lenno, Italy) for flame ionization detectors. The certificates provided by the different companies are presented in Annex 4-1.

- Analytical Instrumentation

The systems used for the analysis of the adsorbent tubes are:

- An automated thermal desorption (ATD) system to concentrate and inject sampled VOCs

- A gas chromatograph (GC) equipped with a column suitable for the VOC separation

- A universal detector system, i.e. either the flame ionization detector (FID) or a mass spectrometer (MS)

The total range of target VOCs (except heavy aldehydes) were analyzed by GC-FID by means of its dual column that allows the separation of a wide range of VOCs in a single run as developed by Liaud (2014), unlike the case of GC-MS where it was not possible to separate light VOCs. However, by using GC-FID it was not possible to quantify benzene (due to co-elution), heavy aldehydes, nor unknown peaks. Thus, GC-MS was used for this purpose. Therefore, both systems were necessary and complementary.

Thermal Desorption

Thermal desorption is a widespread technique that utilizes heat and a flow of inert (carrier gas) to allow the extraction of VOCs trapped on a non-volatile matrix to be transferred to downstream system elements such as the analytical column of a GC (Gallego *et al.*, 2012, 2011). It is used in several official methods like the EPA TO-14 and the EPA TO-17 for

VOCs (U.S. Environment Protection Agency, TO-14A, 1999; U.S. Environmental Protection Agency, 1999).

Thermal desorption was chosen in this study because, in comparison to the other used method, the solvent extraction method, it is 1000 times more sensitive since the whole sample is analysed. Thus, it possesses the best repeatability and recovery (Ramírez *et al.*, 2010; Woolfenden, 2010b).

The two stages of the thermal desorption process are illustrated in Figure 4-4. In the first stage or primary (tube) desorption (Figure 4-4(b)), a reverse stream of inert carrier gas (opposite direction to the sampling flow) is used to sweep adsorbed VOCs from the heated sample tube, to a low mass, electrically cooled cold trap which refocuses the VOCs into a narrow band by means of the Peltier effect which permits to trap VOCs at sub-ambient temperatures. In addition to a carrier gas pressure, a desorb flow should be set and optionally, and inlet split flow. The second stage of thermal desorption or secondary (trap) desorption (Figure 4-4(c)), involves the transfer of the VOCs from the cold or focusing trap to the inlet of the analytical column through a line transfer (deactivated silica) by means of the rapid heating of the trap (to ensure the rapid transfer of analytes and limit their diffusion), where the direction of the carrier gas flow through the trap is reversed.

Our samples were injected using Turbomatrix 350 ATD (Automated Thermal Desorber) provided by Perkin Elmer (Waltham, MA, USA). It is a multifunctional system that contains an on-line accessory and an autosampler, which makes possible the analysis of air samples *via* one of the two injection modes: the 2-stage-desorb mode (as discussed in the previous paragraph) with an autosampler for air samples collected previously on adsorbent tubes; or *via* the “on-line” mode where air samples are trapped directly at low temperature with the online accessory of the ATD. The 2-stage-desorb mode was used for the analysis of the air samples taken on the adsorbent tubes as well the analysis of liquid standards, whereas the “on-line” mode (Liaud, 2014) was used for the analysis of known gaseous concentrations of VOC mixtures generated from gaseous standard bottles and a dilution bench.

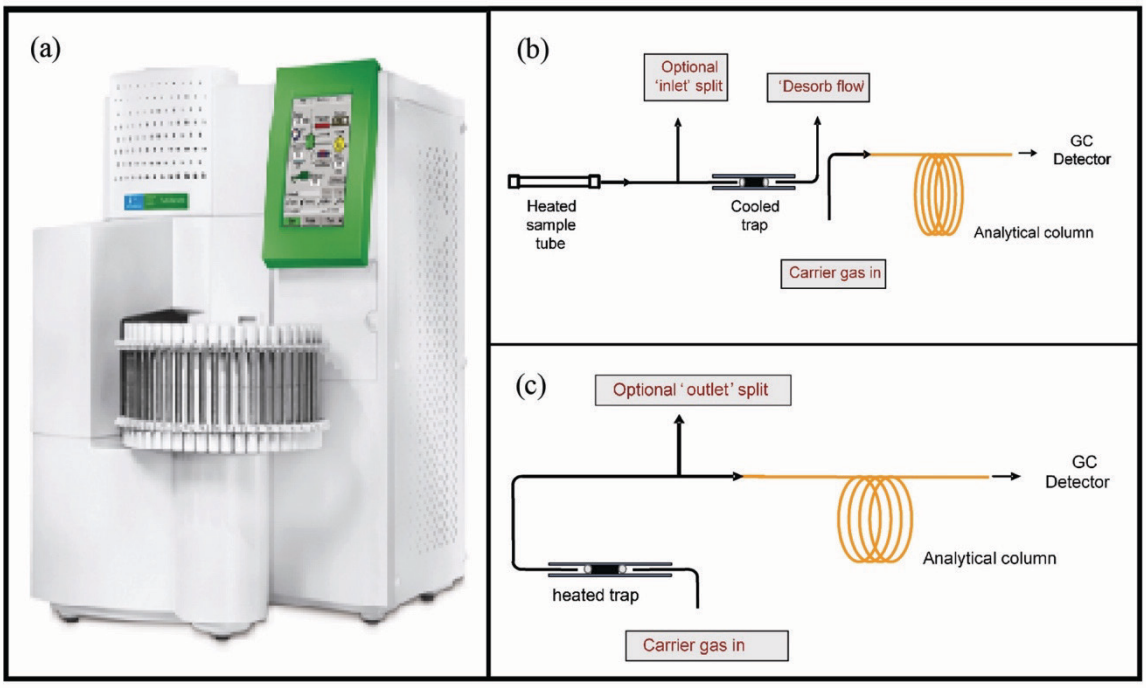

Figure 4-4: Schematic principle of thermodesorption (a) Turbomatrix 350 ATD, (b) Desorption of the sample from the tube to the trap, (c) Transfer of the analytes from the trap to the column by heating ("ATD Quick Start" Guide by Perkin Elmer)

Optimization of ATD parameters

The use of this thermal desorption apparatus requires the optimization of several parameters (composition of the trap, duration and desorption temperature, inert gas flow rate for the desorption and split, etc.) to achieve a quantitative transfer of all of the analytes trapped on the tubes (or only a portion if a split inlet flow is operated) during sampling (Liaud, 2014). The cold trap chosen was the "Air monitoring Trap" (Perkin Elmer) because its composition is equivalent to that of the adsorbent used for air sampling, and thus able to trap our target analytes (C_2-C_{12} molecules). For the "on-line" mode used for calibration, the optimal flow rate selected was 25 mL min^{-1} for a sampling duration of 20 min, thus the total sampled volume was 500 mL. For sorbent tube analysis or 2-stage-desorb, primary desorption (tube to trap) of the adsorbent tubes was carried out at 320°C with a helium flow rate of 25 mL min^{-1} in order to maintain consistency with the "on-line" mode. The cold trap was maintained at -30°C. During secondary desorption (trap to GC), the cold trap was rapidly heated from -30°C to 300°C at a rate of 40°C s^{-1} and maintained at this temperature for 5 min. Analytes were then injected onto the capillary column *via* a

transfer line heated at 250°C and chromatography conditions were exactly the same as the on-line analysis. The outlet split was fixed at 5 mL min^{-1}.

Gas chromatography Coupled with Flame Ionization Detector (GC-FID)

Analysis of the full range of VOCs (except heavy aldehydes) was performed with ATD-GC-FID (Figure 4-5). The analysis of light VOCs was made possible because GC-FID has the advantage of separating light VOCs on a second analytical column.

Indeed, the gas phase chromatograph Clarus® 580 (Perkin Elmer) is equipped with 2 columns and 2 detectors. This analytical chain is equipped with a switching system, Dean switch, which permits the use of one or two chromatographic columns connected in series.

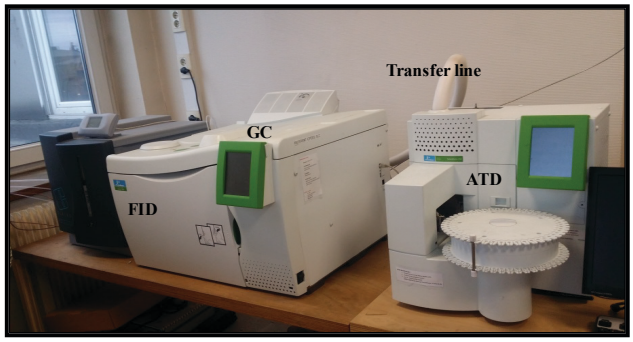

Figure 4-5: ATD-GC-FID

The schema for the analytic chain is presented in Figure 4-6. The columns chosen for this study were selected because they allow the separation of a wide range of VOCs of a relatively weak polarity:

- Column 1: Restek Rt®-Q-BOND, 100 % divinylbenzene, 30 m × 0.32 mm ID × 10 µm (film thickness). This nonpolar column is adapted to the separation of light hydrocarbons consisting of 2 to 6 carbons.

- Column 2: Perkin Elmer Elite-1, 100% polydimethylsiloxane, 60 m × 0.25 mm ID × 0.25 µm (film thickness). This non-polar column, adapted for the separation of a wide range of VOCs, was used to separate the heavier VOCs (nC > 6).

After a first separation on the Elite-1 column (column 2), a Dean switch system allows the division of the sample into 2 fractions depending on the properties of the analytes, such that VOCs are either transferred to the first FID for detection, through a restrictor, or to the

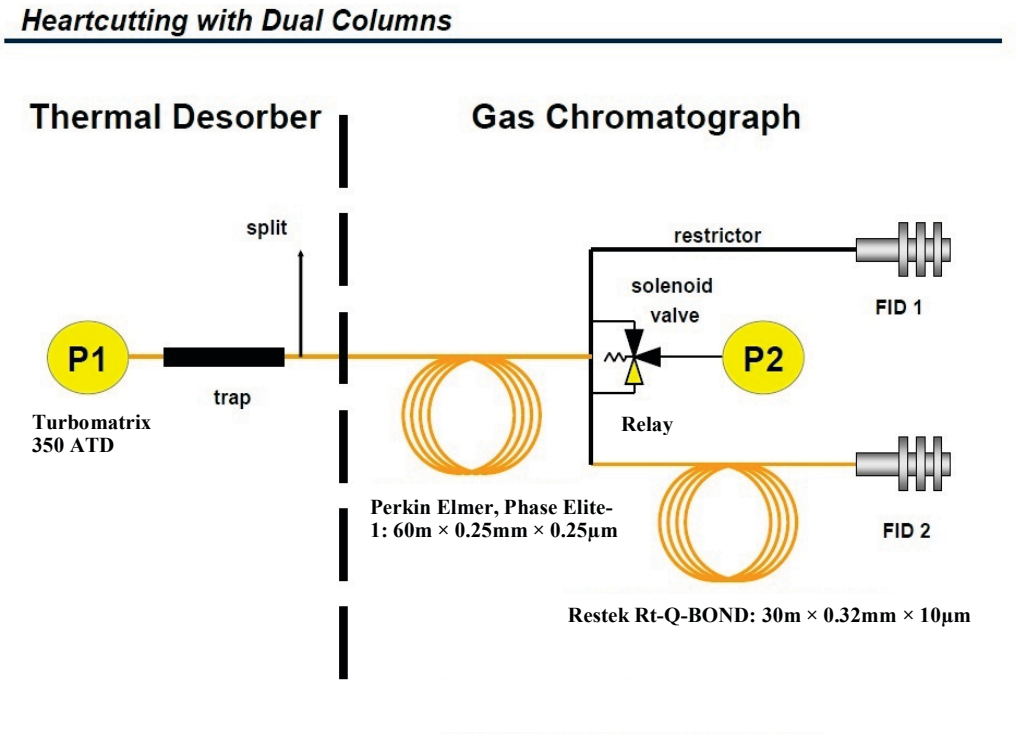

Figure 4-6: Illustration of the analytical chain of ATD-GC-FID (Perkin Elmer)

Rt®-Q-BOND column in order to separate out light VOCs (Figure 4-7). The flow of helium through the system is maintained at 1.2 mL min^{-1}. At the exit of each of the 2 columns, VOCs were detected by an FID. Detectors were operated by hydrogen gas at a flow rate of 40 mL min^{-1} and synthetic pure air at a flow rate of 400 mL min^{-1}; the temperature of flame was maintained at 250°C. The attenuation was fixed to -6, and the offset value was set to 5 mV. The optimization of the chromatographic separation was conducted by Liaud (2014) and was as follows:

(i) The oven program had the following temperature ramp (Table 4-2): initial temperature 40°C hold 5 min, 10°C min^{-1} to 100°C, 2°C min^{-1} to 120°C, 10°C min^{-1} to 180°C hold 10 min.

(ii) The analysis lasted for 37 min.

(iii) The Dean switch time was set to 10.6 minutes and operated as follows: light compounds (C_2-C_6) were eluted first from 0 to 10.6 min on the second column, while the heavier compounds (pentanal to d-Limonene) eluted after 10.6 min on the first column. Co-elutions at the RT®-Q-Bond column involved ethene and acetylene (t = 9.6), n-butane and cis-2-butene (t = 17.1), as well as n-pentane and cis-2-pentene (t = 25.1).

Table 4-2: Temperature Gradient for GC-FID

Instrument Name: Clarus® 580	
Run Time: 37 min	
Dean switch: 10.6 min	
Oven Temperature Program:	**Initial Temperature**: 40°C for 5.00 min
	Ramp 1: 10°C/min to 100°C, hold for 0.00 min
	Ramp 2: 2°C/min to 120°C, hold for 0.00 min
	Ramp 3: 10°C/min to 180°C, hold for 10.00 min

The identification of VOCs was based on the matching of retention times, and the quantification was performed by the use of the external standard method using the software *Totalchrom*.

Although FID is a universal detector, mass spectrometry has also been used to allow the identification of unknown VOCs emitted in the field campaigns, and to measure the concentrations of compounds of particular interest such as benzene and heavy aldehydes, which were not quantified using GC-FID.

Gas Chromatography Coupled with Mass Spectrometry (GC-MS)

GC-MS is the basis for many Environmental Protection Agency (EPA) official methods, and its greatest use is the determination of volatile and semi-volatile organic compounds in complex mixtures as well as waters, soils, and other environmental samples (Sneddon *et al.*, 2007). By combining the two techniques, gas chromatography and mass spectrometry, GC-MS enables the evaluation of a gas mixture both qualitatively and quantitatively. The ability of the mass spectrometer to identify unknowns in the full scan mode and to quantitate known target analytes makes it one of the most powerful tools available for trace level quantitative analysis in the laboratory today.

In our study (see Figure 4-7), GC-MS was implemented to detect and identify the unknown VOCs emitted from aircraft sources as well as VOCs present within or outside the airport vicinity. Afterwards, it was used to identify and quantify heavy alkanes (C_8-C_{14}), heavy aldehydes (C_9-C_{10}), monoaromatics, and chlorinated alkenes in a single run. Due to the presence of blank residues that co-eluted with benzene using GC-FID (Liaud, 2014), it was only possible to accurately quantify benzene using GC-MS.

In this work, the analytical system used is equipped with a gas chromatograph, Agilent 6890N Network coupled to a mass selective detector, Agilent 5973N Network MSD (Figure 4-7).

Figure 4-7: ATD-GC-MS used in this work

GC (Agilent 6890N Network)

Separation was achieved using a DB-5MS column (Agilent), 60 m × 0.25mm × 1 μm, constituted 95% of dimethylpolysiloxane groups and 5% of phenyl groups. Like the column used in GC-FID, this column is non-polar and thus suitable for the separation of the majority of target VOCs. For the sake of consistency between the two analytical systems, helium flow rate through the system was maintained at 1.2 mL min^{-1}.

Table 4-3 below summarizes the final gradient settings adapted. The initial oven temperature was maintained at 40°C for 5 min, increased by 5°C min^{-1} for 2.60 min up to 80°C, increased by 1ºC min^{-1} up to 90°C, increased by 5°C min^{-1} up to 180°C and maintained for 5 min, and finally increased by 30°C min^{-1} to 280°C and maintained for 1 min, for a total run time of 50.33 min. It should be noted that the absence of a second type of column Rt-Q-BOND in this system does not allow the separation of lighter compounds.

Table 4-3: Temperature gradient chosen for GC-MS

Instrument Name: Agilent 6890 N	
Run Time: 50.33 min	**Initial Temperature**: 40°C for 5.00 min
Oven Temperature Program:	**Ramp 1**: 5°C/min to 80°C, hold for 0.00 min
	Ramp 2: 1°C/min to 90°C, hold for 0.00 min
	Ramp 3: 5°C/min to 180°C, hold for 5.00 min
	Ramp 4: 30°C/min to 280°C hold for 1.0 min

MSD (Agilent 5973N Network MSD)

Within the MSD, the analyzer is divided into four components: Ion source, mass filter, detector, heaters, and radiators (Agilent Technologies, 2016). The ionization source used was electron ionization (EI) with an ionization energy fixed at 70 eV. This source is widespread. The classical procedure involves shooting highly energetic electrons, emitted by a filament and guided by a magnetic field, on a gaseous neutral. This induces ionization by the ejection of one electron generating a molecular ion, a positive radical ion, as shown in the following equation (J.T. Watson *et al.*, 2007):

$$M + e^{-}(70eV) \rightarrow M^{\bullet +} + 2e^{-} \quad (4\text{-}1)$$

The radical cation formed ($M^{\bullet +}$) is called a molecular ion. Electron ionization is known as a "harsh" technique because of the degree of fragmentation generated. Indeed, from this molecular ion, it is possible to generate other fragments of lower masses, called ion fragments. Although the mass spectra are very reproducible, EI causes extensive fragmentation so that the molecular ion is not observed for many compounds. The positive voltage on the repeller pushes the positive ions into the lens stack, where they pass through several electrostatic lenses. These lenses concentrate the ions into a tight beam, which is directed into the mass filter and are separated according to their mass to charge ratio (m/z). In our case, the mass filter is a single quadrupole. At the output of the mass filter, the detector collects the ions. The detector in the MSD analyzer is a high-energy conversion dynode (HED) coupled to an electron multiplier (EM). It generates an electronic signal proportional to the number of ions striking it, and the signal is expressed by relative abundance. The electron multiplier is the most common detector. It has a good sensitivity with a high amplification due to the secondary electron formation by the angle (inclination) of dynodes. However, its lifetime is limited. The radiators control the

distribution of heat in the analyzer. For this study, the mass spectrometer was used in full scan mode (m/z 40–400 a.m.u.).

MSD ChemStation software (Agilent, USA) was used to acquire mass spectrometric data. The qualitative identification of VOCs was based on the comparison of the mass spectra of the detected compounds in the total ion current (TIC) chromatogram with spectra in the NIST library. For quantitative assessment, the extracted ion chromatograms (EICs) were recovered with the target ions and quantification was performed by the use of the external standard method. The most specific fragment ion in the spectra of each identified VOC was determined as the target ion.

- Calibration and Analytical Performance

Calibration curves were prepared using the 2 modes of injection of the ATD, "on-line" mode for gaseous standards, and 2-stage desorb mode for liquid standards. It has been shown by Liaud *et al.* (2014) that these 2 injection modes give equivalent results in terms of calibration and sensitivity for BTEX. The method of the ATD in both injection modes, "online" and 2-stage desorb, are identical for the analysis in GC-FID and GC-MS.

Calibration from Liquid Standards (Liquid Spiking)

Liquid standard concentrations ranged from 0.2 to 100 mg L^{-1} for light aldehydes, ketones, and d-Limonene; 20 to 100 mg L^{-1} for n-nonane and n-undecane; and 100 to 500 mg L^{-1} for nonanal and decanal. As for the mixture D3710 (Annex 4-1), which contains the other heavy alkanes and 4 monoaromatics, the concentrations varied between 1.5-7 mg L^{-1} to 8.5-39 mg L^{-1}. The variation in concentration for each VOC is according to the mass fraction of each component in the mixture. For BTEX, 1,2,4-trimethylbenzene, 1,4-dichlorobenzene, and styrene, the standard concentrations varied between 2.5 and 40 mg L^{-1}. The standard concentrations varied between 25 and 400 mg L^{-1} for tetrachloroethene and trichloroethene.

Cartridge (Carbopack™ B) spiking with liquid standards was performed with 2 methods, depending on the physical properties (boiling point) of the liquid analytes injected.

Automatic Liquid Spiking

In order to prepare calibration curves for light aldehydes and ketones, d-limonene, chlorinated alkenes, and monoaromatics, automatic spiking was adopted to deposit small volumes (1 to few µL) of previously prepared liquid standard solutions on the adsorbent tubes. This method, suggested by the TO-17 protocol of the US EPA (U.S. Environmental Protection Agency, 1999), was optimized by Liaud *et al.* (2014) with a spiking time of 10 min. This technique was used because (i) it solves the problem of the injection of an excessive amount of solvent (10-20 µL) that is difficult to be eliminated and (ii) it minimizes the uncertainty in the volume manually deposited upon using µ-pipettes when depositing volumes of less than 10-20 µL.

Automatic liquid spiking was carried out through a home-made converted GC injection port, ThermoFinnigan AS3000 (Milan, Italy) with a syringe as illustrated in Figure 4-8. Carbopack™ B adsorbent tube and the injector were connected by means of a 40 cm deactivated silica column, with a ¼ inch stainless steel connection fitted with a polytetrafluoroethylene (PTFE) ferrule. The temperature of the injector and oven were set at 250°C and 30-35°C, respectively. A 30 kPa nitrogen pressure was applied at the head of the column to make sure that the adsorbent tube was traversed by a flow rate of about 50 mL min^{-1}.

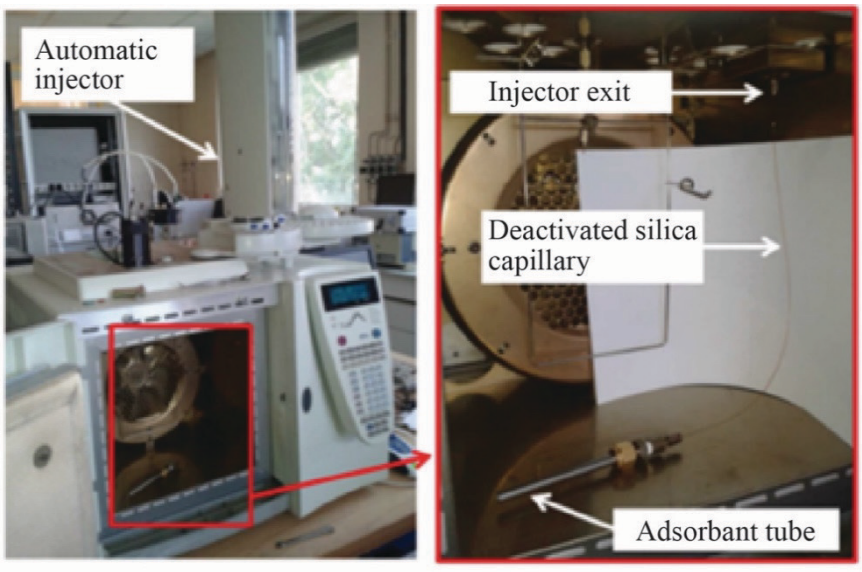

Figure 4-8: Automatic liquid spiking system, taken from Liaud (2014)

Manual Liquid Spiking

Due to the high boiling point of heavy alkanes (C_9-C_{14} in specific) and heavy aldehydes (C_9-C_{10}), it was not possible to perform liquid spiking for these VOCs using the converted injection port, and automatic spiking was replaced with manual spiking. 10 µL of the previously prepared standard solutions were manually injected with a micropipette, followed by purging the spiked tube for 10 min with N_2 at a flow rate of 50 mL min^{-1} to remove excess methanol (Figure 4-9). In a previous study done by Liaud *et al.* (2014) on BTEX, results showed that the overall BTEX were trapped with no losses after purging and upon the evaluation of the breakthrough volume.

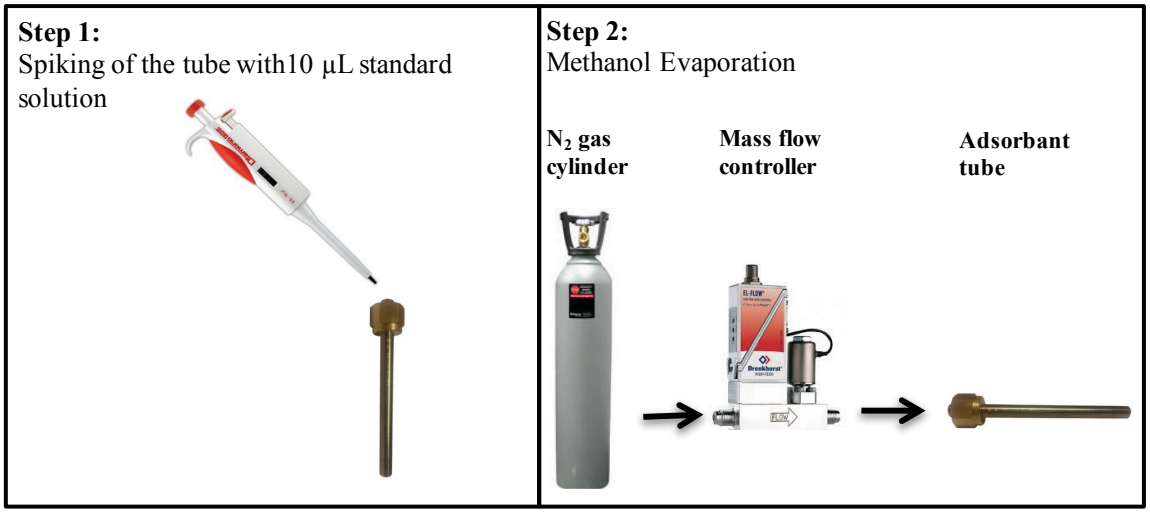

Figure 4-9: Schematic of manual liquid spiking

Calibration from Gaseous Mixtures (On-line Calibration)

To perform calibration curves from gaseous standards, on-line calibration was adapted. The standard gas cylinder containing light alkanes, acetylene, and alkenes was diluted from a concentration of 100 ppb with nitrogen gas (99.999% purity), in order to reach concentrations of the order of 0.1 to 20 ppb conventionally encountered in ambient air. To complete the dilution bench, two mass flow controllers were used. During dilution, the dynamic range used was 0-5 L min^{-1} for nitrogen and 0-100 mL min^{-1} for the mixture of alkanes, alkenes, and acetylene. The total flow rate generated for on-line calibration was fixed at 500 mL min^{-1}. The uncertainty in the mass flow controllers on full scale was 0.1%, whereas the accuracy on the measured value was 0.5%.

Analytical Performances: Calibration Curves and Limits of Detection

Calibration curves were obtained by plotting the peak areas versus the real injected mass for the standards (Figures 4-10 and 4-11). These plots were fit to straight lines using linear regression analysis. The linear calibration parameters were calculated by least-squares regression, and the determination coefficient (R^2) was used for estimation of linearity.

The Limit of Detection (LOD) (ng) was calculated as the quantity of analyte (ng) that will yield a signal to noise ratio (S/N) equal to 3, where S is the peak intensity (a.u.) and N is the mean noise signal (a.u.) before and after the retention time of the compound giving rise to the peak (Shrivastava and Gupta, 2011). Thus, LOD_i(ng) was determined according to the following equation:

$$LOD_i(ng) = \frac{3 \times N \times m_{standard}}{S_i} \quad (4\text{-}2)$$

where S_i is the height of the peak, corresponding to the component concerned, measured from the maximum of the peak to the extrapolated baseline of the signal, N is the peak-to-peak background noise, and $m_{standard}$ is the injected mass (ng) of the standard. For GC-MS, LOD calculations were performed with extract ion chromatograms.

Two calibrations were prepared for GC-FID (June and October 2014) and GC-MS (June and September 2015) to perform quantifications for the campaigns done at different time intervals. All the analytical parameters and the type of calibration chosen for each VOC are listed in Tables 4-4 to 4-7.

It is important to note that for GC-FID, it was not possible to perform standard calibrations for n-nonane, n-decane, n-dodecane, n-tridecane, and n-tetradecane (due to the delay of the arrival of the standards); however, their slopes were determined by **extrapolating** the linear relationship between the slope and the carbon number for all the other n-alkanes for which calibrations were made. This was based on the fact the FID signal is proportional to the number of carbon atoms in a hydrocarbon molecule (Kallai *et al.*, 2001). An example of this strong linear relationship (r = 0.95) is illustrated in Figure 4-10, which depicts the relationship between n-alkane slopes and the corresponding carbon number for the calibrations performed in June 2014. Accordingly, slopes for higher alkanes can be extrapolated using the following equation:

$$y = -131.25x + 5922.9 \quad (4\text{-}3)$$

where y is the slope of the n-alkane and x = n i.e. its carbon number. The LODs of these compounds were similarly extrapolated by determining the linear relationship between LODs and n-alkane carbon number.

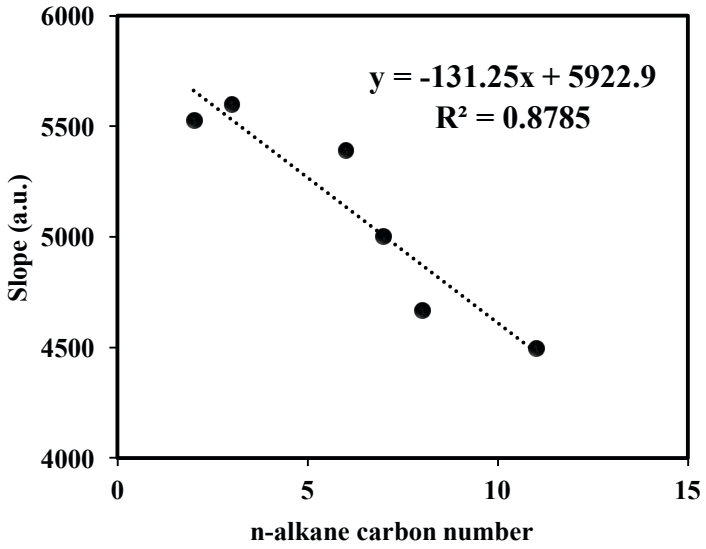

Figure 4-10: The linear relationship between n-alkane slopes vs carbon number in order to extrapolate slopes for higher alkanes (June 2014).

Analytical Performances obtained by GC-FID

Calibration curves performed by GC-FID showed excellent linearity (Figure 4-11), with a determination coefficient (R^2) equal to 0.99 for all VOCs except for propanal (0.98) and acetone (0.98), for both June and October 2014 calibrations (Tables 4-4 and 4-5).

LOD values varied between 0.1 (acetone) and 0.8 ng (hexanal) for most compounds. However, higher LOD values were observed for acrolein and propanal (aldehydes). LOD values (October calibration) were transposed to airborne concentrations for a sampling volume of 0.3 L and 3 L to correspond to both sampling techniques used in the October campaign. For a sampling volume of 3 L, LOD values (µg m^{-3}) varied between 0.04 and 0.47 µg m^{-3} for acetone and propanal respectively for both calibrations (Tables 4-4 and 4-5). These values are similar to those obtained by other studies (except for light aldehydes) and are convenient for quantification of compounds in air (Hollender *et al.*, 2002; Lai *et al.*, 2004). Blank values used and the uncertainties in concentrations are also listed in the tables.

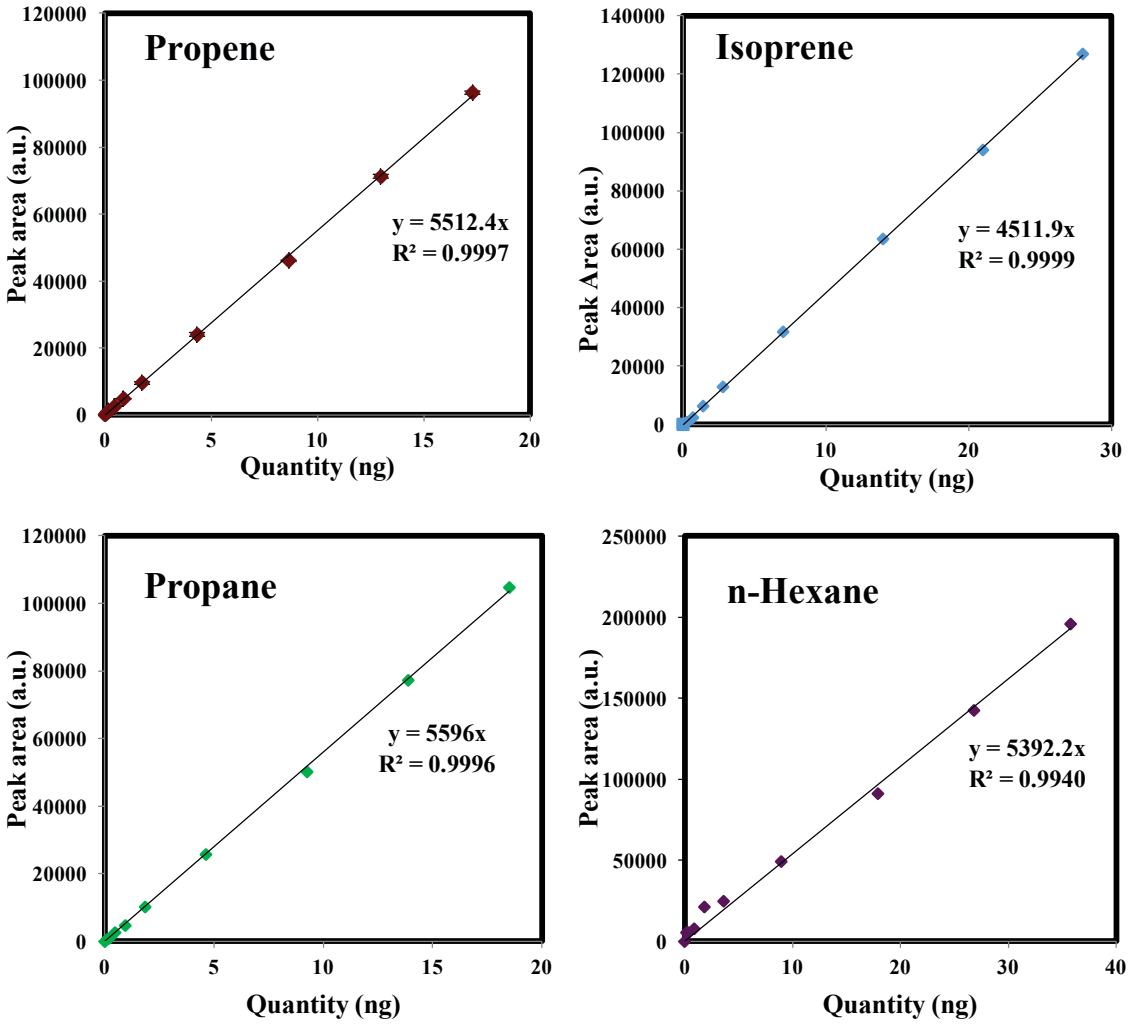

Figure 4-11: GC-FID calibration curves (on-line calibration done in June 2014)

Table 4-4: GC-FID analytical performance parameters (June 2014)

Family	VOC	Linear Regression[a]	Determination Coefficient R^2	LOD[b] (ng)	LOD[c] (µg m^{-3})	Blank[d] (ng)
		LIQUID SPIKING				
HEAVY ALKANES (C_8-C_{14})	n-Octane	y=4666.7x	0.9992	0.10	0.04	0.01
	n-Nonane	y=4741.7*x	-	0.10**	0.03	0.09
	n-Decane	y=4610.4*x	-	0.08**	0.03	0.03
	n-Undecane	y=4496.6x + 1468.6	0.9989	0.10	0.05	0.00
	n-Dodecane	y=4347.9*x	-	0.06**	0.02	0.08
	n-Tridecane	y=4216.7*x	-	0.05**	0.02	0.08
	n-Tetradecane	y=4085.4*x	-	0.03**	0.01	0.00
LIGHT ALDEHYDES (C_2-C_6)	Acrolein	y =383x + 2278	0.9955	1.40	0.46	4.53
	Propanal	y=616x + 543	0.9812	1.40	0.47	3.64
	Butanal	y=1647x + 2328	0.9991	0.40	0.12	0.97
	Pentanal	y=2901x	0.9930	0.50	0.16	0.29
	Hexanal	y=2903x	0.9971	0.80	0.26	0.38
LIGHT KETONES	Acetone	y=1248x	0.9832	0.10	0.04	4.62
	2-Butanone	y=2402x + 4308	0.9991	0.40	0.15	0.46
TERPENE	D-Limonene	y=5163x	0.9977	0.20	0.05	0.01
		ON-LINE				
LIGHT ALKANES (C_2-C_7)	Ethane	y=5528x	0.9989	0.20	0.06	0.00
	Propane	y=5596x	0.9996	0.20	0.06	0.02
	Isobutane	y=5029x	0.9998	0.40	0.05	0.00
	n-Butane+cis-2-Butene	y=11020x	0.9997	0.10	0.14	0.07
	Isopentane	y=3861x	0.9986	0.60	0.21	0.00
	n-Pentane+cis-2-Pentene	y=10228x	0.9999	0.10	0.05	0.02
	n-Hexane	y=5392x	0.9940	0.20	0.06	0.39
	n-Heptane	y=5001.2x	0.9998	0.10	0.03	0.01
ACETYLENE/ ALKENES (C_2-C_6)	Ethene +Acetylene	y=3971x	0.9990	0.20	0.06	0.80
	Propene	y=5512x	0.9997	0.10	0.04	1.23
	1-Butene	y=5426x	0.9998	0.10	0.05	0.68
	1,3-Butadiene	y=5070x	0.9997	0.20	0.06	0.20
	Trans-2-butene	y=4852x	0.9997	0.20	0.07	0.06
	1-Pentene	y=4838x	0.9994	0.30	0.09	0.04
	Trans-2-pentene	y=5016x	0.9999	0.30	0.09	0.40
	Isoprene	y=4512x	0.9999	0.40	0.12	0.12
	1-Hexene	y=5036x	0.9999	0.30	0.09	0.33

*Extrapolated slopes (ng)
**Extrapolated LOD (ng)
[a]Slopes in ng
[b]Instrumental LOD converted to injected quantity
[c]LOD transposed to airborne concentrations for a sampling volume of 3L
[d]Average blank

Table 4-5: GC-FID Analytical performance parameters (October 2014)

Family	VOC	Linear Regression[a]	Determination Coefficient R^2	LOD[b] (ng)	LOD[c] (µg m^{-3})	Δc/c[d] (%)	Blank[e] (ng)	LOD[f] (µg m^{-3})	Blank[g] (ng)
LIQUID SPIKING									
HEAVY ALKANES (C^8-C^{14})	n-Octane	y=4104	0.9993	0.1	0.4	23.6	0.01	0.04	0.01
	n-Nonane	y=4259*x	-	0.1**	0.3	-	0.05-0.12	0.03	0.05
	n-Decane	y=4216*x	-	0.08**	0.3	-	0.02-0.04	0.03	0.04
	n-Undecane	y=3875x+1468	0.9989	0.1	0.5	24.0	0.00	0.05	0.00
	n-Dodecane	y=3859*x	-	0.06**	0.2	-	0.02-0.12	0.02	0.02
	n-Tridecane	y=3726*x	-	0.05**	0.2	-	0.04-0.11	0.02	0.04
	n-Tetradecane	y=3593*x	-	0.03**	0.1	-	0.00	0.01	0.00
LIGHT ALDEHYDES (C_2-C_6)	Acrolein	y =330x + 2278	0.9955	1.4	4.58	24.70	1.76-3.56	0.46	0.00
	Propanal	y=530x + 543	0.9812	1.4	4.69	24.88	0.70-3.62	0.47	0.68
	Butanal	y=1419x + 2328	0.9991	0.4	1.24	25.02	0.02-0.43	0.12	0.00
	Pentanal	y=2500x	0.9930	0.5	1.61	22.99	0.00-0.39	0.16	0.23
	Hexanal	y=2502x	0.9971	0.8	2.61	23.65	1.37-3.3	0.26	1.18
LIGHT KETONES	Acetone	y=1076x	0.9832	0.1	0.44	30.40	3.50-4.87	0.04	2.59
	2-Butanone	y=2226x+4308	0.9991	0.4	1.46	25.27	1.76-3.56	0.15	0.51
TERPENE	D-Limonene	y=5163x	0.9977	0.2	0.54	20.92	0.00-0.07	0.05	0.00
ON-LINE									
LIGHT ALKANES (C_2-C_7)	Ethane								
	Propane	y=4817x	0.9989	0.2	0.61	22.08	0.00-0.12	0.06	0.06
	Isobutane	y=5222x	0.9998	0.2	0.52	21.15	0.01-0.09	0.05	0.04
	n-Butane+cis-	y=4923x	0.9999	0.4	1.40	21.42	0.00-0.31	0.14	0.00
	2-Butene	y=10910x	0.9999	0.1	0.40	20.82	0.10-0.30	0.04	0.06
	Isopentane	y=3733x	0.9997	0.6	2.11	22.04	0.23-0.46	0.21	0.01
	n-Pentane+cis-	y=10191x	0.9999	0.1	0.53	21.25	0.06-0.1	0.05	0.04
	2-Pentene	y=5125x	0.9995	0.2	0.51	23.47	0.50-1.68	0.05	0.74
	n-Hexane	y=4678	0.9995	0.1	0.3	24.50	0.01	0.03	0.01
	n-Heptane								
ACETYLENE/ ALKENES (C_2-C_7)	Ethene	y=3971x	0.9986	0.1	0.47	21.86	0.02-5.22	0.05	0.00
	+Acetylene	y=5512x	0.9998	0.1	0.43	21.29	1.90-2.35	0.04	1.24
	Propene	y=5426x	0.9998	0.1	0.47	21.64	1.06-1.42	0.05	0.97
	1-Butene	y=5070x	0.9999	0.2	0.56	20.90	0.35-0.48	0.06	0.29
	1,3-Butadiene	y=4852x	0.9999	0.2	0.74	20.42	0.06-0.17	0.07	0.13
	Trans-2-butene	y=4838x	0.9999	0.3	0.89	20.59	0.63-0.82	0.09	0.49
	1-Pentene	y=5016x	0.9999	0.3	0.87	21.05	0.02-0.07	0.09	0.04
	Trans-2-pentene	y=4512x	0.9999	0.4	1.20	20.48	0.23-0.46	0.12	0.32
	Isoprene	y=5036x	0.9999	0.3	0.88	21.60	0.35-0.76	0.09	0.40
	1-Hexene								

[a]Slopes in ng
*Extrapolated slopes (ng)
**Extrapolated LOD (ng)
[b]Instrumental LOD converted to injected quantity
[c]LOD transposed to airborne concentrations for a sampling volume of 0.3L
[d]Uncertainty corresponds to "30 sec × 6" samples
[e]Blank corresponds to the series used for "30 sec × 6" samples
[f]LOD transposed to airborne concentrations for a sampling volume of 3L
[g]Blank corresponds to the series used for "30 min" samples

Analytical Performances obtained by GC-MS

The liquid calibration curves performed by GC-MS showed also very good linearity as shown in Figure 4-12.

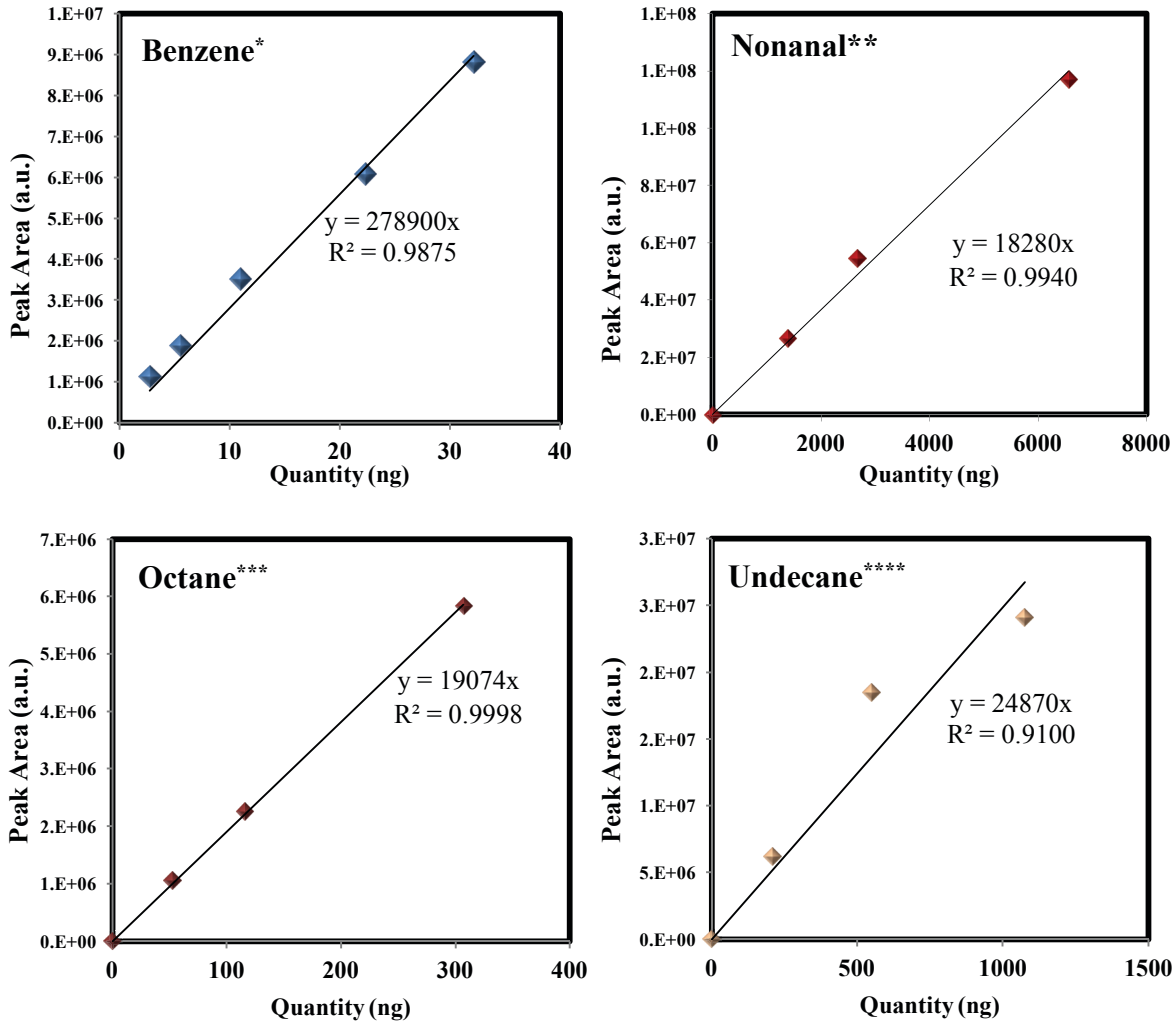

Figure 4-12: GC-MS Calibration Curves (Liquid Spiking done in June 2015)
*Target Ion: 78, **Target Ion: 98, ***Target Ion: 114, ****Target Ion: 156

Table 4-6: GC-MS Analytical Parameters (June 2015)

Family	Compound	Target Ion	Linear Regression	Determination Coefficient R^2	LOD[a] (ng)	LOD[b] (µg m^{-3})	LOD[c] (µg m^{-3})	Δc/c[d]	Blank[e] (ng)
				Manual Liquid Spiking					
Heavy Alkanes (C_7 - C_{14})	n-Heptane	100	26684x	0.9995	0.63	2.09	0.21	22.65	0.00
	n-Octane	114	19074x	0.9998	1.26	4.21	0.42	21.76	0.00
	n-Nonane	128	18297x	1	1.07	3.57	0.36	25.71	0.00
	n-Decane	142	22522x	0.9995	0.70	2.34	0.23	22.55	0.00
	n-Undecane	156	24870x	0.9100	0.73	2.43	0.24	55.76	0.00
	n-Dodecane	140	25408x	0.9121	0.42	1.41	0.14	51.90	0.00
	n-Tridecane	184	17331x	0.9900	0.63	2.10	0.21	35.53	0.00
	n-Tetradecane	198	9346x	0.9400	1.23	4.10	0.41	55.60	0.00
Heavy Aldehydes	Nonanal	98	18280x	0.9940	1.22	4.08	0.41	29.39	0.00
	Decanal	112	15779x	0.9800	0.63	2.09	0.21	22.65	0.00
Monoaromatics	Propyllbenzene	91	424081x	0.9996	0.05	0.16	0.02	22.43	0.00
	Butylbenzene	91	552788x	0.9995	0.04	0.14	0.01	22.52	0.00
				Automatic Liquid Spiking					
Benzene & Other Monoaromatics	Benzene	78	278900x	0.9875	0.05	0.18	0.02	24.77	2.15
	Toluene	91	387547x	0.9923	0.06	0.20	0.02	22.18	0.12
	Ethylbenzene	91	414845x	0.9984	0.05	0.18	0.02	24.59	0.00
	m, p-Xylene	91	639164x	1	0.07	0.22	0.02	23.55	0.00
	o-Xylene	91	327120x	0.9980	0.07	0.22	0.02	24.09	0.00
	1,2,4-TMB	105	343520x	0.9976	0.06	0.19	0.02	24.57	0.00
	1,4-DCB*	146	294758x	1	0.06	0.21	0.02	22.91	0.00
Chlorinated Alkenes	Trichloroethene	130	93970x	0.9995	0.18	0.59	0.06	22.00	0.00
	Tetrachloroethene	164	102600x	0.9998	0.23	0.76	0.08	21.34	0.00

[a]Instrumental LOD converted to injected quantity
[b]LOD transposed to airborne concentrations for a sampling volume of 0.3 L
[c]LOD transposed to airborne concentrations for a sampling volume of 3 L
[d]Uncertainty corresponds to "30 sec × 6" samples
[e]Average blank
*1,4-Dichlorobenzene

Table 4-7: GC-MS Analytical Parameters (September 2015)

Family	VOC	Target Ion	Linear Regression	Determination Coefficient R^2	LOD[a] (ng)	LOD[b] (µg m^{-3})	Blank[c] (ng)
Manual Liquid Spiking							
Heavy Alkanes (C_7 - C_{14})	n-Heptane	100	35790x	0.9881	0.90	0.30	0.00
	n-Octane	114	25780x	0.9927	1.16	0.39	0.00
	n-Nonane	128	26640x	1	1.11	0.37	0.00
	n-Decane	142	31180x	0.9971	0.67	0.22	0.00
	n-Undecane	156	24780x	0.9700	0.84	0.28	0.00
	n-Dodecane	140	18390x	0.9885	1.40	0.47	0.00
	n-Tridecane	184	8095x	0.9800	4.76	1.59	0.00
	n-Tetradecane	198	3440x	0.9400	7.11	2.37	0.00
Heavy Aldehydes	Nonanal	98	33340x	0.9998	0.99	0.33	0.00
	Decanal	112	29090x	1	0.99	0.33	0.00
Monoaromatics	Propyllbenzene	91	872320x	0.9992	0.04	0.01	0.00
	Butylbenzene	91	655840x	0.9994	0.07	0.02	0.06
Automatic Liquid Spiking							
Benzene & Other Monoaromatics	Benzene	87	257950x	0.9847	0.06	0.02	39.17
	Toluene	91	315426x	0.9700	0.06	0.21	0.67
	Ethylbenzene	91	348007x	0.9780	0.07	0.02	0.00
	m.p-Xylene	91	527160x	0.9800	0.09	0.03	0.10
	o-Xylene	91	272660x	0.9813	0.14	0.05	0.39
	Styrene	104	225900x	0.9800	0.13	0.04	0.00
	1,2,4-TMB	105	286520x	0.9695	0.07	0.02	1.12
	1,4-Dichlorobenzene	146	243970x	0.9700	0.12	0.04	0.00
Chlorinated Alkenes	Trichloroethene	130	78442x	0.9807	0.22	0.07	0.01
	Tetrachloroethene	164	91042x	0.9756	0.29	0.10	0.00

[a]Instrumental LOD converted to injected quantity
[b]LOD transposed to airborne concentrations for a sampling volume of 3 L
[c]Average blank

Tables 4-6 and 4-7 list the analytical parameters for the calibrations of June and September 2015 using GC-MS. For June calibration, R^2 values were 0.99 for all VOCs except for n-undecane (0.9100), n-dodecane (0.9121), and n-tetradecane (0.9400). LOD values ranged between 0.05 ng for benzene, ethyl benzene, and propyl benzene and 4.1-4.21 ng for heavy alkanes (4.1 ng for tetradecane and 4.21 ng for octane). For September calibrations, R^2 values were greater or equal to 0.9700 for all VOCs except for tetradecane (0.9400). LOD values ranged between 0.06 ng for benzene and 7.11 ng for n-tetradecane. LOD values for most of the VOCs are similar to those obtained by other studies, except for heavy alkanes, which possess slightly higher LOD values (Chin and Batterman, 2012; Lai *et al.*, 2004; Parra *et al.*, 2008; Volden *et al.*, 2005).

LOD values were transposed to airborne concentrations (µg m^{-3}) for sampling volumes of 0.3 L and 3 L to correspond to both sampling techniques used and detailed above in this chapter. For a sampling volume of 3 L, LOD values varied between 0.02 and 0.42 µg m^{-3} for benzene and octane respectively for June calibrations; while they varied between 0.02 and 2.37 µg m^{-3} for benzene and tetradecane respectively for September calibrations (Tables 4-4 and 4-5). Blank values used and the uncertainties in the concentrations are presented in Tables 4-4 and 4-5.

- Evaluation of Uncertainty (Calibration and sampling)

The uncertainty of the measurement of the final concentration was evaluated as follows:

$$\frac{\Delta C}{C} = \frac{\Delta a}{a} + \frac{\Delta b}{b} + \frac{\Delta V_{sample}}{V_{sample}} \quad (4\text{-}4)$$

Where:

- $\frac{\Delta a}{a}$ and $\frac{\Delta b}{b}$ are the relative errors on the slope and intercept (if any) by considering the equation of the fit straight line obtained during calibration: $y = ax + b$, where Δa and Δb are equal to 2 times the value of the standard deviations of the slope and intercept, respectively.
- $\frac{\Delta V_{sample}}{V_{sample}}$ is the uncertainty of the sampled volume (V) and was calculated according to the following equation:

$$\frac{\Delta V_{sample}}{V_{sample}} = \frac{\Delta D_{sample}}{D_{sample}} + \frac{\Delta t}{t} = \frac{0.003 D_{set} + 0.01 D_{max}}{D_{set}} + \frac{\Delta t}{t} \quad (4\text{-}5)$$

Where:

V = D × t

0.3 % = precision on the measurement of the mass flow controller

1 % = precision on the full scale of the mass flow controller

D_{max}, the maximum flow rate delivered by the mass flow controller (500 mL min^{-1})
D_{set}, the flow rate fixed (set) during sampling (100 mL min^{-1} in our case)

Considering that 3 s was the individual time uncertainty for a given sampling since the fluctuations of the flow rate were observed during the first 3 seconds, $\frac{\Delta V_{sample}}{V_{sample}}$ was calculated as follows:

(i) In the case of "30 s×6"-sampling:

$$\frac{\Delta t}{t} = \frac{3\times6}{180}\times100 = 10\%$$

Thus, the uncertainty of the sampled volume was:

$$\frac{\Delta V_{sample}}{V_{sample}} = 0.53\% + \ 10\% = 10.53\ \%$$

(ii) In the case of 30-minute sampling:

$$\frac{\Delta t}{t} = \frac{3}{1800} \times 100 \ = 0.16\%$$

Thus, the uncertainty of the sampled volume was:

$$\frac{\Delta V_{sample}}{V_{sample}} = 0.53\% + \ 0.16\% = 0.69\ \%$$

Using equation (4-4), the uncertainty of the concentrations measured by the two main sampling techniques used in this thesis was determined. In our case, the uncertainty of the flow rate $\frac{\Delta D_{sample}}{D_{sample}}$ is equal to 0.53%, and the fluctuations of the flow rate were observed during the first 3 seconds. Tables 4-5 and 4-6 present the values of the uncertainty of the calculated concentrations using GC-FID and GC-MS respectively for the "30 s × 6"-technique. For GC-FID (Table 4-5), the uncertainty of the measured concentrations ranged between 21 and 25% for most of the VOCs except for acetone (30%). For GC-MS (Table 4-6), the uncertainty of the measured concentrations ranged between 21 and 26%, except for n-undecane (56%), n-dodecane (52%), and tetradecane (56%), which possess lower R^2 values.

4.2 Sampling and Analysis of NO_2

In order to simultaneously assess the spatial distribution of nitrogen dioxide in ambient air across a wider spatial area, within or away from the airport vicinity, and to measure NO_2 concentrations inside the airport buildings, sites were equipped with a network of passive diffusion tube (PDT) samplers, Passam tubes, for the measurement of average NO_2 concentrations. The collected NO_2 were determined spectrophotometrically based on the well-established Saltzman method (Saltzman, 1954).

4.2.1 Passive Diffusion Tubes (PDTs) for NO_2 Measurements

NO_2 is usually measured either by using continuous measurement techniques such as chemiluminescence analysers, or by using passive/diffusive samplers (Serevicien *et al.*, 2014). However, the continuous measurements involve costly equipment and require continuous maintenance, calibration, and electricity. Passive sampling has been proven to be a practical alternative for atmospheric monitoring at low cost and high spatial resolution; because passive samplers are: (1) small and lightweight, (2) unobtrusive and thus more readily acceptable to study participants, (3) easier to use and handle (no battery or electricity is required), and (4) cost-effective (Yu *et al.*, 2008). Thus, passive sampling facilitates the assessment of air quality in remote places where no electric power nor trained human resources are available; in addition to facilitating indoor measurements where people are acting under noise restriction such as residences, school, offices, and hospitals. Passive sampling has been frequently used in recent simulations with mathematical models and scenario-building on regional and global scales, as well as in studies of environmental personal exposure (Campos *et al.*, 2010). For all these reasons, it has been chosen for the measurement of NO_2 concentrations in this thesis.

A passive/diffusive sampler is a device capable of taking samples of gases or vapors to the collection medium from the atmosphere at a rate controlled by a physical process, such as gaseous diffusion through a static air layer or a porous material and/or permeation through a membrane, but does not involve the active movement of air through the device (Brown, 2000). The driving force is the concentration gradient between the surrounding air and the absorbing surface, where the pollutant concentration is zero (Hangartner *et al.*, 1998). However, diffusive samplers have lower equivalent sampling rates than active methods and usually require relatively longer sampling times; consequently, diffusive samplers

including those used for NO_2 monitoring provide integrated but not short term concentration measurements (Yu *et al.*, 2008).

In this study, passive sampling of NO_2 was performed employing the diffusion tubes of Passam AG (Switzerland), which are passive devices requiring no power for operation (Figure 4-13). They possess a detection limit of 2.1-5.1 μg m^{-3} for short-term exposure (8 – 48 h) and a detection limit of 0.38 μg m^{-3} for long term exposure (1-4 weeks) (Yu *et al.*, 2008). Passam tubes are accredited according to ISO/IEC 17025. They are based on that of Palmes (Palmes *et al.*, 1976), which were introduced for occupational exposure monitoring but were later adapted for ambient air monitoring purposes (Campbell *et al.*, 1994; Ferm *et al.*, 1998; Gottardini *et al.*, 2008). Passam tubes have been used in several applications, such as the validation or calibration of dispersion models where input data such as emission factors or meteorological data are often inaccurate (Rava *et al.*, 2007); to measure concentrations at hot spots; to follow trends of air pollution; or for mapping of air pollution.

In our field campaigns, samplers were placed in a special shelter to be protected from rain and minimize the wind influence (Figure 4-13). Shelters were fixed by means of a cable tie. It is important to mention that we had to open the cages from both sides since, in some cases; VOC and NO_2 passive sampling was taking place inside the same cage (VOC adsorbent tubes were opened from the upper side). The other cages were open from both sides for the sake of conformity. In compliance with Passam instruction manual, and in the absence of any restrictions, samplers were exposed at heights of 2-3 m above ground in positions of unrestricted air movement. In order to avoid sampling in the NO_2 depleted boundary layer close to walls, cages were installed at free-standing columns. These

Figure 4-13: (a) NO_2 Passam passive tube (b) Plastic shelters

samplers were not easily reached by unauthorized persons. At the beginning of the sampling, the lower stopper was removed from the sampler to allow NO_2 to diffuse along the tube, until the end of the sampling period when the stopper was replaced. In our study, the duration of exposure times varied between one day and one week. After exposure, the cartridges were collected and stored in the refrigerator at -4°C until preparation for analysis in the USJ-Chemistry laboratory. Except during sampling, all samplers were kept in airtight bags.

4.2.2 DIFFUSIVE SAMPLING THEORY

Passam tubes collect NO_2 by molecular diffusion (Fick's first law of diffusion) along an inert polypropylene tube (I.D.: 9.5 mm, L: 7.4 cm) to an absorbent adjusted to capture NO_2, in this case triethanolamine ($N(CH_2CH_2OH)_3$), according to the following equation (Delgado *et al.*, 2006):

$$F = -D\frac{dC}{dL} \tag{4-6}$$

Where F is the molar flux (µg cm^{-2} min^{-1}), D is the diffusion coefficient (cm^2 min^{-1}), C is the concentration (µg cm^{-3}), and L is the diffusion path (cm).

After integration and rearrangement, the following equation can be used for calculation of the average ambient concentration C (µg cm^{-3}) using the exposure time (Palmes *et al.*, 1979):

$$C = \frac{Q \times L}{D \times A \times t} = \frac{Q}{S \times t} \tag{4-7}$$

where:

- t is the exposure time (min)
- Q (µg) is the total quantity of gas transferred along the tube (determined by chemical analysis)
- $S = \frac{D \times A}{L}$ where S is the theoretical collection/sampling rate (cm^3 min^{-1}) for the passive sampler, A is the cross-sectional area (cm^2) of the diffusion zone, L is the length of diffusion zone (cm), and D is the diffusion coefficient (cm^2 min^{-1}). For a given passive sampler, A and L are constant. Furthermore, the diffusion coefficient of a gas A (here NO_2) in a gas B (air) is also well known and constant; thus S should be constant.

4.2.3 ANALYSIS OF NO_2 USING UV-VIS

- Chemicals and Materials

The reagents sulfanilamide (SA) (99%) and N(-(1naphthyl) ethylenediamine dihydrochloride (NED 2HCL) (99%) were obtained from Aldrich. The 100-mM SA (B1) and 10-mM NED (B2) stock solutions were prepared by dissolving 20 g SA and 50 mL orthophosphate in 300 mL water; and 70 mg NED in 300 mL water, respectively. The working reagent solution was prepared by mixing (B1) and (B2) and completed to 1 L, to be later stored in a borosilicate bottle. This solution was stable for at least 3 months when stored in the dark under refrigeration. Standard solutions of nitrite were prepared from commercially ultra-pure (99.999%) sodium nitrite obtained from Aldrich.

- Technical analysis

The collected NO_2 were determined spectrophotometrically based on the well-established Saltzman method (Saltzman, 1954). Accordingly, NO_2 is transformed into nitrite ions after the reaction with triethanolamine (TEA) present in Passam tubes with 1:1 conversion; the product is identified as TEA-NO_2 (Glasius *et al.*, 1999). Afterwards, derivatization proceeds when nitrite is converted to an azo dye by means of its reaction with sulfanilamide (SA)/N(-(1naphthyl) ethylenediamine dihydrochloride (NED). The formation of the azo dye proceeds in two steps (Figure 4-14):

(R1) Diazotization: In this step, the nitrite ion reacts with SA in acidic conditions to form a diazonium compound.

(**R2**) Diazo-coupling: This step involves the coupling of the diazonium compound with NED that plays the role of the nucleophile (attacks the diazonium compound), forming a purple azo dye, which is measured with a Vis spectrophotometer at 540.0 nm. R2 is an example of an electrophilic aromatic substitution (Figure 4-14).

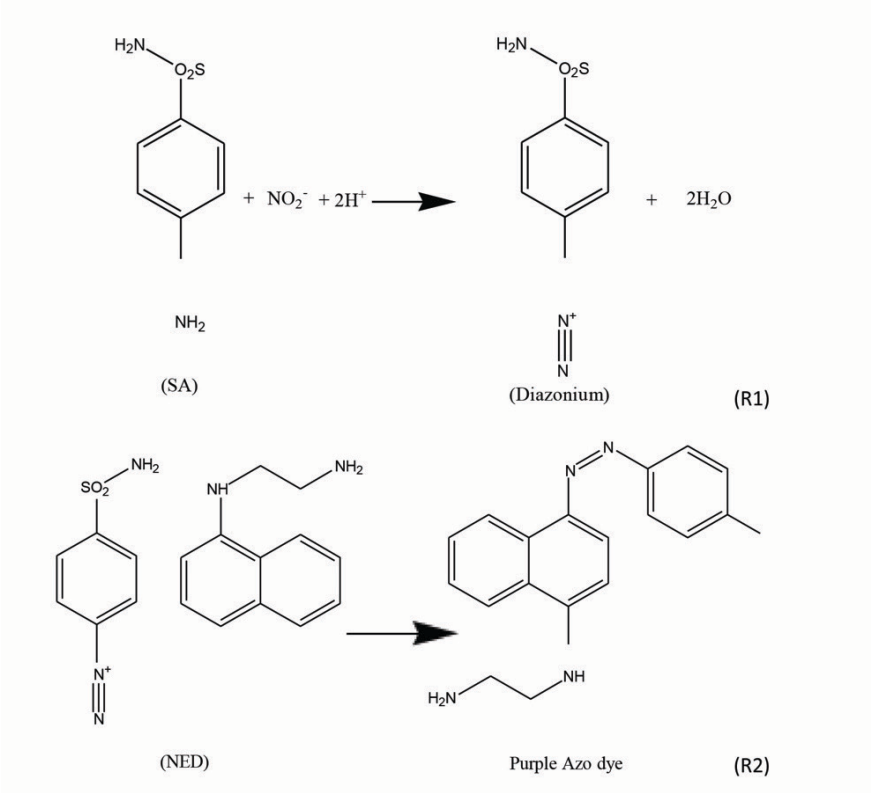

Figure 4-14: Derivatization Reactions

For the analysis of the sample, 2 mL of the colored reagent (SA/NED) were poured into the passam tube containing the sample using a micropipette. The sampler was stirred vigorously for 3 minutes by a vortex to allow the nitrite to dissolve in the solution, and was then left for two hours to allow the derivatization to be completed. The NO_2 - captured reddish purple azo dye was then determined colorimetrically by means of a Nicolet 300 spectrophotometer at 540.0 nm (Figure 4-15).

Figure 4-15: Analysis of the NO_2 collected tubes at the USJ-Chemistry laboratory: (a) Standard solutions and tube preparation, (b) Nicolet 300 spectrophotometer

Calibration

A stock solution (M) of nitrite was prepared by dissolving 0.1543 g of sodium nitrite ($NaNO_2$) in 100 mL distilled water. A secondary solution (N) was prepared from the stock solution by diluting 10 mL of (M) with distilled water in a 100 mL volumetric flask. To prepare the standard solutions, several dilutions were made by withdrawing different amounts of solution (N) with (SA/NED) solution in a 50 mL volumetric flask to obtain NO_2 concentrations between 0.04 and 0.3 mg L^{-1}. The prepared solutions were left for 2 hours for the reaction to take place (development of the purple color) (Figure 4-15). A linear plot (Figure 4-16) was obtained upon plotting the absorbance versus the concentration of nitrite standard solutions, and the following equation was obtained (R^2 = 0.999):

$$y = 1.1325x + 0.1179 \quad (4\text{-}8)$$

Where y is the measured absorbance and x is the concentration of nitrite. Once the quantity of NO_2 (Q) was calculated by means of equation (5-8), and since the time of exposition t and the collection rate S were also known (S = 0.8536 mL min^{-1} for NO_2 passam tubes[5]), the average concentration of nitrogen dioxide present in the atmosphere during the sampling period was calculated by means of equation (4-7).

All necessary quality control and quality assurance of sampled and blank tubes, reproducibility and error estimation were assessed prior and during tube analysis. Blank values (negligible) were subtracted from the measured absorbance of our samples.

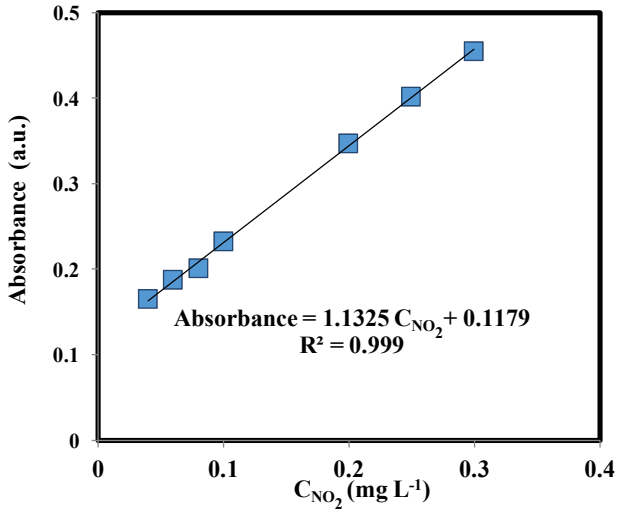

Figure 4-16: NO_2 Calibration Curve

[5] www.passam.ch

Chapter 5 : Sampling Methodology

This chapter provides a description for all the measurement campaigns conducted in this study whether outdoor (5.1-5.3) or indoor (5.4). Campaigns conducted within the airport vicinity (5.1, 5.3, 5.4) required official permissions from the Directorate General of Civil Aviation (DGCA) and Airport Security. Installations took place with the supervision and approval of several departments in Beirut Airport, all according to safety measures and without affecting the airport activities. Similarly, campaigns conducted outside the airport required official permissions but from several other authorities (e.g. university president, the governor of Beirut, and others).

Section 5.1 provides a description of the sampling methodology adapted during the signature campaigns, the main aim of which was to identify aircraft VOC tracers. Section 5.2 presents the sampling locations for the transect campaigns, which were conducted to track the identified aircraft VOC tracers using passive and active sampling. Section 5.3 describes the NO_2 passive campaigns, the aim of which was to validate ADMS-Airport model (chapter 9) and assess NO_2 levels in the airport vicinity. The last section assesses indoor air at Beirut Airport at 2 different locations (maintenance room and the arrivals hall).

5.1 OUTDOOR CAMPAIGNS

5.1.1 SIGNATURE CAMPAIGNS

The main objective of these campaigns was to identify aircraft tracers by characterizing the relative emissions of 50 VOCs (C_2-C_{14}) from the exhaust of around 100 commercial aircraft under real-world conditions and comparing these emissions with gasoline exhaust emissions. The second aim was to determine the average VOC speciation from aircraft exhaust. To the best of our knowledge, this is the first study covering a wide range of VOCs to assess emissions from a large number of in-use aircraft at various modes of operation.

Four signature campaigns have been conducted, however, only the second and third campaigns will be presented. During the first campaign a technical problem occurred with the sampler, whereas the last campaign has not been analysed due to a sudden breakdown

of the GC-MS requiring to return the instrument to the company for inspection which has taken more than 3 months.

- Measurement Sites

VOC measurements were carried out to pursue three different goals, thus 3 different subsets of samples were collected. The first subset aimed at identifying typical fingerprint emissions related to aircraft activities. Measurements were done to sample aircraft exhaust emissions during the 3 different phases of the LTO-cycle (i.e., idle, approach, take-off) as well as APU emissions. As expected, it was not possible to sample aircraft emissions during the climb-out phase of the LTO cycle since these emissions occur above ground level. Sampling was performed as close as possible to the emission sources within the constraints of the airport rules (Figures 5-1 and 5-2). However, the distance between the aircraft and the sampler was sufficient to allow for plume dilution. On these sites, samples were taken from aircraft operating in real conditions, where one sample contained average emissions from several aircraft operating at a similar thrust setting.

Measurements were conducted on days when wind was south-westerly favoring runways 16 for landing and 21 for take-off (see Figure 3-4, chapter 3). The first series of samples, called “approach”, was taken at the first sequence flash light around 8-9 m below the aircraft performing its approach. The second series, called “touch down”, was taken downwind around 17 m away (sideways) from the aircraft engines. After touch down on runway 16, the aircraft starts taxing and exits the runway mostly *via* taxiway Kilo. The series of taxi samples was taken at downwind location about 32 m (sideways) from the aircraft engines for aircraft idling at taxiway Kilo. The “take-off” site was located at the physical beginning of runway 21 at a distance of 120-190 m behind the aircraft engine at its maximum thrust setting. This location was ideally positioned to capture emissions affected by the take-off thrust. Planes initiate take-off in front of the sampling site and then accelerate southward down the runway and away from the sampling site. At this location, the sampler was placed at a downwind location to capture the aircraft plumes at the prevailing wind conditions.

In fact, it was not feasible to obtain exact information regarding thrust settings at each site and for every aircraft. However, estimated thrust settings were determined from pilots and based on the ICAO standard thrust settings. According to ICAO (2008a), the thrust levels

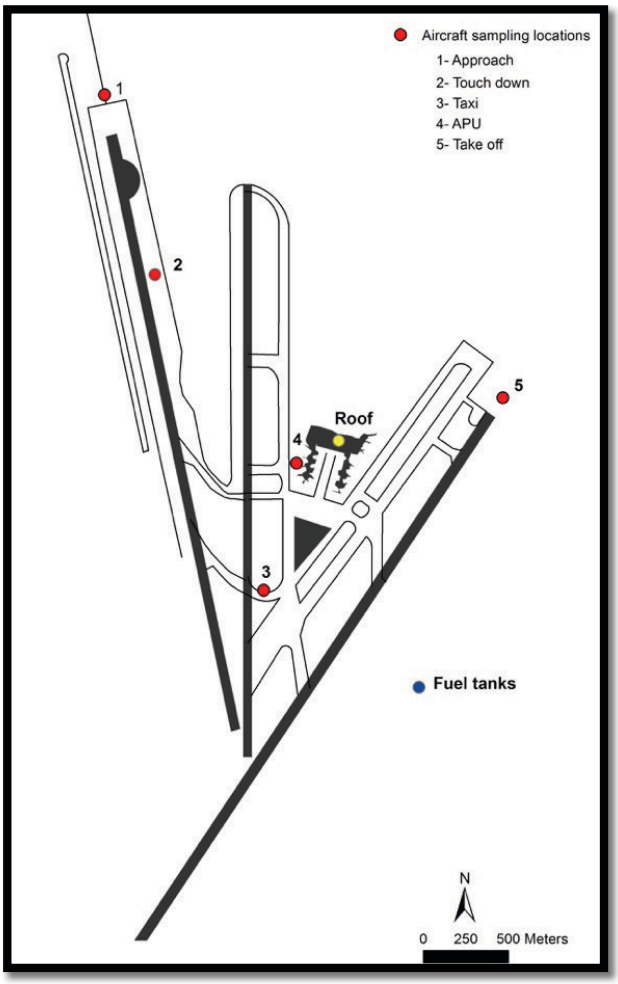

Figure 5-1: Location of the measurement sites for the signature campaigns conducted at Beirut Airport (October 2014 and June 2015)

for idle, approach, and take-off are respectively 7%, 30%, and 100% of the rated thrust. It is important to note that in real operation, the take-off thrust varies from aircraft to another according to the aircraft type and engine model, flight load, meteorological conditions, runway conditions, etc. Thus, in reality, the "take-off" sample collects a variety of different take-off thrusts that vary between 85 and 100%.

At the aircraft gate, the emissions from Garrett-AiResearch (now Honeywell) Model GTCP 331–350C auxiliary power unit (APU) on an A330 were determined by taking air samples at a distance of 10 m downstream from the aircraft tail. For the sake of consistency, all samples were taken from the same APU on an A330.

The kerosene type fuel used in civil aviation at Beirut Airport is Jet A-1. A sample of Jet A-1 fuel was also collected for analysis from the airport fuel farm by dipping the Teflon tube inside the valve of the fuel tank at first, and later by sampling close to the valve to

Figure 5-2: Photographs taken during the signature campaigns at each of the measurement sites at Beirut Airport (October 2014 and July 2015)

avoid the saturation of the GC detector. The aim of these samples was to determine whether aircraft exhaust samples reflected any contribution from raw (unburned) jet fuel that might escape from the aircraft or their engines.

To compare aircraft emissions to vehicle emissions, it was important to assess VOCs from vehicle exhaust using the same sampling and analysis techniques as the aircraft-related samples. In addition to this, due to the strong correlation between fuel composition and VOC emissions (Wang *et al.*, 2013), gasoline exhaust samples were taken without just relying on bibliographical studies. Thus, the second subset aimed at identifying fingerprint emissions related to vehicle emissions. The main focus was on gasoline exhaust emissions, which were chosen to represent vehicle emissions since the majority of vehicles in Beirut operate on gasoline. In Lebanon, light duty vehicles operate on gasoline while only heavy duty vehicles are allowed to run on diesel that constitute only 4% of the total vehicle fleet (Waked and Afif, 2012). The vehicle exhaust gas sample was sampled *via* a Teflon tube from a sampling point located about 30 cm after the tailpipe end. Gasoline exhaust sampling was conducted on Dacia Logan 2007 (4 cylinders 1600 cc) which was in good working conditions and is a good stereotype of automobiles currently found in Beirut area. The gasoline used was the representative of average composition in the Lebanese fuel market. Of course, sampling from gasoline exhaust took place away from direct aircraft sources.

To assess ambient concentrations, a third subset of samples was taken at the airport roof (see Figure 5-1), adjacent to the air traffic control tower at the center of the aerodrome in between the west and east jetties. All samples were collected under the guidance of the airport staff to conduct measurements at the minimal distance permissible from aircraft operations.

- Sampling and Analysis Techniques

Air samples of ambient air and diluted exhaust gases were collected inside homemade stainless steel thermal desorption tubes (Air Toxics) using a portable battery-operated automatic sampler (chapter 4). By means of its practical dimensions (width: 61 cm, height: 32 cm, depth: 20 cm, weight: 4 kg) and its **battery power** supply, this sampler facilitated sampling at any site in the airfield without being constrained with the necessity of electrical supply. Furthermore, its configuration can be operated unmanned with the

remote control option, which made it possible to control the auto sampler without having to access unsafe sites close to aircraft. This sampler, designed in the laboratory at the University of Strasbourg, was composed of a pump located downstream of a mass flow controller. The sampling flow rate was fixed at 100 mL min^{-1} for most of the samples, whereas the sampling duration varied. Two sampling techniques were adapted to sample aircraft signature emissions: (i) 30 seconds sampling repeated 6 times to collect emissions from 6 aircraft for a total volume of 0.3 L or (ii) continuous 30 min sampling during rush hours for a total volume of 3 L. In both techniques, plumes of 6 aircraft were sampled. Emissions from APU, Jet A-1 vapor, and gasoline exhaust were taken by continuously sampling for 3 min in order to get a total volume of 0.3 L, similar to the 30 s × 6 sampling technique. In these aforementioned sites, continuous sampling was performed due to the constant flow of emissions. To measure the average ambient airport concentration, samples were taken from the airport roof for a duration of 6 hours at 25 mL min^{-1}. The choice of a lower flow rate was to avoid the breakthrough of the sampled VOCs through the adsorbents cartridge.

Analysis was performed on 2 analytical systems, described in details in chapter 5, to cover the wide range of the target C_2-C_{14} VOCs. These systems were: (i) ATD-GC-MS: Automated Thermal Desorber (ATD) with capillary gas chromatography (GC) coupled with a Mass Selective Detector (MSD) used for the **assessment of heavy VOCs** and the **identification of aircraft tracers** and (ii) ATD-GC-FID: Automated Thermal Desorber (ATD) with capillary gas chromatography (GC) coupled with Flame Ionization Detector (FID) used for the assessment of the **total VOC speciation**.

A total of 60 samples from aircraft exhaust, 10 from the airport roof, and 12 samples from gasoline exhaust were collected. However, due to technical problems which occurred either with the sampler, or the gas chromatographs especially due to humidity of the air samples, 31 samples from aircraft exhaust, 5 samples from the airport roof, and 4 samples from gasoline exhaust were able to be analyzed. More than 15 samples from Jet A-1 vapor were taken at different sampling durations (3 – 30 min). However, all samples saturated the GC detector, and only 1 sample (3 min duration) was not saturated and successfully analyzed. This is why new samples, with a duration of 30 sec repeated 6 times, have been taken but unfortunately were not analyzed due to the sudden GC-MS breakdown.

- Sampling Schedule

VOC measurements were carried out during 4 measurement campaigns performed in June 2014 (2 weeks), October 2014 (2 weeks), June 2015 (3 weeks), and October 2015 (2 weeks). As mentioned before, only 2 measurement campaigns will be presented.

Measurements conducted in October 2014 aimed at identifying the speciation of VOC groups using GC-FID whereas measurements done in June 2015 targeted heavy VOCs using GC-MS for the identification of aircraft tracers.

Sampling of aircraft exhaust using the 30-min approach took place during rush hours to minimize the dilution of the sample by ambient air or the interference of other emission sources. Sampling using the 30 s × 6 approach took place preferably during rush hours as well. Table 5-1 presents the sampling schedule only for the tubes that were analyzed, whose corresponding results will be presented in section 6.1.

Table 5-1: Sampling schedule for the signature campaigns conducted at Beirut Airport

	Site	Oct-14	Jun-15
		Analysis Method	Analysis Method
		GC-FID	GC-MS
Aircraft-Related	**LTO Cycle**		
	Approach	30 s × 6 (n=1) 30 min (n=1)	30 s × 6 (n=2) 30 min (n=1)
	Touch down	30 s × 6	Not available
	Taxi	30 s × 6 (n=1) 30 min (n=1)	30 s × 6 (n=2) 30 min (n = 1)
	Take-off	30 s × 6 (n=1) 30 min (n=1)	30 s × 6 (n=2) 30 min (n=1)
	Non-LTO		
	APU	30 min, A330 (n=1)	30 s × 6 (n=2) 30 min (n=2)
	Kerosene vapor	Not available	3 min (n=1)
Vehicle	Gasoline Exhaust	Not available	3 min (n=4)
Ambient Air	Airport Roof	30 min (n=2)	6 h (n=3)

5.1.2 TRANSECT CAMPAIGNS

Transect studies were undertaken to investigate the impact of the airport activities on the air quality in the vicinity and on Beirut area. Note that a transect is a representation of space along a linear path along which observations are made or measurements are taken. These preliminary investigations aimed at assessing the impact of Beirut Airport activities on the air quality of Beirut and its suburbs, by determining if measurements of air pollutants could be attributed to aircraft activities.

Four transect campaigns have been conducted covering several locations within Beirut and its suburbs. During the first campaign (June 2014), a technical problem related to the sampling flow occurred with the active sampler. The last exhaustive campaign which involved more than 13 sites have been conducted; however, due to GC-MS breakdown, it has not yet been analyzed within the time limit of this thesis.

Thus, only 2 campaigns, conducted in 20-22 October 2014 (passive) and 13-21 July 2015 (active), will be presented in the following paragraphs. This section provides a description of the sampling methodology (site location, sampling schedule, etc.) adapted during the transect campaigns.

All sites were chosen in a way to be minimally affected by vehicular traffic and direct emission sources. As much as practicable, polyethylene cages were installed on roof tops to allow the sampling of background air. Installations were conducted only after obtaining official permissions from the appropriate responsibles, especially with the security cautions that existed during the past years.

- Passive Campaign (20-22 Oct-2014)

Sampling Sites

Measurements taken on 20-22 October 2014 involved several sites located along 4 main transects, centered at the airport roof and extending towards Beirut and its suburbs (Figures 5-3 and 5-4).

The first transect, located along the seashore, was chosen to estimate the impact of aircraft emissions on the air quality along the seashore area, since most frequently aircraft overfly the seashore before landing on runway 16 at an altitude of 200-500 m above sea level. The first site in this transect is the golf club (golf), which is green space located approximately 2.8 km north of the airport (sampling took place at 31 m AMSL). The second site, CNAM

(Conservatoire National des Arts et des Metiers), is an educational establishment located approximately 4.4 km north of the airport, 60 m AMSL. A major highway is located to the east of the site, however, tubes were installed at the roof and as far as possible from vehicular emission sources. The third sampling site was at the rooftop of the Issam Fares Institute for Public Policy and International Affairs (IFI) building at the American University of Beirut (AUB) campus located approximately 8.3 km north of the airport, 65 m AMSL. This site is located away from direct emission sources, in the campus center.

The second transect was selected to cover areas towards the northeast of the airport. The first sampling site was located 1.1 km away from the airport center, 40 m AMSL, at the radar station related to Beirut Airport. This site is closer to airport emissions than to road traffic emissions. The second sampling site was the pine forest, located approximately 5.3 km away from the airport, 52 m AMSL. The pine forest is an urban park that covers about 400,000 m² of green space within Beirut municipality.

To assess the impact of the airport activities at downwind locations, and since the prevailing wind conditions are southwest (Chelala, 2008), a third transect (Northeast Beirut Airport) was studied to cover downwind locations. Sampling locations on this transect, especially near Beirut Airport (Beirut southern suburbs) was limited by the security constraints. The first sampling site was located at the rooftop of a 2 floor building at Hay el Sellom, approximately 1.5 km northeast Beirut Airport and 48 m AMSL Hay el Sellom is a very urbanized residential area located in the southern suburbs of Beirut. The second site was at the rooftop of the student dorms near USJ (Saint Joseph University) at Mansourieh, approximately 7.8 km northeast Beirut Airport located at a mountainous area. Mansourieh slopes upwards from an elevation of approximately 200 m to reach its highest at around 350 m.

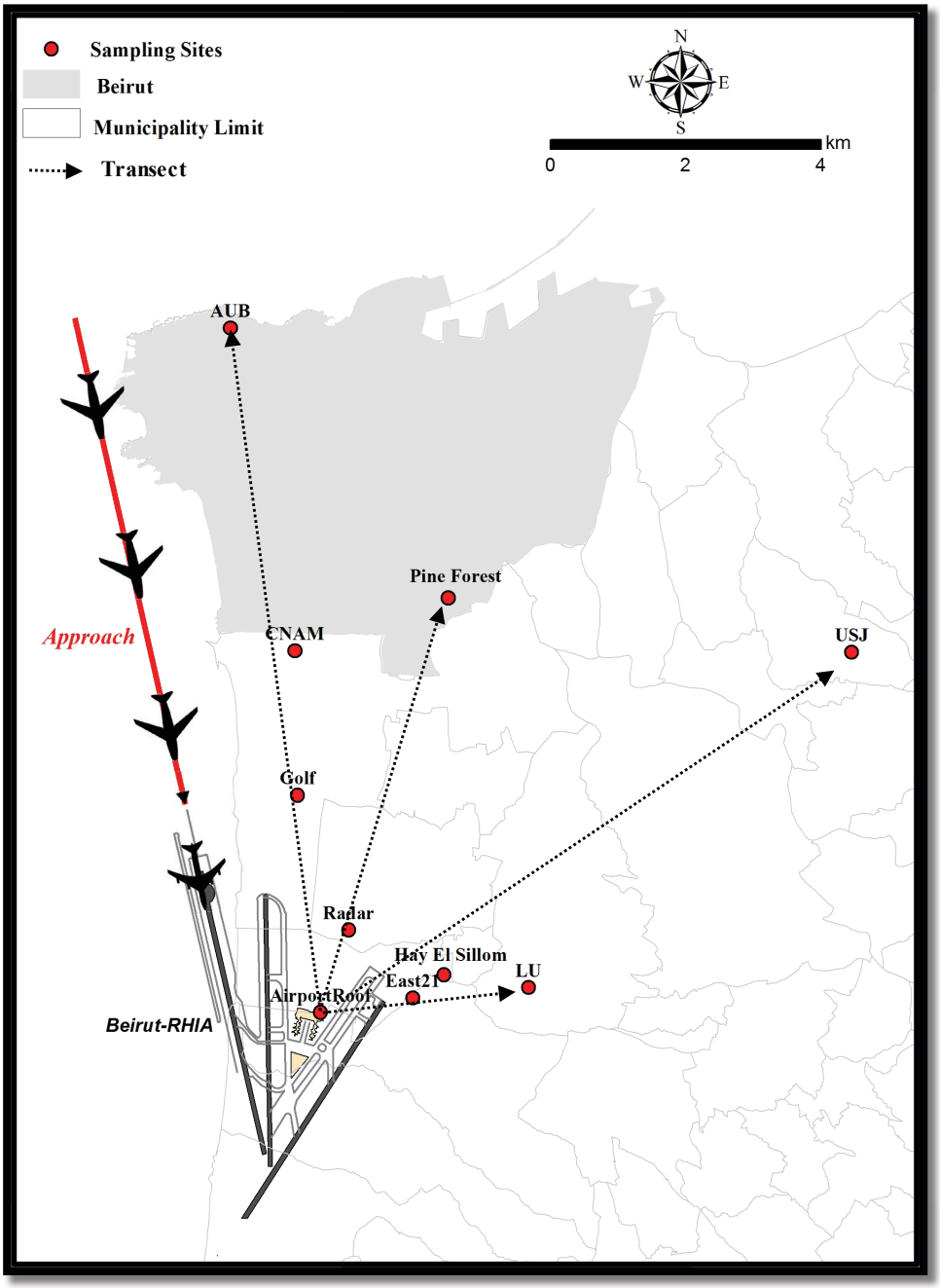

Figure 5-3: Location of sampling sites (Transect Campaign, 20-22 Oct-2014).
The red dotted line reflects the main jet trajectory used for landing in Beirut-RHIA.

Figure 5-4: Photographs taken during the campaign at each of the measurement sites (20-22 Oct-2014)

The fourth transect constituted of sites located to the east of the airport, representing sites that are not downwind of the airport. Measurements taken along this transect were also constrained by security measures in the southern suburbs of Beirut. The first site was located near the airport fence to the east of runway 21 (East 21), 1.15 km away from the airport center, 18 m ASL, near a main highway. This was the most convenient location due to security reasons. The second site was the Lebanese University (LU) located 2.6 km east

of the airport at 51 m AMSL, inside the campus and away as much as possible from vehicular emissions.

In this preliminary campaign, sampling focused on locations in the upper right quadrant with respect to the airport location. This is mainly because the aim of the thesis is to study the impact of the airport's activities on the air quality of Beirut, and because the airport emissions are expected to disperse mainly towards that quadrant as a result of the prevailing southwest wind conditions.

Sampling and Analysis Techniques

Measurements taken on 20-22 October 2014 involved passive sampling of pollutants (2 tubes per site). The selected duration of passive sampling was 48 hr, as the recommended sampling duration by Perkin Elmer is a minimum of 8 hr and depends on the ambient measured concentrations. All these tubes were analyzed using GC-FID (chapter 4) to identify the total VOC distribution.

- Active Campaign (13-21 July 2015)

Sampling Sites

During this campaign, active samples were taken from several sites (1 site per day) at the southern part of Beirut and its suburbs (Figures 6-5 and 6-6). However, this campaign was interrupted by the occurrence of the garbage crisis that has led to elevated pollutant levels, and it was no longer possible to compare new measurements with the previous ones.

Active samples were collected from the golf club, radar station, and pine forest as described above. Primary results obtained in the campaign conducted in October showed an impact of aircraft emissions along the seashore. To verify this, active sampling was performed exactly at the seashore to monitor the difference in concentration levels. The site chosen was next to the Coral beach (Coral) at approximately the same distance (4.9 km) from the airport center (airport roof) as CNAM (4.3 km) and exactly at the seashore (14 m AMSL).

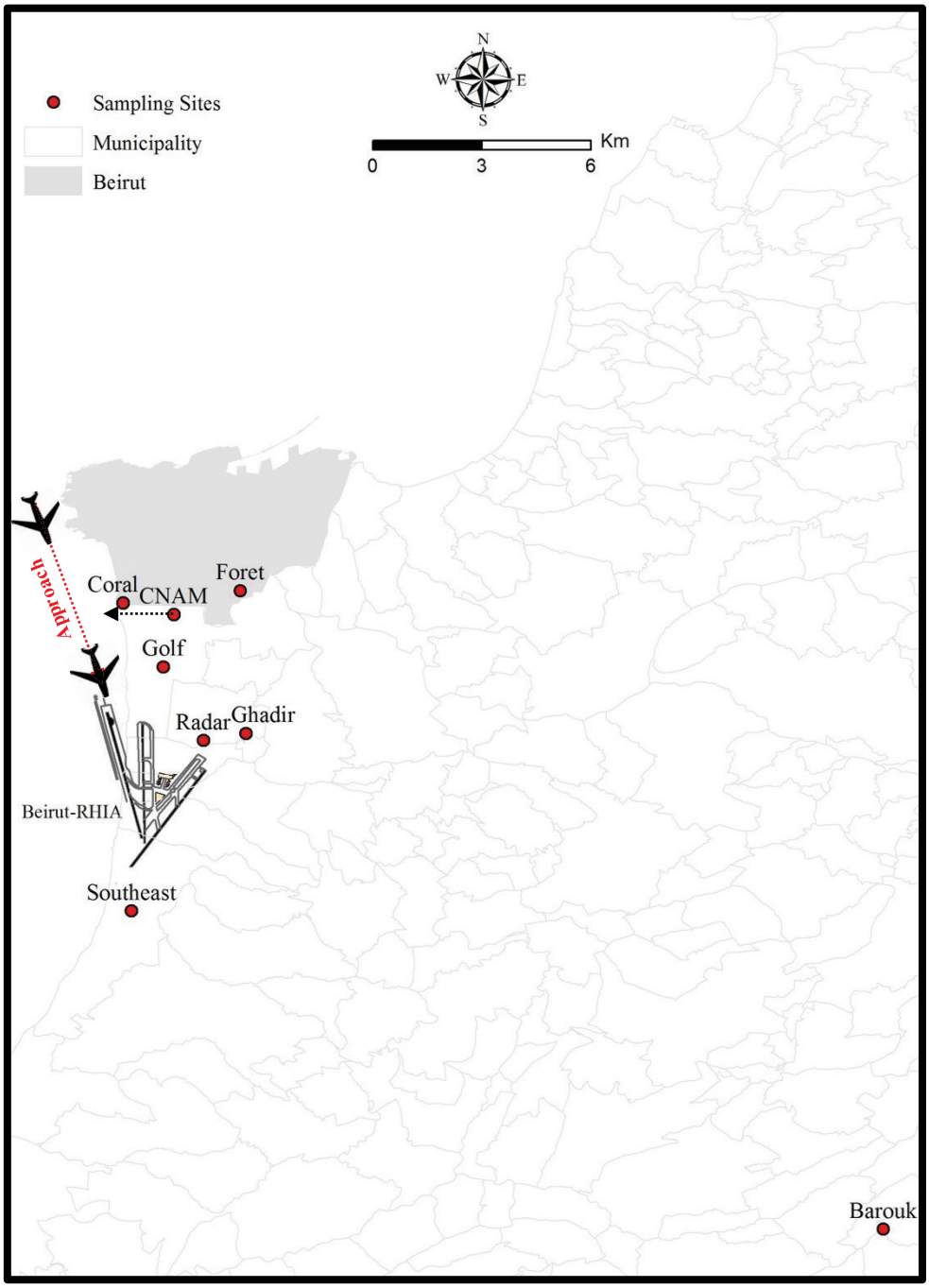

Figure 5-5: Location of sampling sites (Transect Campaign, 13-21 July 2015).
The red dotted line reflects the main jet trajectory used for landing in Beirut-RHIA.

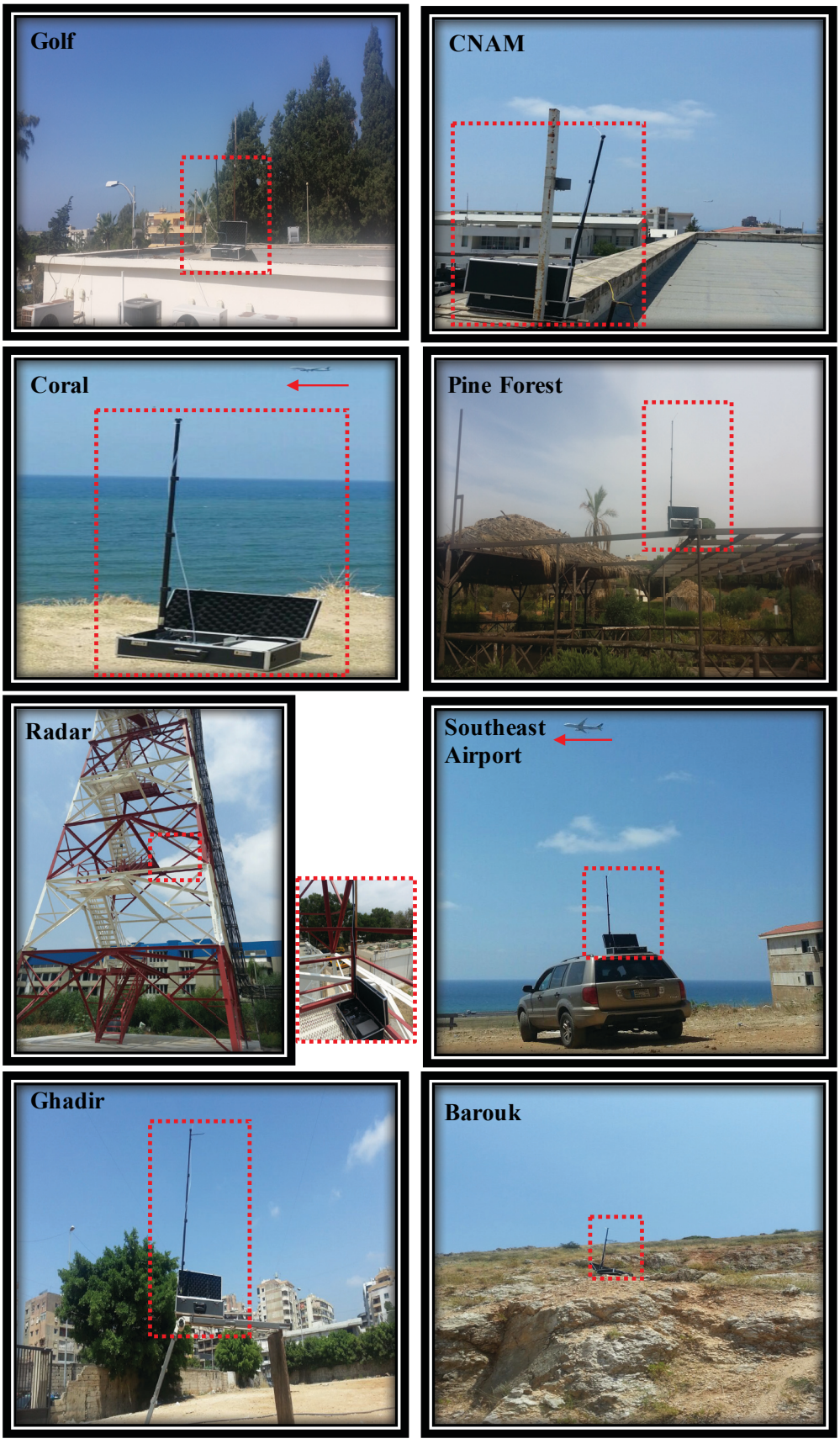

Figure 5-6: Photographs taken during the campaign at each of the measurement sites (13-21 July-2015). The autosampler and aircraft are marked with a red dotted square and a red arrow respectively.

Another measurement was taken from Ghadir which is an urbanized location near Hay El Sellom towards the northeast direction (2 km from the center of the airport, 43 m AMSL). To determine if the southeast areas are affected by airport emissions, measurements were taken to the southeast (Khaldeh) at 4.1 km from the airport center, 52 m AMSL. Another site, Barouk, very far from the airport has been chosen to represent clean air at a distance of about 20.3 km southeast the airport and an elevation of 1120 m AMSL.

Sampling and Analysis Techniques

Measurements taken on 13-21 July 2014 involved active sampling of pollutant concentrations at the sampling sites described above. Active sampling was performed in triplicates with a duration of 30 min at a sampling rate of 100 mL min^{-1}. Each site was assessed at a different day, but at approximately the same time interval between 13:00 and 14:30 (arrivals rush hours during summer 2015) except for 2 sites either due to the proximity to another site (Coral) or due to traffic delay (Southeast airport). This study took place over 8 days between 13 and 21 July 2015 (Table 5-2). All tubes were analyzed using GC-MS (chapter 4) in order to quantify heavy aldehydes and detect any unidentified VOCs. Again, few tubes were lost due to the humidity of the air samples.

Table 5-2: Sampling schedule for the active transect campaign
(July 2015, 3 samples per site)

Sampling Site	Date	Sampling time (Center)
Golf	13/07/15	13:45
Barouk	14/07/15	13:45
Radar	15/07/15	13:45
Coral	16/07/15	11:45
CNAM	16/07/15	13:45
Pine forest	17/07/15	13:45
Ghadir	20/07/15	13:45
Southeast Airport (Khalde)	21/07/15	14:30

5.1.3 NO_2 PASSIVE CAMPAIGNS

The goal of this campaign was to assess NO_2 levels in the airport vicinity and to validate ADMS-Airport (chapter 9) according to parameters of the study area. Model results are often calibrated with measured results to determine the ability of a model to characterize current conditions with some degree of confidence (ICAO, 2011). Once ADMS-Airport is

verified for baseline conditions, it can be used with greater confidence (chapter 9) to predict future scenarios accurately.

- Sampling Sites

NO_2 samples were collected at 9 sites inside the airport (Figure 5-7). Validation sites were selected according to guidelines recommended by ICAO's Airport Air Quality Guidance Manual (ICAO, 2011). The sites and the rationales for their selection are described in Table 5-3.

The first site, approach, was located near the first sequence flash light around 8-9 m below the aircraft performing its approach (see photos in Figure 5-8). After touch down on runway 16, the aircraft starts taxiing and exits the runway mostly *via* taxiway Kilo. The taxi site was located at a downwind location about 32 m (sideways) from the aircraft engines for aircraft idling at taxiway Kilo. The site take-off (1) was located at the physical beginning of runway 21 at a distance of 190 m behind the aircraft engine at its maximum thrust setting. This location was ideally positioned to capture emissions affected by the take-off thrust. Planes initiate take-off in front of the sampling site and then accelerate southward down the runway and away from the sampling site. Optionally, measurement sites are located directly upwind and downwind (and sideline) of the runways, often at the airport boundary. For this purpose, the sites take-off (2) (41 m away aircraft engines) and take-off (3) (42 m away from aircraft engines) were selected.

The site Ozaii was situated in a residential area away from the immediate proximity of emission sources as the case of the other sites (e.g. taxi, take-off, approach, gate 12). This site, located to the east of the landing runway at about 180 m (sideways) from aircraft engines, assesses the average situation of a residential area with permanent housing closest to the airport. The site near the cargo, was located 30 m to the right of aircraft taxiing and 115 m away from handling aircraft. This site reflects medium airport activities without being affected by direct emissions. The site "gate 12" was selected to measure the concentration of NO_2 affected by emissions from APUs and aircraft ground handling equipment (e.g. emissions from baggage truck, fuel dispenser, catering truck, etc. (see chapter 2)), which service the aircraft prior to departure and after arrival to the gate.

Table 5-3: Description of the selected sampling sites for the NO_2 model validation campaigns

Airport Site	Description	Justification
Background	Background concentration site, undisturbed by any polluting activities.	This site provides the background and baseline data for the region where the airport is located.
Take-off (1) Take-off (2) Take-off (3) Taxi Approach Gate 12	These sites are located within the airport area with intense airport activities. Optionally, sites are located directly upwind and downwind (and sideline) of the runways, often at the airport boundary (take-off (2) and take-off (3)).	It can be expected that these sites will most likely best reflect the airport activities (aircraft and/or handling and infrastructure). Those activities will dominate the pollution concentrations, and significant concentration changes will likely be caused by these sources.
Ozaii	This site is located in a residential area downwind of the airport, but without a dominant emissions source in its proximity relative to the sites near intense airport activities.	This station will give the average situation of a residential area with permanent housing closest to the airport.
Cargo	This site is located facing the cargo area, with medium traffic.	This site reflects medium airport activities without being affected by direct emissions.

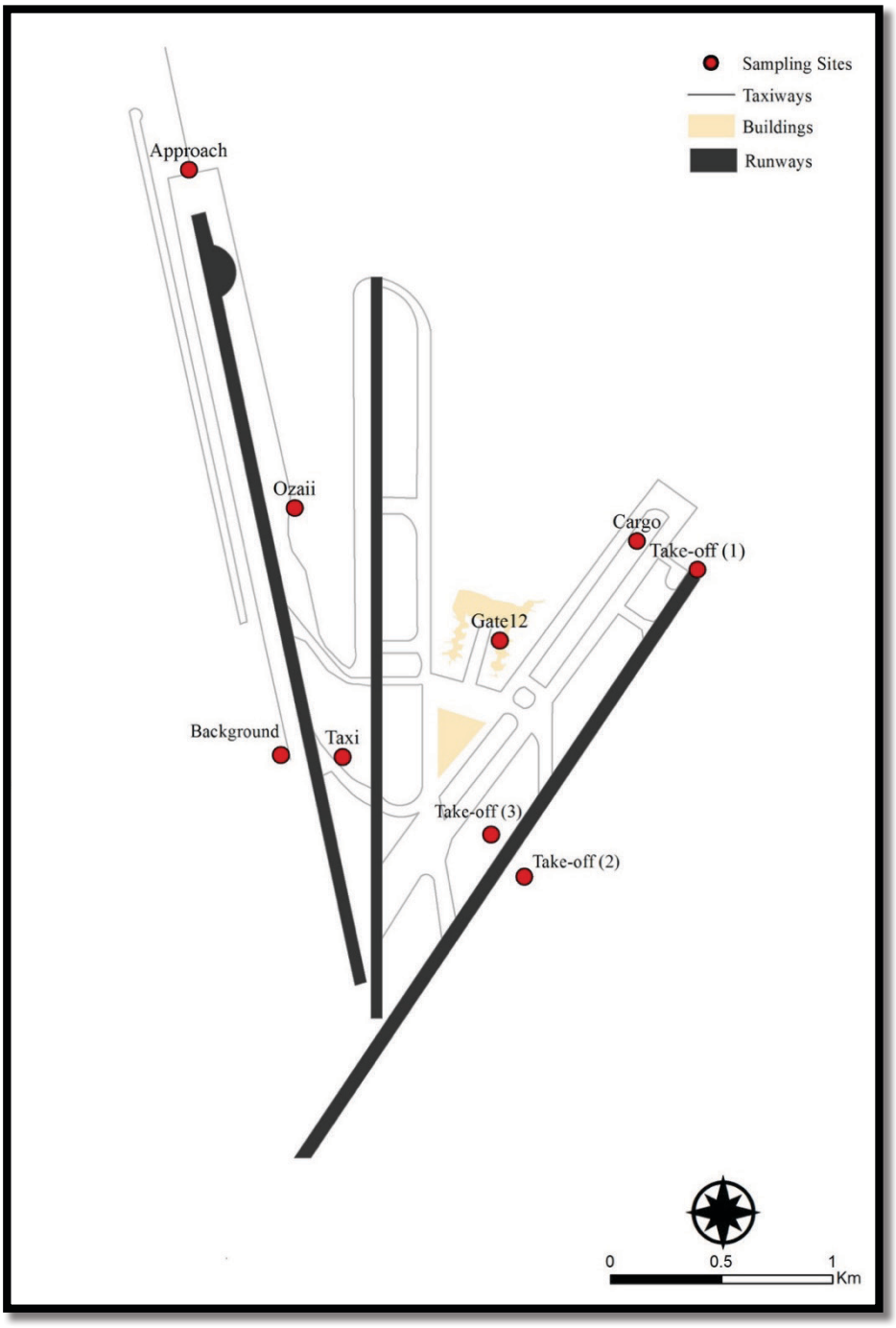

Figure 5-7: Sampling sites chosen for NO_2 validation campaigns at Beirut Airport (May/June-2015)

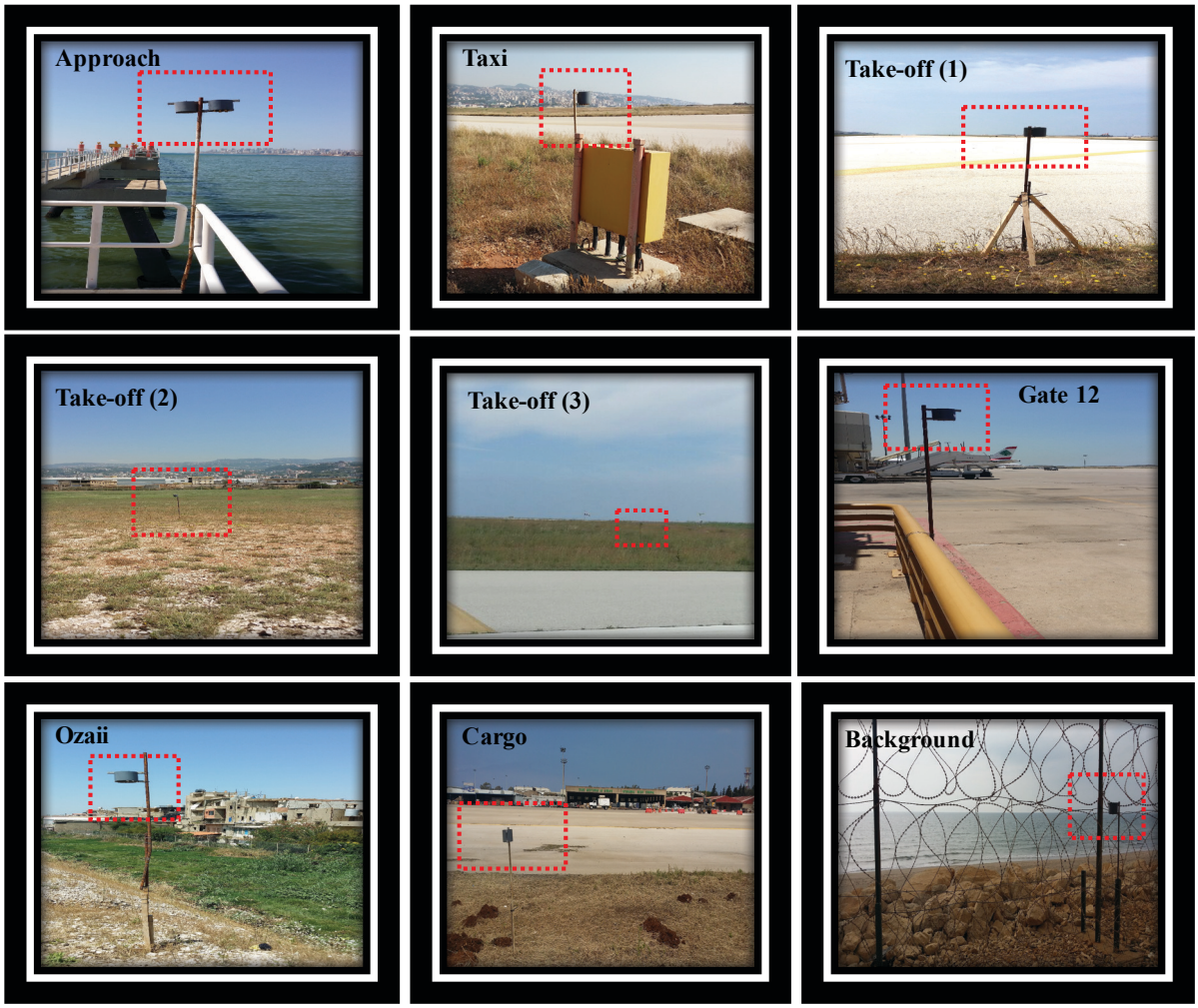

Figure 5-8: Photographs taken during the NO_2 validation campaigns at each of the measurement sites at Beirut Airport (May/June-2015)

-5.3.2 Sampling and Analysis Techniques

Due to the absence of monitoring stations within the airport vicinity and in order to simultaneously assess the spatial distribution of nitrogen dioxide within the airport vicinity, sites were equipped by a network of passive diffusion tube samplers, passam tubes, for the measurement of average NO_2 concentrations. Passive sampling was chosen as it is a practical alternative for atmospheric monitoring at low cost and high spatial resolution and because passive samplers are: (1) small and lightweight; (2) unobtrusive and thus more readily acceptable to study participants; (3) easier to use and handle (no battery or electricity is required); (4) and cost-effective for such campaigns (Yu *et al.*, 2008). Protective cages were installed within the airport at a height of 110-200 cm above ground, without affecting the regulations and the airport operations. It was not possible to

maintain a constant height for the cages due to the different airport operations and restrictions or practical constraints.

In general, 1 tube was used for sampling at most locations. However, to evaluate the accuracy of measurements, 3 tubes were installed at 2 sites (take-off (3) and approach) during the first campaign. As already mentioned in chapter 4, the collected NO_2 were spectrophotometrically quantified based on the well-established Saltzman method (Saltzman, 1954). Three validation campaigns were conducted at a convenient duration of 1 week (Table 5-4).

Table 5-4: Sampling schedule for NO_2 validation campaigns at Beirut Airport (May/June 2015)

Campaign	Duration
1	16-23 May-2015
2	04-11 June-2015
3	11-18 June-2015

5.2 INDOOR CAMPAIGNS

Indoor air pollution at airports can impact both airport personnel and the public/passengers (Witten *et al.*, 2011). For this reason, indoor measurements (Figure 5-9) were conducted at Beirut Airport in the maintenance room (workplace) to assess the impact on airport personnel, and in the arrivals hall to assess the impact on public/passengers as well as on airport personnel. Measurements and installations were conducted with the assistance of the Mechanical Department at the Middle East Airports Services (MEAS).

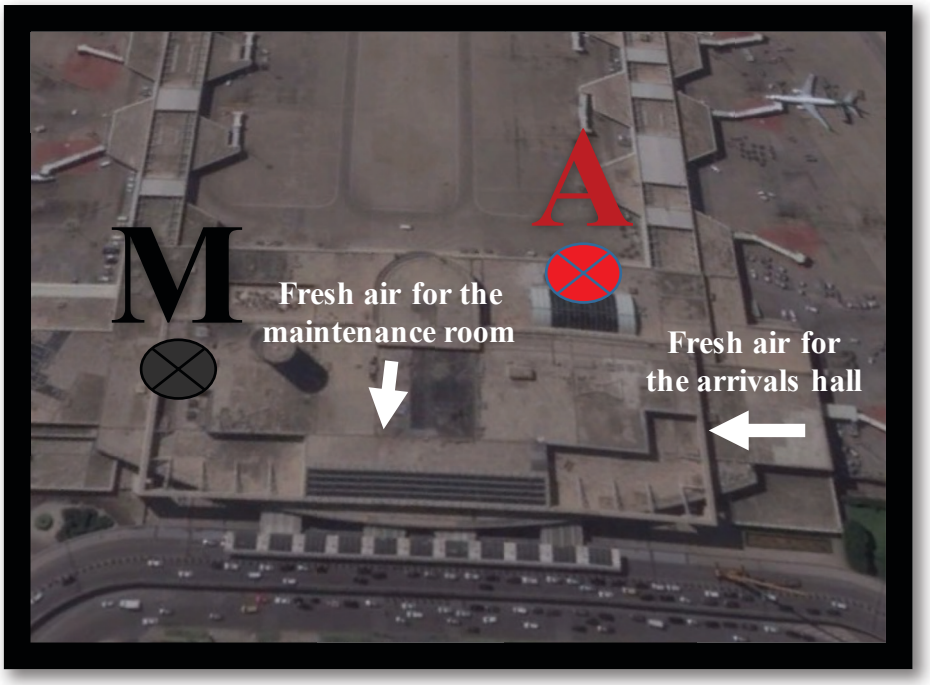

Figure 5-9: Location of the studied rooms. **M**: Maintenance room and **A**: Arrivals Hall (White arrows indicate the direction of fresh air flow into the mechanical rooms)

5.2.1 VENTILATION PRINCIPLE IN BEIRUT AIRPORT

For each room there exists an air climate unit located inside a mechanical room not necessarily adjacent to the room (Figures 5-9 and 5-10). Within this air climate unit, the system of ventilation works in the following manner: 80% of the returning indoor air (return duct) is mixed with 20% of fresh air which are afterwards filtered with Aluminum filter (to remove big dust particles and protect the air bag filter from being clogged) and an air bag filter (to remove particles with diameters of 0.03-1.0 microns which include bacteria, most tobacco smoke, proplet nuclei (sneeze), and dust particles). According to the required indoor temperature, this air is heated or cooled before it enters the indoor room again through the supply duct (Figure 5-10).

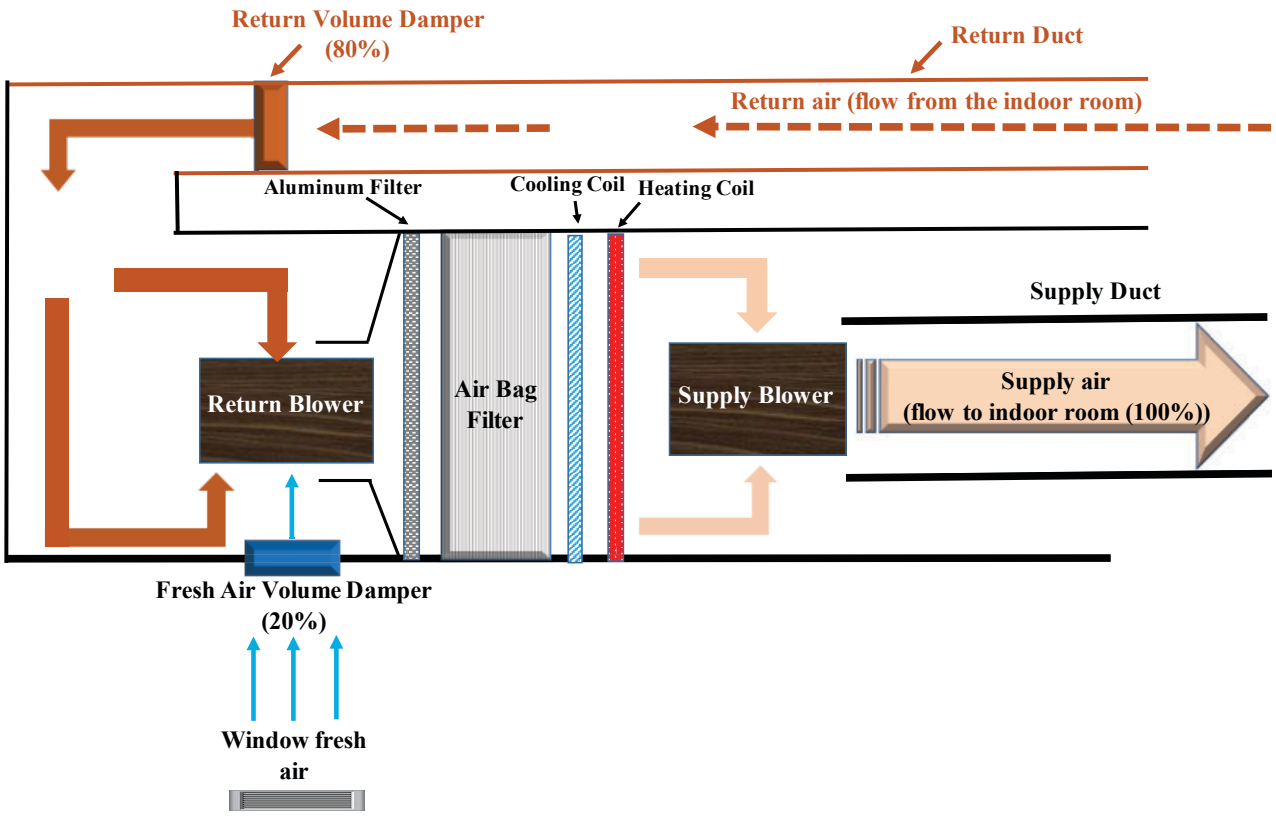

Figure 5-10: Top view of a typical air climate unit at Beirut Airport

5.2.2 MAINTENANCE ROOM

The maintenance room is a workplace where full-time maintainers stay for at least 12 hr. Moreover, the air quality inside this room is similar to the one inside several workplaces in the same floor including the Area Control Center (ACC) in the Air Navigation Services Department.

For VOC measurements, air samples of indoor air were collected inside stainless steel thermal desorption tubes of the type "Air Toxics" using 2 types of autosamplers. The sampling flow rate was fixed at 100 mL min^{-1} at a sampling duration of 30 min resulting in a total sampled volume of 3 L. VOC sampling was taken at a height of 1.5 to 2 m above the floor level in the breathing zone. Sampling was performed over 3 days in July using an 8-channel programmable autosampler and 2 days in November 2014 using a one-channel portable battery-operated automatic sampler collecting a total of 27 air samples (the 2 autosamplers possess the same sampling principle and accuracy). Sampling times (Table 5-5) were set to take account for the different levels of activity at the airport (low traffic, rush hours, morning hours, etc.). All samples were subsequently analyzed mainly using

GC/FID, with the exception of few samples which were analyzed with GC/MS to identify unknown VOCs.

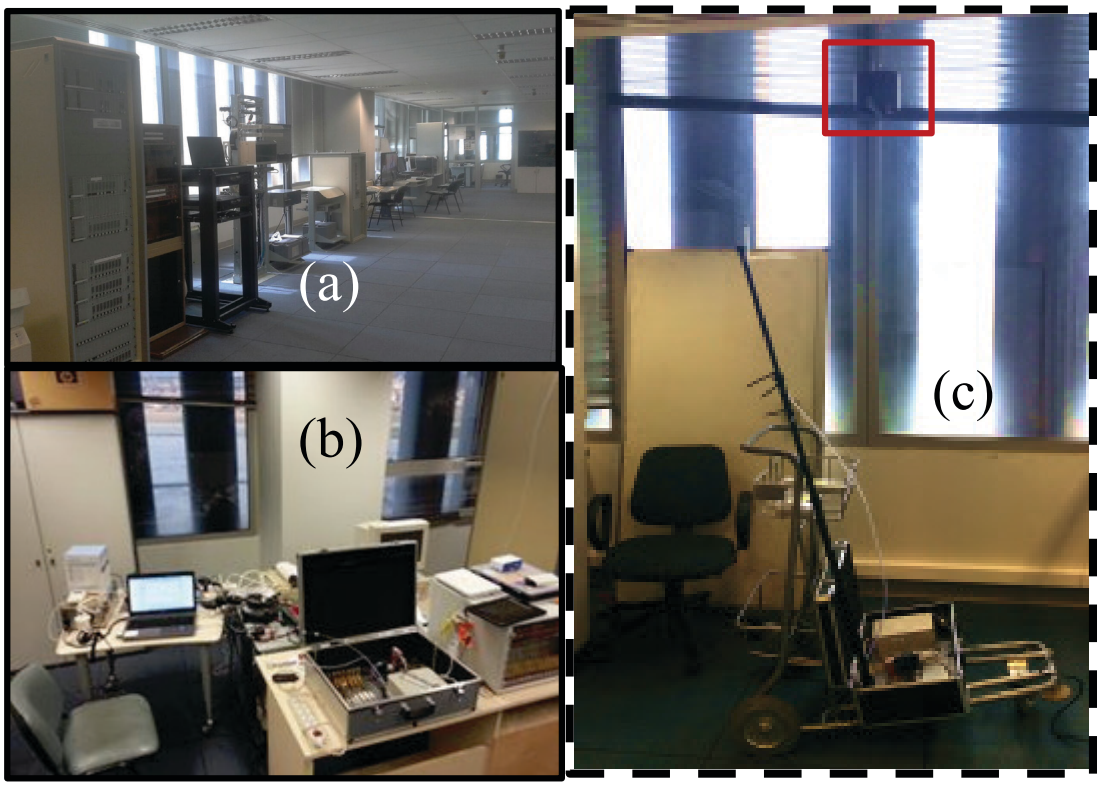

Figure 5-11: (a) Maintenance room at Beirut Airport (b) 8-channel autosampler (June 2014) (c) one-channel autosampler and NO_2 cage (red square) (November 2014)

To measure NO_2 levels, air samples were taken using Passam passive samplers placed in polypropylene cages. These cages were tied to the ceiling of the maintenance room at a height of 2.1 m above ground to measure indoor NO_2 levels. To assess the average NO_2 concentration of the fresh air that supplies the maintenance room, a cage (2.5 m above floor level) was tied adjacent to the window (Figure 5-12) through which fresh air enters before getting mixed with the returning indoor air, as previously explained. These measurements were taken simultaneously with the VOC campaign (28-29/11/14), as well as during summer 2015 (Table 5-6).

Table 5-5: Sampling schedule for VOC measurements taken in the maintenance room (Beirut Airport, 2014)

10-14 June 2014 (Summer)		28-29 November 2014 (Fall/winter)	
Programmable 8-channel autosampler		one-channel autosampler	
Date	**Sampling time (Center)**	**Date**	**Sampling time (Center)**
10-Jun-14	16:15	28-Nov-14	11:15
10-Jun-14	18:00	28-Nov-14	14:15
10-Jun-14	21:00	28-Nov-14	17:15
11-Jun-14	05:15	28-Nov-14	22:30
11-Jun-14	08:00	28-Nov-14	01:30
11-Jun-14	10:45	29-Nov-14	6:45*
11-Jun-14	16:00	29-Nov-14	10:45*
11-Jun-14	18:00	29-Nov-14	11:15
11-Jun-14	21:00		
12-Jun-14	00:30		
12-Jun-14	05:15		
12-Jun-14	08:00*		
12-Jun-14	08:45		
12-Jun-14	10:45		
12-Jun-14	14:15		
12-Jun-14	16:30		
12-Jun-14	21:00		
13-Jun-14	05:15		
13-Jun-14	12:15		

The duration of sampling was 30 min at a rate of 100 mL min^{-1} (total volume of 3L). All the tubes were analyzed with GC/FID except those marked with an asterix (*Analyzed with GC/MS).

Table 5-6: Sampling Schedule for NO_2 measurements taken in the maintenance room (Beirut Airport, 2014)

Date	26-27/11/14	28-29/11/15	17-24/6/15	24-29/6/15
Location	**Sampling Duration**			
Indoor	24 h	24 h	7 d	7 d
Fresh Air	24 h	24 h	7 d	7 d

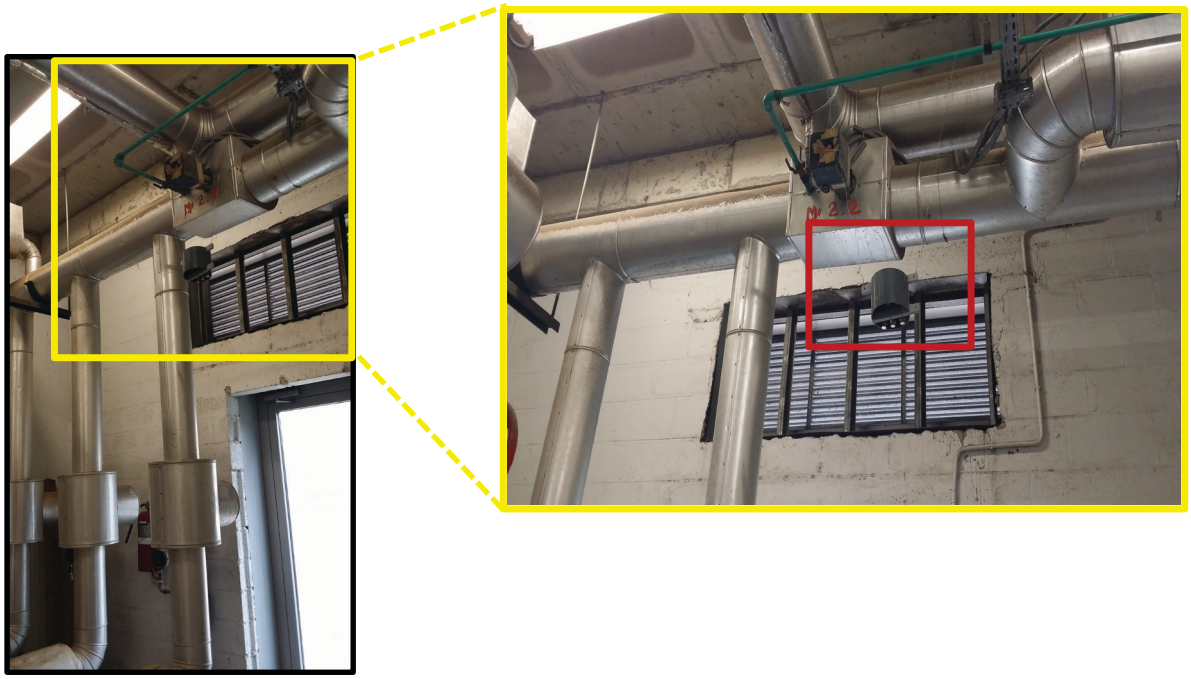

Figure 5-12: Installation of polyethylene cage (red square) in the mechanical room to measure NO_2 levels in fresh air supplying the maintenance room at Beirut Airport (November 2014)

5.2.3 Arrivals Hall

The arrivals hall is the area of an airport where the incoming passengers arrive and spend at least 1 hr. Moreover, it has the same air quality as in the offices and duty free shops located in the same airport section where employees spend at least 12 hr/day (case of RHIA).

For VOC measurements, air samples of indoor air were collected inside stainless steel thermal desorption tubes of the type "Air Toxics" using 2 types of autosamplers. The sampling flow rate was fixed at 100 mL min^{-1} at a sampling duration of 30 min resulting in a total sampled volume of 3 L. VOC sampling was taken at a height of 1.5 to 2 m above the floor level to acquire samples at a typical breathing zone. Sampling was performed during the summer of 2014 over 2 days in July using an 8-channel programmable autosampler, and during the winter of 2014 over 2 days in October and 2 days in November using a portable battery-operated autosampler collecting a total of 22 air samples. Sampling times (Table 5-6) were set to take account for the different levels of activity at the airport (low traffic, rush hours, morning hours, etc.). During the summer campaign, VOC samples were taken by inserting a Teflon tube in the return duct to assess the VOC concentrations in the returning indoor air from the arrivals hall using the

programmable 8-channel autosampler, whereas the one-channel sampler was used to take samples directly from the arrivals hall during the fall/winter campaigns (Figure 5-13). During the campaign conducted in November, an exceptional malfunction in the air conditioning system took place which necessitated the change of the ventilation procedure from mixing 20% fresh air with 80% returning indoor air, to mixing 50% fresh air with 50% indoor air. All the collected samples were analyzed mainly using GC/FID, with the exception of few samples which were analyzed with GC/MS to identify unknown VOCs.

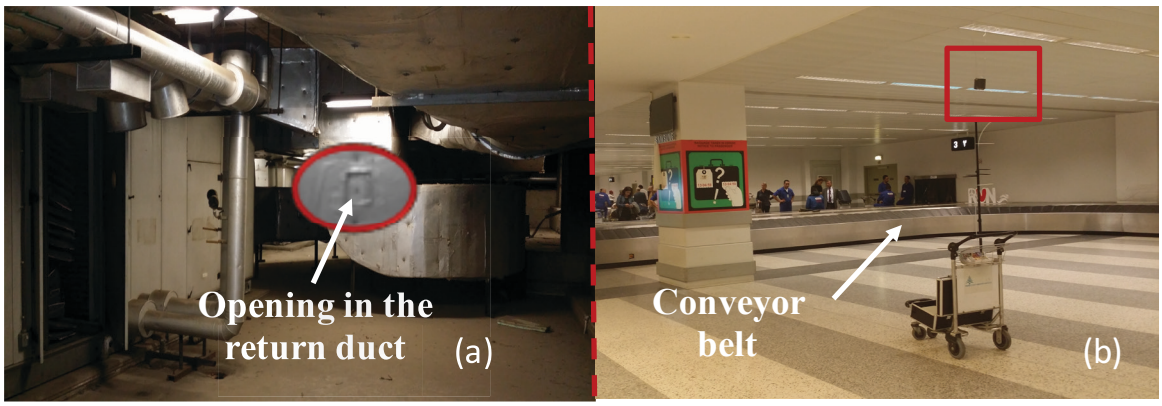

Figure 5-13: (a) Sampling through the opening in the return duct at the mechanical room at which the air climate unit for the arrivals hall is installed (Beirut Airport, June 2014) (b) one-channel autosampler during the winter campaign and NO_2 cage (red square) (Beirut Airport, October and November 2014)

Again, to measure NO_2 levels, air samples were taken using Passam passive samplers placed in polypropylene cages. These cages were tied to the ceiling of arrivals hall at a height of 2.5 m above floor level to measure indoor NO_2 levels. To assess average NO_2 concentration of the fresh air that supplies the arrivals hall, a cage (1.5 m above floor level) was tied adjacent to the window through which fresh air enters before getting mixed with the returning indoor air (Figure 5-14), as previously mentioned. NO_2 sampling took place just outside the arrivals hall to measure the NO_2 levels (2.8 m above floor level) of the air that enters into the arrivals hall through openings associated with the conveyor belts. These openings lead to the flow of contaminated air from the ramp into the arrivals hall. All NO_2 measurements (Table 5-8) were taken simultaneously with both VOC winter campaigns as well as during summer 2015.

Table 5-7: Sampling Schedule for indoor VOC measurements at the arrivals hall (Beirut Airport, 2014)

17-18 June, 2014 Summer Regular ventilation		30-31 October, 2014 Fall/Winter Irregular ventilation		25-26 November, 2014 Fall/Winter Regular ventilation	
8-channel sampler		1-channel sampler		1-channel sampler	
Date	**Sampling time (Center)**	**Date**	**Sampling time (Center)**	**Date**	**Sampling time (Center)**
17-Jun-14	16:00	30-Oct-14	10:15	25-Nov-14	09:15
17-Jun-14	18:00	30-Oct-14	13:15*	25-Nov-14	12:15
17-Jun-14	20:45	30-Oct-14	16:15	25-Nov-14	15:15
18-Jun-14	00:30	30-Oct-14	19:15	25-Nov-14	18:15*
18-Jun-14	07:30	30-Oct-14	22:15	25-Nov-14	21:15
18-Jun-14	10:45	31-Oct-14	04:15	25-Nov-14	23:15
18-Jun-14	13:30	31-Oct-14	08:45	26-Nov-14	08:45
18-Jun-14	16:00				

-Regular ventilation corresponds to the mixing of 20% fresh air with 80 returning indoor air, while irregular ventilation corresponds to the mixing of 50% fresh air with 50% returning indoor air.
-The sampling duration was fixed at 30 min at a rate of 100 mL min^{-1} (total volume of 3L). All of the tubes were analyzed with GC/FID except those marked with an asterix (*Analyzed with GC/MS).

Table 5-8: Sampling schedule for NO_2 measurements at the arrivals hall (Beirut Airport, 2014-2015)

Date	30-31/10/14	25-26/11/14	17-24/6/15	24-29/6/15
Location	**Duration**			
Indoor	24 hr	15 hr	7 d	7 d
Outdoor Baggage	24 hr	15 hr	7 d	7 d
Fresh Air	24 hr	15 hr	7 d	7 d

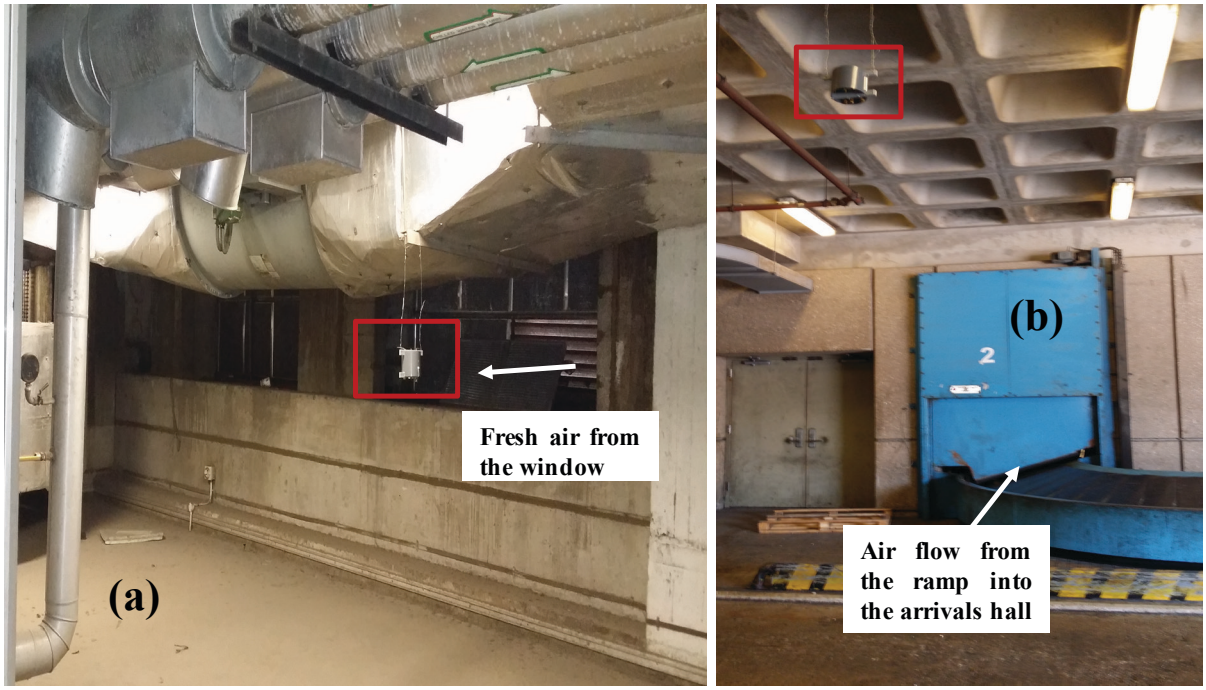

Figure 5-14: Installation of polyethylene cage (red square) (a) in the mechanical room to measure NO_2 levels in fresh air supplying the arrivals hall at Beirut Airport and (b) near the baggage loaders to measure NO_2 levels in the air that enters from the ramp into the arrivals hall through openings

Chapter 6 : Experimental Results and Discussion

This chapter presents the main findings for the previously described measurement campaigns (chapter 5). The results of signature campaigns are presented in section 6.1. Using the fingerprint results of the signature campaigns, it was possible to track the impact of aircraft activities in preliminary investigations presented in section 6.2, which corresponds to transect campaigns as described in the previous chapter. The results of NO_2 passive campaigns for ADMS-Airport model validation are presented in section 6.3.

Indoor VOC measurements conducted in the maintenance room and arrivals hall are presented in section 6.4. These measurements showed an interesting relation between aircraft number and VOC levels in the arrivals hall.

6.1 OUTDOOR CAMPAIGNS

6.1.1 SIGNATURE CAMPAIGNS

The 48 VOCs measured mainly represent the most abundant compounds from aircraft emissions according to previous studies (chapter 2). They are divided into different chemical families, i.e. light alkanes (C_2-C_7), heavy alkanes (C_8-C_{14}), alkenes (C_2-C_6), light aldehydes and ketones (C_2-C_6), heavy aldehydes (C_9, C_{10}), monoaromatics, and d-limonene. The detailed results of the measured VOCs in the exhaust at the various modes of the LTO cycle as well as the APU emissions are summarized in Table 6-1. It is important to note that chlorinated alkenes (trichloroethene and tetrachloroethene) were absent from all the samples. This result is in accordance with the study done for the City of Park Ridge (City of Park Ridge, 2000) which reported that both chloroalkenes were not found in jet exhaust.

The first subsection describes the campaigns conducted to identify aircraft tracers by performing comparisons between the speciation of heavy VOC emissions from aircraft exhaust and gasoline exhaust. The second subsection describes the speciation of the total VOC groups measured in real conditions and at various thrust settings. The last subsection presents comparisons between the speciation of VOC groups obtained in this study and various other studies obtained whether through engine tests or under real conditions (case of idle power).

Because sampling conditions could be very different from one sample to another or from one day to another, the results will often be presented and discussed in terms of percentages and not as quantitative data.

- Aircraft Tracers

We have defined a speciation by averaging all data collected with the same sampling conditions, 30 min or 30 s × 6. The profile labelled “Aircraft” constitute the average of samples collected near the aircraft when either the APU or the main turbine engines were running. In the case of 30 s × 6 technique, 6 samples were averaged to assess heavy VOCs, while 3 samples were averaged to represent the speciation obtained using the 30-min technique. The profile labelled “Airport” constitutes of 3 samples taken at the airport roof to assess the ambient airport concentrations affected by the total airport activities

including aircraft, ground support equipment (GSE), APU, refuelling, etc. The profile "gasoline" corresponds to the average of 4 samples which represent gasoline exhaust.

As mentioned in chapter 5, several samples were taken for Jet A-1 vapor, however only 1 sample was analyzed and interpreted Jet A-1, as all the other samples overloaded the GC column and saturated the detector.

Distribution of Heavy VOCs by Family

It is important to assess the distribution by family of aircraft VOC emissions because each family has its different environmental and health effects. Heavy VOCs emitted are broken down into heavy alkanes (C_8-C_{14}), heavy aldehydes (C_9, C_{10}), benzene, and other monoaromatics. The 20 measured heavy VOCs using GC-MS accounted for only a portion of aircraft exhaust since the target VOC species covered only a limited range (C_6-C_{14}). This range was chosen because it showed significant differences between aircraft and vehicle exhaust during our primary qualitative study.

Our first objective was to identify emission tracers from aircraft by comparing the emission profile of aircraft engines to that of vehicle exhaust gas. As shown in Figure 6-1, the profiles "aircraft" and "gasoline" illustrate significant differences. Indeed, the most prominent difference is the dominance of heavy alkanes (C_8-C_{14}) in the aircraft profiles and their absence from the profile of gasoline. The total concentration of heavy alkanes was 53 $\mu g\ m^{-3}$ for the profile "aircraft" (30 s × 6), which accounted for 51% of the total heavy VOCs. Similar speciation was observed for the 30-min sampling, where heavy alkanes (C_8-C_{14}) constituted 64% of the mass of aircraft sources with a smaller magnitude of 9.2 $\mu g\ m^{-3}$. In addition to heavy alkanes, heavy aldehydes (C_9, C_{10}) were present only in aircraft sources with average concentrations of 2.6 and 0.2 $\mu g\ m^{-3}$ for the 30 s × 6 and 30-min and techniques respectively. These heavy aldehydes are mainly generated by the atmospheric photoxidation of heavy alkanes, kerosene combustion, and/or evaporation of raw fuel.

Table 6-1: Volatile organic compounds in jet engine emissions (units converted to μg m^{-3})
(Spicer *et al.*, 1994; Eichkoff, 1998; Anderson *et al.*, 2006; Schürmann *et al.*, 2007)

	This Study							***Spicer***			***Eichkoff[a]***	***Anderson (RB211-535E4)***			***Schürmann[b]***
Sampling distance (m)/position wrt engine	**10 m/ down- stream**		**17 m/ left**	**8-9 m/ below**		**130-190m/ behind**		**0.3-0.6 m/behind**			**30 m/ behind**	**1 m behind**			**50 -100 m behind**
Engine Status*/ Flight mode	APU A330 (GC-FID)	APU A330 (GC-MS)	Touch down (GC-FID)	Approach (GC-FID)	Approach (GC-MS)	Take-off (GC-FID)	Take-off (GC-MS)	Idle	30%	80%	Averaged run	4-7%	26%	61%	***Taxi***
n-Octane	1.52	bDL	0.78	0.21	22.10	2.10	3.31	664.96	bDL	bDL	0-120				
n-Nonane	2.97	6.53	1.70	0.64	55.96	2.72	bDL	746.63	53.33	bDL	20-760				
n-Decane	4.66	9.70	1.39	0.87	34.63	3.88	3.77	4259.53	76.91	11.83	30-1480				bDL
n-Undecane	2.32	bDL	0.40	n.d.	8.62	2.83	4.52	6499.38	58.49	129.99	30-1010	7.71	2.54	8.54	0.56-11.74
n-Dodecane	2.57	bDL	0.57	0.13	2.67	2.87	2.90	7365.62	502.85	297.46	20-850				1.13-35.96
n-Tridecane	0.36	bDL	0.42	0.16	bDL	0.97	2.89	9275.49	114.99	168.65	20-570				
n-Tetradecane	bDL	bDL	bDL	bDL	bDL	bDL	bDL	7754.12	156.73	164.98	20-270				
Nonanal	-	bDL	-	-	bDL		2.37	-	-	-	-				
Decanal	-	bDL	-	-	2.02		3.60	-	-	-	-				
Benzene	-	3.74	-	-	bDL	-	22.52								
Toluene	15.69	3.63	4.35	1.59	9.98	17.94	10.77					36.70	1.17	1.62	
Ethylbenzene	2.45	0.24	0.11	n.d.	4.99	2.59	2.47	13413.48	64.96	64.96	60-690	15.55	3.60	3.14	7.77-39.20
m, p-Xylene	7.92	0.77	2.48	0.94	13.66	7.18	3.16	5976.65	38.31	NA	70-260	2.87	0.57	0.44	6.06-28.37
o-Xylene	4.32	1.95	n.d.	0.72	13.06	4.06	2.70	1854.1	bDL	bDL	10-180	6.40	1.77	2.25	1.42-12.19
Styrene	0.95	0.62	1.74	0.18	0.45	0.71	0.37	3001.6	bDL	bDL	20-450	4.99	1.28	1.46	4.03-25.90
1,2,4-TMB	7.25	1.92	1.91	n.d.	36.67	8.47	0.95	1765.6	bDL	bDL	10-350	NA	NA	NA	1.89-17.97
1,4-DCB	-	bDL	-	-	bDL	-	bDL	3291.23	43.31	-	10-90	3.55	1.85	2.05	1.75-17.95
Propyllbenzene	-	0.59	-	-	2.36	-	0.11								
Butylbenzene	-	0.53	-	-	4.19	-	0.18								
Acrolein	54.74	-	7.87	bDL	-	46.87	-								
Propanal	9.23	-	bDL	bDL	-	37.23	-								
Butanal	bDL	-	bDL	bDL	-	4.18	-	9790.10	23.31	23.31	62-190				
Pentanal	2.44	-	1.00	bDL	-	2.87	-	2897.96	24.15	24.15					
Hexanal	bDL	-	bDL	bDL	-	bDL	-								
Acetone	13.67	-	60.37	38.75	-	26.92	-	1473.13	386.40	166.63					
2-Butanone	bDL	-	bDL	bDL	-	0.87	-								

Table 6-1 (Continued): Volatile organic compounds in jet engine emissions (units converted to μg m^{-3})

	This Study							*Spicer*			*Eichkoff*[a]	*Anderson (RB211-535E4)*			*Schürmann*[b]
Sampling distance (m)/position wrt engine	**10 m/ down- stream**		**17 m/ left**	**8-9 m/ below**		**130-190m/ behind**		**0.3-0.6 m/behind**			**30 m/ behind**	**1 m behind**			**50 -100 m behind**
Engine Status*/ Flight mode	**APU A330 (GC-FID)**	**APU A330 (GC-MS)**	**Touch down (GC-FID)**	**Approach (GC-FID)**	**Approach (GC-MS)**	**Take-off (GC-FID)**	**Take-off (GC-MS)**	**Idle**	**30%**	**80%**	**Averaged run**	**4-7%**	**26%**	**61%**	***Taxi***
D-Limonene	5.90	-	1.00	bDL	-	2.29	-								
Ethane											-				
Propane	1.05	-	2.23	1.94	-	1.23	-	1388	50.01	bDL	-	21.51	3.93	2.40	4.46-24.51
Isobutane	4.08	-	8.15	9.31	-	5.14	-	312	18.34	bDL	-	9.11	3.12	1.93	2.75-5.15
n-Butane+cis-2-Butene	2.90	-	9.07	4.05	-	6.56	-	-	-	-	-	1.81	0.77	0.65	0.39-3.24
Isopentane	1.69	-	5.44	6.46	-	9.30	-	-	-	-	-	8.14	2.27	1.74	1.80-9.73
n-Pentane+cis-2-Pentene	3.14	-	bDL	0.35	-	0.80	-	-	-	-	-	3.45	1.32	0.81	1.80-49.52
n-Hexane	0.81	-	0.82	bDL	-	10.18	-	-	-	-	-	1.05	0.45	0.30	1.15-7.14
n-Heptane	bDL	-	bDL	bDL	-	bDL	-	-	-	-	10-50	0.79	0.36	0.36	0.33-1.45
	2.07	bDL	0.77	1.40	4.80	0.87	8.73	583.34	bDL	bDL					
Ethene															
+Acetylene	16.28	-	20.30	16.73	-	10.57	-	48892	bDL	bDL					58.37-191.13
Propene	1.39	-	7.88	0.74	-	3.08	-	18092	18	bDL					18.89-159.55
1-Butene	bDL	-	1.20	2.45	-	bDL	-	9332	23	47		579.66	2.40	1.78	4.64-43.18**
1,3-Butadiene	bDL	-	0.53	bDL	-	0.07	-	8974	bDL	22.5		118.98	0.38	0.42	bDL-11.11
Trans-2-Butene	bDL	-	0.86	bDL	-	0.80	-	11120***	23***	bDL		31.03	0.12	0.16	0.56-5.42
1-Pentene	bDL	-	2.64	0.27	-	bDL	-	5161	bDL	bDL		34.19	bDL	bDL	bDL-19.95
Trans-2-Pentene	bDL	-	bDL	bDL	-	bDL	-	-	-	-		3.13	0.12	0.05	bDL-3.91
Isoprene	2.10	-	6.69	4.21	-	1.04	-	-	-	-					0.84-9.43
1-Hexene	bDL	-	2.20	bDL	-	bDL	-	5879	35	-					
TVOC (μg m^{-3})	174.7	30.2	155.9	92.11	216.2	227.2	75.3	113311	601	283	62-190	820	15	10	140-400

*Engine power setting is given in percent of maximum rated thrust.
**1-Butene coelutes with propyne
***cis-2-butene + trans-2-butene
[a]CF6-50C2/E2, CFM56-3B1
bDL: below Detection Limit

Another difference is that the total concentration of monoaromatics in the profile "gasoline" is around 3 times higher than the profile "aircraft" at 122 and 44 μg m^{-3} respectively. Benzene dominates the mass emissions in gasoline exhaust (77% of the total mass emissions) while in aircraft exhaust "other monoaromatics" dominate (82% of the mass of monoaromatics emitted). The absence of heavy alkanes and aldehydes from the VOC speciation of the gasoline exhaust is in accordance with previous studies, which reported that heavy alkanes especially C_8-C_{14} were negligible or almost not present in gasoline exhaust (Liu *et al.*, 2008; Wang *et al.*, 2013). These results are not surprising because jet aircraft use a kerosene-based fuel (Jet A-1) with a higher overall molecular weight than gasoline. This was confirmed by the analysis of unburned Jet A-1 vapor used in Beirut Airport. Results show that heavy alkanes constitute 57% of the mass of unburned kerosene vapor. Kerosene vapor, in turn, constitutes up to 30% of aircraft emissions (Ritchie *et al.*, 2003a). This explains the presence of heavy alkanes as fuel-derived emissions. Heavy aldehydes can be either combustion products (fuel oxidation) or due to unburned fuel. Jet A-1 fuel may have significant amount of species of carbons i.e. more than 14, but it was not suitable to measure them because the sampling method involving carbopack B as adsorbent, was adapted for gaseous species up to C_{12}-C_{14} only. It is known that the average chemical formula for kerosene (Jet A-1) differs from one source to another and ranges from $C_{10.9}H_{20.9}$ to $C_{12}H_{23}$ (Dagaut and Cathonnet, 2006).

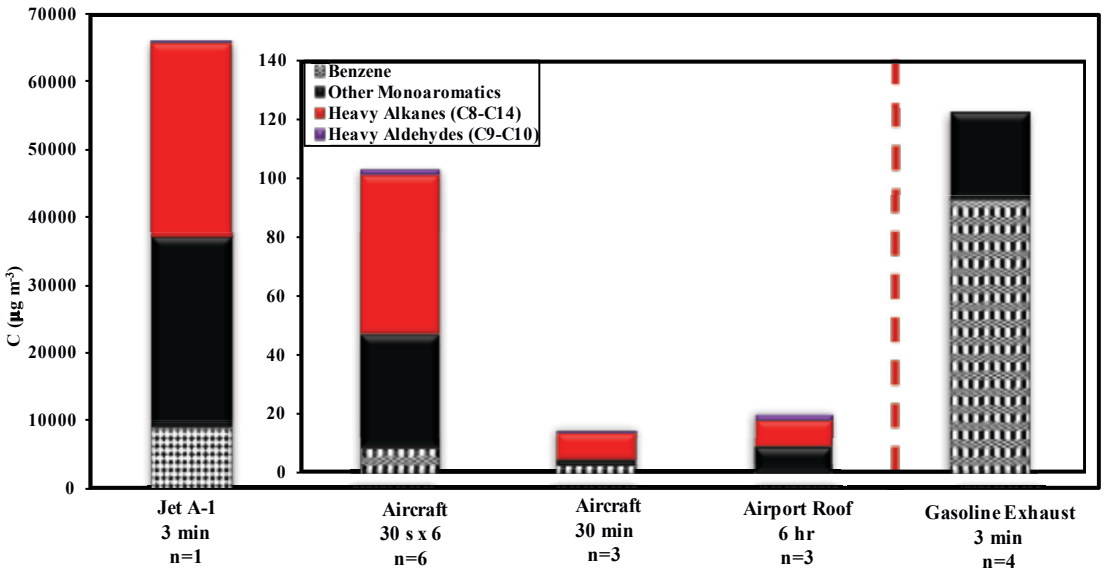

Figure 6-1: Heavy VOC groups (GC-MS)

Conner *et al.* (1995) averaged 2 air samples collected near an aircraft at the gate that was refuelling and preparing for departure, with running engines. Similar observations were found as heavy alkanes and monoaromatics constituted 66% and 44% of the heavy VOC composition (considering our target heavy VOCs).

For the "airport" profile, highest concentrations were found during the noon rush hours between 13:00 and 17:00, while lower concentrations were observed between 01:00 and 07:00. This change in concentration is dependent on the traffic intensity. The average heavy TVOC was 20.5 $\mu g\ m^{-3}$ of which 47.5% was heavy alkanes, 45% monoaromatics, and 7.5% heavy aldehydes.

In all the profiles, benzene had the highest concentration among the monoaromatics except for the airport roof (see Figure 6-1).

Results show that aircraft samples taken using the 30 s × 6 technique have a higher TVOC concentration (88 $\mu g\ m^{-3}$) than those taken with the 30-min technique (15 $\mu g\ m^{-3}$). The 30-min samples have a TVOC closer to that of the airport roof and thus are more representative of ambient airport concentrations rather than aircraft signature emissions. This conclusion is explained by the fact that with the 30 s × 6 technique, sampling was done just when the aircraft passed near the sampler to take exclusively (as much as possible) aircraft engine emissions with least interference from the ambient concentration. Results from the 30 s × 6 technique will be chosen in the next paragraphs to discuss the speciation of aircraft emissions at different thrust settings.

Speciation of Heavy VOCs

Information regarding the distribution of emissions by carbon number is important because such data can distinguish the cracking and partial oxidation products from unburned fuel. The carbon number distribution of Jet A-1 vapor shows that C_8-C_9 compounds have the highest mass contribution, followed by the contribution of n-decane, n-undecane, n-dodecane, n-tridecane, and n-tetradecane mentioned in decreasing order of contribution (Figure 6-2 (a)). Results also indicate the presence of nonanal and decanal in jet vapor. Upon previous analysis of JP-4 jet fuel by Spicer *et al.* (1984), it was seen that C_7-C_9 dominated the speciation for a wide range of VOCs and little high volatility (light) VOCs were seen. As deduced by Spicer *et al.*, we can conclude that the exhaust species found in

C_2-C_6 were probably products of combustion, referred to as "combustion derived", and VOCs C_8 and higher were "fuel-derived".

The fraction of each species of the TVOC is known as the species "abundance", presented as a percent of TVOC on the basis of μg m^{-3} (weight %). The set of species abundances for a source is known as the "source profile" or "source fingerprint" (Conner *et al.*, 1995; Henry *et al.*, 1994). Source profiles are illustrated in Figure 6-2. Figure 6-2 (a) illustrates the speciation of heavy alkanes. n-Nonane and n-decane dominate the speciation in the profiles "aircraft" (30 s × 6) and "airport". The airport roof source profile is in close resemblance to the samples collected with the 30 s × 6-technique. The 30-min aircraft source has a different VOC speciation where C_9-C_{13} have almost equal contribution. It is important to note that this difference in speciation between the 2 sampling techniques is also attributed to the different sites used to calculate the average emissions. The speciation of heavy alkanes in kerosene vapor is as follows: n-octane (67%), n-nonane (26%), n-decane (4%) and others (<1%). This explains the presence of these high alkanes in aircraft and airport emissions, as they are components of jet fuel. These results are similar to results obtained within the platform of the airport of Charles De Gaulle, where n-nonane was found to be the dominating species (50%) among C_6-C_9 measured alkanes (Lelievre, 2009). In our work, the speciation of other monoaromatics for "aircraft" (30 s × 6) and "gasoline" is dominated by toluene that has a higher contribution in the "gasoline" profile (91%) than in the "aircraft" profile (45%) (Figure 6-2 (b)). 1,2,4-trimethylbenzene, emitted by aircraft as well as vehicles, dominates the airport roof source profile. It is important to note that inhalation of air containing trimethylbenzene can lead to irritation of the respiratory tract, sore throat, headache, wheezing, vomiting, anxiety, tension and may affect the blood.

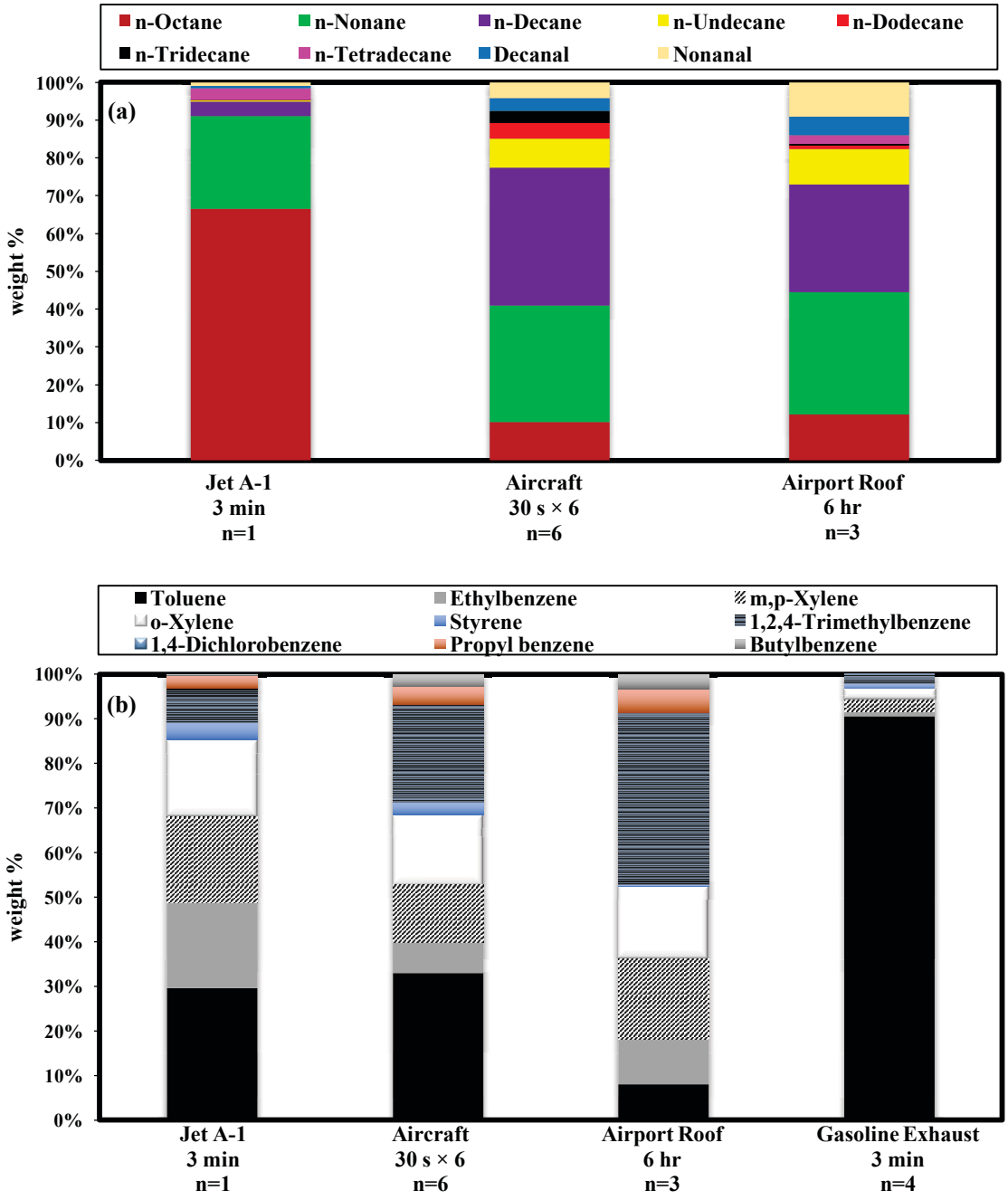

Figure 6-2: (a) Speciation of heavy alkanes and aldehydes (b) Speciation of "other monoaromatics" determined from measurements conducted in July 2015 (GC-MS)

Speciation of VOCs with Engine Power

It should be emphasized that the measurements presented are not subject to a normative character and that the variety in the conditions (sampling distance, aircraft type, engine type, etc.) doesn't permit to compare the emission concentrations between the different studies. However, these results illustrate the variability of concentrations and speciation in the plume of the aircraft. Results confirm that VOC compositions decreased with increased

engine power settings as can be seen for concentrations of approach (30% of the rated thrust) compared to that of take-off (85-100% of the rated thrust) (Figure 6-3). The observed TVOC equal to 216 µg m^{-3} for the approach profile decreased by a factor of 3 for the take-off, i.e. down to 75 µg m^{-3}. For the same power range, the observed levels of monoaromatics and heavy alkanes decreased by factors of 4 and 5 respectively. The highest drop in concentration was observed for 1,2,4-trimethylbenzene with a factor of 39. These results could be expected. Indeed, turbine engines primarily emit CO and NMHC species as a result of incomplete combustion of jet fuel. The relative amounts of NMHC emissions depend on combustor temperature and pressure, fuel to air ratio, and the extent to which fuel is atomized and mixed with inlet air. VOC emissions are higher at low power settings when the temperature of the air is relatively low and the fuel atomization and mixing process is least efficient. This is also according to ICAO databank sheets for unburned hydrocarbons (UHC) for all modern turbine engines; all engines produce less CO and NMHC emission per kg of fuel burned as their power levels are increased above idle (Anderson *et al.*, 2006). In comparison to our observations, Spicer *et al.* (1994) found that TF-39 and CFM-56 engines exhibited larger decreases in NMHC emissions with increasing engine power. These differences can be mostly accounted for by fact that the TF-39 and CFM-56 engines produce much higher levels of emissions at idle (low power) than do the newer commercial engines.

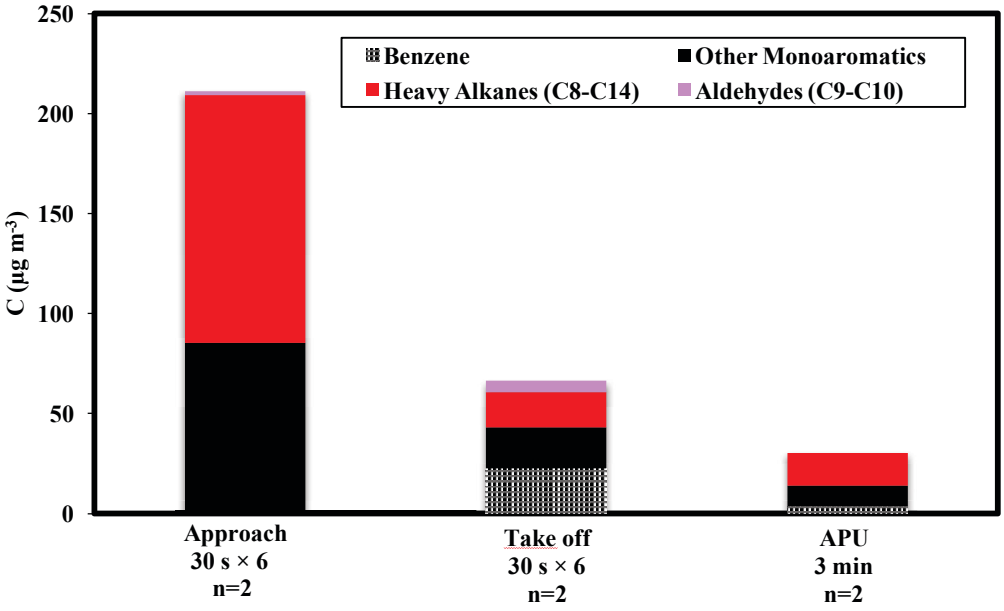

Figure 6-3: Heavy VOC emissions for different aircraft operations (GC-MS)

The concentration of benzene increased from approach (bDL) to take-off (22.5 μg m^{-3}) while the concentration of "other monoaromatics" decreased from 85 to 21 μg m^{-3}. This is due to the cracking of higher aromatics upon the increase in temperature which leads to less amounts of these species, but increased amounts of benzene (Schürmann *et al.* 2007). Figure 6-4 (b) compares the speciation of "other monoaromatics" in aircraft and gasoline profiles. Benzene dominates the mass speciation of the monoaromatics in all the sites except for approach. It is 92 μg m^{-3} for gasoline exhaust. As previously noted, toluene dominates the monoaromatic speciation in aircraft and gasoline exhaust.

The speciation of both heavy alkanes and heavy aldehydes is dominated by n-nonane and n-decane for approach and APU and by n-undecane and n-decane for take-off (Figure 6-4 (a)). The heavy alkanes in APU emissions are only n-nonane and n-decane. The presence of these heavy alkanes is a result of unburned kerosene vapor (Spicer, 1984). It should be noted that emissions during take-off are partially composed of unburned fuel; they contain C_8-C_{13} alkanes and contain nonanal and decanal coming either from kerosene combustion or from the raw fuel. Airport roof, which is present between the 2 jetties, is in close proximity to the gates and is consequently affected to a great extent by APU emissions. This explains the dominance of n-nonane and n-decane on the VOC mass at this site. Nonanal and decanal are also present at the airport roof and are probably oxidation derived. Similarly, higher alkanes (C_8-C_{14}) and nonanal have been found at increased levels at the fence of O'Hare International Airport and was attributed to airport activities (City of Park Ridge, 2000). Decanal has been previously identified as a VOC associated with exhaust from tested commercial aircraft engines (EPA, 2009b).

The absence of 1,4-DCB is not surprising as it a chlorinated aromatic compound not expected to be present in combusted fuel. It is worth mentioning that, in addition to heavy alkanes, the following compounds were present at high intensities in take-off and approach source profiles: 1,1,2,3-tetramethylcyclohexane, 1,1,3-trimethylcyclohexane, and 2-butyl-1,1,3-trimethylcyclohexane.

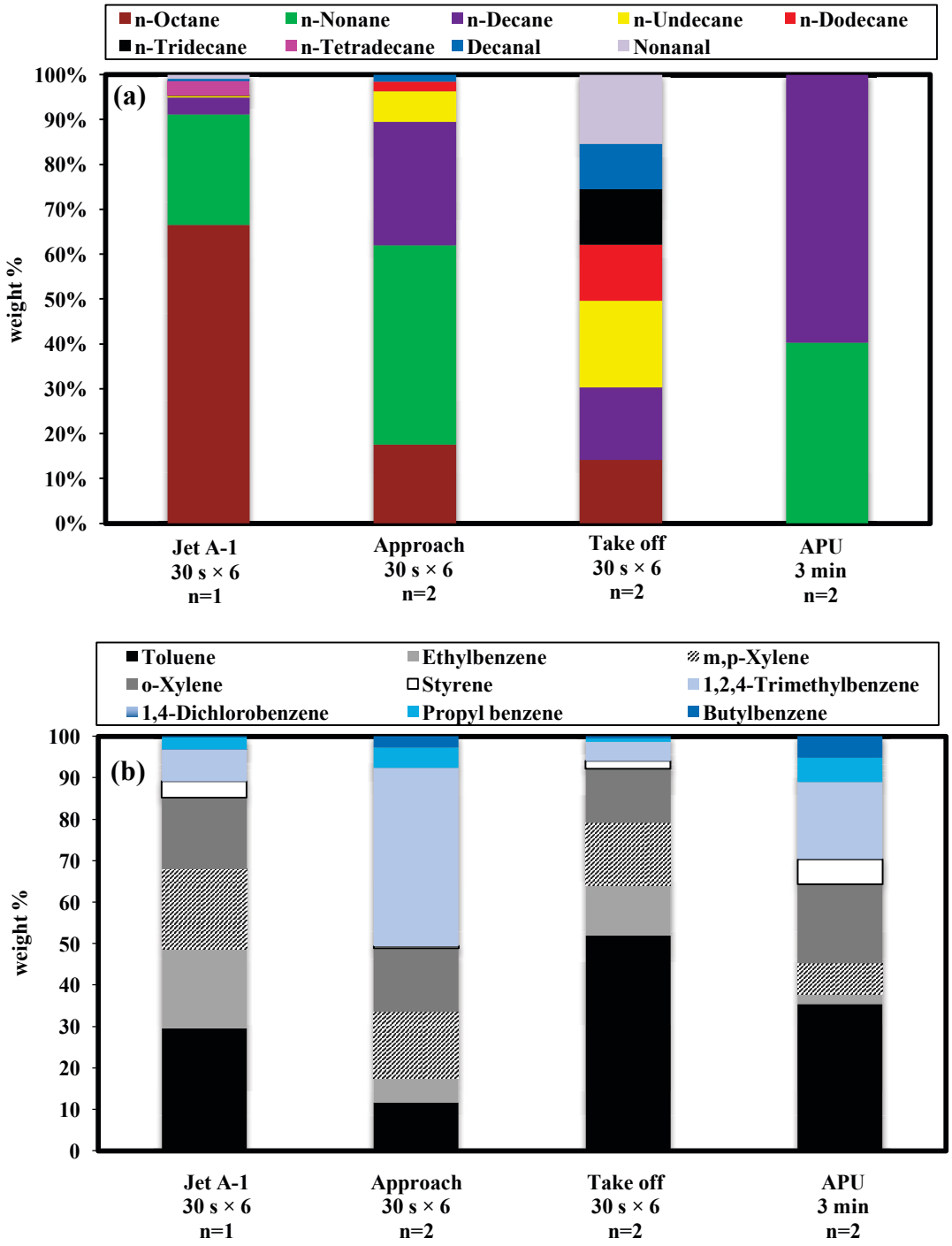

Figure 6-4: Comparison of the speciation between the different modes of aircraft operation (a) Heavy alkanes and aldehydes (b) "Other monoaromatics" (GC-MS)

- Complete Speciation of VOCs (GC-FID)

Figure 6-5 shows that the total concentration of VOC groups in the "aircraft" source profile taken using the 30 s × 6 technique has a higher TVOC (160.8 µg m^{-3}) than that taken by the 30-min technique (28.3 µg m^{-3}), as found in our previous measurements

(GC/MS) with the exception of heavy alkanes (Figure 6-5). Again, it can be deduced that the 30 s × 6 samples are more representative of aircraft emissions rather than the 30-min samples which were closer to the airport ambient concentration (82.61 µg m^{-3}). Indeed, it is expected and consistent to obtain higher concentrations in aircraft exhausts than in ambient concentrations. The 30 min samples are finally more influenced by ambient concentrations than by aircraft exhaust.

The average aircraft profile, represented by the 30 sec technique, was dominated by light aldehydes and ketones (48% of TVOCs) followed by alkenes (16% of TVOC), monoaromatics (14.5% of TVOC), and light alkanes (14.5% of TVOC). Light aldehydes and alkenes are mainly combustion derived VOCs previously reported as part of the major VOC groups emitted from aircraft exhaust (EPA, 2009a). As illustrated in Figure 6-5, the VOC speciation at the airport roof was dominated by monoaromatics (38.5%), light alkanes (29%), aldehydes and ketones (16.5%), and heavy alkanes (9%), listed in decreasing order of magnitude. The dominance of monoaromatics and light alkanes is probably enhanced by emissions from vehicles and ground support equipment (GSE) near the airport roof. The difference in speciation between VOCs measured in the airport roof for the campaign conducted in October 2014 and that conducted in July 2015 can be probably explained by the difference in time conditions (weather, light, etc.).

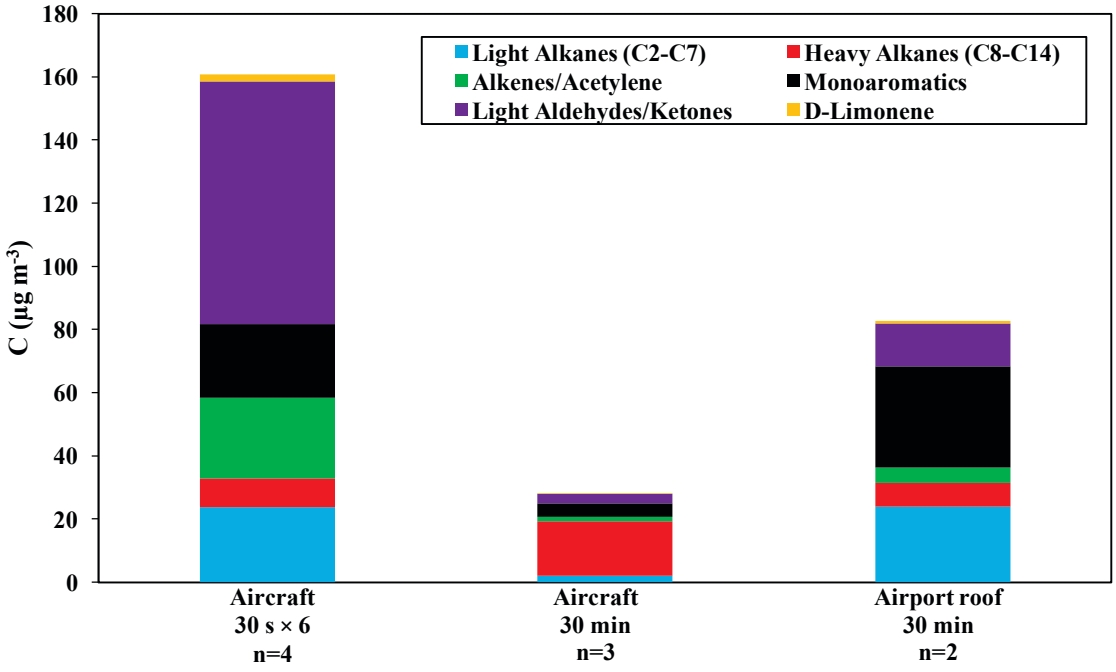

Figure 6-5: VOC distribution by compound class determined from measurements performed in October 2014 (GC-FID)

Distribution of VOC Groups at Different Engine Powers

Technical errors occurred during sampling at the "taxi" location. New samples have been taken and will be analyzed. To assess emissions at idle power, the sample taken at the location "touchdown" will be used after confirming with several pilots that the engine settings at this point are idle settings.

Results confirm that VOC compositions in jet exhaust vary with engine power settings (see Figure 6-6). As the engine power increased from idle (touchdown) to approach phase, TVOC decreased by a factor of 1.7 from 154 µg m^{-3} to 91 µg m^{-3}. The take-off profile would have had as well a lower value of TVOC than approach and idle values, if acrolein (47 µg m^{-3}) were excluded.

As for aliphatic hydrocarbons, the predominant presence of alkenes and acetylene (unsaturated aliphatic hydrocarbons) over alkanes was observed at idle power (62% of the total aliphatic hydrocarbon species). The predominance of unsaturated HCs is consistent with observations by Anderson *et al.* (2006), Spicer *et al.* (1994), and Schürmann *et al.* (2007).

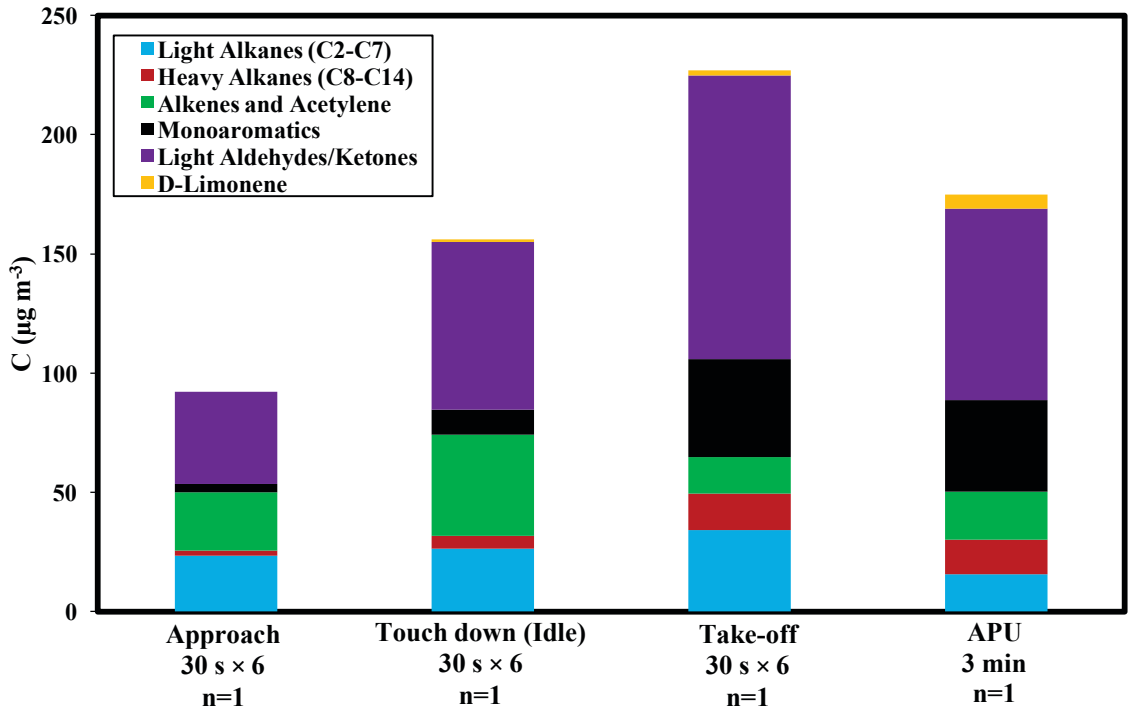

Figure 6-6: Exhaust VOC distribution by compound class (GC-FID)

The effect of engine thrust settings on the relative contribution of the different families is evident by the decrease in the concentration of alkenes from idle power (42.0 μg m^{-3}) (touchdown) to take-off (15.4 μg m^{-3}). Alkenes and alkynes (represented by acetylene) are generally products of incomplete combustion, and consequently are present at much higher concentrations at idle compared with high power settings (Spicer *et al.*, 1992). With higher speed, the contribution of alkanes increased accounting for 68% of the mass of aliphatic HCs. In fact, increasing the engine power drives a lower contribution of unsaturated aliphatic compounds in favor of alkanes and aromatics (Anderson *et al.*, 2006). This increase results from the temperature rise within the combustor. These observations are consistent with those of Lelievre *et al.* (2009). Another effect of engine power was seen in the increase of the contribution of heavy alkanes from 2 to 8% from approach to take-off, corresponding to 2 and 15 μg m^{-3} respectively. As mentioned by Anderson *et al.* (2006), at higher engine powers, species with low carbon number disappear, and VOCs with higher carbon numbers become more dominant. These could be either fuel or combustion derived (Anderson *et al.*, 2006).

Finally, for APU emissions, results show that they were of the same order as main engine emissions with TVOC equal to 172 μg m^{-3}.

Speciation of VOC Groups at Different Engine Powers

Figure 6-7 presents the speciation of the previously discussed VOC groups with engine power. Light alkanes from aircraft emissions were mainly dominated by propane and isobutene (idle and approach). According to previous studies (Anderson *et al.*, 2006; Schürmann *et al.*, 2007), light alkanes were dominated by ethane and propane at these thrust settings. The fact that ethane contributes less to the light alkane speciation in our study can be attributed to the weak adsorption properties of the used adsorbent. i.e. Carbosieve^{TM} S-III for light VOCs, with C_2 molecules, as previously mentioned by Liaud (2014). Figure 6-7 (b) presents the speciation of heavy alkanes at different engine powers and from APU emissions. The first interesting observation to note is that, for the same mode of operation, the speciation of heavy alkanes using GC/FID is similar to that obtained using GC/MS (previously discussed, see Figure 6-4 (a)). For example, with both techniques n-nonane and n-decane dominate the speciation of heavy alkanes for the approach phase, and for APU emissions. Moreover, in both measurements, the speciation for the take-off phase is more distributed as a result of higher engine powers.

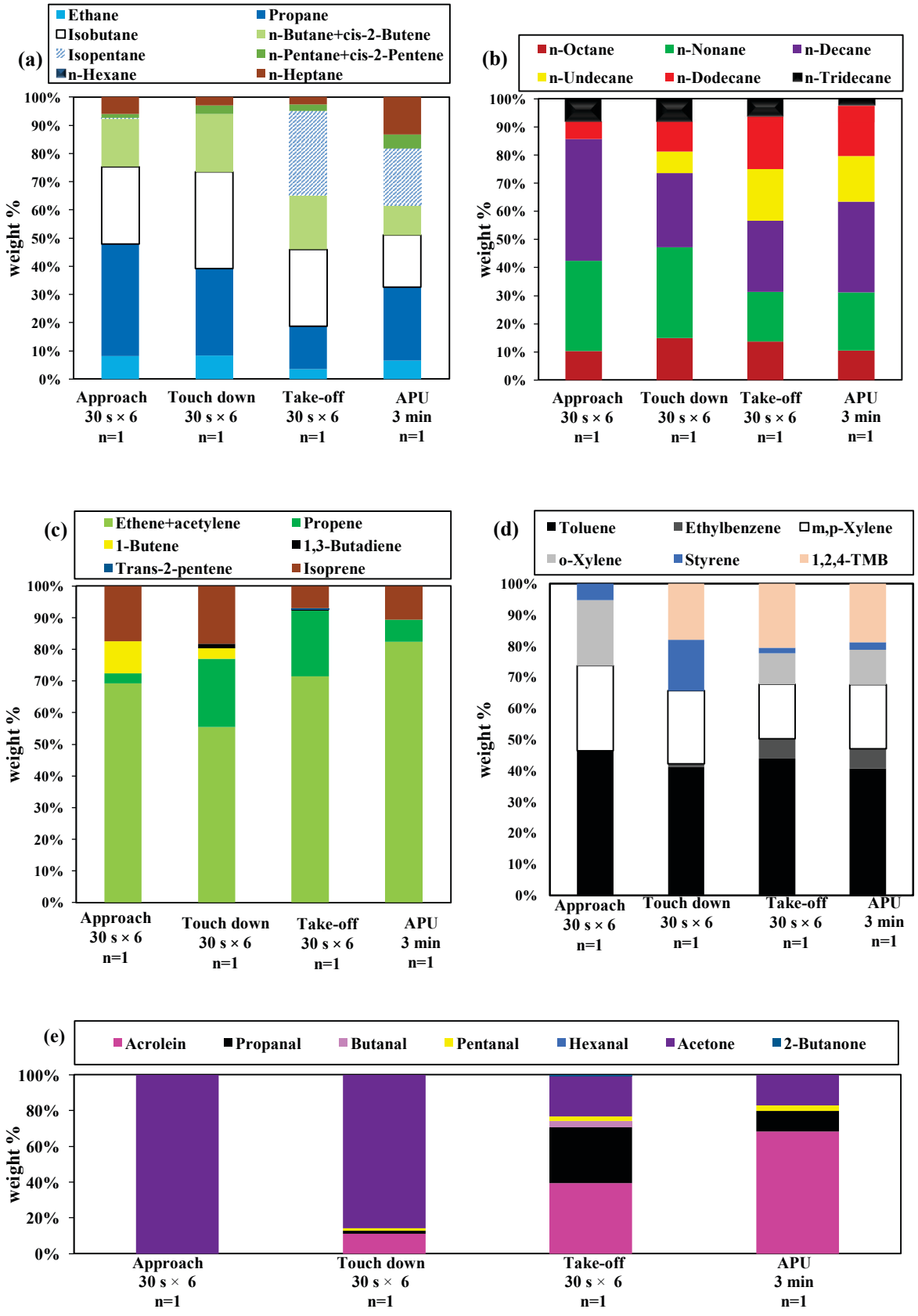

Figure 6-7: Speciation of VOCs by family: (a) light alkanes, (b) heavy alkanes, (c) light alkenes/acetylene, (d) monoaromatics, (e) light aldehydes and ketones (GC-FID)

Ethene, acetylene, and propene clearly dominate the speciation of unsaturated aliphatic hydrocarbons in aircraft emissions, they alone represent 66-88% of the average aliphatic hydrocarbon mass emitted (Figure 6-7 (c)). According to experimental and kinetic modelling studies conducted by Dagaut *et al.* (2006), alkene and alkyne emissions are mainly dominated by light compounds (2 to 3 carbon atoms) produced as intermediate products during the oxidation of jet fuel. Previous studies conducted during engine tests or in real aircraft operations reported the dominance of C_2-C_3 over unsaturated HCs (Anderson *et al.*, 2006; Lelievre, 2009; Schürmann *et al.*, 2007). According to Anderson *et al.* (2006), C_2-C_3 compounds constituted 90-92% of unsaturated HC emissions from RB211-535E4. During measurements of real aircraft operations (taxi) by Schürmann *et al.* (2007), C_2-C_3 unsaturated aliphatics constituted 73-91% of the total HC emissions.

Another significant alkene is isoprene which has been previously found in both jet and traffic exhaust (Borbon *et al.*, 2001). Isoprene, which constitutes between 11-16% of the mass of unsaturated aliphatic hydrocarbons, was previously detected in aircraft exhaust emissions and not in refuelling emissions (Schürmann *et al.* 2007). Thus, it is "combustion-derived". As for monoaromatics, toluene and m, p-xylene dominated the speciation with approximately equal contributions for the different engine powers.

Aldehydes and ketones (oxygenated VOCs) in aircraft emissions were also dominated by C_2-C_3 compounds. Acetone, acrolein, and propanal constituted between 91-100% of the total oxygenated VOCs. Acrolein and propanal are included in the list of 14 Hazardous Air Pollutants (HAPs) present in the exhaust of aircraft according to the US EPA Clean Air Act (FAA, 2003) and have been identified as major components of jet exhaust (City of Park Ridge, 2000; EPA, 2009a). The highest concentrations of acrolein and propanal were found during take-off and in APU emissions (A330). The concentrations of acrolein ranged between bDL and 112 $\mu g\ m^{-3}$ while the concentration of propanal ranged between bDL and 37 $\mu g\ m^{-3}$. Acetone has been previously considered as a component of jet engine exhaust. Other sources that can contribute to the acetone levels may be due to maintenance activities performed on planes, like painting and parts cleaning. Butanal and hexanal which have been previously associated with jet exhaust (City of Park Ridge, 2000) are only present in jet and not in gasoline exhaust.

- Comparison with Bibliography (Total Results: GC-FID and GC-MS)

The comparison of aircraft exhaust emission measurements with previous studies needs to be conducted with caution. Several parameters like the sampling distance, sampling techniques, sampling conditions (real operations or in a test bed), age, model, and type of the engine (commercial or military), can strongly affect the magnitude of the obtained results (Table 6-1). Therefore, the safest way to compare results is through VOC speciation (expressed in % weight) even though the above mentioned parameters could still play a role in the difference or similarity of results.

Figure 6-8 presents the comparison of the speciation of VOC groups obtained in this study with those obtained by other studies. To conduct the comparisons, VOCs were reduced to cover exactly the same species for all the studies. Thus, in Figure 6-8 light alkanes are constituted of ethane, propane, n-heptane; aldehydes/ketones are constituted of acrolein, propanal and acetone; monoaromatics include toluene, ethyl benzene, m, p-xylene and o-xylene; and heavy alkanes are constituted of nC_8-nC_{12} straight chain alkanes. Comparisons were divided into comparisons with engines tests (Figure 6-8 (a), (b), (c)) and comparisons with measurements taken under real aircraft operation that took place during taxi or idle power (Lelievre, 2009; Schürmann *et al.*, 2007). This study is probably the first study to cover this range of VOC species at different thrust settings measured under real conditions. As a reminder, according to ICAO (2008a), the thrust levels for idle, approach, and take-off are respectively 7%, 30%, and 80% of the rated thrust. However, in real operation, the take-off thrust varies from aircraft to another according to the aircraft type and engine model, flight load, meteorological conditions, runway conditions, etc. Thus, in reality, the "take-off" sample collects a variety of different take-off thrusts which vary between 85 and 100% (Dennis Ting, 2009).

Figure 6-8 (a) presents the comparison of the total VOC groups obtained in this study, at the average of 3 powers, with that of Spicer *et al.* (1994). Figure 6-8 (b) presents the comparison of total VOC groups obtained in this study (minus aldehydes and ketones) with that obtained by Spicer *et al.* (1994), Lelievre (2009), and Anderson *et al.* (2006). It can be seen that alkenes dominate the VOC mass in the results obtained by Spicer *et al.* (Figure 6-8(a)), whereas light aldehydes/ketones dominate the speciation in our study. On the other hand, by comparing our results to those obtained by Lelievre, a similar speciation can be seen upon averaging the idle and approach powers, whereas results obtained by Anderson *et al.* (2006) and Spicer *et al.* (1994) still show higher domination of alkenes.

This is probably due to the difference in the sampling location; contrary to the mentioned studies in which sampling was done behind the engine exhaust as small distances (0.3-30 m) behind the engine, sampling in our study was done either sideways at relatively smaller distances (17-32 m to the left) or behind (130-190 m behind) to be able to sample several aircraft in real operation without interfering with aircraft operations. The difference can be also attributed to the difference in emissions between the CFM-56 engine studied by Spicer *et al.* (1994), RB211-535E4 measured by Anderson *et al*. (2006), and our averaged emissions for several engine types. The difference in emissions at idle power measured in our study and taxi emissions measured during real aircraft operation by Schürmann *et al.* (2007) can be related to the difference in aircraft type, age, engine type, etc. However, results obtained by Schürmann *et al.* are of the same order as our results.

Finally, Figure 6-8 (c) presents the speciation of heavy alkanes and monoaromatics measured in this study (GC/FID and GC/MS) compared to the results obtained with Spicer *et al*. (1994), Lelievre, and Eickhoff (1998). It can be seen that the speciation obtained in this study (GC/MS) is very similar to that obtained by Eickhoff for the averaged test run of the engine CFM56-3B1, while the speciation obtained with GC/FID (34% heavy alkanes) is similar to that obtained with CF6-50C2/E2.

Figure 6-8 (d) presents the comparison between results obtained in this study at idle power, to real measurements taken for real in-use aircraft. A similar speciation is observed between our study and that obtained by Lelievre (2009). Results obtained by Schürmann *et al.* (2007) (representing 3 aircraft engines) show a higher contribution of alkenes and heavy alkanes and a less contribution of light alkanes.

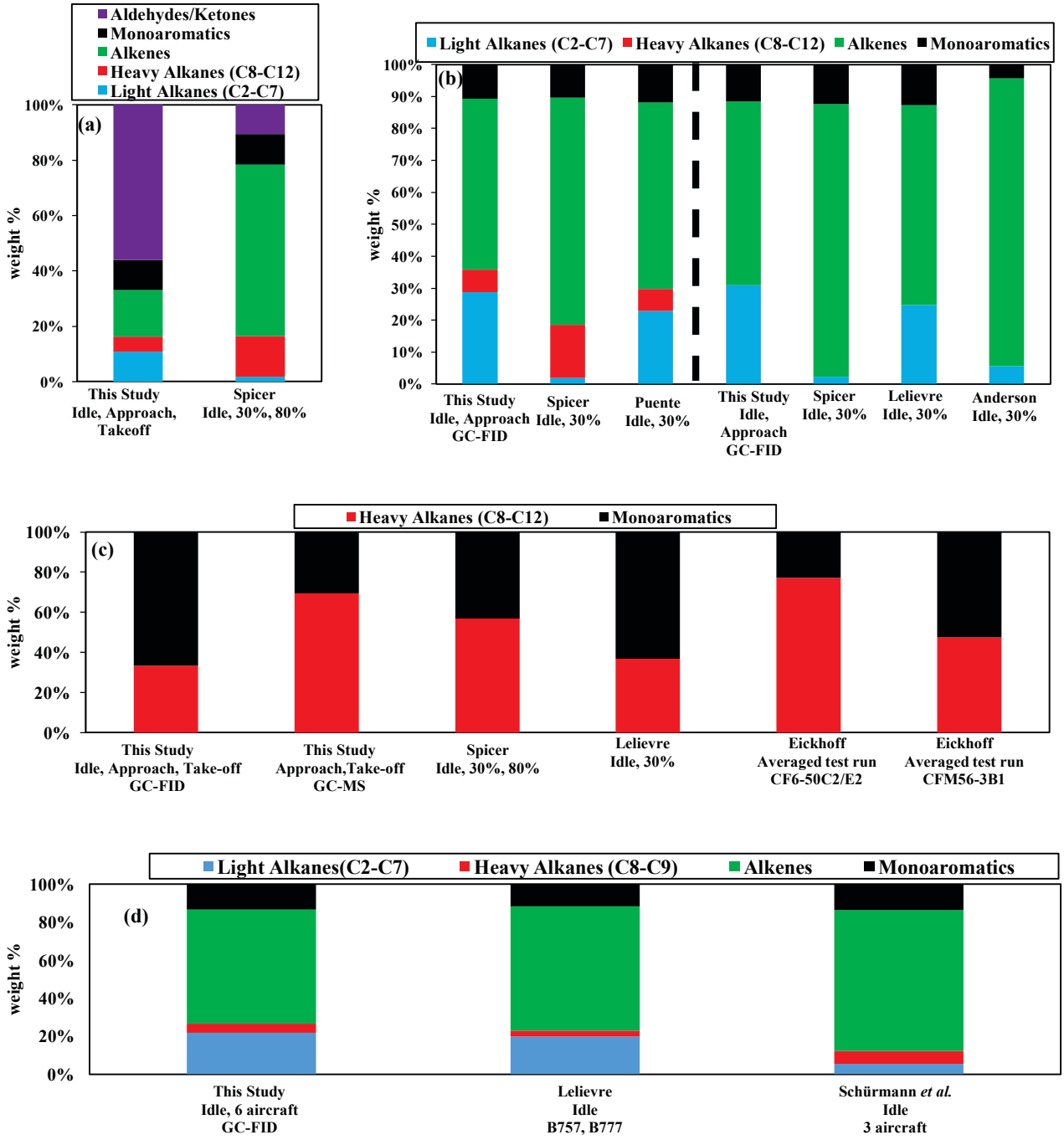

Figure 6-8: Comparison with bibliography (a) Total VOC groups, (b) Total VOC groups except aldehydes and ketones and TVOC except aldehydes/ketones and heavy alkanes, (c) heavy alkanes and monoaromatics, (d) comparison with real measurements at idle power (light alkanes, heavy alkanes, alkenes, and monoaromatics) (Note: In this Figure, light alkanes are constituted of ethane, propane, and n-heptane; light aldehydes/ketones include acrolein, propanal and acetone; monoaromatics comprise toluene, ethyl benzene, m,p-xylene and o-xylene; and heavy alkanes are constituted of nC_8-nC_{12} straight chain alkanes.

Conclusion

This is the first study covering a wide range of VOCs to assess emissions from a large number of in-use aircraft at various modes of operation. Results have shown that heavy alkanes and heavy aldehydes may be the best compounds used to resolve jet exhaust emissions from gasoline sources in air quality monitoring studies. These differences in the types of VOCs emitted act as "fingerprints" for the sources. The main reason for the presence of heavy alkanes is that jet aircraft use a kerosene based fuel (Jet A-1) that is mainly composed of heavy alkanes (11-14 carbon atoms) in contrast to gasoline fuel. On the other hand, the presence of heavy aldehydes is due to both kerosene combustion and the photo-oxidation of heavy alkanes. The identification of jet exhaust tracers opened the door for the next study, the objective of which was to identify the spatial extent of the impact of airport activities in environments polluted by vehicle and aircraft emissions.

In the present work, alkanes, alkenes, alkynes (represented by acetylene), aldehydes, and ketones were detected in jet exhaust as observed by Spicer *et al.* (1994). Since jet fuel is mainly composed of long heavy alkanes, then the presence of light VOCs in aircraft exhaust was a result of incomplete combustion rather than being unburned fuel. As for the total speciation of VOCs, results confirmed the dominance of light aldehydes and ketones, followed by alkenes.

The difference in aircraft engines, operating conditions, meteorological conditions, and sampling conditions made it difficult to compare emission levels with literature data. However, the comparison of percent compositions by mass showed resemblance to few studies (Eickhoff, W., 1998; Lelievre, 2009) and differences with other studies (Spicer *et al.*, 1994).

6.1.2 TRANSECT CAMPAIGNS: PRELIMINARY INVESTIGATIONS

In the previous section (6.1.1), both heavy alkanes and heavy aldehydes were identified as significant VOC tracers of aircraft exhaust engines among which n-nonane and n-decane were two significant VOC molecular tracers of aircraft. Also, it has been reported elsewhere that ambient air concentrations of n-nonane, n-decane, n-undecane, and n-dodecane are potentially elevated along the perimeter of airports due to airplane exhaust and volatilized jet fuel (American Chemistry Council, 2004; Lai *et al.*, 2004), but with a very limited number of studies (Lai *et al.*, 2004) to support this hypothesis. Moreover, a

complete fingerprint profile for aircraft exhaust emissions has been established in our study (section 6.1.2) based on real measurements in Beirut Airport. Previous studies conducted to measure the speciation of road emissions in Lebanon indicated that roadway emissions are mainly composed of high percentages of isopentane, n-butane, toluene, m,p-xylenes, ethylene and acetylene, and isobutane (Salameh *et al.*, 2014).

Based on this given, our preliminary investigations aimed at assessing the impact of Beirut Airport activities on the air quality of Beirut and it suburbs, by determining if measurements of air pollutants could be attributed to aircraft activities.

Two parallel tracks were followed to achieve this purpose. The first focused on comparisons with "chemical fingerprints" related to aircraft exhaust emissions. Because fuels differ in their VOC constituents and are burned at different temperatures in different sources, emissions from categories of sources (e.g. aircraft, gasoline engines) have subtle but important distinctions that constitute the "fingerprints" for the source categories (KM Chng, 1999). The chemical fingerprinting procedure uses gas chromatography (GC) with mass spectrometry (MS) or flame ionization detection (FID) to establish the chemical constituents of environmental samples. The GC/MS or GC/FID results show the relative abundance or concentration of each VOC in a sample.

The second track focused on assessing the spatial distribution of the molecular tracers (heavy alkanes and heavy aldehydes) identified as aircraft exhaust tracers (section 6.1) by comparing their concentrations at different locations near the airport vicinity all the way to Beirut.

- Passive Campaign (20-22 October 2014)

Samples were analyzed to characterize VOC distributions at different locations, so that contributions from aircraft operations could be distinguished from other VOC sources. VOC profiles were assessed based on the average mass (ng) of VOCs measured using GC-FID for samples taken *via* passive sampling (Table 6-2).

Figure 6-9 shows that the VOC speciation profiles (VOC distributions) at the airport roof and along the seashore bare great chemical resemblance to aircraft fingerprint emissions (source profile) obtained previously during the signature campaigns using GC-FID (section 6.1, Figure 6-5). This resemblance is manifested by the dominance of light aldehydes/ketones and monoaromatics, followed by light alkanes, alkenes, and heavy

alkanes. This resemblance seems to clearly highlight that the sites along the seashore are most probably affected by aircraft exhaust emissions during jet landing, which will be confirmed later through modelling (chapter 9). This conclusion is fortified by the relatively higher mass of heavy alkanes for the sites extending from the airport roof to Beirut along the coastline and which range from 3.05 to 7.65 ng for the airport roof and AUB respectively.

The resemblance of the VOC speciation at the pine forest to aircraft exhaust and the presence of heavy alkanes at relatively higher quantities than south west Beirut is probably due to the dispersion of pollutants under the effect of wind. It is interesting that the VOC distribution at USJ (Mansourieh), which is 8 km Northeast the Airport at an altitude of 200-330 m above sea level, is similar to that at sites along the coastline (Western part of Beirut). This observation is scientifically limited, but it triggers questions. The dispersion of pollutants between 0 and 300 m is unknown. Is this the effect of dispersion of pollutants from the airport under the effect of wind (southwest)? Or is this the effect of emissions from aircraft during the final approach phase also in the range of 200-500 m above sea level? What is the effect of the combination between wind and topography present to the East of Beirut Airport on the dispersion of pollutants? This would be the subject of a future study.

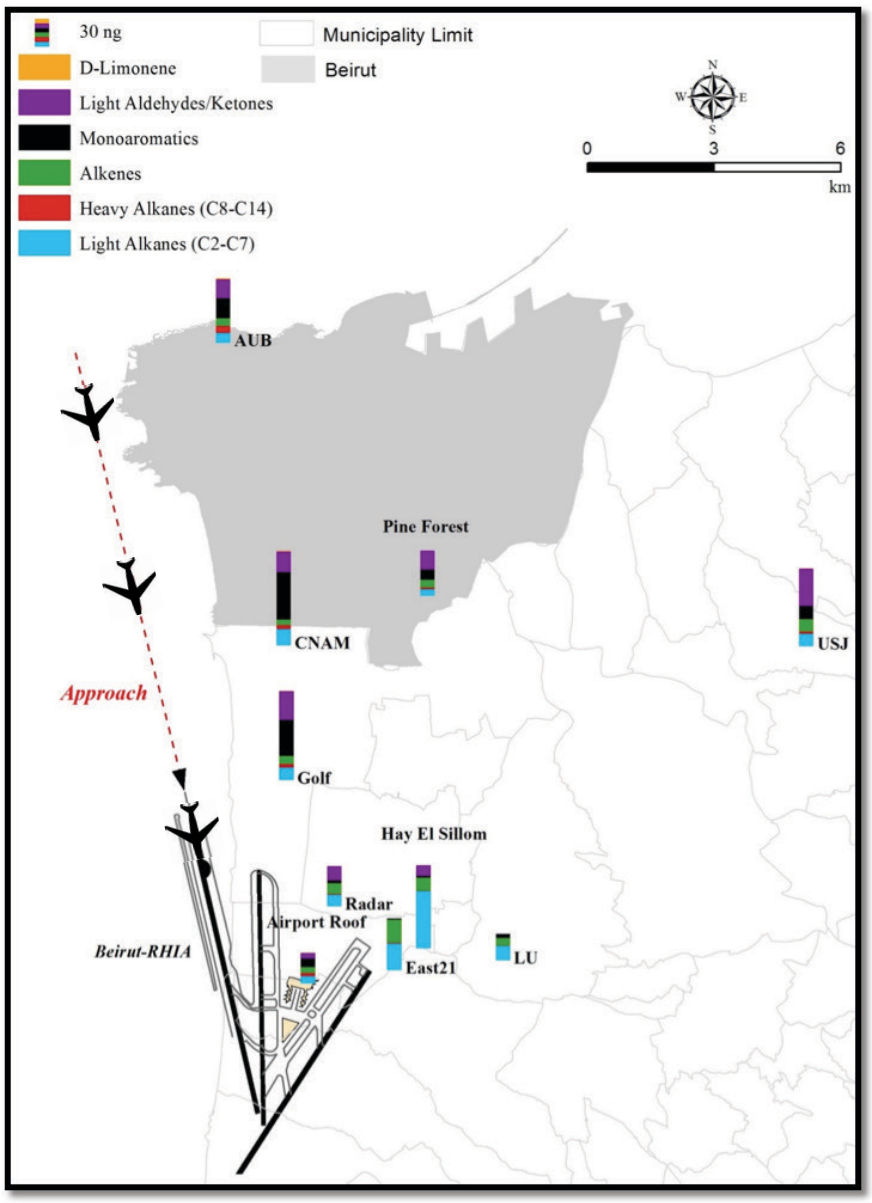

Figure 6-9: Mass (ng) distributions of VOC groups for the transect campaign conducted during 20-22 October 2014 (GC-FID). The red dotted line reflects the main jet trajectory used for landing in Beirut-RHIA.

Table 6-2: Average mass (ng, n=2) of the total VOC groups for the transect campaign conducted in October 2015 (GC-FID)

VOC group/Site	Airport Roof	Golf	CNAM	AUB	USJ	LU	Pine Forest	Radar	East 21	Hay El Sellom
Light Alkanes (C_2-C_7)	7.98	13.83	17.41	10.67	13.90	15.76	6.92	12.60	28.98	62.55
Heavy Alkanes (C_8-C_{14})	3.05	3.55	4.36	7.65	2.23	0.61	2.01	1.08	0.74	0.81
Alkenes	6.79	9.21	6.10	8.50	13.58	8.00	8.43	11.73	25.49	13.69
Monoaromatics	9.25	39.36	52.22	21.83	14.32	4.45	11.17	2.96	1.47	2.29
Light Aldehydes/Ketones	6.36	31.22	22.46	20.87	41.13	0.42	20.42	6.36	n.d.	11.45
D-Limonene	0.31	0.53	0.76	1.41	0.55	0.11	0.29	0.31	0.08	0.08

To the east of the airport, samples taken at LU, East 21, and Hay El-Sellom were significantly different from jet exhaust. The most abundant VOC group was light alkanes which accounted for 51% (East 21) to 69% (Hay El-Sellom) of the total VOC mass, followed by alkenes which accounted for 45 to 15 % also at East 21 and Hay El-Sellom respectively. It should be noted that these VOCs may be emitted by vehicle exhaust near the airport as well as airport emissions, and therefore they cannot be defined as indicators of airport emissions.

The fact that sites along the seashore up to 8 km away from the airport (AUB) possess VOC distributions that resemble aircraft signature emissions and showing the presence of heavy alkanes, and the fact that this distribution and aircraft tracers (heavy alkanes) are absent from sites geographically closer (LU, Hay El-Sellom) to the airport, is a strong indicator that the seashore areas are majorly affected by aircraft emissions during the final approach phase.

- Active Campaign (13-21 July 2015)

The overall results of heavy VOCs, summarized in Table 6-3, are presented in Figure 6-10 as a map plot for measured concentrations during July 2015. It was apparent that aircraft emissions have brought great impacts on sites located in the vicinity of the airport. The speciation profile at radar and southeast the airport is very similar to aircraft speciation profile determined in section 6.1.1. The site Ghadir also possesses a similar distribution, however, with a higher contribution of monoaromatics that can be attributed to vehicle

emissions. On the other hand, the concentrations of heavy alkanes were highest at the site "radar" (2.4 μg m^{-3}), followed by the sites "Ghadir" and "southeast" with a concentration of 1.7 and 1.6 μg m^{-3} respectively. The highest concentrations of heavy aldehydes, which are most probably oxidation products from jet fuel and/or heavy alkane emissions, were found in the golf club (5.41 μg m^{-3}). This can be most probably due to the photochemical oxidation of higher alkanes that is maximum during summer conditions. The impact of the airport probably reached to the pine forest, however with very little contribution (the concentration of heavy aldehydes and heavy alkanes were 0.13 and 0.16 μg m^{-3} respectively). The wind effects can possibly explain the presence of heavy alkanes in the pine forest.

To understand the effect of aircraft emissions during the approach phase on air quality, measurements were undertaken at CNAM and the Coral beach. Heavy alkanes were not detected in CNAM; however, heavy aldehydes were detected at a concentration of 1.2 μg m^{-3}, which could possibly be a result of jet exhaust oxidation. The absence of heavy alkanes maybe attributed to their faster photochemical degradation. The presence of both heavy alkanes and heavy aldehydes at the Coral beach, located at the same distance from the airport as CNAM, confirmed the effect of aircraft emissions on the jet landing trajectory.

An interesting observation was the presence of aircraft tracers at Barouk located around 18 km away from the airport. This is scientifically limited, because it is the result of one campaign but we can consider it as an indicator of the complexity of the dispersion of air pollutants due to the aerodynamic effect resulting from the interaction between topography and wind in a country with geographical characteristics like Lebanon.

Since heavy alkanes are of particular interest as aircraft emission tracers, Figure 6-11 shows the speciation of heavy alkanes at the different measurement sites. It is interesting that the speciation at the sites closest to the airport (radar and southeast the airport) resembles the aircraft fingerprint emissions, Jet A-1 vapor, as well as the airport roof (6.1.1) in which all are dominated by n-nonane and n-decane.

Table 6-3: Average concentration (µg m^{-3}) of heavy VOCs for the transect campaign conducted in July 2015 (GC-MS)

	VOC (µg m^{-3})	Radar (n=3)	Southeast (n=1)	Ghadir (n=3)	Golf (n=2)	Coral (n=2)	CNAM (n=2)	Pine Forest (n=3)	Barouk (n=2)
	n-Heptane	0.19	0.57	0.44	nd	nd	nd	nd	0.23
Heavy Alkanes (C_8-C_{14})	n-Octane	nd	0.30	nd	nd	nd	nd	nd	nd
	n-Nonane	0.78	0.56	0.10	nd	nd	nd	nd	nd
	n-Decane	1.03	0.40	0.21	0.03	nd	nd	0.10	nd
	n-Undecane	0.35	0.33	nd	nd	nd	nd	nd	nd
	n-Dodecane	0.19	nd	0.37	nd	nd	nd	nd	nd
	n-Tridecane	nd	nd	nd	nd	nd	nd	0.03	nd
	n-Tetradecane	nd	nd	1.01	nd	0.87	nd	nd	0.14
Heavy Aldehydes	Nonanal	0.56	nd	0.37	5.41	0.29	1.18	0.12	1.33
	Decanal	0.70	0.30	0.39	nd	0.31	nd	0.04	0.42
	Benzene	158.73	17.69	28.40	nd	21.37	nd	4.17	80.91
Other Monoaromatics	Toluene	2.51	2.18	4.59	0.59	0.49	0.02	nd	1.46
	Ethylbenzene	0.07	0.11	0.14	nd	0.02	nd	nd	0.05
	m,p-Xylene	0.06	0.09	0.20	nd	0.05	nd	nd	0.05
	o-Xylene	0.08	0.02	0.12	nd	nd	nd	nd	nd
	Styrene	0.08	0.32	0.09	nd	0.04	nd	nd	0.08
	1,2,4-TMB	0.19	nd	0.05	nd	nd	nd	nd	nd
	1,4-DCB	nd	nd	nd	nd	nd	nd	nd	nd
	Propyl benzene	0.06	0.05	0.03	nd	0.02	nd	0.01	nd
	Butyl benzene	0.04	0.01	0.01	nd	nd	nd	nd	nd
	Heavy Alkanes (C_8-C_{14})	2.35	1.59	1.69	0.03	0.87	nd	0.13	0.14
	Benzene	158.73	17.69	28.40	nd	21.37	nd	4.17	80.91
	Other Monoaromatics	3.09	2.78	5.23	0.60	0.62	0.02	0.01	1.64
	Heavy Aldehydes (C_9,C_{10})	1.26	0.30	0.76	5.41	0.60	1.18	0.16	1.75
	TVOC (µg m^{-3})	165.61	22.93	36.53	6.03	23.46	1.20	4.47	84.66

nd: not detected

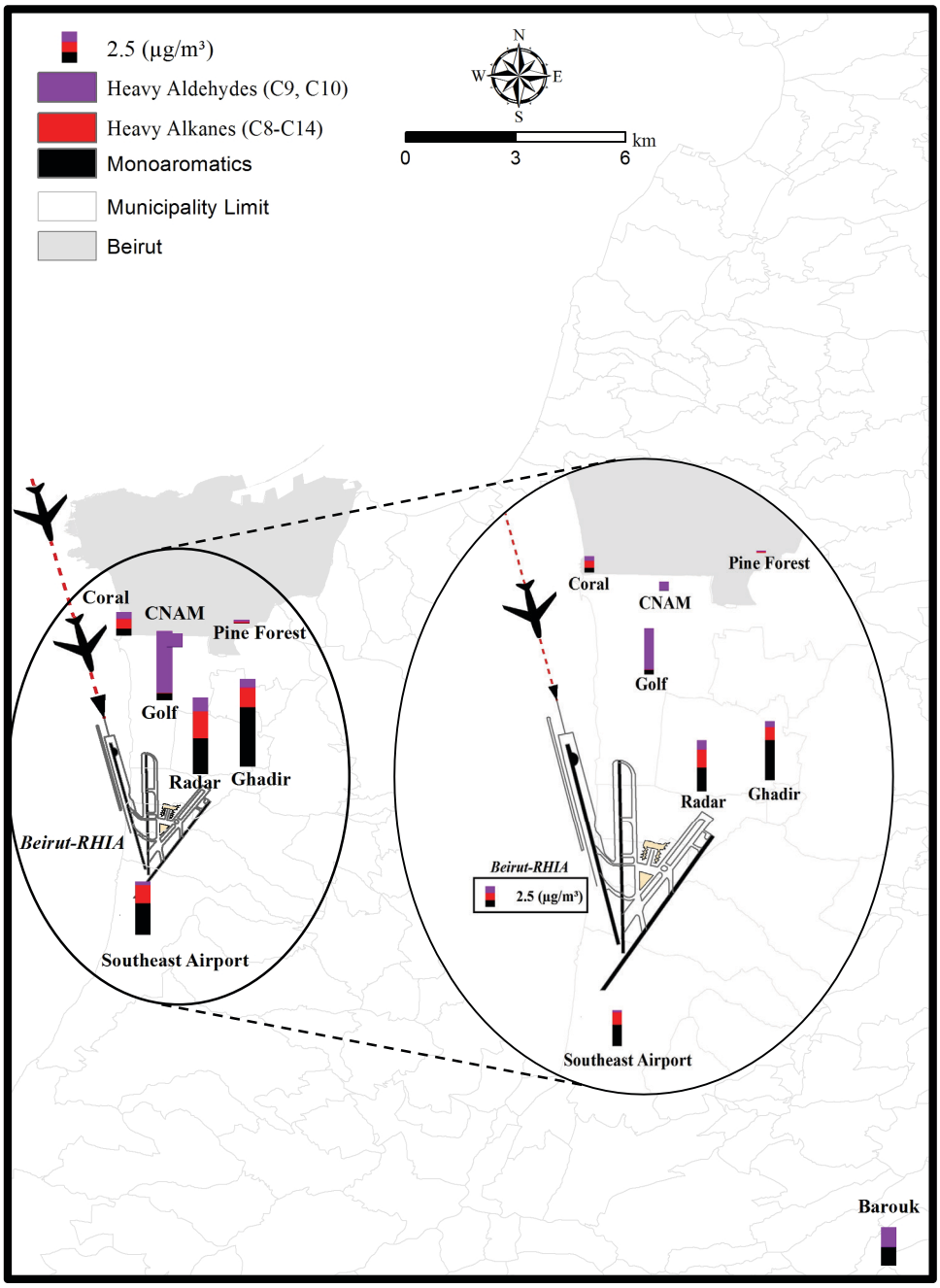

Figure 6-10: Concentrations (µg m^{-3}) of heavy VOC groups for the transect campaign conducted in 13-21 July 2015 (GC-MS). The red dotted line reflects the main jet trajectory used for landing in Beirut-RHIA.

Another observation is that Coral and Barouk share the same speciation with the sole presence of n-tetradecane. Another exhaustive campaign is needed to better understand these observations.

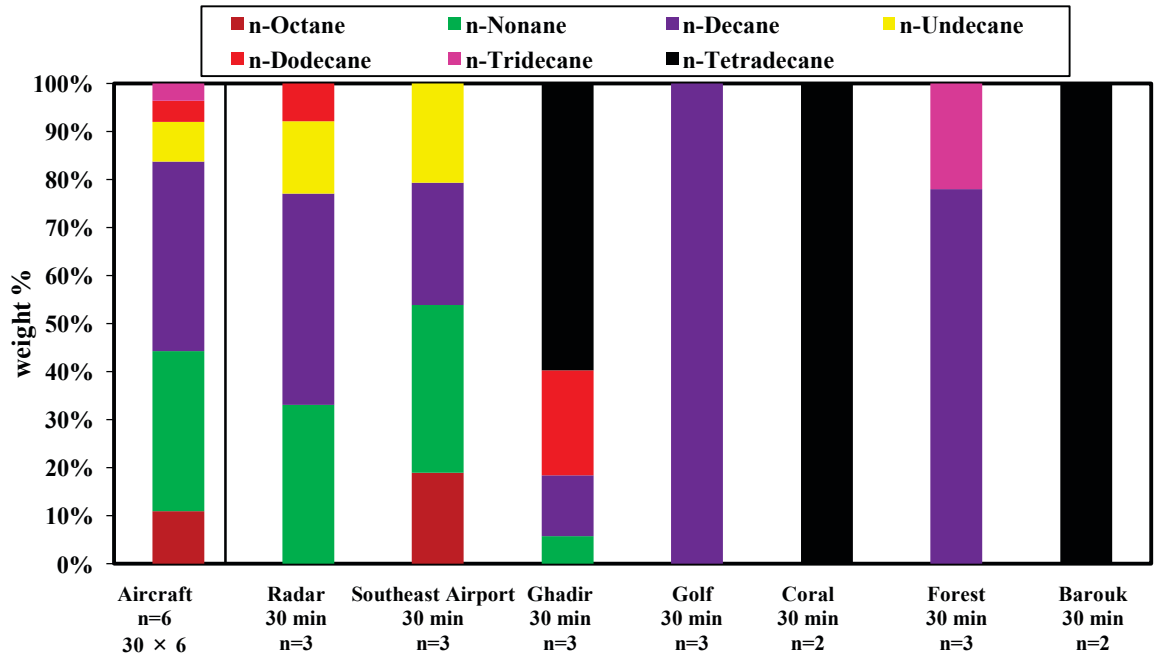

Figure 6-11: Speciation of heavy alkanes for measurements taken in July 2015 (Active Sampling)

Conclusion on Transect Campaigns

This investigation was able to demonstrate the feasibility of collecting and analyzing meaningful data that could determine the extent to which Beirut Airport is contributing to the overall burden of air pollution in the surrounding communities.

The comparison between aircraft fingerprint emissions and VOC profiles for both passive and active campaigns provided consistent results concerning the impact of aircraft activities on air quality. Both studies confirm the impact on the air quality of the airport vicinity. The resemblance of VOC distributions for sites along the seashore to aircraft signature profiles indicated that probably these sites were affected by aircraft activities (October 20-22, 2015). This hypothesis was confirmed by measurements taken at the Coral and CNAM, which proved that higher amounts of heavy alkanes were present at the seashore. This observation was in accordance with results obtained by ADMS-Airport (see chapter 9).

We have assumed that the mountainous areas were not affected by aircraft emissions, however 2 indicators have hinted that mountainous areas may be influenced by airport emissions. However, this is preliminary and needs further investigation to understand the importance of this influence, the interaction between air quality and topography, and what the extent of this probable contribution is.

This study opens the door to implement a more comprehensive investigation that will provide a more detailed picture of the effect that air pollution from Beirut Airport has on the surrounding communities.

6.1.3 NITROGEN DIOXIDE PASSIVE CAMPAIGNS

The average NO_2 concentration for the 3 validation campaigns, summarized in Table 6-4, ranged between 27.6 µg m^{-3} at the approach site and maxima of 56.9 µg m^{-3} at gate 12 and 56.7 µg m^{-3} at take-off (1). The higher concentration levels at take-off (1) with respect to approach and taxi is expected. At low engine speeds (e.g. taxiing of aircraft), the combustion temperature is low (680°K-1700°K) (Dagaut *et al.*, 2006; Tsague *et al.*, 2006) and does not guarantee optimum combustion (Heland and Schäfer, 1998). The emission of NO_2 is minimal. However, at high speed (e.g. departing aircraft), the temperature within the combustion chamber is higher (around of 2300°K) (Dagaut *et al.*, 2006). This leads directly to the increase in NO_x emissions (chapter 3) (Heland and Schäfer, 1998; Tsague *et al.*, 2006).

NO_2 concentrations at the site take-off (2) (average of 43.5 µg m^{-3}) were slightly greater than that at the site take-off (3) (average of 39.3 µg m^{-3}), even if the relatively small difference between both values cannot be considered as fully significant regarding their uncertainties which are close to 2 µg m^{-3} for each (see Table 6-4, repetitive tests performed during the 1st campaign). Nevertheless, this nearly significant small difference is probably due to the effect of the prevailing southwest wind conditions as illustrated in Figures 6-12, 6-13, and 6-14; the site take-off (2) was chosen to measure concentrations at a downwind location, whereas take-off (3) was chosen to measure concentrations at upwind locations. These 2 sites assess emissions during the take-off phase. In addition, it is interesting to underline that NO_2 concentrations at take-off (2) were always slightly higher than that at the site take-off (3), whatever the field campaign.

The extremely high concentrations at gate 12 (56.9 μg m^{-3}) is a resultant of the accumulation of emissions from aircraft at the gate, as well as ground support equipment which comprises a diverse range of vehicles and equipment necessary to service aircraft at the gate. These high values are in agreement with modelling results (chapter 9). The average background concentrations were about 31 μg m^{-3}, majorly affected by road traffic.

Finally, the difference in concentrations between the 3 campaigns could be attributed to many factors such as meteorological and weather conditions, type of aircraft fleet, etc. Despite the difference, the relative contribution to the total emissions remained the same, with highest contribution from take-off (1) and gate 12 and lowest contribution from approach and background (see Table 6-4).

Table 6-4: NO_2 concentrations (μg m^{-3}) for validation campaigns (passive sampling) conducted at Beirut Airport (2015)

Site	May 16-23, 2015	June 4-11, 2015	June 11-18, 2015	Mean	SD
Gate 12	72.4	49.2	49.0	56.9	13.4
Take-off (1)	77.1	47.2	45.8	56.7	17.7
Take-off (2)	57.2	42.1	31.3	43.5	13.0
Take-off (3)	54.5±2.1*	34.9	28.4	39.3	13.6
Cargo	NA	42.9	31.5	37.2	8.1
Taxi	53.0	26.4	26.1	35.2	15.5
Ozaii	47.3	22.6	22.9	30.6	14.5
Background	43.6	27.3	22.1	31.0	11.2
Approach	42.3±2.2*	21.9	18.6	27.6	12.8

*The standard deviation (n=3) for NO_2 concentrations measured during the first campaign (May 16-23, 2015) was 2.1 μg m^{-3} for take-off (3) and 2.2 μg m^{-3} for approach corresponding to 4% and 5% of their mean NO_2 concentration (μg m^{-3}) respectively. This signifies the precision of measurements taken using one Passam tube.

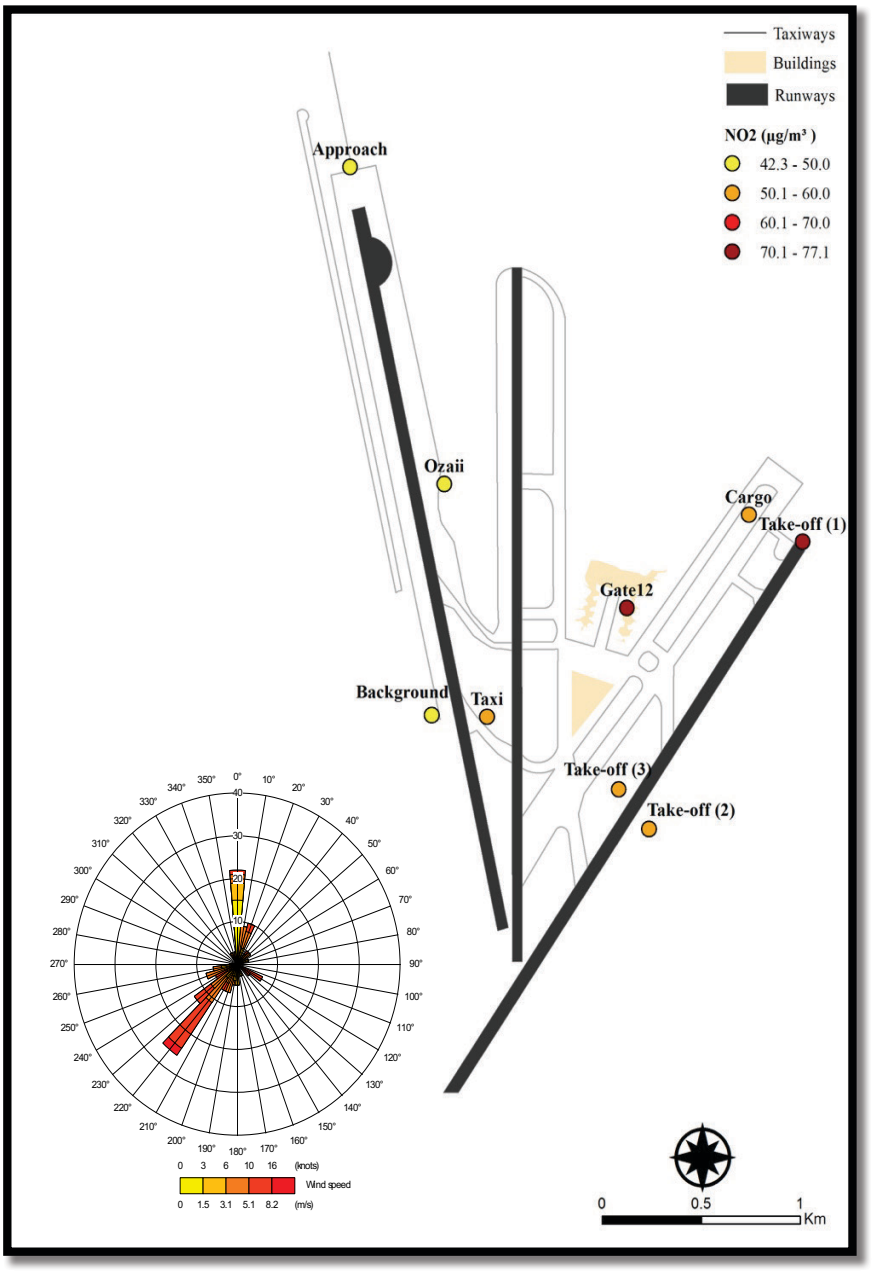

Figure 6-12: Measured NO_2 Concentrations (µg m^{-3}) at Beirut Airport (May 16-23, 2015)

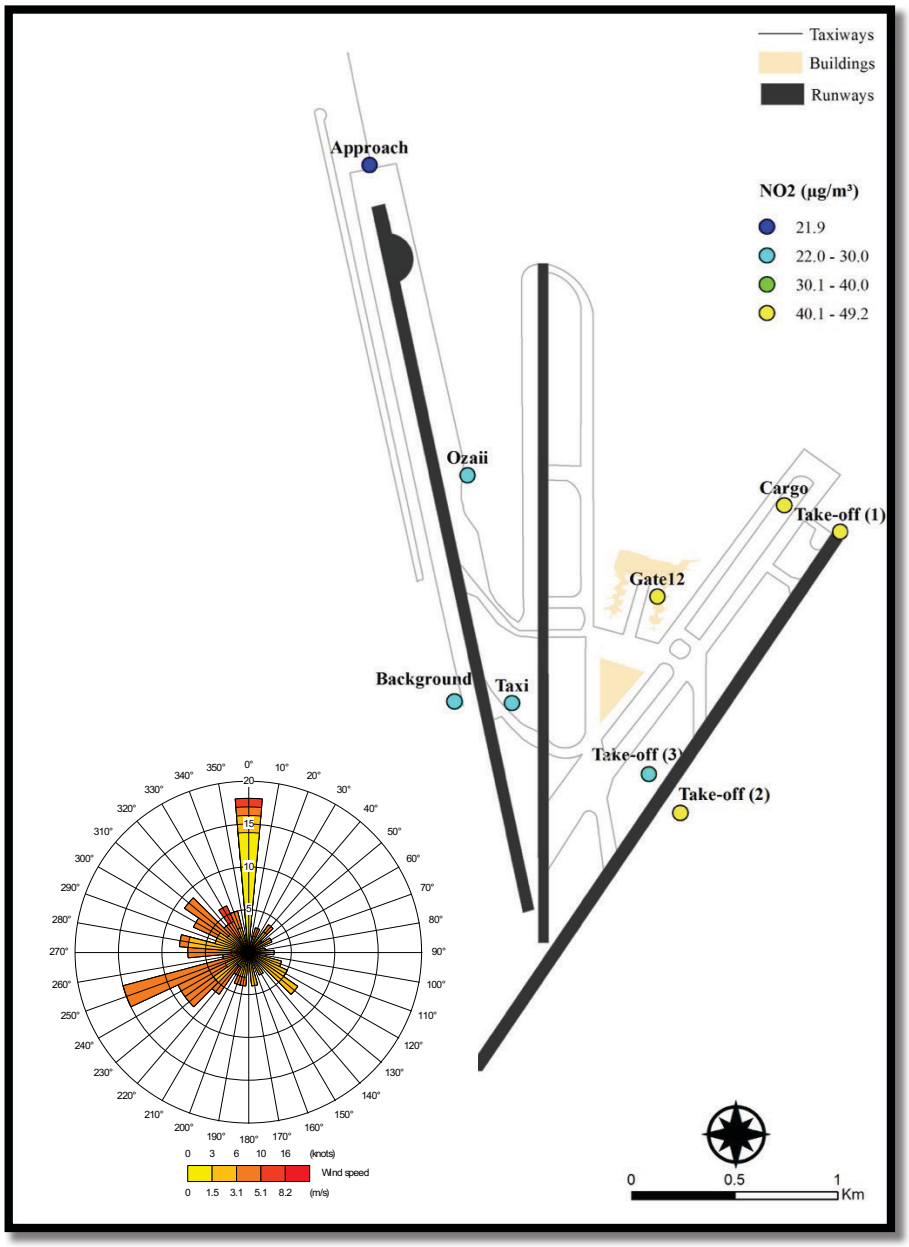

Figure 6-13: Measured NO_2 Concentrations (µg m^{-3}) at Beirut Airport (June 04-11, 2015)

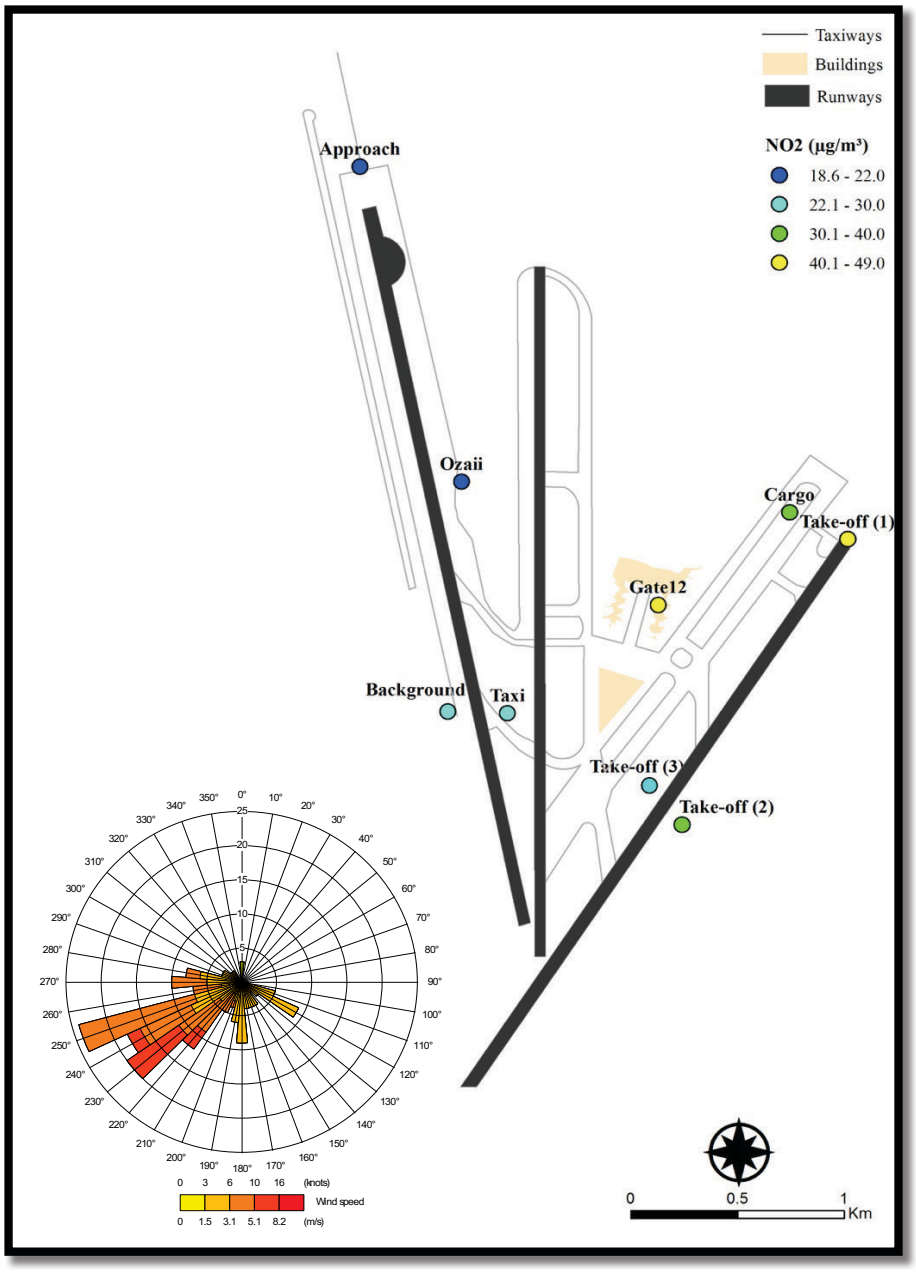

Figure 6-14: Measured NO_2 Concentrations (µg m^{-3}) at Beirut Airport (June 11-17, 2015)

6.2 INDOOR Campaigns

6.2.1 VOC CONCENTRATIONS

- Maintenance Room

Comparison of TVOC Concentrations between the 2 Campaigns

All VOC concentrations (μg m^{-3}) presented in this section were measured using GC-FID. n-Tetradecane was not detected and thus will not be included in Tables and Figures. The seasonal variation of the mean total VOC (TVOC) concentration (μg m^{-3}), as well as the individual VOC groups, measured inside the maintenance room are presented in Figure 6-15. Results show that lower mean TVOC concentrations existed during the summer campaign (123 μg m^{-3}) and higher concentrations existed during the fall/winter campaign (250 μg m^{-3}). These observations are similar to results obtained in Cairo (Matysik *et al.*, 2010) and Europe (Rehwagen *et al.*, 2003) which reported that seasonal variations existed for alkanes, BTEX, and terpenes for both indoor (measured in apartments) and outdoor concentrations. The lower indoor concentrations of monoaromatics in summer months can be explained by a faster photochemical degradation in the lower troposphere (chapter 1). Benzene and alkyl-substituted benzenes react with OH and NO_3 radicals, with the OH radical reaction being the dominating tropospheric removal process (Atkinson, 2000). This process can only partly explain these variations, other complex influences might also play a role e.g. meteorological conditions (Matysik *et al.*, 2010).

The increase in the total concentration of aldehydes and ketones are less pronounced i.e. the increase is from 23 to 36 μg m^{-3} (a factor of 1.5), which is related to the production of aldehydes and ketones during the summer when photo-oxidative reactions are at maximum. The total concentration of heavy alkanes increased by a factor of 10 from summer to winter (5 to 50 μg m^{-3} respectively). The total monoaromatic concentration increased by a factor of 2 (from 11 to 23 μg m^{-3}). During both campaigns, alkanes (45-108 μg m^{-3}) were the major contributors to the total VOC concentrations, followed by aldehydes and ketones (23 μg m^{-3}) during summer and heavy alkanes (49 μg m^{-3}) during the winter campaign. It is important to note that when calculating the average monoaromatic concentrations for the summer campaign, the first 3 data points were not accounted for because they presented extremely high values of toluene (probably due to smoke).

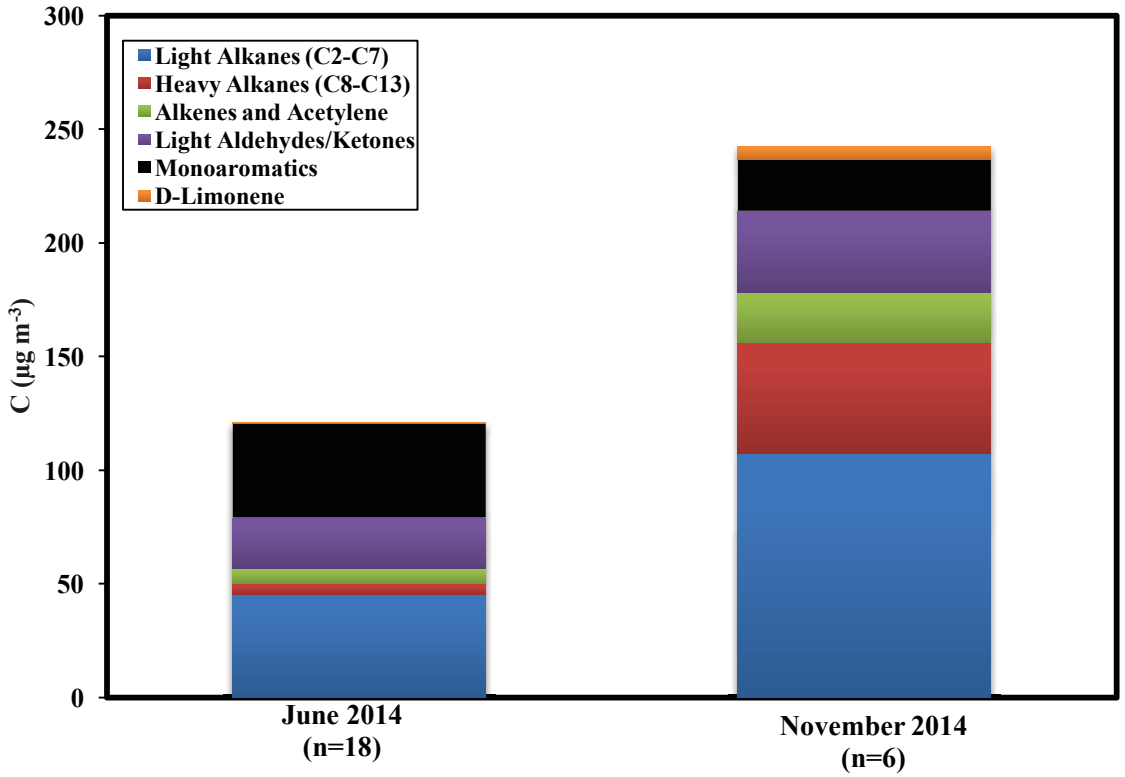

Figure 6-15: Comparison of TVOC (µg m^{-3}) measured in the maintenance room at Beirut Airport (June and November 2014)

Temporal Variations of VOC Groups

The temporal variations of the various VOC groups measured in the maintenance room are presented in Figure 6-16, along with the variations in air traffic. The total aircraft number for each measurement was calculated by summing up the total aircraft movement starting 2 h before the end of the sampling (sampling duration = 30 min). This was an approximate way to identify the relation to air traffic, taking into account that the smallest lifetime of our target VOCs is 2 hours, corresponding to isoprene and 1,3-butadiene. Results show an interesting relation between light aldehydes/ketones and the total aircraft number, and a less pronounced relation between other VOC groups and aircraft number with the exception of 10/06/14 where the variation in VOC groups seem more related to the variation in aircraft number (Figures 6-16 (a) and 6-16 (b)). The reason could be that aldehydes/ketones are the major aircraft fingerprint emissions (section 6.1) and with a relatively slower photochemical degradation rate.

During the first day of the summer campaign (Figure 6-16 (a)), the concentration of total monoaromatics was maximum at 16:15 (215 µg m^{-3}) due to extremely high toluene

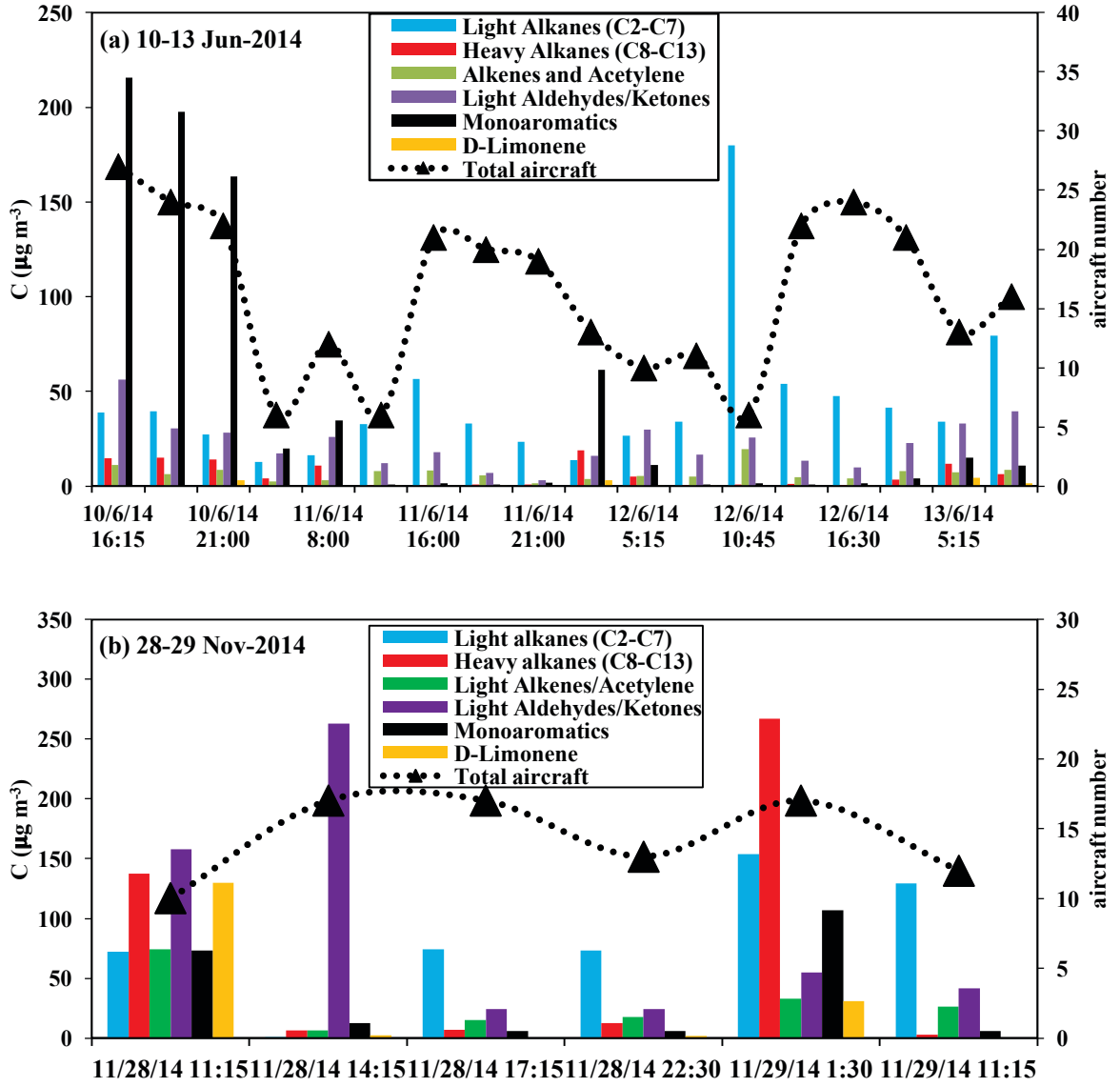

Figure 6-16: Temporal Variation of VOC Groups with Aircraft Number (a) Maintenance Room, June 2014 (b) Maintenance Room, Nov. 2014. (The total number of aircraft represents the sum of the number of aircraft that have departed and arrived within 2 h before the end of sampling).

concentration (179 µg m^{-3}). These high values are probably related to increased personal activities (smoking) and airport emissions associated with rush traffic. The concentration of total monoaromatics remained extremely high until the morning of 11/6/14 and decreased in accordance with total aircraft number. Also, the concentrations of all the VOC families decreased at 5:15 A.M., a time which corresponds to extremely low air traffic and personal activities. During the next day (11/06/14), a similar trend existed between 16:00 and 21:00 followed by an increase at time 5:15. At 10:45 on 12/06/14, a huge increase in the concentration of light alkanes was observed reaching 180 µg m^{-3}

which was probably due to the different activities taking place inside the room, as well as airport activities (vehicles, air traffic, etc.).

During the winter campaign, it was seen that the concentrations of the VOC groups are maximum in the morning-noon time as a result of increased personal and airport activities. Another peak time was observed just after midnight (01:30), as observed in the summer campaign. This was due to the rush hour of arrivals preceding that time, accompanied with increased personal activities.

VOC Speciation

The mean, maximum, and minimum concentrations (μg m^{-3}) of the individual VOCs measured in the maintenance room during summer (June) and winter (October) 2014 are summarized in Table 6-5. It is important to note that when calculating the average monoaromatic concentration for the summer campaign, the first 3 data appoints were not accounted for because they presented extremely high values of toluene.

The occurrence of a VOC, in percent, describes the proportion of the dataset in which the VOC was detected. The percentage occurrence was more than 50% for most of the VOCs measured during June 2014 except for tetrachloroethene that is rarely detected at airports. Acetone (9.85 μg m^{-3}), propanal (6.53 μg m^{-3}), toluene (6.23 μg m^{-3}), isobutane (6.21 μg m^{-3}), and acrolein (4.10 μg m^{-3}), listed in descending order of predominance, were the major VOCs found during the summer campaign. n-Octane (1.77 μg m^{-3}), n-undecane (1.13 μg m^{-3}), and n-decane (1.07 μg m^{-3}) were the major heavy alkanes found. All these values were below the recommendation levels set by INRS[6] (National Institute of Scientific Research in France). The average toluene concentration was 6.23 μg m^{-3} upon excluding the average concentration during 10/06/2015, which was equal to 169.26 μg m^{-3}.

During the winter campaign, the percentage occurrence was more than 50% for most of the VOCs except for propanal and hexanal (17 % each). Isobutane (43.34 μg m^{-3}), n-undecane (28.63 μg m^{-3}), acetone (24.24 μg m^{-3}), toluene (11.47 μg m^{-3}), propene (8.89 μg m^{-3}), and acrolein (4.95 μg m^{-3}) were the major VOCs found during the winter campaign. Among the heavy alkanes, n-undecane (28.63 μg m^{-3}), n-decane (8.89 μg m^{-3}), and n-nonane (3.13 μg m^{-3}) were the major contributors, listed in descending order of magnitude. The tube analyzed with GC-MS confirmed the presence of heavy alkanes and mainly nC_{10}-nC_{12}.

[6] en.inrs.fr

Table 6-5: Mean VOC concentrations (µg m^{-3}) measured during the two campaigns conducted in the maintenance room (June 10-13 and Nov 28-29, 2014)

		June 10-13, 2014 (µg m^{-3}) (Summer Campaign)				Nov 28-29, 2014 (µg m^{-3}) (Fall/Winter Campaign)			
	VOCs	**Mean (n=18)**	**Min**	**Max**	**% occurrence**	**Mean (n=6)**	**Min**	**Max**	**% occurrence**
Heavy Alkanes (C_8-C_{13})	n-Octane	**1.77**	n.d.	9.28	94	1.56	0.13	8.02	100
	n-Nonane	0.36	0.03	0.95	100	3.13	0.08	15.77	100
	n-Decane	1.07	0.18	2.86	100	8.89	0.30	46.68	100
	n-Undecane	1.13	0.10	3.45	100	**28.63**	0.01	157.76	100
	n-Dodecane	0.33	n.d.	1.05	94	5.30	0.03	29.70	100
	n-Tridecane	0.11	n.d.	0.45	94	1.00	0.05	5.17	100
Monoaromatics	Benzene	invalid results			100	invalid results			100
	Toluene	**6.23**	0.47	24.21	100	**11.47**	2.44	39.67	100
	Ethylbenzene	0.68	n.d.	4.47	89	1.55	n.d.	7.53	83
	m,p-Xylene	1.11	n.d.	6.40	94	3.44	0.01	15.90	100
	o-Xylene	1.00	n.d.	9.12	78	1.86	0.03	8.90	100
	Styrene	1.54	n.d.	18.93	56	0.91	n.d.	4.30	67
	1,2,4-TMB	0.55	n.d.	1.93	94	6.62	0.10	30.50	100
Chloroalkenes	Trichloroethene+Isooctane	**1.29**	n.d.	5.51	94	**4.48**	3.81	4.89	100
	Tetrachloroethene	0.38	n.d.	1.66	44	0.70	n.d.	2.82	50
Light Aldehydes and Ketones	Acrolein	4.10	n.d.	10.24	94	**4.95**	n.d.	8.93	100
	Propanal	**6.53**	n.d.	30.56	94	n.d.	n.d.	n.d.	17
	Butanal	0.46	n.d.	2.22	67	0.64	n.d.	2.98	100
	Pentanal	2.15	n.d.	8.94	61	2.23	0.75	6.03	100
	Hexanal	0.53	n.d.	1.81	83	0.49	n.d.	2.47	17
	Acetone	**9.85**	2.43	51.55	100	**24.48**	16.45	31.53	100
	2-Butanone	2.05	n.d.	7.55	72	2.68	0.52	4.76	100
Terpene	D-Limonene	1.12	n.d.	8.67	56	6.75	0.02	31.02	100
Light Alkanes (C_2-C_7)	Ethane	0.17	0.09	0.36	100	0.57	0.34	0.83	100
	Propane	5.44	1.56	16.07	100	25.10	15.45	41.62	100
	Isobutane	**6.21**	0.04	31.60	100	**43.34**	25.60	59.68	100
	n-Butane+cis-2-Butene	4.82	0.71	22.58	100	21.29	12.93	31.04	100
	Isopentane	1.18	0.16	5.53	100	20.04	14.42	27.68	100
	n-Pentane+cis-2-Pentene	0.20	0.03	0.91	100	1.95	1.06	3.36	100
	n-Hexane	0.26	n.d.	1.52	72	0.82	n.d.	2.34	83
	n-Heptane	1.34	0.01	4.90	100	0.91	0.10	4.04	100
Light Alkenes and Acetylene	Ethene+acetylene	**2.25**	n.d.	7.43	72	3.53	2.23	5.06	100
	Propene	1.57	0.43	4.97	100	**8.89**	6.07	11.52	100
	1-Butene	1.15	n.d.	4.42	94	3.64	3.15	4.42	100
	1,3-Butadiene	0.15	n.d.	0.65	89	0.62	0.50	0.83	100
	trans-2-butene	0.45	n.d.	1.90	94	2.00	1.42	2.48	100
	1-Pentene	0.18	n.d.	1.08	61	0.76	0.51	1.56	100
	Isoprene	0.43	n.d.	2.77	78	1.32	0.12	4.24	100
	Trans-2-pentene	0.03	n.d.	0.28	28	0.34	0.14	0.99	100
	1-Hexene	1.00	n.d.	3.21	83	2.62	1.63	5.02	100

C(µg m^{-3})	**Average**	**Min**	**Max**	**Average**	**Min**	**Max**
Light Alkanes (C_2-C_7)	45.27	13.80	180.06	107.52	72.36	157.86
Heavy Alkanes (C_8-C_{13})	4.77	0.37	15.79	48.51	0.60	263.09
Light Alkenes/Acetylene	6.71	1.49	19.65	22.32	15.31	33.14
Monoaromatics	11.11	0.79	61.35	22.57	2.64	106.79
Aldehydes/Ketones	22.49	2.97	56.31	35.87	24.08	54.69
D-Limonene	0.72	n.d.	4.30	5.71	0.02	31.02
Total VOC	88.87	30.76	229.61	247.46	125.25	654.29

The highest concentration per VOC group is formatted in bold
n.d.: not detected

Among the heavy alkanes, n-undecane (28.63 μg m^{-3}), n-decane (8.89 μg m^{-3}), and n-nonane (3.13 μg m^{-3}) were the major contributors, listed in descending order of magnitude. The tube analyzed with GC-MS confirmed the presence of heavy alkanes, mainly nC_{10}-nC_{12} in aircraft exhaust and/or their ground support equipment (GSE). The U.S. EPA has listed 14 airport-related HAPs (Hazardous Air Pollutants), generally defined as those pollutants that are known or suspected of being able to cause serious health effects such as cancer, birth defects, etc. (Kim, 2015). Ten individual HAPs comprise the vast majority of HAPs (FAA, 2003; Wood, 2008), five of which were assessed in this study which are (listed in descending order of importance): acrolein, 1,3-butadiene, toluene, xylene, and propanal. The average concentration levels for these species were below the acute toxicity criteria (see chapter 3) reported by Wood (2008) except for **acrolein** which was found to be above the reference exposure level (0.19 μg m^{-3}) for 1-6 hr exposure. According to US EPA, acute (short-term) inhalation exposure of acrolein may result in upper respiratory tract irritation and congestion.

Correlation of Outdoor (Airport roof) and Indoor (Maintenance room) VOC levels

To better understand the correlation between outdoor and indoor levels, mean VOC concentrations (n=6), measured in the maintenance room during 28-29 November 2014, were compared with mean outdoor concentrations (n=2) measured at the airport roof during the same month. These correlations are made between measurements conducted in the same season, i.e. similar meteorological conditions and air traffic intensity.

Figure 6-17 (a) presents a scatter plot of the correlations between indoor and outdoor VOCs excluding monoaromatics which possess a different behavior and were plotted in Figure 6-17 (b). Both Figures show strong to very strong correlations with correlation coefficients (r) equal to 0.78 and 0.90 respectively. This shows a direct indoor to outdoor correlation in general. Figure 6-17 (a) also shows that indoor concentrations are higher than outdoor concentrations which is signified by points plotted above Y=X. On the other hand, the indoor concentration for monoaromatics is very close to outdoor values. Figure 6-18 presents the indoor/outdoor correlations by VOC group. Heavy alkanes possess the strongest correlation (r = 0.99) while both alkenes and aldehydes/ketones exhibit the weakest correlations (r = 0.6).

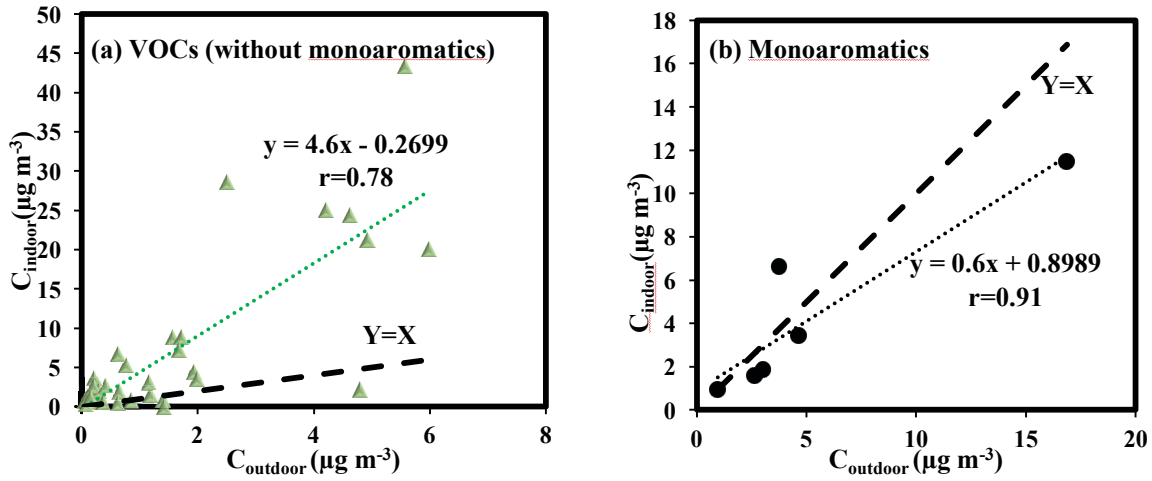

Figure 6-17: VOCs measured in the maintenance room (28-29/11/14, n = 6) vs Airport Roof (20-21/10/14, n = 2) (a) All the VOCs without monoaromatics, (b) Monoaromatics

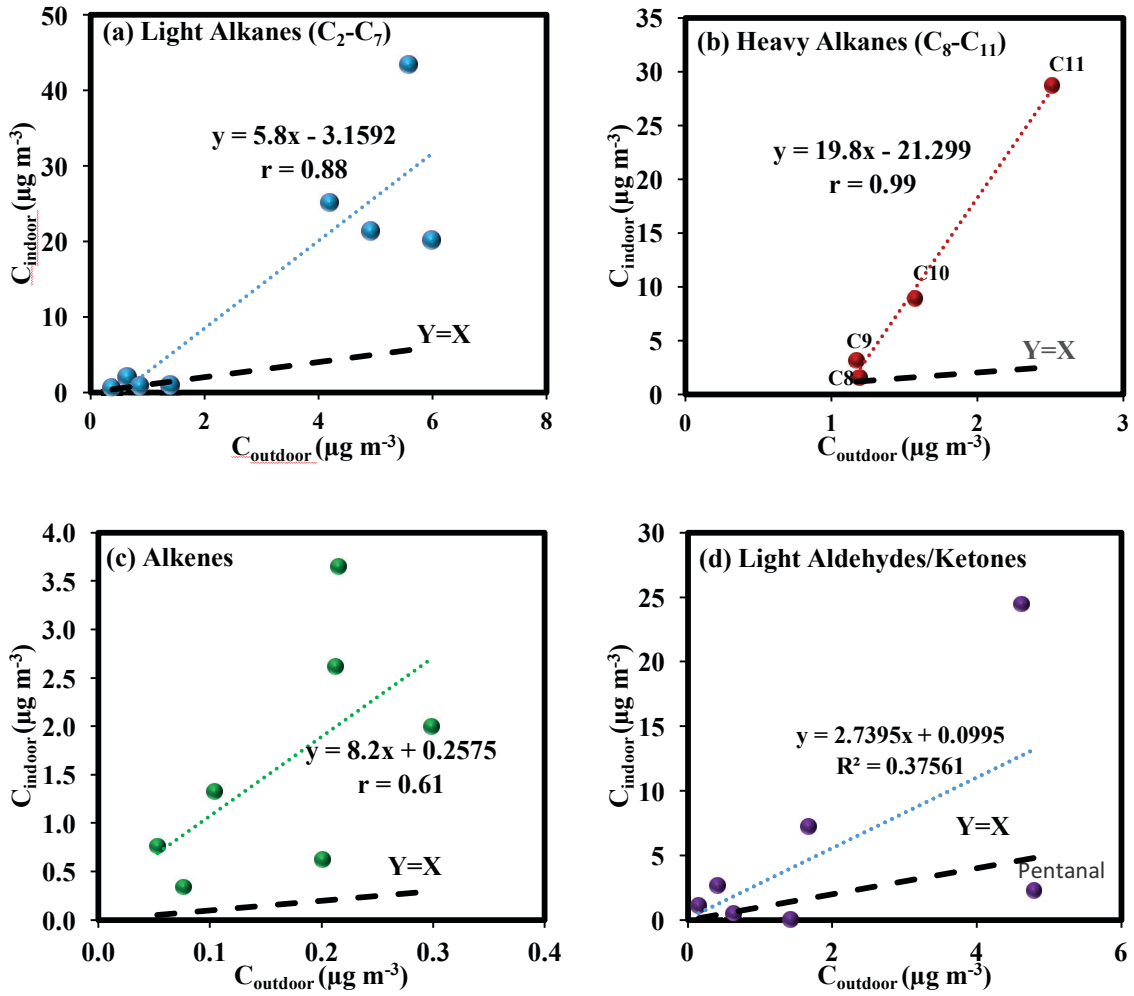

Figure 6-18: Concentrations (µg m^{-3}) of VOC groups measured in the maintenance room (28-29/11/14, n = 6) vs Airport Roof (20-21/10/14, n = 2): (a) Light alkanes (C_2-C_7), (b) Heavy alkanes (C_8-C_{11}), (c) Light alkenes, (d) Light Aldehydes/Ketones (after removing an outlier (pentanal))

Correlation analysis

Pearson's correlations and p-values[7] have been calculated taking into account a subset of the heavy alkanes (C_8-C_{11}) and monoaromatics quantified in the indoor rooms, as it is an important method to determine common sources for these VOCs (Villanueva *et al.*, 2015; Wang *et al.*, 2014). The correlations of aldehydes and C_{12}, C_{13} straight chain alkanes were not presented due to the lack of optimal adsorption of these species. The classification of Pearson's correlations was according to Evan's classification (Divaris *et al.*, 2012; Kowang *et al.*, 2015) as shown in Table 6-6.

Table 6-6: Interpretation of Pearson's correlation coefficient (r)

R	Strength
< 0.2	very weak correlation
0.20-0.39	weak correlation
0.40-0.59	moderate correlation
0.60-0.79	strong correlation
> 0.8	very strong correlation

Pearson's correlations have been quantified taking into account a subset of the heavy alkanes (C_8-C_{11}) and monoaromatics measured inside the maintenance room during the summer campaign (June, 2014). The correlations between VOCs measured during the fall/winter campaign were not presented due to the presence of an outlier (1 out of 6 measurements) which leaves insufficient data points for reliable correlation analysis.

Examination of the concentrations of the selected VOCs across the 18 measurements revealed that some had markedly consistent behavior. Table 6-7 shows the correlation coefficient (r) between pairs of VOCs. Most correlations between VOCs were statistically significant ($p < 0.001$); and VOC pairs were strongly correlated with a partial correlation coefficient ($r) > 0.8$ and $p < 0.001$. Of special significance are the very strong correlations ($r = 0.93$-0.98) between n-nonane, n-decane, and n-undecane which are the identified aircraft tracers presented in the previous sections. Monoaromatics also correlate very well between themselves except for styrene and toluene ($r = 0.52$). It is important to note the very strong correlations exist between 1,2,4-TMB and m, p-xylene with aircraft tracers (C_8-C_{11} alkanes) (r ranges between 0.80 and 0.96).

[7] p-values help to determine the statistical significance of results.

Table 6-7: Pearson's correlation coefficients of VOCs quantified in the maintenance room at Beirut Airport (June, 2014)

VOC	1.	2.	3.	4.	5.	6.	7.	8.	9.	10.
1. n-Octane	1									
2. n-Nonane	0.74	1								
3. n-Decane	0.78	**0.98**	1							
4. n-Undecane	0.66	**0.93***	**0.94**	1						
5. Toluene	0.32	0.72***	0.72	0.64	1					
6. Ethylbenzene	0.68*	**0.84**	**0.86**	0.72	0.79	1				
7. m,p-Xylenes	**0.80**	**0.92**	**0.95**	**0.85**	0.77	**0.91**	1			
8. o-Xylene	**0.87**	0.78	**0.82**	0.65	0.47	**0.87**	**0.83**	1		
9. Styrene	0.78*	0.73	0.76	0.57	0.52	**0.90**	**0.80**	**0.98**	1	
10. 1,2,4-TMB	0.70*	**0.92**	**0.96**	**0.94****	0.64**	0.76	**0.89**	0.73	0.65*	1

The absence of an asterix (*) indicates that $p < 0.001$
$0.001 < *p < 0.005$
$0.005 < **p < 0.05$
$***p > 0.1$
Red bold values indicate a very strong correlation ($r > 0.8$)

Figure 6-19 shows scatter plots of n-decane and n-undecane versus n-nonane concentrations; styrene concentrations versus n-nonane concentrations; and xylenes versus toluene. C_9-C_{11} straight chain alkanes were strongly correlated among them for all the samples taken during different sampling times of the study, and m, p-xylene exhibited very strong correlations with ethyl benzene. These results may indicate that the sources of these chemicals were consistent or at least their composition was similar during the different sampling times. On the other hand, n-octane was weakly correlated to toluene ($r = 0.32$), as illustrated in Figure 6-19.

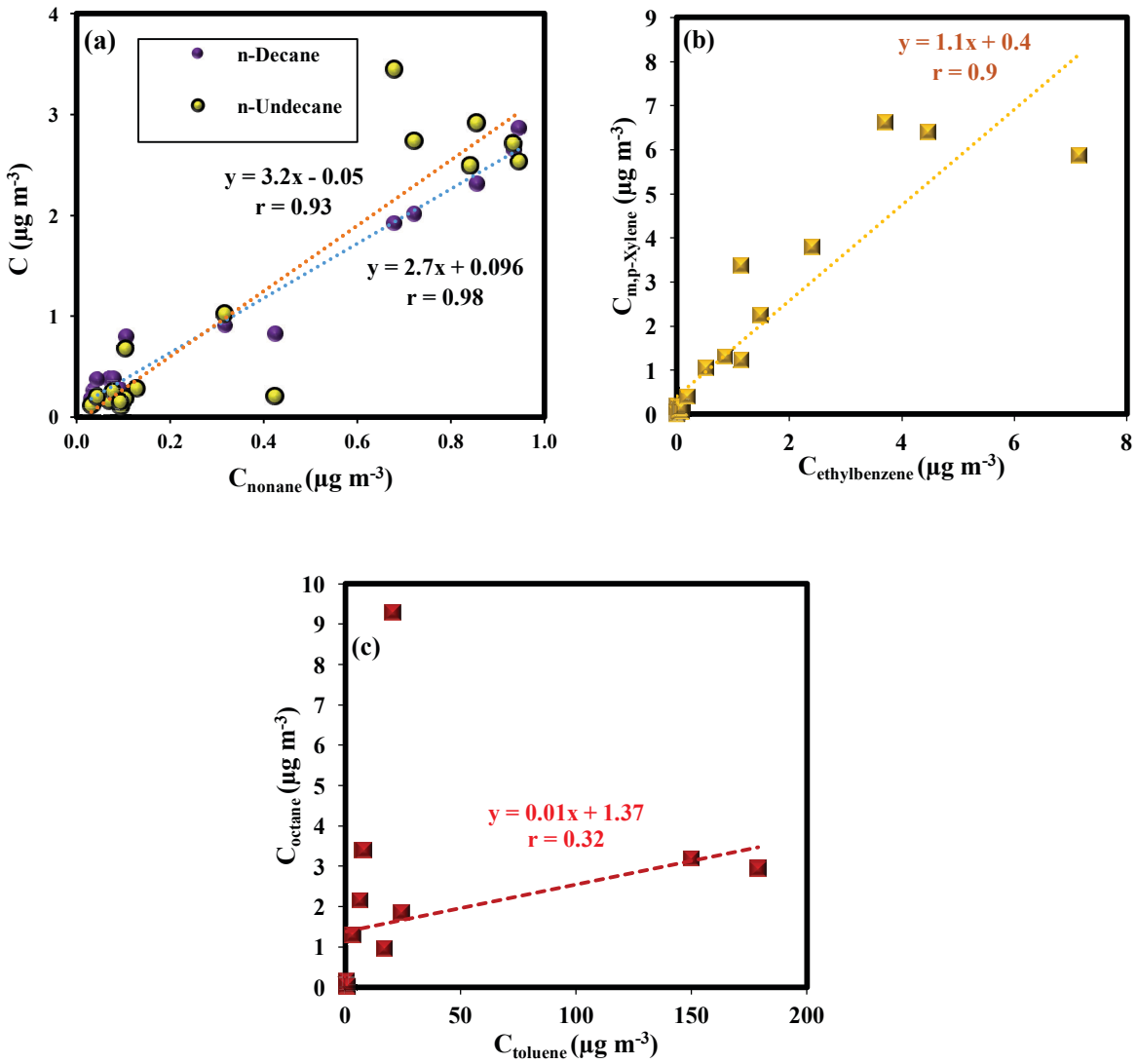

Figure 6-19: Correlations between (a) C_9-C_{11} n-alkanes (b) m,p-Xylene and ethyl benzene (c) n-Octane and toluene (example of a weak correlation) (Beirut Airport, June 2014)

- Arrivals Hall

Variation of TVOCs between the Campaigns

As previously mentioned (chapter 5), the first campaign in the arrivals hall was conducted during summer (June 2014), the second campaign (October 2014) during fall/winter with no rain preceding, while the third fall/winter campaign (November 2014) was conducted on a rainy day. Another variable to consider is the change in the ventilation procedure during the campaign that took place in October 2014 where the supply duct contained 50% fresh air mixed with 50% returned indoor air (and not 20% fresh air mixed with 80% recycled air as usual).

The mean total VOC concentrations (μg m^{-3}), as well as the concentrations of the individual VOC groups, measured inside the arrivals hall at Beirut Airport during the 3 measurement campaigns are presented in Figure 6-20. The mean TVOC concentration decreased by 35% between the summer (98 μg m^{-3}) and the fall/winter (November) campaign (64 μg m^{-3}). In fact, the decrease occurred in the concentration of total monoaromatics (31.4 to 10.10 μg m^{-3}), aldehydes and ketones (32.6 to 9.5 μg m^{-3}), alkenes (8.8 to 5.5 μg m^{-3}), and d-limonene (2.77 to 0.64 μg m^{-3}). Whereas the concentration of light alkanes doubled from summer to winter (11.3 to 22.7 μg m^{-3}), and the concentration of heavy alkanes increased slightly from 11.5 to 14.9 μg m^{-3}. During the summer campaign, the major contributors to TVOC concentrations were aldehydes (32.6 μg m^{-3}, 33%) whereas light alkanes (22.7 μg m^{-3}, 35%) were the major contributors in winter. It is important to note there are three variables between the campaign conducted in June and that in November: (i) the method of sampling: samples were taken through the duct which carries the air entering the indoor room during the summer campaign, whereas sampling during the fall/winter campaign took place inside the arrivals hall (chapter 6); (ii) samples were taken during a rainy day in November; (iii) stronger photochemical reactions take place in the summer. Despite these different conditions, it is remarkable to observe very similar TVOC indoor concentrations.

An exceptional incident took place on 30-31 Oct-2014, where the air conditioning units malfunctioned that necessitated the pumping of 50% of fresh air instead of 20% (usual conditions) in order to provide cooling effects. This implied that more outdoor emissions (rich with aircraft exhaust and other airport-related emissions) were forced to enter the arrivals hall and get confined inside. The most prominent result was the huge increase of the concentration of heavy alkanes up to 407 μg m^{-3}, around 40 times that of the other 2 campaigns, contributing by 66% of the TVOCs measured and remarkably mimicking the speciation observed in aircraft signature measurements (section 6.1). The other VOC family affected by this irregular ventilation was the monoaromatics, reaching a concentration of 135 μg m^{-3}. It is important to note that light alkanes, alkenes, and d-limonene remained in the same order of magnitude as the other campaigns. To conclude, this is another proof that the major aircraft signature emissions are the heavy alkanes, which elevated dramatically when more outdoor emissions were allowed to enter indoors.

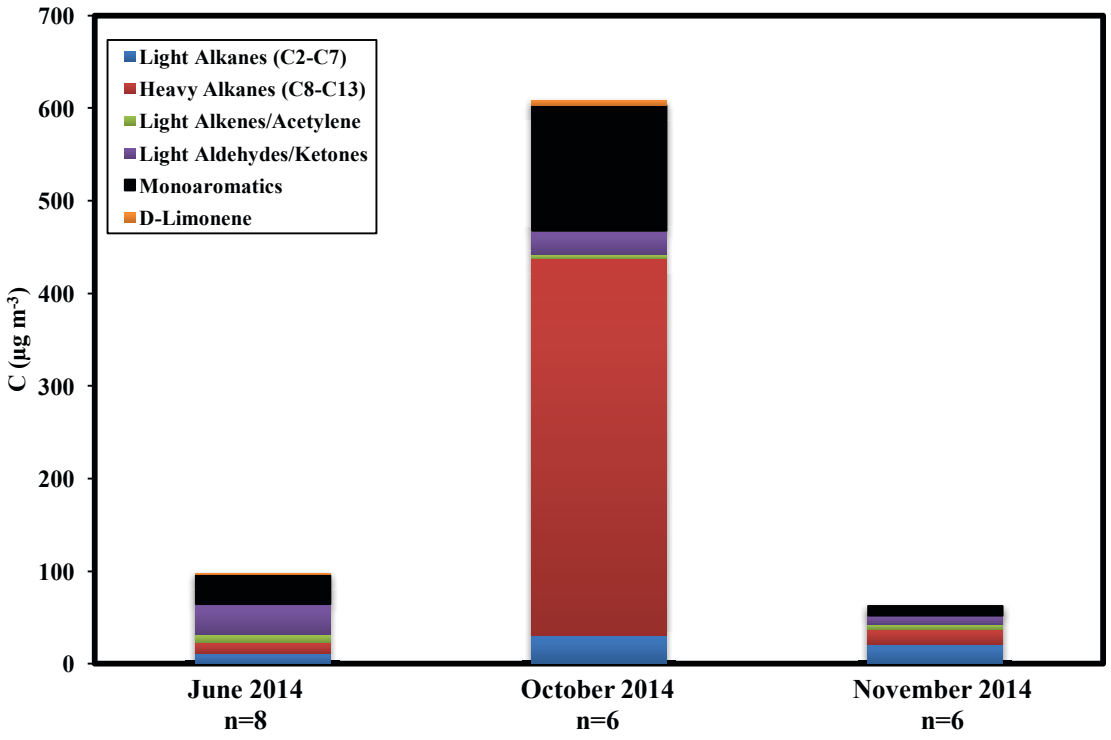

Figure 6-20: Variation of VOC concentrations (µg m^{-3}) between the 3 indoor campaigns conducted at the arrivals hall (Beirut Airport, 2014). Note that C_{14} was not detected during the measurement campaigns.

Temporal Variations of VOC groups

Figure 6-21 presents the temporal variations of the concentrations of VOC families and their correlation to the number of arriving aircraft, calculated by counting the number of aircraft arriving within the past 2 hr before the end of the sampling. The Figure shows a very interesting correlation between VOC groups, specifically heavy alkanes, aldehydes and ketones and monoaromatics with the number of arriving aircraft. For example, at 16:00 on 17/06/2014 (see Figure 6-21 (a)) the concentration of heavy alkanes, light aldehydes/ketones, and monoaromatics (combustion products) is maximum (rush hour). Afterwards, these concentrations decrease gradually until they become very low at 07:30 (very low traffic) and increase again with time to reach another maximum at 16:00 (rush

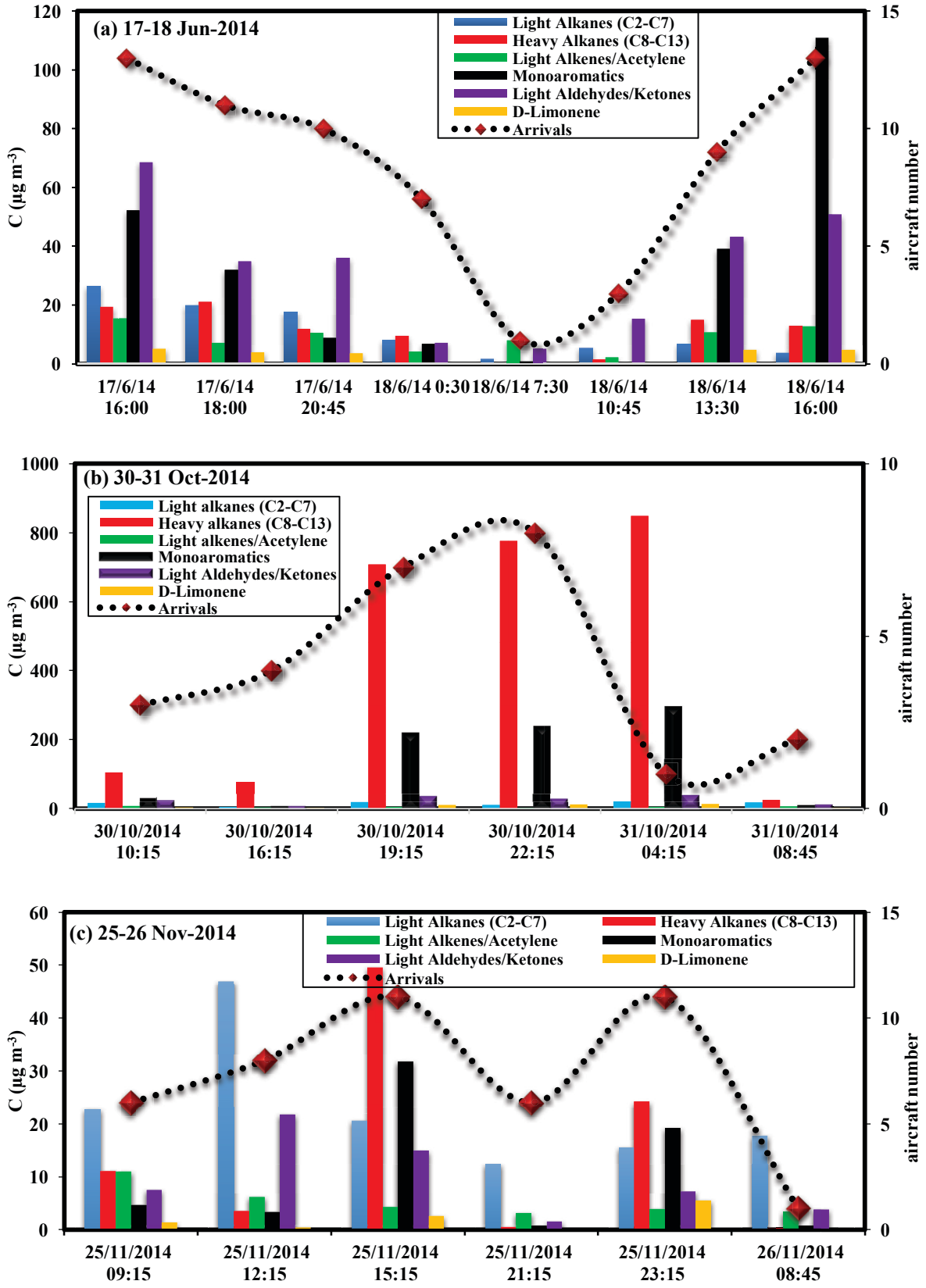

Figure 6-21: Temporal Variation of VOC groups in the arrivals hall during the campaigns conducted in (a) June 2014, (b) October 2014, and (c) November 2014
Note that C_{14} was not detected during the indoor measurement campaigns

hour). In fact, this direct effect of aircraft activity on indoor concentrations is also influenced by the presence of large openings at the baggage belts that provide a pathway for contaminated air near the aircraft gates. The influence of aircraft traffic is also shown in Figure 6-21 (b) where huge concentrations of heavy alkanes entered the arrivals hall when the fresh air flux was increased up to 50%. Again, maxima of heavy alkane concentrations were observed in November 2014 for the third campaign during rush traffic.

VOC Speciation

The mean, maximum, and minimum concentrations (μg m^{-3}) of VOCs measured in the arrivals hall at Beirut Airport during the 3 campaigns are summarized in Table 6-8.

The percentage occurrence was more than 60% for most VOCs (June 2014) except for tetrachloroethene and hexanal, as reported previously in the summer maintenance campaign. Propanal (10.9 μg m^{-3}), toluene (10.3 μg m^{-3}), acetone (9.3 μg m^{-3}), n-butane and cis-2-butene (6.5 μg m^{-3}), ethene and acetylene (4.5 μg m^{-3}), listed in descending order of predominance, were the most abundant VOCs measured in indoor air during the summer campaign.

During the first fall/winter campaign (October 2014), affected to a great extent by outdoor emissions, the most abundant VOCs were n-decane, n-undecane, and n-nonane with mean concentrations of 134.91, 105.52, and 79.30 μg m^{-3} respectively, followed by 1,2,4-TMB (67.1 μg m^{-3}), n-octane (43.5 μg m^{-3}), and n-dodecane (37.8 μg m^{-3}). This confirms again the role of C_8-C_{12} as signature emissions from aircraft and airport activities. The tube analyzed with GC-MS confirmed the presence of heavy alkanes and mainly nC_9-nC_{13}.

During the second winter campaign (November 2014), the most abundant VOCs were acetone (6.8 μg m^{-3}), n-hexane (6.5 μg m^{-3}), n-nonane (5.7 μg m^{-3}), n-decane (4.0 μg m^{-3}), 1,2,4-TMB (3.6 μg m^{-3}), and ethene and acetylene (2.21 μg m^{-3}). The tube analyzed with GC-MS confirmed the presence of heavy alkanes mainly nC_{10}-nC_{12} but at a much lower peak intensity than the previous fall/winter campaign.

Table 6-8: Mean VOC (µg m^{-3}) concentrations during the 3 campaigns conducted in the arrivals hall at Beirut Airport (2014)

	Normal Ventilation: June 17-18, 2014 (n=8)				Irregular Ventilation: October 30-31, 2014 (n=6)				Normal Ventilation: November 25-26, 2014 (n=6)			
VOCs	Average (n=8)	Min	Max	% occurrence	Average (n=6)	Min	Max	% occurence	Average (n=6)	Min	Max	% occurence
n-Octane	2.97	n.d.	9.32	63	43.47	1.98	103.39	100	2.86	0.01	11.19	100
n-Nonane	0.92	0.03	1.81	100	79.30	4.82	181.76	100	**5.70**	0.04	22.25	100
n-Decane	1.81	0.02	3.34	100	**134.91**	6.79	273.58	100	3.97	0.08	13.01	100
n-Undecane	**4.24**	0.04	6.75	100	105.52	5.47	203.21	100	1.56	n.d.	5.37	67
n-Dodecane	1.05	0.02	2.60	100	37.78	3.56	91.95	100	0.65	0.03	2.60	100
n-Tridecane	0.47	0.02	1.05	100	6.13	0.98	16.78	100	0.12	0.02	0.33	100
Benzene	Invalid results				Invalid results				Invalid results			
Toluene	**10.27**	n.d.	44.79	88	20.18	2.56	41.69	100	3.02	0.64	6.73	100
Ethylbenzene	6.00	n.d.	26.10	88	11.95	0.08	30.19	100	0.87	n.d.	2.72	83
m,p-Xylene	6.75	n.d.	28.67	100	16.62	0.59	41.77	100	1.82	n.d.	5.98	83
o-Xylene	3.75	n.d.	16.00	75	12.24	1.40	27.48	100	0.57	0.02	1.75	100
Styrene	0.41	n.d.	1.54	50	2.48	0.13	5.77	100	0.20	n.d.	0.56	67
1,2,4-TMB	3.84	n.d.	24.26	75	**67.10**	2.76	146.28	100	**3.62**	n.d.	15.23	67
Trichloroethene+ Isooctane	**0.84**	n.d.	4.64	63	3.55	0.97	5.86	100	1.07	n.d.	2.92	83
Tetrachloroethene	0.17	n.d.	0.94	38	**6.75**	0.24	15.46	100	n.d.	n.d.	0.02	17
Acrolein	5.01	n.d.	15.86	88	4.57	1.98	7.80	100	1.11	n.d.	2.47	67
Propanal	**10.95**	n.d.	29.40	88	2.09	n.d.	7.36	83	0.44	n.d.	1.39	50
Butanal	1.43	n.d.	4.16	100	0.25	n.d.	1.16	33	0.33	n.d.	1.11	17
Pentanal	0.39	n.d.	1.48	63	7.90	2.03	13.41	100	0.52	0.08	0.79	100
Hexanal	1.24	n.d.	3.26	38	4.28	0.04	9.60	100	0.07	n.d.	0.40	17
Acetone	9.33	n.d.	19.07	88	**6.09**	3.44	9.40	100	**6.80**	0.88	18.76	100
2-Butanone	0.81	n.d.	3.29	88	0.37	n.d.	1.44	50	0.45	n.d.	1.39	67
D-Limonene	2.46	n.d.	5.11	63	6.85	13.95	0.04	100	0.64	n.d.	1.92	83
Ethane	0.06	n.d.	0.14	63	0.10	0.01	0.16	100	0.27	0.06	0.38	100
Propane	0.52	n.d.	1.46	75	2.80	1.02	4.92	100	3.05	1.98	4.81	100
Isobutane	1.05	n.d.	2.58	88	3.14	1.26	6.00	100	5.18	2.41	7.87	100
n-Butane+cis-2-Butene	**6.51**	n.d.	18.76	88	1.96	0.60	2.83	100	3.82	2.44	6.11	100
Isopentane	0.50	n.d.	1.09	88	2.32	0.36	4.65	100	2.49	0.99	5.24	100
n-Pentane+ cis-2-Pentene	0.78	n.d.	1.92	100	0.72	0.19	1.60	100	0.28	0.06	0.55	100
n-Hexane	0.19	n.d.	0.51	88	3.49	0.15	6.89	100	**6.46**	n.d.	37.71	67
n-Heptane	0.49	n.d.	1.07	75	**15.82**	0.82	35.92	100	1.14	0.03	2.57	100
Ethene+acetylene	**4.45**	n.d.	8.56	88	0.24	n.d.	0.76	50	**2.21**	0.63	5.02	100
Propene	1.25	0.30	1.98	100	**1.37**	0.32	2.82	100	1.21	0.68	2.18	100
1-Butene	0.73	0.05	1.24	100	0.56	0.14	1.49	100	0.85	0.24	1.56	100
1,3-Butadiene	0.40	n.d.	2.75	75	0.49	0.05	1.16	100	0.18	n.d.	0.64	83
Trans-2-Butene	0.16	0.02	0.45	100	0.30	0.11	0.56	100	0.35	0.21	0.65	100

Table 6-8 (Continued): Mean VOC (µg m^{-3}) concentrations during the 3 campaigns conducted in the arrivals hall at Beirut Airport (2014)

	Normal Ventilation: June 17-18, 2014 (n=8)				**Irregular Ventilation: October 30-31, 2014 (n=6)**				**Normal Ventilation: November 25-26, 2014 (n=6)**			
VOCs	Average (n=8)	Min	Max	% occurence	Average (n=6)	Min	Max	% occurence	Average (n=6)	Min	Max	% occurence
1-Pentene	0.25	n.d.	0.63	88	0.43	0.01	0.92	100	0.24	n.d.	0.54	83
Trans-2-pentene	0.04	n.d.	0.15	50	0.08	0.01	0.25	100	0.03	n.d.	0.09	67
Isoprene	1.22	0.04	4.42	100	0.48	0.09	1.07	100	0.10	n.d.	0.27	67
1-Hexene	0.35	n.d.	1.35	75	0.37	0.07	1.25	100	0.16	n.d.	0.51	83
C(µg m^{-3})	**Average**	**Min**	**Max**		**Average**	**Min**	**Max**		**Average**	**Min**	**Max**	
Light Alkanes (C_2-C_7)	11.30	1.70	26.64		30.36	6.22	56.26		22.70	12.43	46.92	
Heavy Alkanes (C_8-C_{13})	11.46	0.12	21.04		407.11	23.59	813.17		14.86	0.19	49.61	
Alkenes/Acetylene	8.85	2.18	15.45		4.32	1.33	7.73		5.34	3.15	11.03	
Monoaromatics	31.37	0.24	110.84		135.40	9.64	296.83		10.10	0.76	31.82	
Aldehydes/Ketones	32.67	5.12	68.58		25.54	8.25	40.07		9.47	1.51	21.76	
D-Limonene	2.77	n.d.	5.11		6.85	0.04	13.95		0.64	n.d.	1.92	
Total VOCs	98.98	16.02	197.26		619.88	78.56	1243.97		64.19	18.77	124.27	

The highest concentration per VOC group is formatted in bold
n.d.: not detected

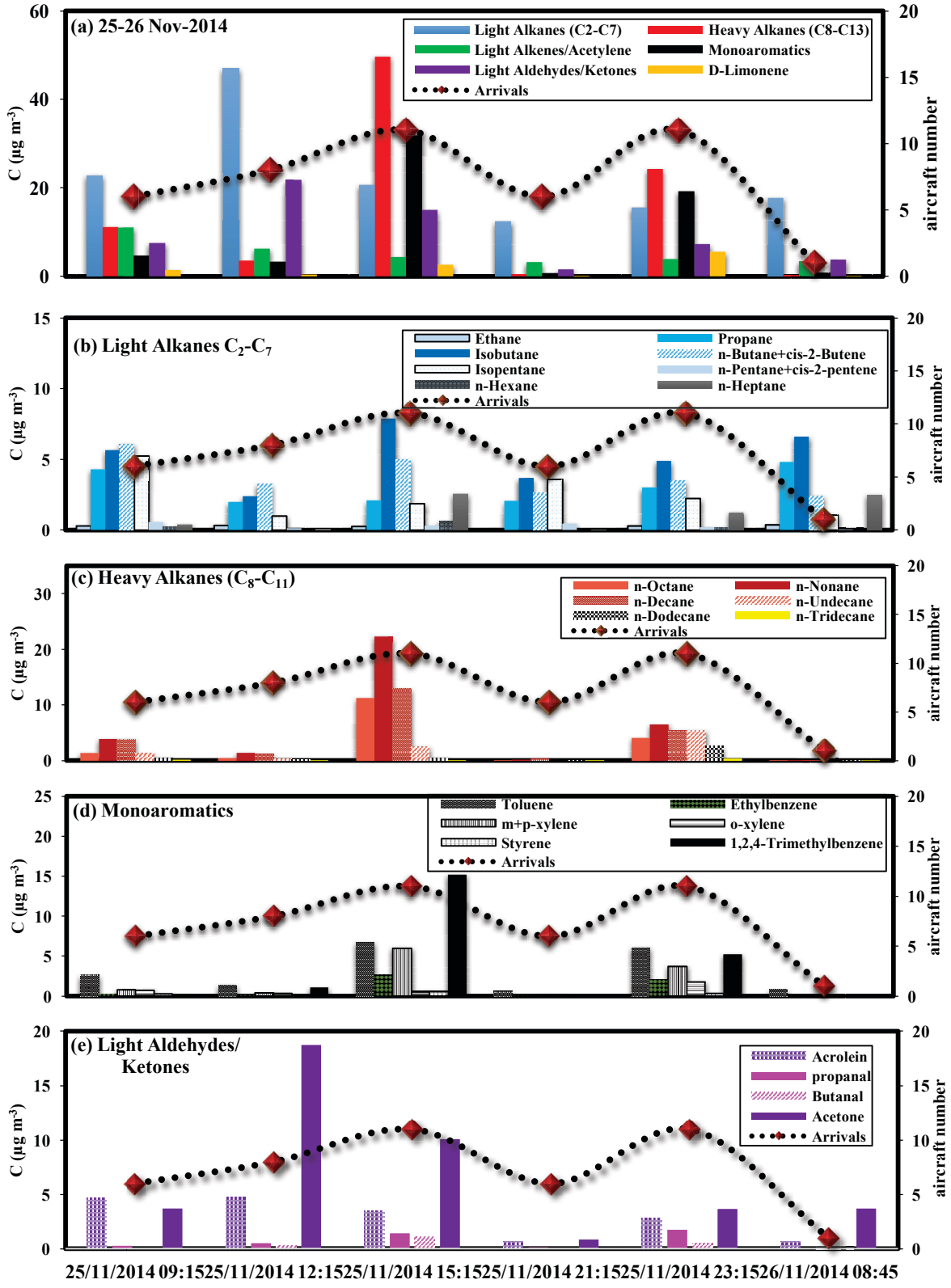

Figure 6-22: Temporal Variations of VOC families for the arrivals hall campaign (Beirut Airport, 25-26 Nov-2014) (a) Total VOC families, (b) Light Alkanes, (c) Heavy Alkanes, (d) Monoaromatics (e) Light Aldehydes and Ketones

For the 3 campaigns conducted at the arrivals hall, HAP levels were below the acute toxicity criteria (see chapter 3) except for acrolein with an average concentration of 5.01 µg m^{-3} (between 0 and 15.86 µg m^{-3}) during the summer campaign, 4.57 µg m^{-3} (between 1.98 and 7.8 µg m^{-3}) during the campaign conducted in 30-31 October 2015, and 1.11 µg m^{-3} (0-2.47 µg m^{-3}) during the campaign conducted in 25-26 November 2015, which may pose a health hazard for passengers and the airport employees.

Figure 6-22 presents the temporal variations of VOC families for the campaign conducted in November 2014. VOC species also exhibit temporal variations related to aircraft activity, mostly heavy alkanes (nC_9 and nC_{10}) and monoaromatics (xylenes and 1,2,4-TMB).

Correlation Analysis

Results show that the correlations between measured VOCs during summer are much weaker (lower correlation coefficients) and less statistically significant (most p-values are above 0.05) than in the winter campaigns (Table 6-9). There is no doubt that indoor VOC levels are affected by outdoor air. In summer, when photochemistry is at a maximum, the variation of outdoor VOC concentrations is affected by photochemistry in addition to emission sources. By contrast, during winter when photochemistry is at a minimum, the changes in VOC concentrations would be majorly affected by the variations in source emissions rather than by photochemistry. It has been previously reported that the tropospheric lifetimes of VOCs are 20 times shorter in summer than in winter, considering OH radical reaction as the rate determining step in the photo-oxidative degradation of VOCs (Atkinson, 1986a; Hellén, 2006).

The correlations between VOCs measured during the summer campaign ranged between very weak (r = 0.08 for 1,2,4-TMB and n-octane) and very strong (r = 1 for o-xylene and m, p-xylene) correlations. These results are not surprising. During summer, the photochemical reactions of VOCs are intensified and consequently strongly contribute to the production/loss processes of VOCs, depending on the rate constant of each VOC. For example, the rate constant of 1,2,4-TMB ($32.5 \pm 5.0 \times 10^{-12}$ cm^3 $molecule^{-1}$ s^{-1}) for its reaction with OH radical is 4 times higher than that of n-octane (8.11×10^{-12} cm^3 $molecule^{-1}$ s^{-1}) at T = 296 - 298 K (around 25°C) which leads to a faster degradation of the former

(Atkinson, 2003; Atkinson and Aschmann, 1989). Consequently, the sink caused by OH radicals will lead to a faster variation of 1,2,4-TMB concentrations than n-octane.

The correlation coefficients during the winter campaigns ranged between 0.62 (styrene/ethylbenzene) and 1 (m, p-xylene/n-octane, m, p-xylene/ethylbenzene, and 1,2,4-TMB/n-nonane). This implies that all the correlations listed are classified as "strong" or "very strong" correlations.

Despite the seasonal differences, some VOCs correlate similarly throughout summer and winter. For example, m, p-xylene and o-xylene present a very strong correlation with toluene with r equal to 0.97 and 0.95 respectively (3 campaigns) (Figure 6-23). A similar very strong correlation exists between aircraft tracers, namely n-nonane and n-decane if the 3 campaigns are taken into account (r = 0.99) (Figure 6-24). This is explained by the fact that they have similar tropospheric lifetimes and same primary emission sources. On the other hand, examples of weakly correlated VOCs are styrene and n-nonane during the summer campaign as illustrated in Figure 6-25.

Table 6-9: Pearson's correlation coefficients of VOCs quantified inside the arrivals hall at Beirut Airport, taken during summer (June) and winter (October/November) 2014

VOC	1.	2.	3.	4.	5.	6.	7.	8.	9.	10.
1. n-Octane	1									
2. n-Nonane	0.68***	1								
3. n-Decane	0.63***	**0.96***	1							
4. n-Undecane	*0.42*	*0.59*	0.59**	1						
5. Toluene	*0.13*	0.76*	0.67*	0.34**	1					
6. Ethylbenzene	*0.35*	0.73**	0.66**	0.49**	0.52**	1				
7. m,p-Xylene	*0.27*	**0.81**	0.72	0.39**	**0.97**	0.59	1			
8. o-Xylene	*0.29*	**0.83**	0.74	0.38**	**0.97**	0.60	**1**	1		
9. Styrene	*-0.27*	*0.23*	*0.12*	*0.45*	*0.65*	*0.07*	*0.56*	*0.52*	1	
10. 1,2,4-TMB	*0.08*	0.66	0.54	0.38**	**0.96**	0.38	**0.92**	**0.91**	**0.80**	1
1. n-Octane	1									
2. n-Nonane	**0.99**	1								
3. n-Decane	**0.98**	**0.99**	1							
4. n-Undecane	**0.97**	**0.98**	**0.99**	1						
5. Toluene	**0.99**	**0.99**	**0.99**	**0.98**	1					
6. Ethylbenzene	**0.99**	**0.98**	**0.96**	**0.96**	**0.99**	1				
7. m+p-Xylene	**1**	**0.99**	**0.97**	**0.96**	**0.99**	**1**	1			
8. o-Xylene	**0.99**	**0.97**	**0.97**	**0.97**	**0.98**	**0.98**	**0.98**	1		
9. Styrene	0.71*	0.75*	0.79*	0.75*	0.72*	0.62*	0.66*	0.72*	1	
10. 1,2,4-TMB	**0.99**	**1**	**0.99**	**0.98**	**0.99**	**0.96**	**0.98**	**0.96**	0.78	1

The absence of an asterix (*) indicates that $p < 0.001$
$0.001 \leq *p < 0.005$
$0.005 \leq **p < 0.05$
$***0.05 \leq p < 0.1$
$p > 0.1$
Red bold values indicate very strong correlations ($r > 0.8$).

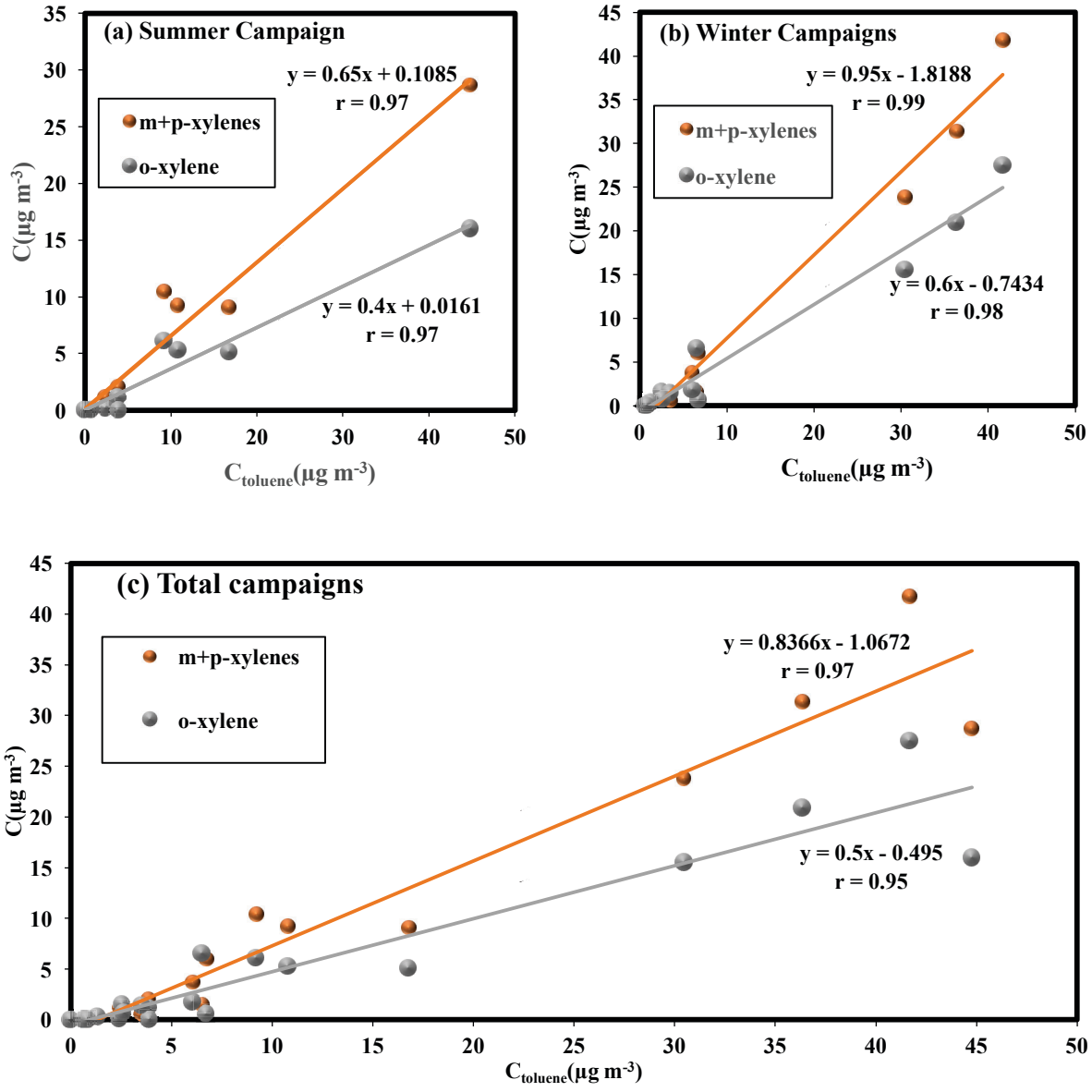

Figure 6-23: Examples of very strong correlations: The correlation between the indoor concentrations (µg m^{-3}) of xylenes (m,p-xylenes and o-xylene) and toluene at the arrivals hall in Beirut Airport during (a) Summer (17-18 June-2014), (b) Fall/Winter (30-31Oct-2014 and 25-26 Nov-2014), and (c) Total Campaigns

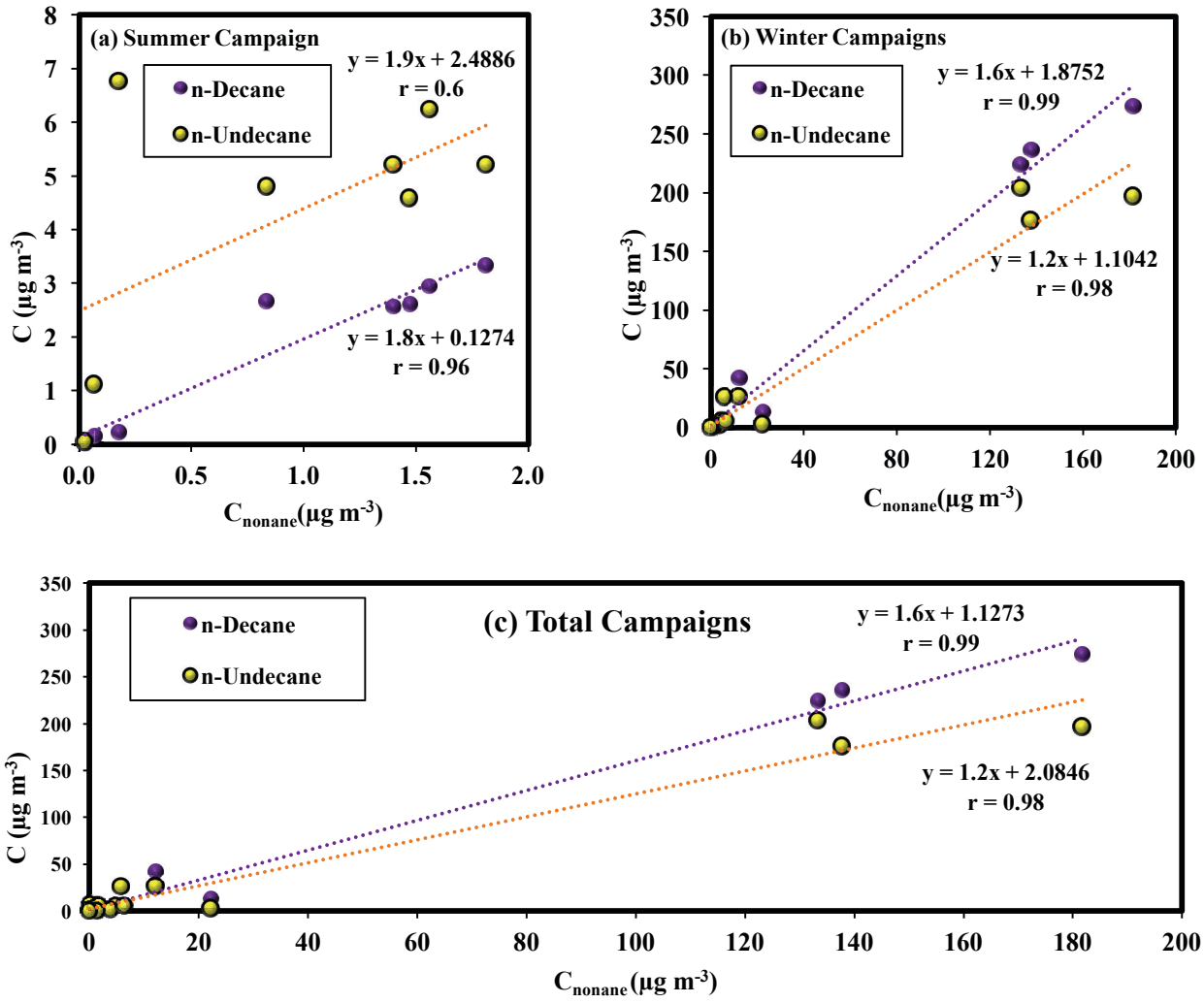

Figure 6-24: Examples of strong and very strong correlations: The correlation between the indoor concentrations (µg m^{-3}) of n-nonane, n-decane, and n-undecane at the arrivals hall in Beirut Airport during the different measurement campaigns: (a) Summer (17-18 June-2014), (b) Fall/Winter (30-31 Oct-2014 and 25-26 Nov-2014), (c) Total Campaigns

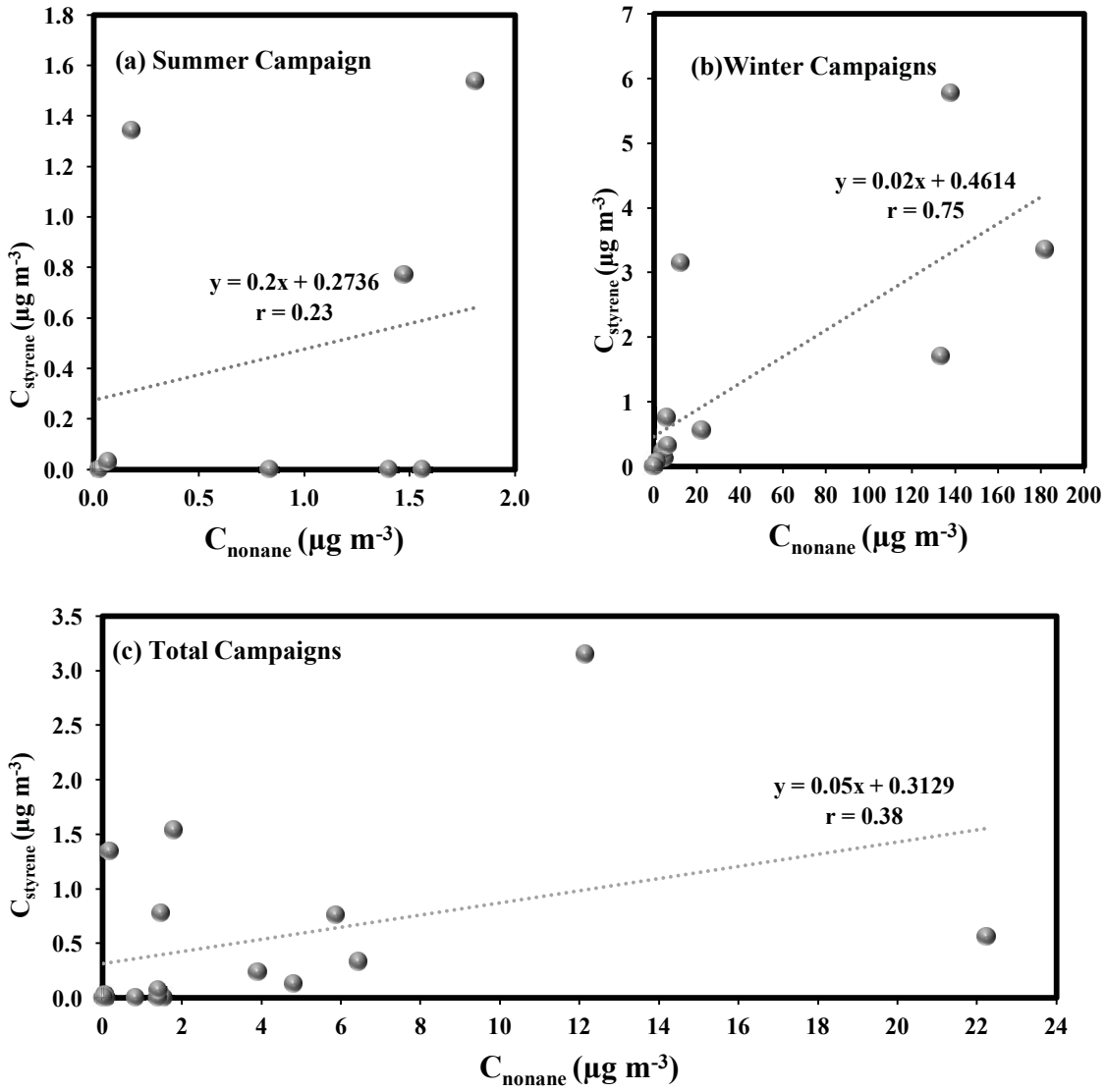

Figure 6-25: Example of weak correlations: The correlation between the indoor concentrations (µg m^{-3}) of styrene and n-nonane at the arrivals hall in Beirut Airport during the different measurement campaigns (a) Summer (17-18 June-2014), (b) Winter (30-31 Oct-2014 and 25-26 Nov-2014), (c) Total Campaigns

6.2.2 NO_2 CONCENTRATIONS

Average NO_2 concentrations (µg m^{-3}) measured in the maintenance room and the arrivals hall are presented in Tables 6-10 and 6-11.

NO_2 concentrations inside the maintenance room ranged between 7.2 and 10.8 µg m^{-3}, which are significantly below the World Health Organization (WHO) annual threshold limit (40 µg m^{-3}). The 2 sources that contribute to indoor NO_2 levels in the maintenance room are the indoor room itself and the measured fresh air (Table 6-10). The fact that indoor room concentrations as well as the fresh air concentrations are below that limit explains the observed relatively clean environment.

On the other hand, results show that NO_2 concentrations exceeded 40 µg m^{-3} in the arrivals hall at two out of 4 measurement campaigns to reach values of 41.6 µg m^{-3} (26-27 October 2014) and 48.4 µg m^{-3} (24-29 June 2015), followed by 36.1 µg m^{-3} (25-26 Nov 2014). These results are threatening since these values, although weekly average concentrations, indicate a big probability that the annual mean NO_2 concentrations might be either above or slightly below the World Health Organization (WHO) annual guideline value for indoor NO_2 of 40 µg m^{-3} (Jarvis *et al.*, 2010), which risks the health of passengers in the arrivals hall. Most importantly, are the airport personnel who stay a minimum of 12 h daily in the offices and duty free shops adjacent to the measurement location. Three sources contribute to pollutant concentrations in the arrivals hall: (i) The return flow from the indoor room itself, (ii) fresh air measured in the mechanical room, and (iii) the air that flows from the ramp into the arrivals hall through the openings associated with the conveyor belts. Table 6-10 presents NO_2 concentrations of the fresh air (52.3 µg m^{-3}) and the outdoor air (64.2 µg m^{-3}) measured in October 30-31, 2014 which are already above the WHO threshold and which consequently contribute to the elevated concentrations in the arrivals hall. Similar observations were found in June 2015 with mean indoor NO_2 concentration of 48.4 µg m^{-3} and a corresponding concentration of 49.5 measured outdoors near the conveyor belt. These results are very significant, as they can point at the causes for pulmonary diseases that Beirut airport employees suffer from, especially workers in the ramp (Yaman, 2001).

Table 6-10: Measured NO_2 concentrations (µg m^{-3}) during the measurement campaigns conducted in the maintenance room (Beirut Airport, 2014-2015)

NO_2 (µg m^{-3})	26-27 Nov-2014	28-29 Nov-2014	17-24 June-2015	24-29 June-2015
Indoor	10.8	14.6	9.6	7.2
Fresh Air	25.8	3.7	NA	NA

NA: Not Available

Table 6-11: Measured NO_2 concentrations ($\mu g\ m^{-3}$) during the measurement campaigns conducted in the arrivals hall (Beirut Airport, 2014-2015)

NO_2 ($\mu g\ m^{-3}$)	30-31 Oct-2014	25-26 Nov-2014	17-24 June-2015	24-29 June-2015
Indoor	41.6	36.1	34.0	48.4
Outdoor Baggage	64.2	NA	49.0	49.5
Fresh Air	52.3	20.6	NA	NA

NA: Not Available

6.2.3 COMPARISON OF RESULTS

- Comparison between Measurements Taken in the Maintenance Room and the Arrivals Hall

Comparisons between VOC levels in the 2 rooms were made according to season. Figure 6-26 (a) shows that although TVOC concentration for the 2 rooms is very similar, nevertheless it was slightly higher in the arrivals hall (98.4 $\mu g\ m^{-3}$) than in the maintenance room (91.1 $\mu g\ m^{-3}$) for the summer campaigns. A difference in the contribution between the VOC groups exists, where light alkanes (45.3 $\mu g\ m^{-3}$) dominate the TVOC mass in the maintenance room accounting for 49.6% of the total mass, whereas aldehydes and ketones (32.7 $\mu g\ m^{-3}$) as well as monoaromatics (31.4 $\mu g\ m^{-3}$) dominate the TVOC mass accounting for 33.2 and 31.8% respectively. These 2 VOC groups are combustion products that diffuse inside the arrivals hall. The concentration of heavy alkanes in the arrivals hall is almost 3 times (11.6% of TVOC) that in the maintenance room (5.2% of TVOC), which confirms that the arrivals hall is more affected by aircraft emissions.

In the fall/winter campaigns, the mean TVOC concentration in the maintenance room (247.5 $\mu g\ m^{-3}$) was around 4 times higher than that measured in the arrivals hall (64.2 $\mu g\ m^{-3}$). This is most probably a result of the heavy rain that occurred during sampling in the arrivals hall (wet deposition). Light alkanes constitute 44% of the total VOC mass in the maintenance room at a concentration of 107.5 ($\mu g\ m^{-3}$). The contribution of heavy alkanes was 19.6% in the maintenance room and 23.2% in the arrivals hall. The mean NO_2 concentration was higher in the arrivals hall by a factor of 2.5.

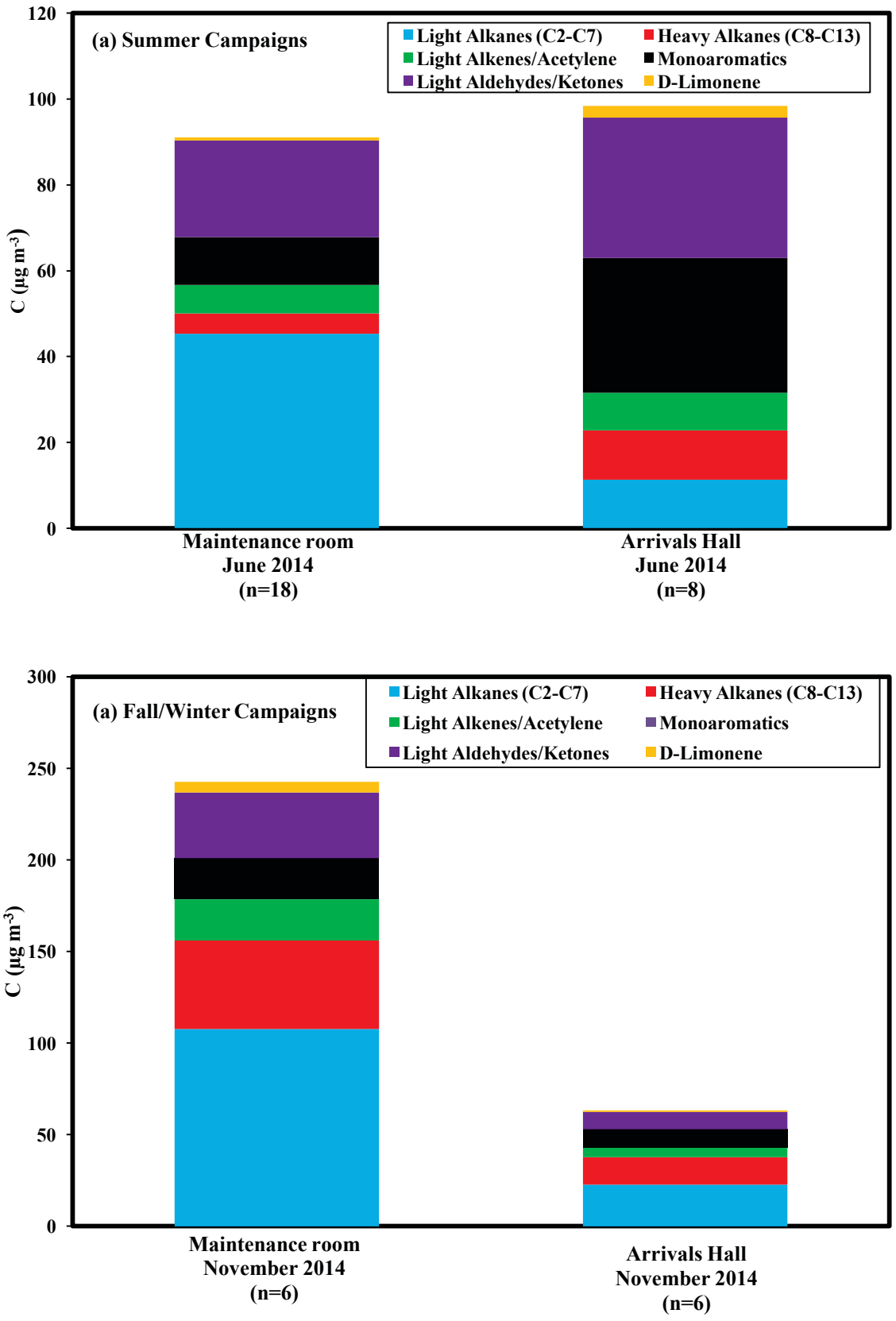

Figure 6-26: VOC groups measured in the maintenance room and arrivals hall in June 2014 and (b) November 2014 at Beirut Airport

- Comparison with Previous Studies

Even if the airport buildings are ventilated using potentially very polluted outdoor air, indoor air was not the main focus in airports so far especially because most buildings have no significant indoor sources (Kim, 2015). Therefore, comparison of our results with previous studies is rather very limited. To the best of our knowledge, this study is the first to assess the speciation and temporal variations of 47 VOCs inside airport buildings. This is also the first indoor VOC study conducted in Lebanon, so it was not possible to compare our results with other indoor Lebanese institutions.

Table 6-12 presents a comparison between measurements taken in this study (maintenance room) and those measured by Pleil *et al.* (2000) taking into account the subset of common VOCs measured. To assess the relative exposures to JP-8 fuel (military jet fuel) vapor, Pleil *et al.* (2000) measured C_6-C_{12} alkanes as well as monoaromatics (the main constituents of JP-8 fuel) in the Air Force base shops (break rooms, office areas, etc.) using a battery-operated machine. The maintenance room was chosen for comparison purposes since it is closer to office areas and break rooms studied by Pleil *et al.* Indoor concentrations in the Air Force base shops represent the average of 5 samples taken in July 1997 and February 1998. Therefore, to conduct a comparison, the maintenance summer and winter campaign were averaged.

Results show that concentrations are somehow similar, with a higher total VOC concentration measured in the U.S Air Force base. The difference in total concentration might be due to the difference in location and emission sources and meteorological conditions (rain). The concentrations of monoaromatics in the maintenance room are similar to those measured by Pleil *et al.* In the 2 measurements, styrene is the least contributor among the monoaromatics whereas toluene is the highest contributor. In both studies, n-undecane dominated the speciation of heavy alkanes followed by n-decane.

Table 6-12: Comparison of our data with those obtained by Pleil et al. (2000)
(Concentrations measured by Pleil et al. were converted from ppb to µg m^{-3})

VOC group	VOC	This Study Maintenance room Summer/Winter 2014 (n = 24)	Pleil et al., 2000 U.S. Air Force base (AFB) Break rooms, offices July 1997, Feb 1998 (n = 5)
Heavy Alkanes	n-Octane	1.67	0.85
	n-Nonane	1.75	6.33
	n-Decane	4.98	15.94
	n-Undecane	14.88	16.49
Monoaromatics	Toluene	8.85	9.62
	Ethylbenzene	1.12	1.77
	m,p-Xylene	2.28	4.46
	o-Xylene	1.43	3.05
	Styrene	1.23	1.43
Chloroalkenes	Tetrachloroethene	0.54	0.48
Light Alkanes	n-Hexane	0.54	1.51
	n-Heptane	1.13	0.58
	TVOC (µg m^{-3})	40.37	62.51

Conclusion

Our study is the first assessment that covers 47 VOCs measured inside an airport building to understand the impact of airport activities on the airport personnel exposure (maintenance room) and passengers' exposure (arrivals hall). Moreover, it is the first study that correlates air traffic with indoor air pollutants. Results showed a strong relation between VOC groups and aircraft number in the arrivals hall, due to the presence of a direct opening that provides a pathway for air from the ramp into the arrivals hall. A much less pronounced correlation was observed between VOC groups and aircraft number in the maintenance room. This is explained by the contribution of other indoor sources to the total VOC budget. In general, VOC concentrations were below recommendations (INRS), however, NO_2 concentrations hinted at a potential risk to the health of airport employees since some measurements were slightly higher than the threshold annual value of 40 µg m^{-3}. Also, HAP levels were below the acute toxicity criteria except for acrolein which might pose a health hazard.

Conclusion - Part II

Part II presented the experimental approach followed to track the impact of Beirut Airport activities on the air quality of Beirut and its suburbs. The technique adapted was *via* identifying aircraft tracers and tracking the variation in their concentrations, as well as conducting comparisons with aircraft fingerprint emissions obtained using real measurements. The focus was on VOCs as due to the higher probability to identify special markers using these species than using NO_2 due to the existence of a tremendous number of VOCs. Results showed the impact Beirut Airport activities is mainly concentrated in its vicinity, while a more interesting observation signalled the impact of aircraft emissions during the approach phase over the seashore. Emissions during the approach phase were also expected to be dispersed to remote mountainous locations > 8 km away from the airport. These studies were the first to identify aircraft exhaust makers using real operations and tracking their resemblance to assess the airport impact. At the indoor level, the variation of heavy alkanes in the arrivals has confirmed their significance as aircraft tracers, when a greater amount of outdoor air supplied from the ramp was accompanied with a large increase in their concentration levels.

Part III: MODELLING WITH ADMS-AIRPORT

Part III presents the other approach adapted to assess the impact of Beirut airport, using an advanced dispersion model, ADMS-Airport, which will be described in the following chapters.

Chapter 7 : Presentation of ADMS-Airport

Another approach to assess the impact of Beirut Airport on air quality was by utilizing an advanced dispersion modelling system, ADMS (Atmospheric Dispersion Modelling System)-Airport. The first step to preform dispersion modelling was to conduct an emission inventory, which calculates the emission rates (e.g. in $g/m^3/s$) for all the emissions sources. The output of this inventory was later exported to ADMS-Airport for dispersion modelling taking into account the influence of meteorological factors (wind, turbulence, and boundary layer). To apply this European model was a real challenge because no previous inventory has been conducted for airport-related emission sources or for road traffic around the airport. However, intensive work was dedicated to produce the first emission inventory for Beirut Airport in the medium approach for the year 2012, which was followed by dispersion modelling using an advanced dispersion modelling system, ADMS-Airport. ADMS-Airport results were validated with measured air quality data (NO_2 concentrations) at selected receptor points, and the first model for the impact of Beirut Airport activities was executed for the year 2012.

7.1 Description of ADMS-Airport

Atmospheric dispersion modelling is the mathematical simulation of the physics and chemistry governing the transport, dispersion, and transformation of pollutants emitted into the atmosphere under the effects of meteorological, terrain, and other influencing factors (FAA, 2014). Most modern air pollution models are computer programs that calculate the pollutant concentration using information on source parameters (e.g. location, shape), emissions parameters (e.g. emissions strength), substance parameters (e.g. chemical reactions, deposition), atmospheric parameters (e.g. wind speed and direction, turbulence properties, and temperature), and terrain parameters (e.g. surface roughness) (ICAO, 2011). Dispersion modelling fills in the gaps between monitoring sites, which gives a much clearer picture of emission spatialization over a large area. Moreover, this simple but powerful ability means that dispersion models can be used in situations where real world measurements are rather too expensive, difficult, or destructive (BC Air Quality, 2016). The results of this modelling allow for the prediction of pollutant concentrations at or near an emission source (s) and enable the comparison of these results to air quality standards (FAA,

2014). Because the modelling is based on an estimate of emissions in and around the airport, the impact of changing these emissions and carrying out future projections is also possible. Dispersion model types include Gaussian models, Lagrangian models, Eulerian models, etc. According to ICAO's Airport Air Quality Manual (ICAO, 2011), the typical 4 models approved for use in the advanced approach for modelling in the vicinity of airports (local air quality) are ADMS-Airport[8] (UK Department for Transport), ALAQS-AV[9] (EUROCONTROL), AEDT/EDMS[10] (US FAA), and LASPORT[11] (Swiss Federal Office for Civil Aviation (FOCA) and German Ministry of Transport (BMVBS)). According to the Department for Transport's (DfT, 2006) Project for Sustainable Development of Heathrow (PSDH) Model Inter-comparison Study (ADMS, EDMS, LASPORT, etc.): "ADMS-Airport should be used for future air quality modelling studies at Heathrow, associated with PSDH". Consequently, ADMS-Airport was chosen to model Beirut Airport emissions, as will be discussed in chapters 8 and 9.

Atmospheric Dispersion Modelling System (ADMS)-Airport is a local air quality model, developed by Cambridge Environmental Research Consultants (CERC), to model concentrations of pollutants in the vicinity of an airport. ADMS-Airport is an extension of the well-known ADMS-Urban air quality model; the additional features of ADMS-Airport compared to ADMS-Urban are related to modelling aircraft exhaust as accelerating jet sources by using algorithms designed specifically to model dispersions from aircraft engines. This PC-based air quality management system includes emission tools, GIS tools and a model of dispersion in the atmosphere of pollutants released from aircraft, road traffic, industrial and area sources for airports in rural or complex urban environments. ADMS-Airport models (simulates) emissions sources using aircraft jet, point, line, area, volume, and grid source models. Aircraft engine (jet) sources are modelled as jets from accelerating sources (CERC, 2015a). ADMS can predict both short-term (1 to 24 hours) and long-term (annual) average concentrations (in $\mu g\ m^{-3}$ or ppb) at each receptor.

ADMS employs a Gaussian dispersion model (Figure 7-1) in the near field that is nested within a trajectory model (used to model large areas). The dispersion equations are described in the technical specification at the CERC website, with the basic Gaussian dispersion described in P10/01X/12. However, additional calculations also affect the plume dispersion,

[8] www.cerk.co.uk
[9] www.eurocontrol.int
[10] www.faa.gov
[11] www.janicke.de

and are described in the other technical specification documents (CERC, 2016). ADMS-Airport models NO_x chemistry based on the ***Generic Reaction Set (GRS)*** (Azzi *et al.*, 1992; Venkatram *et al.*, 1994) which uses explicit reactions for NO, NO_2 interactions with ozone and a limited set of surrogate reactions for the impact of VOCs on O_3 and NO_x (Carruthers *et al.*, 2011) In fact, the GRS Chemistry scheme is a semi-empirical photo-chemical model that reduces the complicated series of chemical reactions involving NO, NO_2, O_3 and VOCs (Annex 7-1).

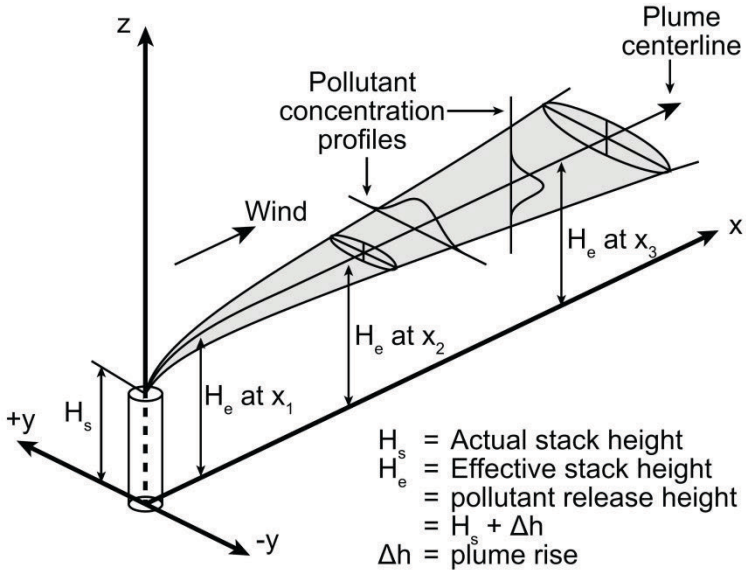

Figure 7-1: Schematic of Gaussian plume, taken from Aliyu *et al.* (2015) in Turner *et al.* (1996)

7.2 Reasons for Using ADMS-Airport

7.2.1 ACCURACY

ADMS-Airport is one of the approved models by the International Civil Aviation Organization, Committee on Aviation Environmental Protection (ICAO CAEP), Models and Databases Group. ADMS-Airport was one of the 4 participating local air quality models in the ICAO CAEP (Committee on Aviation Environmental Protection) model exercises (CAEP, 2008) and contributed to studies of the impact of aviation as part of the Modelling and Databases Group (MDG) of ICAO CAEP (CAEP 9, 2013). The ICAO Airport Air Quality Manual (ICAO, 2011) classified ADMS-Airport as a typical model used in the advanced and sophisticated approaches for dispersion modelling in the vicinity of airports. It has been used to model air quality at London's Heathrow airport for the 2002 base case and

future year scenarios as part of the Department for Transport's (DfT) Project for Sustainable Development of Heathrow (PSDH)-Adding capacity at Heathrow (DfT, 2007). This followed the recommendations of the PSDH Model Inter-comparison Study (ADMS, EDMS, LASPORT, etc.) that: "ADMS-Airport should be used for future air quality modelling studies at Heathrow, associated with PSDH" (DfT, 2006).

The indication of the accuracy of the model was provided by the comparisons of the model with measured concentrations, and also by the sensitivity of the model to the different parameters. Studies showed that there is no significant trend to over or under-prediction by ADMS-Airport (McHugh, 2007). It was found that calculated annual means were generally within ±10 or 20% of measured concentrations for each monitoring site with an overall fractional bias, taking account of all sites, of 0.045 or approximately 5%. The sensitivity of the model to mean wind speed, surface roughness and 'chemical reaction time' showed sensitivity to these parameters but within the range of accuracy detailed above (DfT, 2006). The ADMS model response for variations in wind data have been reported in a study done by (Leuzzi, 2002). The model showed a high sensitivity at low wind speed; however, it was very sensible to wind direction variations, a difference of 45° around to 270° introduces an error of 200% on the concentration.

To simulate the impact of aircraft exhausts, ADMS-Airport can make use of the ADMS jet model, which "calculates an integral solution to the equations of conservation of mass, momentum, heat and species, capturing the effect of the movement of the jet engine source in reducing the effective buoyancy of the exhaust". This is particularly important in capturing the near-field dispersion from the high momentum, buoyant take-off ground roll sources[12]".

7.2.2 PRINCIPLE FEATURES

This system has a number of distinct features summarized below (CERC, 2015a):

1- It is an advanced dispersion model in which the boundary layer is characterized by its height and Monin-Obukhov length. Also, the local Gaussian model is nested within a trajectory to include more significant areas (e.g. 50 km x 50 km).

2- Distinguishing Feature: It can model emissions (aircraft exhausts) from the important sources in the LTO cycle as moving jet sources (jets from an accelerating source) and not as volume sources, as is the case in some other models, to capture the near field

[12] www.cerc.co.uk

plume rise and dispersion characteristics (aircraft jet emissions are released as a jet i.e. at high temperature and pressure). It is important to note that this is taken into account in ADMS-Airport using Air File sources.

3- It can be used to model emissions for up to 6500 sources simultaneously: up to 500 aircraft jet sources, 1500 road sources (up to 50 vertices), 1500 industrial, point, line, area and volume, and up to 3000 grid cells.

4- It involves the modelling of chemical reactions with NO, NO_2, VOCs, and ozone and the generation of sulphate particles from SO_2.

5- INPUT: It possesses a direct link to EMIT (Emission Inventory Toolkit) that contains emission factors for various aircraft and other airport sources.

6- OUTPUT: It is integrated with the commercial Geographical Information System (GIS).

7- It includes a meteorological pre-processor that calculates the boundary layer parameters from a variety of input data (e.g. wind speed, day, time and cloud cover).

8- It possesses an ability to incorporate detailed time-varying emissions.

Chapter 8 : APPLICATION OF ADMS-AIRPORT TO RHIA

8.1 Methodology

The overall air quality assessment methodology includes both quantification of emissions (EMIT) and atmospheric dispersion modelling (ADMS) (Figure 8-1). The first step for conducting an airport air quality study was to produce an emissions inventory in order to calculate and store emissions from different sources, to be later exported to ADMS for dispersion modelling by taking into account different dispersion equations and meteorological conditions. Emissions data were calculated and stored in EMIT, the emissions inventory toolkit (EMIT) developed by CERC, requiring **more than one year** of exhaustive work. Emissions from EMIT were exported to ADMS as sources with emission rates. The dispersion of emissions from these sources was then calculated by the ADMS model using a series of equations, taking meteorological conditions and a number of other effects into account.

The approach adapted in ADMS involved the use of hourly varying meteorological data, emissions data, and background pollutant data as input in order to calculate hourly pollutant concentrations. The meteorological data were obtained from the meteorology department at Beirut Airport from station 16 and converted to comma separated. met files. The meteorological input data include Julian day, number, and hour (which along with latitude determine solar elevation), along with hourly wind speed, direction, cloud cover, and temperature that are used to calculate the boundary layer height, friction, convective velocity scales, and Monin-Obukhov length. Using these quantities, the vertical profiles of mean velocity, turbulence, temperature, etc. were derived to be used in the dispersion algorithm. The background data of pollutant concentrations (NO_2, O_3) were taken from a measurement site (AUB) outside the emissions domain in the upwind direction. The concentrations in the calculation domain consist of the background and those calculated by ADMS-Airport from the emissions, using the local ADMS model for explicitly defined sources. The medium approach was employed in this study and will be described in the following paragraphs. The additional features of ADMS-Airport, as compared to ADMS-Urban, relate to its treatment of aircraft as jet sources using an *AirFile* (complex

approach); however, due to the complexity of this approach it was not employed in this study but will be the aim of our next study.

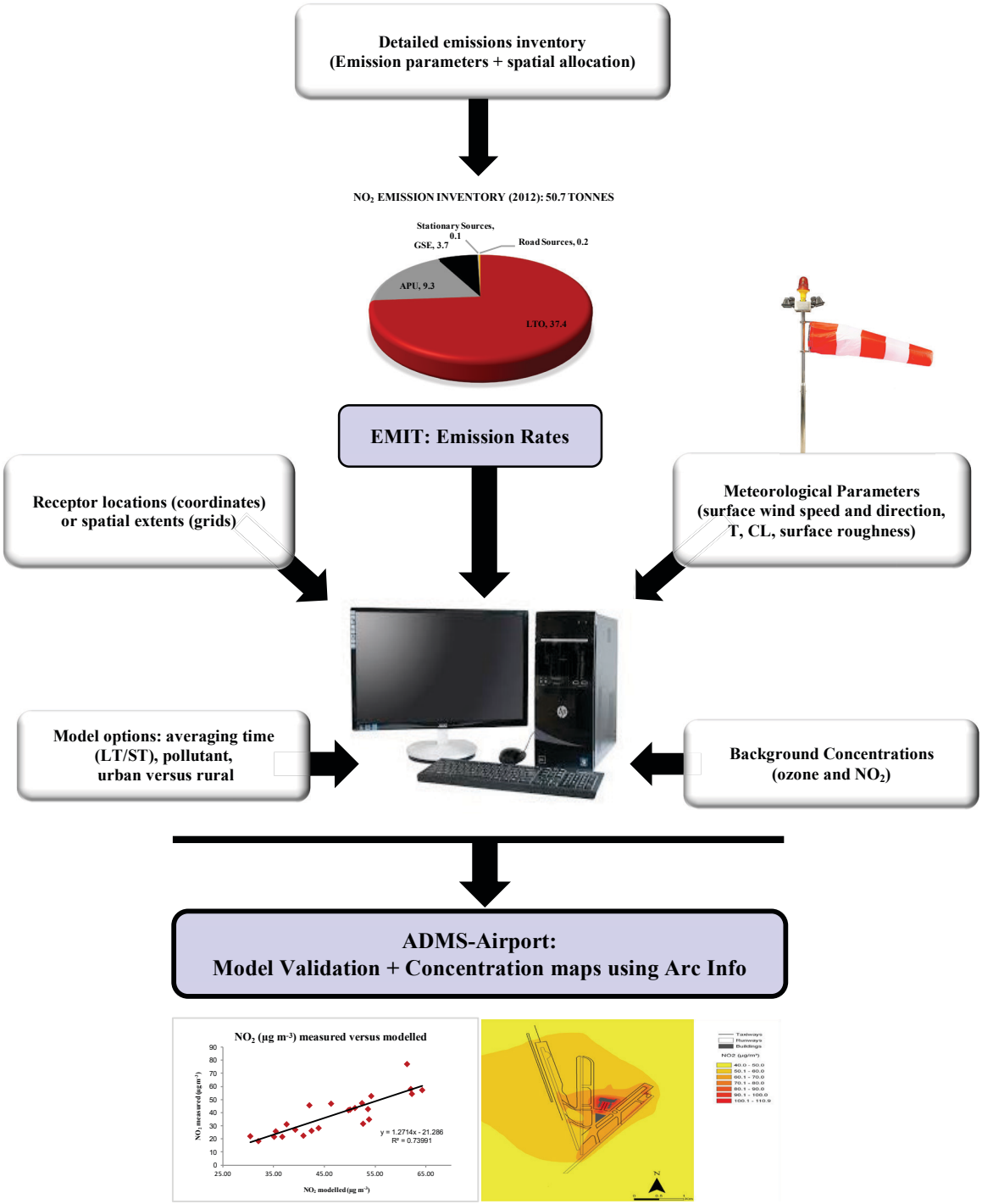

Figure 8-1: ADMS-Airport model input and data requirements

The emissions inventory for the year 2012 was used to estimate pollutant concentrations for that year. Another objective was to validate the model against measured data (3

measurement campaigns, 2014). To achieve that, the emission rates were calculated using the emissions inventory (2012) taking into account that most flights are scheduled and are similar every year. However, specific background and meteorological data were used for each of the validation campaigns.

8.1.1 GENERATING AN EMISSIONS INVENTORY (EMIT)

An emissions inventory contains information regarding airport emissions (magnitude of emissions and the spatial allocation of emissions). Using appropriate input data, it calculates the total mass of emissions released into the environment from specific emission sources for a selected period of time (e.g. tonnes/yr) to be used as input for modelling pollutant concentrations (ICAO, 2011).

EMIT (Emissions Inventory Toolkit), developed by CERC, was used to generate and store the airport emissions inventory. Full details about EMIT are found in EMIT User Guide (CERC, 2015b). Within EMIT, the emissions inventory (*.mdb*) contains several groups. Each group can contain one to several source types organized that share the same modelling (volume, point, area, road, etc.). The magnitude of emissions for each source was calculated from source activity data (such as aircraft model, engine type and time in mode for aircraft; traffic flow speed and source length for roads, etc.) using emission factor datasets stored in EMIT (Table 8-1), whereas the spatial allocations were plotted in ArcMap based on the real locations of the operations taking place in Beirut Airport. The data output from EMIT are the magnitude and spatial information on emissions sources. Details about the activity data and the spatial allocations for Beirut Airport's Emissions inventory (2012) are provided in Annex 8-1.

EMIT contains emission factor datasets for all Landing and Take-off (LTO) modes (taxi, take-off, climb, approach), Ground Support Equipment (GSE) (e.g. belt loaders, push back tug, etc.), stationary sources (e.g. power plants) and Auxiliary Power Units (APU). These datasets are activity datasets i.e. for these source types the total emission E of a particular pollutant in tonnes/year is equal to the product of the activity, A (unit activity)/year and the emission factor, e_f, in tonnes of pollutant/unit activity ($E=Ae_f$). For example, the activity A can be the number of LTO cycles per year or working hours of APU per year. EMIT holds the emission factors and thus calculates the emission rate E (tonnes/year) when the activity data are entered by the user. This is applied to point, area, line, and volume sources modelled. These emission rates (tonnes/yr) were then converted by EMIT to units of

$g/m^3/s$ (volume source) or $g/m^2/s$ (area source) or g/s (industrial point source), etc. according to the dimensions of each source group used. Emissions rates and spatial allocations were exported directly to ADMS-Airport as input for air dispersion modelling.

- Emission Sources

This study was based on Beirut Airport's 2012 operational data. The full range of sources (Table 8-1), which are important in calculating air quality in the vicinity of Beirut Airport, were modelled and included in the emissions inventory. These sources have been grouped into the following 5 categories (Figure 8-2):

- Aircraft main engine emissions (about 63 000 arriving and departing aircraft) during the different modes of operation: taxi-in and taxi-out, take-off, climb, arrival (approach (3000-1500 ft), approach (1500 ft-touchdown), landing roll)

- Auxiliary power unit (APU) for 30 000 aircraft

-Aircraft GSE, which included both GSE operating at the stand (e.g. GPU) and mobile sources across the apron (called airside vehicles (e.g. crew buses))

- Airport static sources that included power plants and fuel tanks

- Urban Sources, which included airport landside traffic, constituting road traffic at major roads close enough or directly related to the airport to require explicit modelling (airport main entrance road).

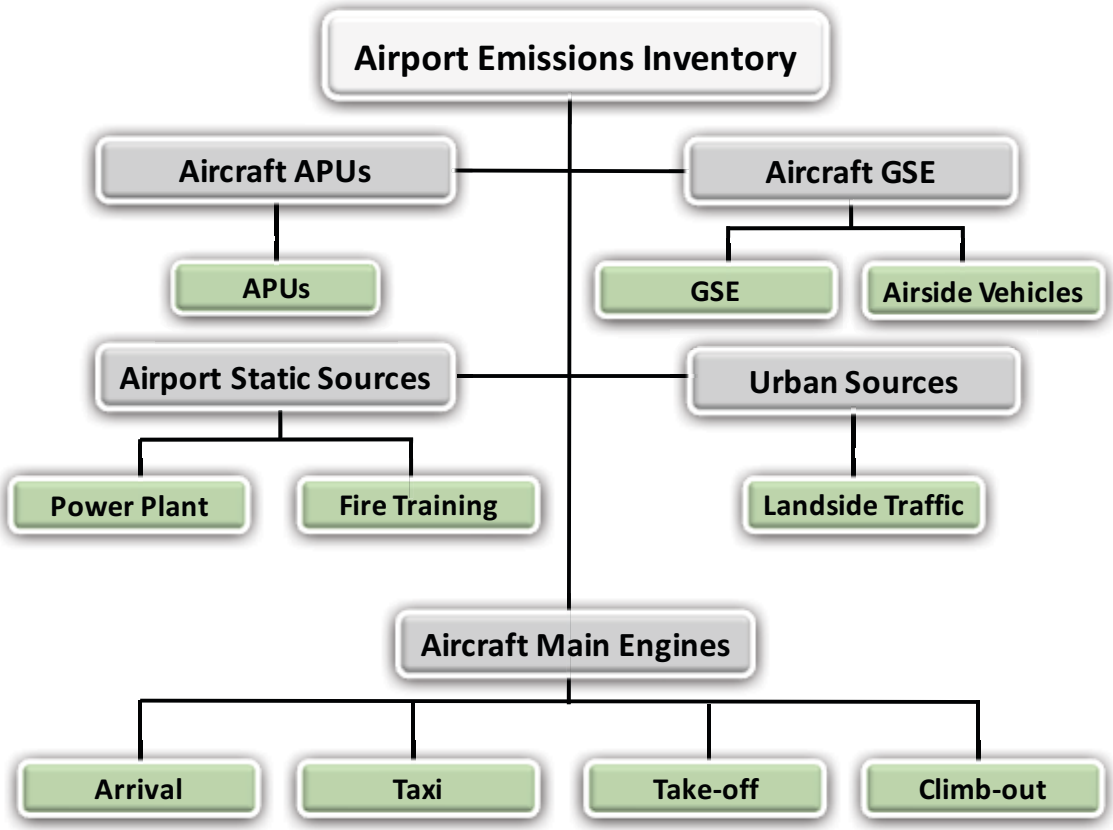

Figure 8-2: Airport emissions inventory plan: Grey boxes represent the main airport emission source categories, and the green boxes represent the different groups entered into EMIT, adapted from CERC (2015).

Table 8-1: Emission inventory parameters used in EMIT

Category	Group (EMIT)	Source Type	EMIT Factors	Source	Parameters required
AIRCRAFT ENGINES	Aircraft main engines -Approach -Landing roll -Taxi-in -Taxi-out -Take-off ***-Climb-out***	***Volume***	***ICAO 17 + Other***	Approach ***(3000 ft-1500 ft)*** ***Approach 1500 ft-touchdown*** ***Landing Roll*** ***Taxi-in*** ***Taxi-out*** ***Take-off*** ***Climb-out***	**Activity Data:** -Aircraft-engine combination (e.g. B777-200 may have different engines installed: 2 × General Electric GE90-90B or 2 × Pratt & Whitney PW4084, or 2 × Rolls Royce Trent 892) - Thrust for each aircraft mode - Annual number of LTO cycles for each aircraft-engine combination (aircraft timetable) -Time-in-mode (TIM) for each mode in a single flight **Physical location** **Spatial Characteristics (volume source):** -Depth and elevation are required. ***-Area is calculated by EMIT from the vertices data***
APU	***APU***	***Volume***	***APU 2004***	***APU***	**Activity Data:** APU type, operation time (annual) **Physical location** **Spatial Characteristics (volume source):** ***Depth and elevation are required. Area is calculated by EMIT from the vertices data.***
GSE	***GSE at stands***	***Volume***	***AIRPORT GSE 2007***	***GSE***	**Activity Data:** **-**Operation time (annual) per type **Physical location** **Spatial Characteristics (volume source):** -Depth and elevation are required. Area is calculated by EMIT from the vertices data.
	Airside Vehicles	***Road***	***EURO SCALED 03***	*Gate 1→7* *Gate 7→16* ***Gate 18→24***	**Activity Data:** Traffic: Cars/hr (motorcycles/light/heavy), hourly speed, **Spatial Parameters**: road width (m), elevation (m), canyon height (m) and gradient **Physical location** (Vertices)
Static Sources	***Power plants***	***Point***	UKEFD07 OR ***Manual***	***Power plants***	**Activity Data:** working hrs, Exit Velocity (m/s), Exhaust gas temperature(°C), molecular weight, specific heat capacity, density **Spatial Characteristics**: stack height (m), stack diameter (m) *Physical Location:* ***Vertices (X, Y)***
Urban Sources	***Landside (Road)*** **Sources:**	***Road***	EURO SCALED 03	***Airport main entrance***	**Activity Data:** Traffic: Cars/hr (motorcycles/light/heavy), hourly speed, **Spatial Parameters**: road width (m), elevation (m), canyon height (m) and gradient **Physical location** (Vertices)

- Aircraft Main Engines

The assessment of aircraft main engine emissions included several types of aircraft modelled as volume sources. There are various approaches or methodologies to quantify aircraft emissions, with varying degrees of accuracy and what determines the choice of approach (basic, medium, and complex) is the availability of information (magnitude and spatial allocation) and the required accuracy of the concentration output (CERC, 2015a). In brief, the basic approach requires basic knowledge with easily available data; the medium approach is more airport specific and requires additional information, whereas the complex approach requires in-depth knowledge (ICAO, 2011).

Despite the absence of any previous database or inventory for Beirut Airport, intensive work was done to conduct the modelling of aircraft engine emissions using the medium approach for the year 2012. To achieve that, the detailed emissions inventory for about 63000 aircraft movements (31620 arriving and 31600 departing aircraft) commercial, cargo, and general aviation) was conducted. These movements included all commercial, cargo, and general aviation flights; however, it was impossible to access information regarding military fleet (2.5 % of the total fleet) due to security reasons. The emissions inventory required detailed parameters like aircraft-engine combination (e.g. B777-200 may have different engines installed: 2 × General Electric GE90-90B or 2 × Pratt & Whitney PW4084, or 2 × Rolls Royce Trent 892), thrust for each aircraft mode, annual number of LTO cycles for each aircraft-engine combination, and time-in-mode (TIM) for each mode in a single flight. Aircraft movements (timetable) for the year 2012 were obtained from the Directorate General of Civil Aviation (DGCA). To obtain the aircraft type and engine model for each and every aircraft, a thorough research was done through visits to all the airline companies at Beirut Airport. Some companies like Middle East Airlines (34% of the total fleet), Kuwait Airlines, British Airways, and Executive Aircraft Services provided the required data. The other fleet information was obtained from pilots and from aircraft type certificate datasheets available online.

For emission calculations, the ICAO 17+ Other dataset installed within EMIT was used along with activity data. For the ICAO data set, main engine emissions are divided into taxi, take-off (ground sources), approach and climb-out (elevated sources). The ICAO 17+ Other dataset provides the mode-specific emission factors for certified engines for NO_x, NO_2, VOCs and others in units of kilogram per min (kg/min), for the four power settings of the engine emissions certification scheme. Multiplying the mode-specific EF by the

TIM yields a mode-specific emission rate in units of grams per LTO for each engine. The calculation of emissions is as follows (CERC, 2015a)

$$\text{Emissions (kg)} = \sum_{i=0}^{n} \text{LTO}_i \times \left[\text{N}_i \times \sum_{j=0}^{3} \text{TIM}_{i,j} \times \text{EF}_{i,j}\right] \quad (8\text{-}1)$$

where i: airframe-engine type

j: aircraft mode (take-off roll, climb-out, approach, taxi-in or out)

n: number of different air frame-engine types (e.g. [A320-200, CFM56-5B4/3, (8CM055)], [Boeing 777-200 series, GE90-94B, (8GE100)], etc.)

$EF_{i,j}$: emission factor for airframe-engine type i in mode j (unit kg/min).

LTO_i: number of landings and take-off cycles of airframe-engine type i

N_i: number of engines installed on an airframe-engine

$TIM_{i,j}$: includes the time an airframe-engine type i spends in each of the four operating modes j (i.e., take-off, climb out, approach, and taxi/idle)

Regarding the spatial references and the real duration of the different modes of the LTO cycle (Annex 8-1), information was obtained from monitoring the aircraft movements through airport visits as well as from pilots, air traffic controllers, and aircraft engineers to obtain representative values. The geographic coordinates for the arrival sources were obtained from pilots and air traffic controllers using real aircraft observations and Standard Instrument Arrival Routes (STARs) that are published procedures followed by aircraft before reaching a destination airport, or Standard instrument departure (SID) routes that are published flight procedures followed by aircraft on an IFR flight plan immediately after take-off from an airport. Aircraft sources used in this study have the same location of emissions for all aircraft types i.e. all aircraft during climb-out are modelled within the same geographical extents although in reality there are differences in the trajectories. This is a simplification, and when modelling an airport more details can be given by assigning different geographical extents to different aircraft types. The depth and elevation (Figure 8-3) used for each mode was adapted from ADMS-Airport Manual for the medium approach and is explained as follows: (i) Take-off and taxi are emissions for the main engines, so the elevation used (1.75 m) represents typical engine heights (ii) the defaults (depth and elevation) for approach were used to represent the descent of aircraft: the first volume source assumes well-mixed emissions between 3000 ft and 1500 ft; and the second

volume source assumes well-mixed emissions between 1500 ft and ground-level. Because approach (elevated source) has a relatively small impact on ground-level concentrations, this relatively simple approach can be used to represent the aircraft.

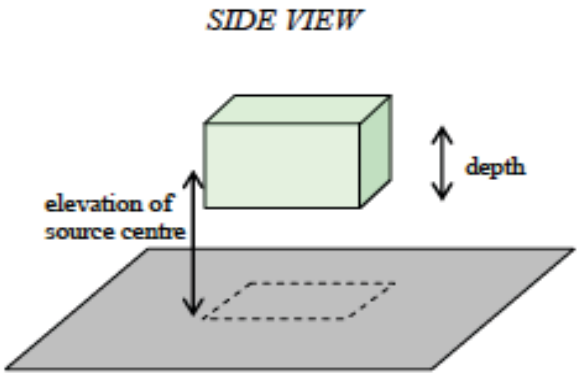

Figure 8-3: Dimensions (depth and elevation) of a volume source as defined by EMIT, taken from (CERC, 2015b)

Auxiliary Power Unit (APU)

APU emissions were also assessed to complement aircraft movements (each aircraft included in the inventory should have an associated APU). These emissions, which take place at the stand prior departure or after landing, were modelled as volume sources. The activity data for APUs (APU type and operation hours) were obtained as follows: (i) An approximate time of 1.5 hr before departure and 1.5 hr after landing was estimated after contacting several airport engineers and pilots; (ii) The APU models were obtained from several companies and by using several references (CERC, 2015b; European Environment Agency, 2009; Unique, 2005). The depth (12 m) and elevation (6 m) were chosen according to ADMS-Airport manual values since APU units, typically located at the back of an aircraft, are located around 6 m above ground-level.

Ground Support Equipment (GSE)

For GSE at the stand, detailed information about the working hours for each GSE type was obtained from the major handling companies like Middle East Airlines Ground Handling (MEAG) responsible for the majority of ground support equipment, Directorate General of Civil Aviation (DGCA) at Beirut Airport, Mideast Aircraft Services Company (MASCO), Middle East Airlines Ground Handling (MEAG), and Middle East Airports Services

(MEAS), Lebanese Air Transport (LAT), Trans Mediterranean Airways (TMA), Executive Air Services, Beirut Wings, and others. This included information about the various types of GSE utilized: baggage belt loader, air climate unit, aircraft tug, baggage cart tractor, cargo loader, cargo loader main deck, catering truck, GPU, refuelling truck, forklift, lavatory truck, narrow body towbarless aircraft tug, passenger stairs, refuelling dispenser truck, refuelling tanker truck, water truck, etc. Since the majority of GSE emissions are from vehicles on the ground, lower values for the depth (2 m) and elevation (1 m) are suggested by CERC. To assess airside vehicles (i.e. road traffic within the airport vicinity), emissions rates were computed using the EMIT datasheet (EUROSCALED 03) with activity data related to traffic (vehicles/hr classified as motorcycles/light/heavy, hourly speed). Due to the lack of any previous assessment, activity data for airside vehicles was obtained by manually counting the vehicles on the airport ramp and classifying them (light or heavy) at low, medium, and high traffic activity during different times of the week.

Fuel Tanks

Airport fuel farm emissions are mainly constituted of VOCs, which result from the evaporation of the fuel stored in the airport tanks (aircraft fuel, GSE fuel, and power plant fuel). Because emissions from fuel tanks are dependent on the type and location of the tanks as well as the ambient temperature, a single set of emission factors are not available for this source type, so are not included in EMIT.

Annual emission rates (tonnes/yr) for VOCs were first calculated using *TANKS* (EPA, 2016), which is a software designed by the US EPA to estimate emissions from organic liquids in storage tanks. *TANKS* allows users to enter specific information about a storage tank which include its dimensions (height and diameter in meters), turnovers/yr, construction, paint condition (roof and shell), roof type, radius, and height; the liquid contents (average and maximum liquid heights (ft), chemical components (chemical category and liquid temperature); and the location of the tank (ambient temperature, etc.), to generate an air emissions report. Report features include estimates of annual emissions for VOCs stored in the tank.

All the parameters required for the 3 kerosene tanks found at Beirut Airport, as well as 20 other tanks (related to generators and GSE) were obtained, and the calculated emissions (kg/yr) were manually entered into EMIT. Upon entering the yearly emission rates and the

spatial allocation of each fuel tank, emission rates for fuel tanks (modelled as area sources) were calculated by EMIT.

Power plants

Airport power plants (19 power plants) were modelled as point sources. Activity data (working hours) was obtained from Middle East Airports Services (MEAS) and Mideast Aircraft Services Company (MASCO). Due to the lack of previous measurements, the power plant stack heights and diameters were manually measured (measuring tape) and their geographic coordinates were taken using a GPS tracking unit.

Landside Traffic (Road Sources)

Emission rates resulting from road traffic at the airport main entrance (landside traffic) were computed using the EMIT datasheet (EUROSCALED 03) with activity data related to traffic, i.e. vehicles/hr (motorcycles/light/heavy) and hourly speed. Spatial Parameters included road width (m), elevation (m), canyon height (m) and gradient, as well as spatial allocation (vertices). Due to the lack of any information about these parameters, the flux of vehicles (count/hr) by vehicle category was determined by manual counting, which took place at the road leading to the airport entrance at different levels of activity (low, medium, high) and repeated several times a week to account for all the traffic variations during the week.

Emission Source Models

All of the above sources were modelled as explicit sources. Once calculated, these emissions were included in ADMS according to several types of groups (volume, area, point, road). In brief, a volume source corresponds to a source where the emissions distributed in a volume, a point source (or industrial point source) represents typically a stack emission, and an area source (or industrial area source) corresponds to an industrial source that is too large to be treated as a point source and is distributed over a large area at ground level (CERC, 2015b).

8.1.2 ADMS-AIRPORT INPUT

Emission sources were exported to ADMS-Airport and the chemistry module was selected.

- Meteorological Data

In the "Site data" section, the latitude entered was 33, corresponding to the location of the meteorological station found near runway 16 in Beirut Airport (Table 8-3). Values used for the surface roughness (0.3 m) and Monin-Obukhov (20 m) were suggested default values used for airports (CERC, 2015a). In the advanced dispersion site screen, default values for surface albedo for a not snow covered site (0.23) and Priestly-Taylor parameter for dry grassland (0.45) was used. In the "Met. Data" section, there are three different types of meteorological data that can be entered (hourly sequential data, series of unrelated meteorological conditions, or statistical data covering a series of years). In this study, modelling was carried out using hourly sequential meteorological data using a *.met* file. These data consisted of: (i) surface wind speed (U, m/s) and direction (PHI, º) and (ii) the Julian day number (TDAY), time of data (THOUR), temperature (TOC, ºC) and cloud cover (CL, oktas). A meteorological pre-processor calculated the boundary layer parameters from these input data (e.g. wind speed, day, time and cloud cover).

The meteorological data used were obtained from actual data at the meteorological station (height = 12.5 m) located on-site at the airport, near runway 16 (Table 8-2). More details about meteorological data are found in ADMS-Airport and ADMS-Urban User Guides. Figure 8-4 shows a wind rose for the year 2012. The wind roses for the 3 validation campaigns were presented in chapter 6.

Table 8-2: Summary of meteorological data at Beirut Airport (2012)

Parameter	**Beirut Airport 2012**		
Height	12.5 m		
Location	Latitude: 33:49 N, Longitude: 35:29 E		
Statistics	Mean	Minimum	Maximum
Temperature (ºC)	21.58	5	36
Wind speed (m/s)	3.26	0	17
Cloud cover (oktas)	3.34	0	9

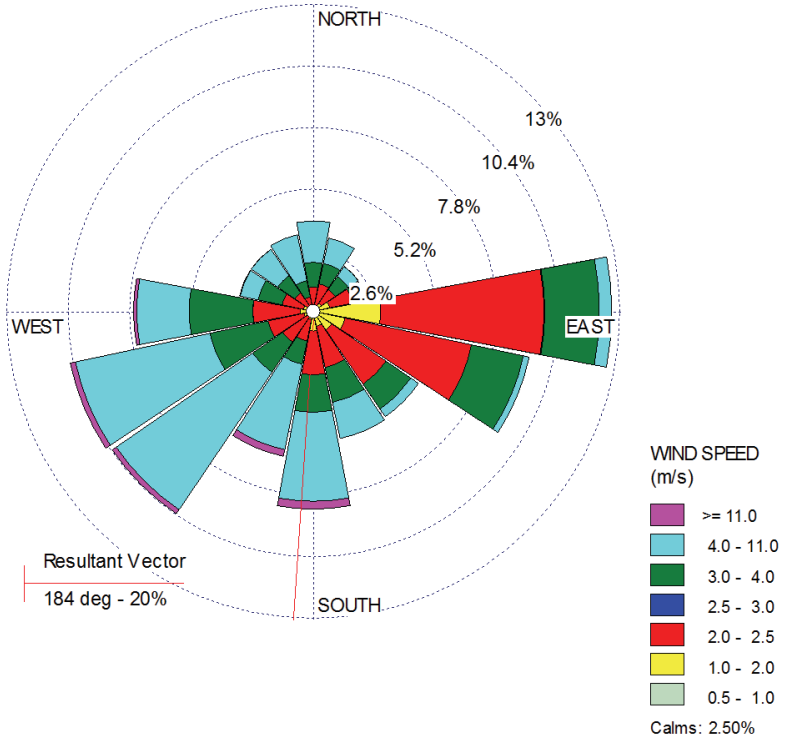

Figure 8-4: Yearly wind rose at Beirut Airport for 2012

Background Concentrations

Background concentrations were obtained from a representative background site (American University of Beirut (AUB)), located a few kilometers upwind north of the airport. Representative background concentrations are normally added to the model predicted concentrations (FAA, 2014). It is important to note that the background values (38 µg m^{-3} for 2012) are near the WHO limits themselves. The background ambient concentrations used for ozone was 30 ppb. For the validation campaigns, background concentrations were measured using passive samplers during each campaign.

Output parameters

Gridded output with regular spacing was used with a resolution of 45 and 138 m along the x-axis and y-axis respectively for modelling at the airport scale, and a resolution of 171 and 233 m along the x-axis and y-axis respectively for modelling at the regional scale. The total height selected was 2 m (z = 2 m) corresponding to the breathing zone and the approximate sampling heights of NO_2 measured during the validation campaigns (see

chapter 5, section 3). The "long term" average with an averaging time of 1 h and output units in μg m^{-3} were selected.

8.2 Emissions Inventory (EMIT Output)

The emission rates calculated by EMIT are presented in Table 8-3, and the source models are viewed in 3-D using ArcGlobe (Figure 8-5). EMIT first calculates the emission rates in tonnes/yr and then converts them to units of $g/m^2/s$ (area source) or $g/m^3/s$ (volume source) by dividing the emission rates in tonnes/yr by the product of the total volume or area with the total time. It is these converted emission rates which are used in ADMS-Airport dispersion modelling equations.

Figure 8-5 depicts the different types of source models used. All the aircraft sources, including APU, were modelled as volume sources. GSE was modelled both as a volume source (GSE at the stand) and a road source (airside vehicles). It is important to note that the GSE at the stand and APU are both located at the gates at the center of the airport, which leads to the increase in the estimated emissions at this location, as will be seen later in the model results.

Figure 8-6 shows the estimated annual airport-related NO_2 and VOC emissions (tonnes/yr) as a function of major source category. The estimated total NO_2 and VOC emissions for the year 2012 are 50.7 and 32 tonnes respectively. Aircraft emissions (APU and LTO cycle) dominate the airport emissions for both NO_2 (92%) and VOCs (68%). Aircraft emissions during the LTO cycle (37.4 tonnes/yr) make the dominant contribution to airport NO_2 emissions, followed by APU (9.3 tonnes/yr), GSE (3.7 tonnes/yr), whereas stationary and road sources are minor contributors. For VOCs, the major source is also the LTO cycle (11.5 tonnes) with levels very close to APU emissions (10.3 tonnes). Actually, this high contribution of APU emissions is not surprising due to the long operating time of APUs at Beirut Airport (can reach up to 3 hr per aircraft) leading to a huge amount of emissions in the zone of the gates. The estimated VOC emissions from GSE are 5.5 tonnes, followed by stationary sources (3.8 tonnes). In fact, the major contributors to these stationary source emissions are fuel tanks (99.7%), especially the 3 kerosene fuel tanks located at the eastern part of the airport.

Table 8-3: EMIT Emission rates calculated for Beirut Airport inventory (2012)

	NO_2		VOCs	
Volume Sources	$g/m^3/s$	tonnes/yr	$g/m^3/s$	tonnes/yr
Approach 3000 - 1500 ft	4.70×10^{-10}	5.53	3.32×10^{-11}	0.39
Approach 1500 - 0 ft	5.01×10^{-10}	5.53	3.57×10^{-11}	0.39
Landing Roll	8.81×10^{-8}	1.33	6.27×10^{-9}	0.09
Climb-out	1.15×10^{-9}	10.95	4.17×10^{-11}	0.40
GSE	3.90×10^{-7}	3.7	5.59×10^{-7}	5.22
Take-off	3.53×10^{-7}	5.09	1.16×10^{-8}	0.17
taxi in (1)	3.73×10^{-7}	0.90	4.14×10^{-7}	1.00
taxi in (2)	6.69×10^{-7}	0.90	7.43×10^{-7}	1.00
taxi in (3)	1.02×10^{-6}	0.90	1.13×10^{-6}	1.00
taxi in (4)	5.81×10^{-7}	0.90	6.45×10^{-7}	1.00
Taxi-in	**$3.73 - 10.2 \times 10^{-7}$**	**3.61**	**$4.14 - 11.3 \times 10^{-7}$**	**4.01**
Taxi out (1)	1.13×10^{-6}	0.90	1.26×10^{-6}	1.00
Taxi out (2)	2.86×10^{-7}	1.80	3.19×10^{-7}	2.01
Taxi out (3)	9.94×10^{-7}	0.90	1.11×10^{-6}	1.00
Taxi out (4)	8.16×10^{-7}	0.90	9.08×10^{-7}	1.00
Taxi out (5)	1.67×10^{-6}	0.90	1.86×10^{-6}	1.00
Taxi-out	**$2.86 - 16.7 \times 10^{-7}$**	**5.41**	**$3.19 - 12.6 \times 10^{-7}$**	**6.03**
APU	1.21×10^{-7}	9.29	3.45×10^{-8}	2.65
Area Sources	**$g/m^2/s$**	**tonnes/yr**	**$g/m^2/s$**	**tonnes/yr**
Fuel Tank	0.00	0.00	$0.035 – 3990 \times 10^{-5}$	3.79
Point Sources (g/s)	**g/s**	**tonnes/yr**	**g/s**	**tonnes/yr**
Generators (g/s)	$8.56 – 646 \times 10^{-6}$	0.11	$0.014 - 1.11 \times 10^{-6}$	0.02
Road Sources (g/km/s)	**g/km/s**	**tonnes/yr**	**g/km/s**	**tonnes/yr**
Main Entrance	0.01	0.15	0.07	0.95
Airside Vehicles (GSE)	0.0015 - 0.0017	0.05	0.007 - 0.008	0.25

Aircraft NO_2 and VOC emissions are broken down further into emissions by flight phase. It is important to differentiate between ground level emissions and elevated emissions associated with aircraft where the former have the biggest impact on local air quality, whereas the latter have less impact as they take place at increasing heights. Aircraft ground NO_2 emissions (Landing roll, taxi-in, taxi-out, take-off) were approximately 15.45 tonnes in 2012 constituting 41% of total aircraft engine emissions, whereas the corresponding VOC emissions were estimated to be 10.29 tones constituting up to 90%. The proportion

of NO_2 and VOC emissions from the different modes of the LTO cycle are summarized in Figure 8-7.

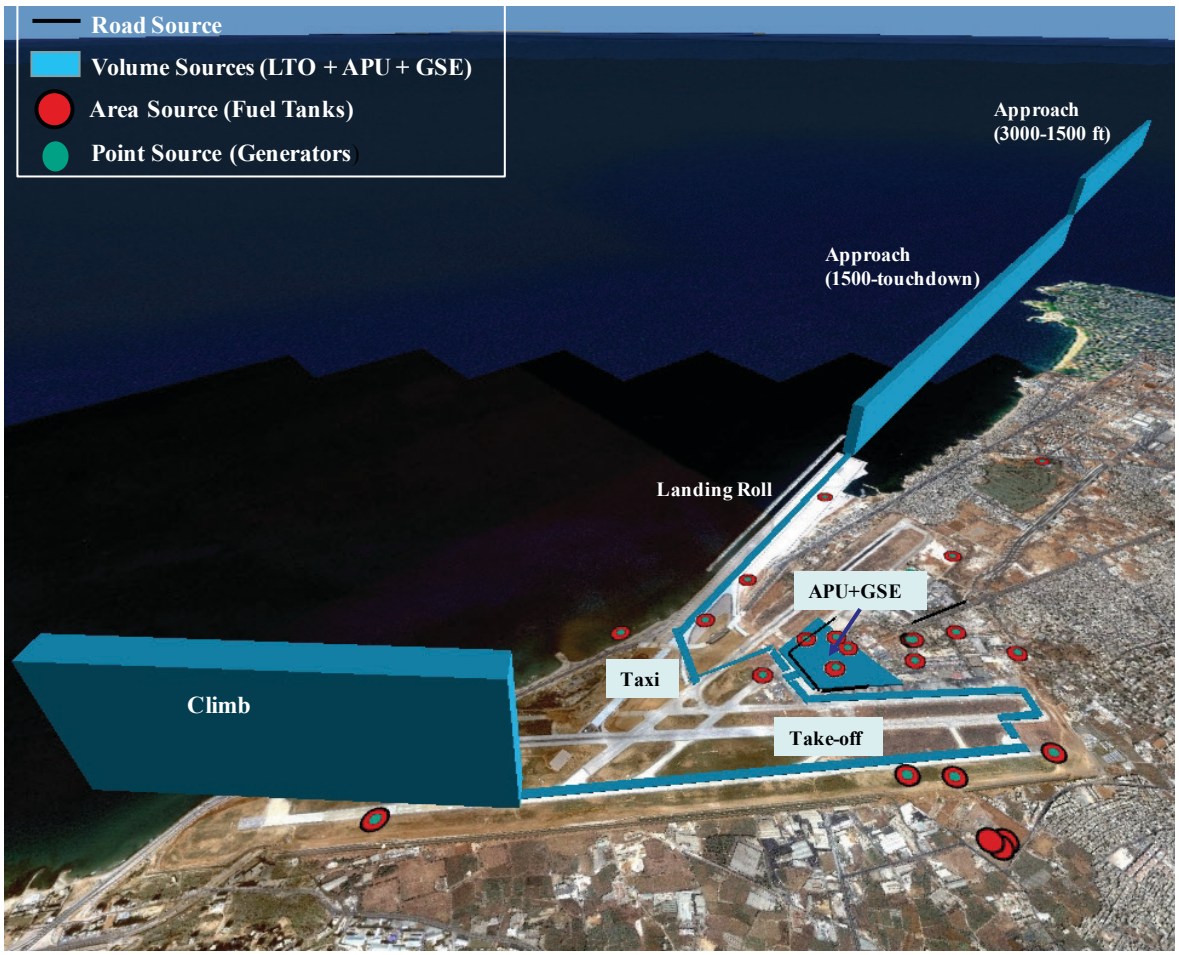

Figure 8-5: 3-D geospatial emissions inventory created by exporting EMIT database to Arc Globe for the sources modelled at Beirut Airport in this study (2012)

The 2 major contributors for NO_2 emissions are the climb and approach phases each contributing to 11 tons per year. In fact, the emission rate per second for the climb phase (1.15×10^{-9} g/m^3/s) is greater than the approach phase ($4.7 – 5 \times 10^{-10}$ g/m^3/s), but the total volume for the approach phase led to equal emissions in tonnes per year. This is significant because this highlights the fact that the climb phase has a higher impact on the concentrations generated by the dispersion modelling. Although the total duration for the take-off phase is 0.7 min, it contributes by 1.3 tonnes/yr to the total NO_2 emissions (14% of the total LTO) with an emission rate of 3.53×10^{-7} g/m^3/s. This is due to the fact that at high speed the temperature within the combustion chamber is higher, which leads directly to the increase in the emission of nitrogen oxides (Dagaut and Cathonnet, 2006; Penner, 1999).

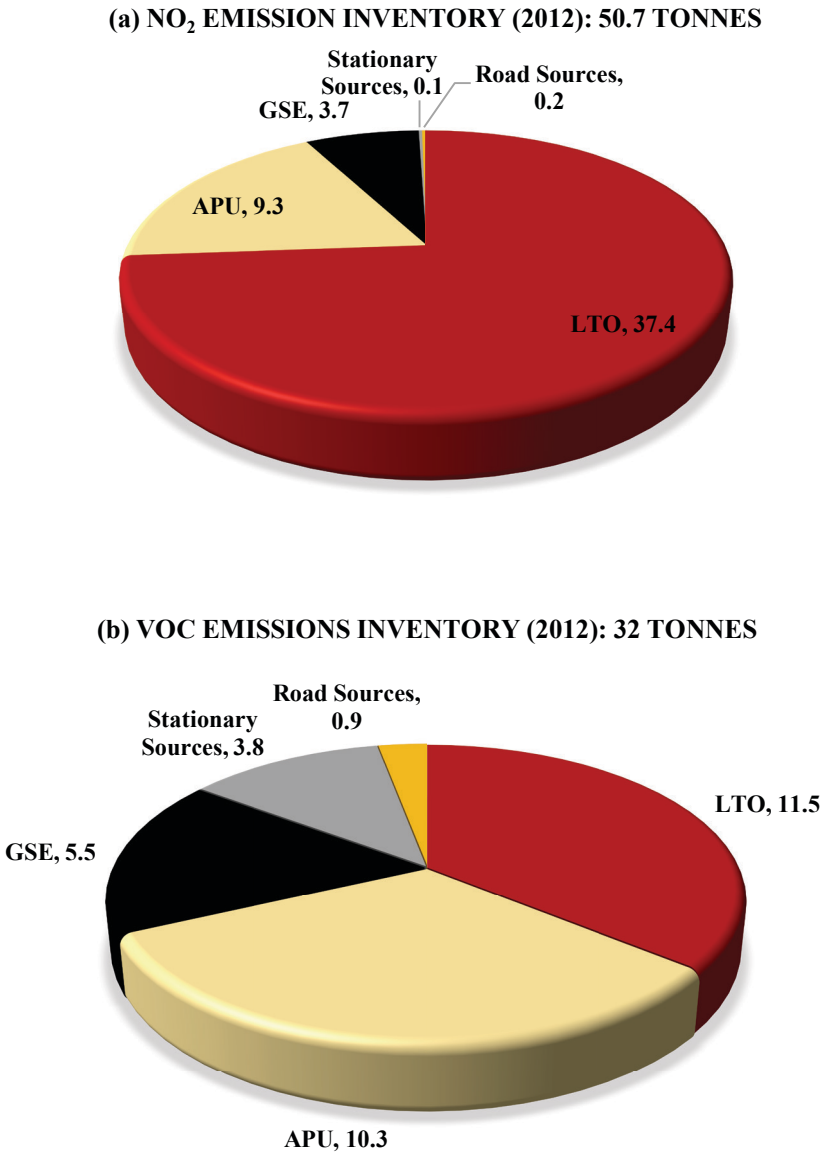

Figure 8-6: Estimated ground level airport-related emissions (tonnes) from Beirut Airport in 2012 (a) NO_2 (b) VOCs

On the other hand, the taxi phase dominates the VOC emission sources with a contribution of 10 tonnes per year or 88% of the LTO cycle contribution. This is followed by the arrival (7%), climb (3%), and take-off (1%). This result is expected as the emission factors for the taxi phase are the highest and that of the take-off phase is the lowest. VOC emissions are higher at low power settings when the temperature of the air is relatively low and the fuel atomization and mixing process is least efficient. This is also according to ICAO databank sheets for unburned hydrocarbons (UHC) for all modern turbine engines; all engines produce less CO and NMHC emission per kg of fuel burned as their power levels are increased above idle (Anderson *et al.*, 2006).

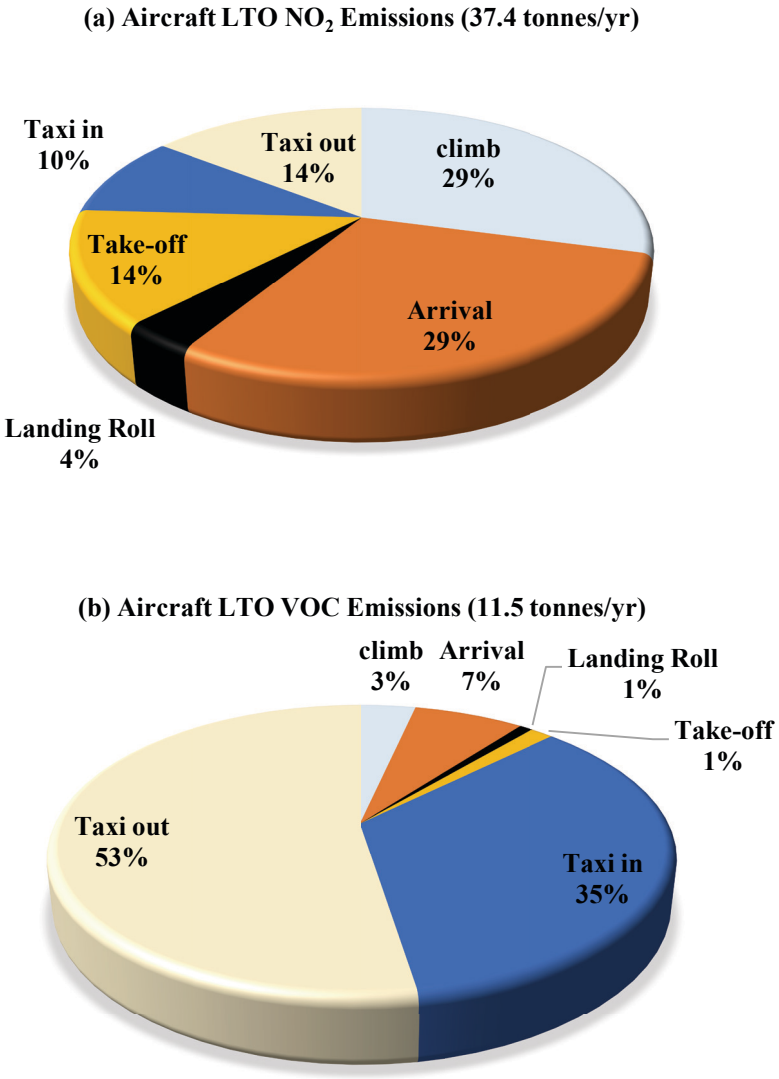

Figure 8-7: Estimated ground-level LTO emissions from aircraft at Beirut Airport in 2012 (% by flight phase) (a) NO_2 (b) VOCs

Chapter 9 : SPATIALIZATION OF EMISSIONS

ADMS-Airport produced the majority of its numerical output in comma separated variable text file format, viewed in a spreadsheet package such as Microsoft Excel or in Windows Notepad. ADMS-Airport also produced contour plots of pollutant concentrations overlaid onto digital map data within ArcGIS 10.1 (ESRI, Redlands CA).

9.1 Model Validation

ADMS dispersion models in general, and ADMS-Airport in specific have been continually validated against available measured pollutant concentration data obtained from real world situation field campaigns (Carruthers, 2006; Carruthers *et al.*, 2011, 2008). Studies show that there is no significant trend to over or under-prediction by ADMS-Airport. ADMS-Airport has been used to model air quality at London's Heathrow airport for the 2002 base case and future year scenarios as part of the Department for Transport's (DfT) Project for Sustainable Development of Heathrow (PSDH)-Adding capacity at Heathrow. The correlation coefficients of annual average model predictions (calculated from hourly time series) of NO_x and NO_2, compared with annual average measured data from 9 automatic monitoring sites, were 0.61 and 0.68 respectively. By comparing the ADMS model predictions against ambient monitoring data, it is not just the model performance that determines the comparison but also the accuracy of the model inputs (spatial and quantitative source data, meteorological data, and background data, model inputs).

Table 9-1 compares monitored and modelled weekly average NO_2 calculated from the hourly time series of concentrations. Measurements were taken by passive methods and the duration of one week was chosen for model validation. More information about the measurement methodology and the average concentrations measured were presented in chapters 4-6. In this study, the (Pearson) correlation coefficient of hourly NO_2 model predictions compared with hourly measured data from 7 sites was 0.86 (Figure 9-1), excluding the site "gate 12" considered as an outlier. According to Evans' (1996) proposed classifications for interpreting correlation strength, 0.85 is considered a "very strong" correlation (Kowang *et al.*, 2015). (Note that the correlation coefficient is 0.7 if the site "gate 12" is included, which is also considered a "strong" correlation). The reason for this

over estimation at gate 12 might be related to the model input or to the modelling of the 3 overlaying sources at this location (APU, GSE on the stand, and airside vehicles). In a study conducted by Peace *et al.* (2006) using ADMS-Urban at Manchester Airport, an overestimation was also observed at the monitoring site near the airport.

Table 9-1: Comparison of measured (µg m^{-3}) and monitored (µg m^{-3}) NO_2 concentrations at 8 measurement sites

	May 16, 23-2015		June 04-11, 2015		June 11-18, 2015	
	Modelled	Measured	Modelled	Measured	Modelled	Measured
Site						
Approach	50.1	42.3	35.0	21.9	31.9	18.6
Ozaii	52.4	47.3	40.8	22.6	36.6	21.9
Taxi	54.2	53.0	42.4	26.4	35.4	26.1
Gate 12	94.3	72.4	96.2	49.2	85.0	49.0
Takeoff (1)	61.3	77.1	46.3	47.2	42.0	45.8
Takeoff (2)	64.3	57.2	49.8	42.1	37.5	31.3
Takeoff (3)	62.2	54.5	53.7	34.9	43.9	28.4
Cargo	61.9	58.0	53.6	42.9	52.6	31.5

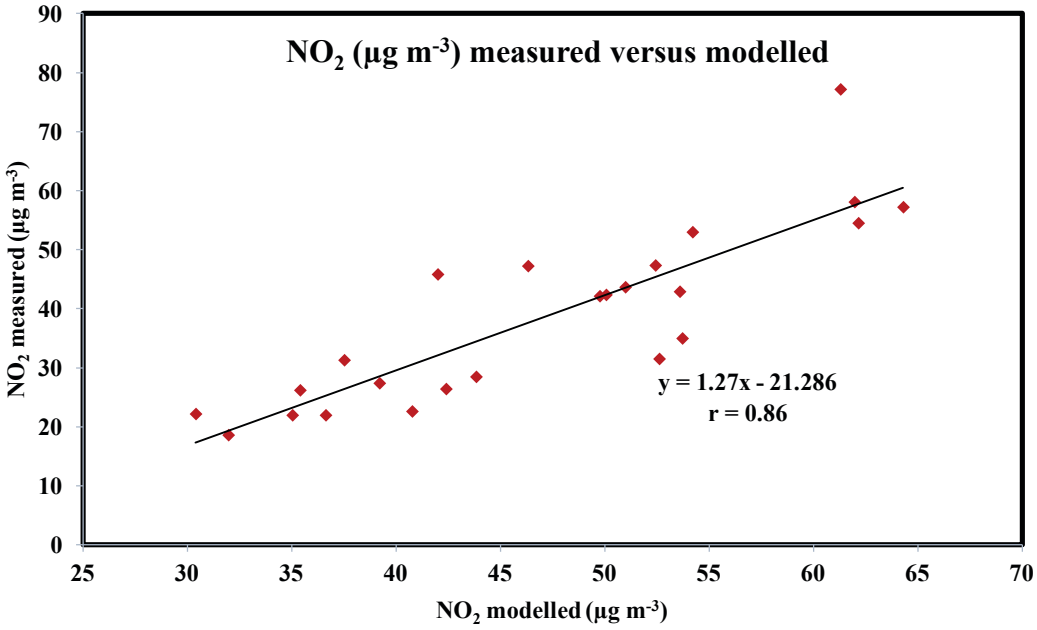

Figure 9-1: Scatter plot of measured (passive samplers) versus modelled NO_2 concentrations (µg m^{-3}) using ADMS-Airport
*Excluding the site "gate 12" which is an outlier

The model response for variations of background NO_x and NO_2 concentrations have been investigated. Several simulations were made by increasing the background values of NO_x and NO_2 consecutively by 20% and 30% while keeping the other fixed. Output concentrations have been calculated at a receptor point positioned behind the take-off runway at a height of 2 m (the "take-off" site, see chapter 6). Results have shown that an increase in NO_x background concentrations by 20 and 30% lead to an increase in NO_2 concentrations at the take-off point by 7 and 11% respectively. On the other hand, an increase in NO_2 background concentrations by 20 and 30% lead to an increase in NO_2 concentrations by 9 and 13% respectively.

Because the model has been verified and adjusted as necessary, there can be reasonable confidence in its simulation of 2012 concentrations, as follows.

9.2 The Impact of Beirut Airport on Air Quality (year 2012)

9.2.1 AIRPORT VICINITY

Figure 9-2 shows contour plots of the estimated NO_2 concentrations ($\mu g\ m^{-3}$) in the vicinity of Beirut Airport affected by aircraft and other airport sources for the year 2012. Results show that NO_2 in the airport vicinity exceeds the World Health Organization (WHO) threshold limit (40 $\mu g\ m^{-3}$). As expected, NO_2 concentrations are highest at the center of the airport near the gates (up to 111 $\mu g\ m^{-3}$) and near the take-off runway (up to 90 $\mu g\ m^{-3}$) where the combustion is maximal. These extremely high concentration levels near the gates (contribution from APU, GSE at the stand, and airside vehicles) have hazardous impacts on the airport employees who spend at least 12 working hours in this area and who suffer from pulmonary diseases as previously reported by Yaman (2008). These observations are consistent with previous observations by Peace *et al.* (2006) which have provided evidence that the highest concentrations occurred close to the stands where planes are idling at Manchester Airport.

Figure 9-3 presents a contour plot of VOC emissions within the airport vicinity. It is important to note that background total VOC measurements were not available, especially that the exact VOCs used in EMIT activity datasheets were not specified. Thus, modelled VOC concentrations represent those emitted from airport sources only rather than the total measured concentrations. The maximum VOC concentrations are emitted by the kerosene fuel tanks reaching up to 87.9 $\mu g\ m^{-3}$. The center of the airport at the gates also has high

VOC levels (reaching up to 40 µg m^{-3}). Also, taxiways show high VOC concentrations, which is not surprising as the taxi operations have been reported to produce the highest amounts of VOC emissions among the other aircraft operations as a result of incomplete combustion at low thrust settings (Anderson *et al.*, 2006). On the other hand, VOC levels near the runways, corresponding to emissions from the climb and approach modes, show minimal VOC concentrations with respect to the other airport sources. In general, VOC concentrations decrease away from the center of the airport to range between 0.02 and 2.0 µg m^{-3}.

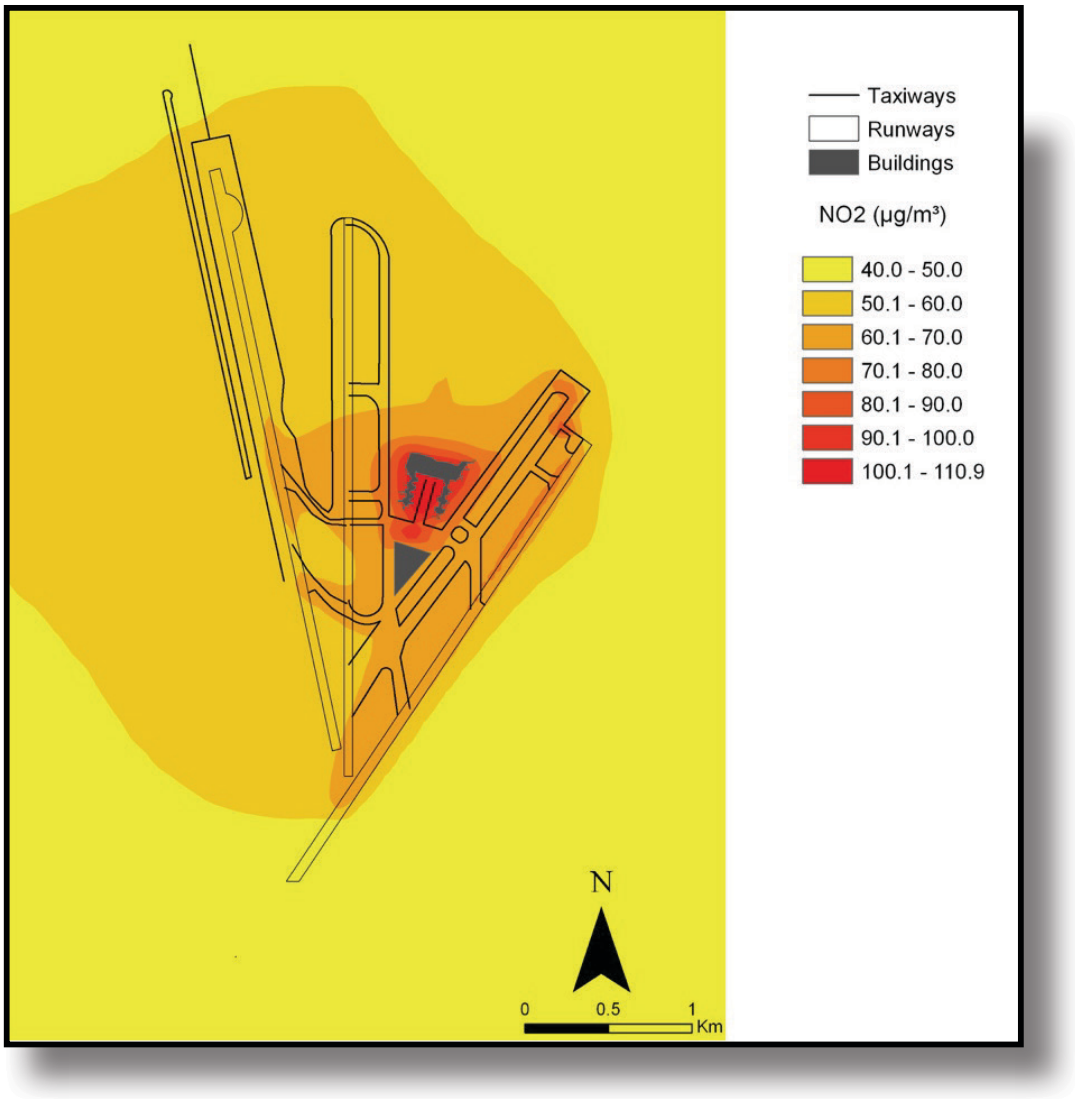

Figure 9-2: Contour plot of modelled total NO_2 concentrations (µg m^{-3}) around Beirut Airport (2012) (z = 2 m)

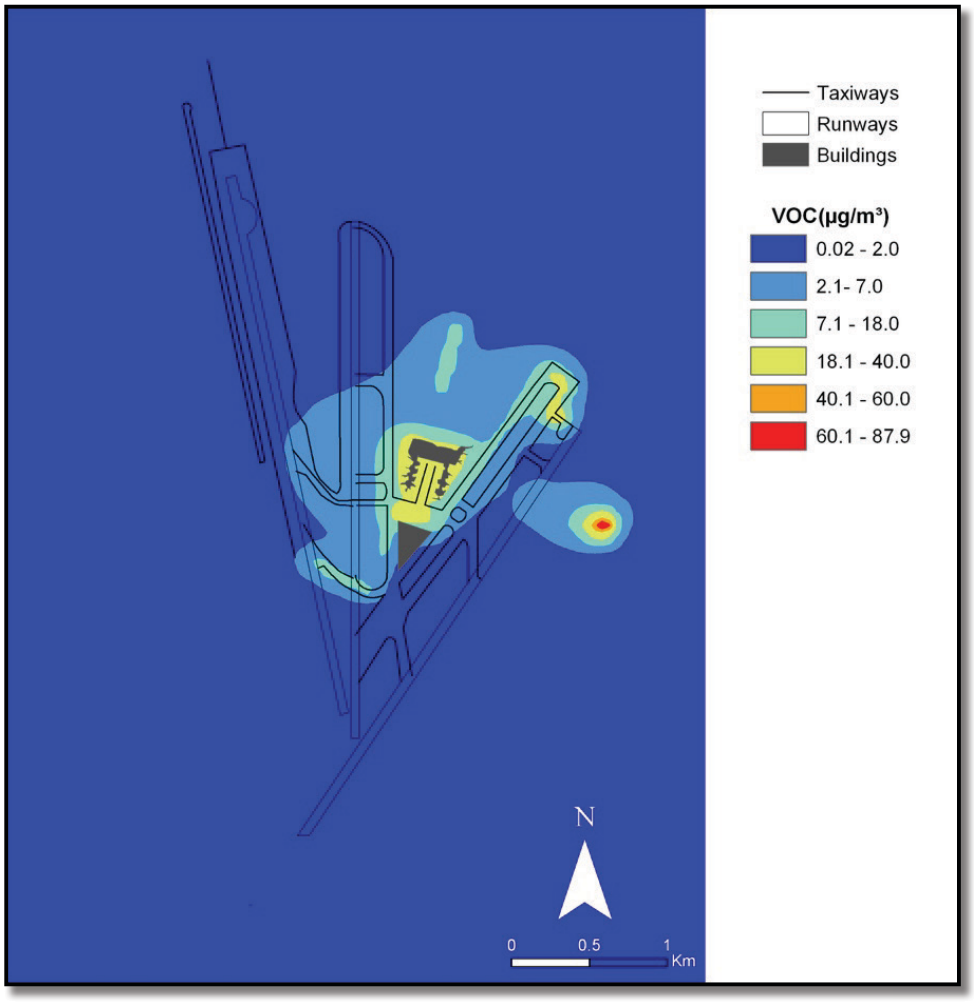

Figure 9-3: Contour plot of modelled total VOC concentrations (µg m^{-3}) around Beirut Airport (2012) (z = 2 m)

9.2.2 IMPACT ON BEIRUT AND ITS SUBURBS

Figure 9-4 shows the average NO_2 concentrations in Beirut and its suburbs, taking into account only emissions from Beirut Airport activities. As shown, the mean value of NO_2 in Beirut and its suburbs exceeds the World Health Organization (WHO) threshold limit (40 µg m^{-3}). NO_2 levels are maximum in the airport vicinity (95 µg m^{-3}) and decrease away from the airport ranging between 40 and 50 µg m^{-3} in Beirut. Our observations are consistent with previous studies (Adamkiewicz *et al.*, 2010; Westerdahl *et al.*, 2008) that have provided evidence of the near-airport influence of airport activities on NO_2 concentrations. In Beirut, concentration levels are above the background value set in the model, which confirms that Beirut Airport activities have an impact on the air quality of Beirut and its suburbs (up to ca. 8 km away from the airport). The area located to the south and southeast of the airport is less affected by the airport emissions, with NO_2 levels

ranging between 39 and 40 µg m^{-3}, similar to the background levels. Carslaw *et al.* (2006) estimated the upper limit of the airport contribution to be less than 15% (<10 µg m^{-3}) at background locations 2–3 km downwind of London Heathrow (LHR) airport. In fact, within 2-3 km the contribution of Beirut Airport (difference between estimated and background NO_2 levels) does not exceed 20% of the total concentration.

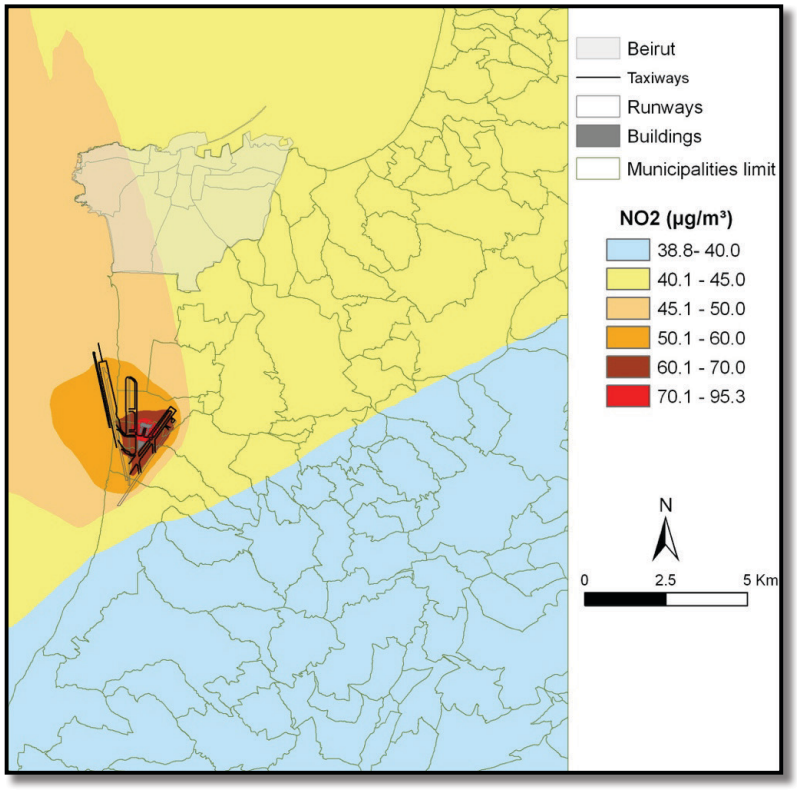

Figure 9-4: Contour plot showing the annual average NO_2 concentrations (µg m^{-3}) predicted by ADMS-Airport for 2012 (z = 2 m)

Another significant observation is that the western part of Beirut, along the seashore, has higher mean NO_2 concentrations (45-50 µg m^{-3}) than the eastern part. This result is not surprising because aircraft overfly the seashore during the approach phase before landing on runways 16 or 17, located at the seashore. It is important to note that the background values (38 µg m^{-3} for 2012) in Beirut are near the WHO limits themselves and the effects of the airport's contribution to the air quality of Beirut are minimal by comparison.

Figures 9-5 presents contour plots of VOC concentrations resulting from Beirut Airport activities. In fact, the impact of the airport activities on air quality is mainly localized in the airport vicinity (1-23 µg m^{-3}) within 0.5 km from the airport boundary, and it decreases away from the airport to range between 0.003 and 1 µg m^{-3} in Beirut.

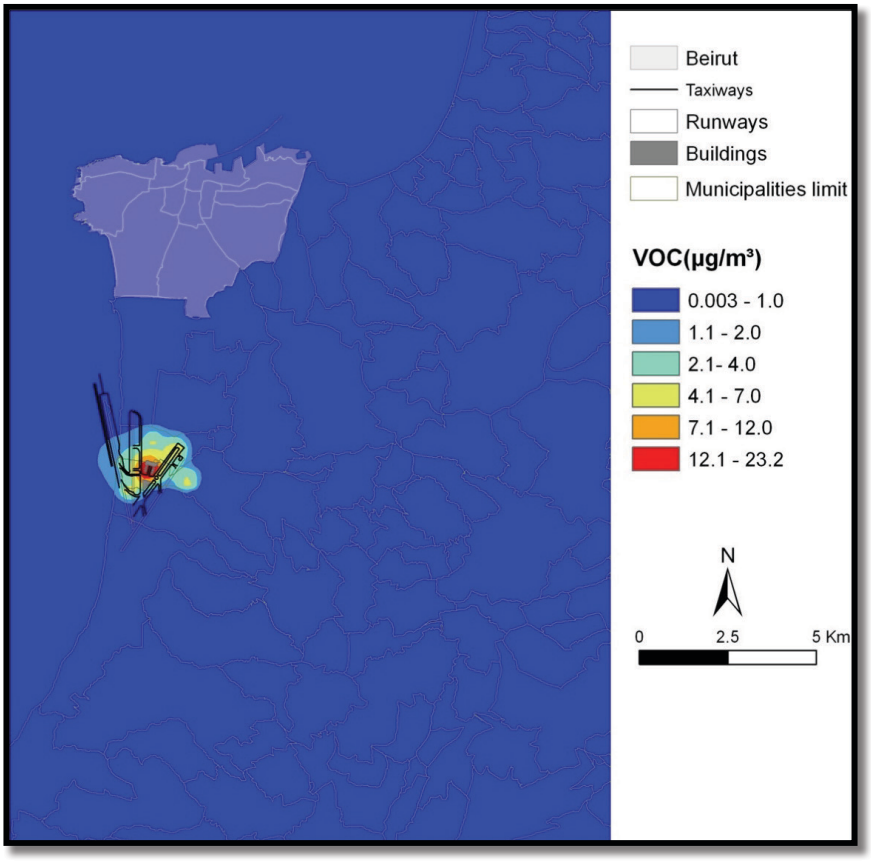

Figure 9-5: Contour plot of Beirut showing the annual average VOC concentrations (µg m^{-3}) predicted by ADMS-Airport for 2012 (z = 2 m)

Conclusion

This study is the first attempt to model the impact of Beirut Airport activities on air quality using a European model. In fact, it is the first study in the Middle East region to model airport emissions using an advanced dispersion model, after conducting the first emission inventory for Beirut Airport. The model results have been compared against measured data located within the airport, which provides a degree of confidence in the results. The use of an up-to-date and comprehensive emission inventory together with an advanced dispersion model has minimized the uncertainties. Modelling (undertaken for a base year of 2012) has shown that the airport activities impact the air quality of Beirut and its suburbs mostly in the vicinity, and to a lesser extent up to 8 km away reaching Beirut. Similar to the experimental findings (chapter 6, section 2), results also confirmed the impact of jet landing emissions on the seashore areas. Future work will involve a sophisticated level of modelling.

Conclusion and Future Work

The main aim of this thesis was to identify the impact of Beirut airport activities on the air quality of Beirut and its suburbs. Both approaches, experimental and modelling, provided pathways to achieve the goal of the thesis. The second aim, indoor measurement, has also shown an interesting relationship between aircraft activity and indoor concentrations as well as very high NO_2 concentrations in the arrivals hall.

Main Findings

Signature Campaigns and Transect Campaigns

The experimental approach used was based on the identification of unique markers and fingerprints related to aircraft exhaust emissions. This was achieved by conducting several measurements of aircraft exhaust under real operation, thereby sampling more than 100 aircraft plumes. This is the first study which identifies aircraft tracers based on real measurements. Results showed that heavy alkanes and aldehydes are the major contributors to VOC emissions from aircraft and appear as the most suitable tracers for distinguishing emissions from aircraft in relation to gasoline exhaust. The contribution of n-octane to n-tridecane was about 57 to 65% of the total mass of heavy VOCs emitted by aircraft. Heavy aldehydes (nonanal and decanal), although to a lesser amount, can also be considered as aircraft related. On the other hand, the total concentration of heavy alkanes in the airport's ambient air was 48% of the total mass of heavy VOCs measured.

Upon assessing the total VOC speciation from aircraft exhaust, the most abundant VOC family was aldehydes/ketones. This family contains VOCs classified as Hazardous Air Pollutants (HAPs) by US EPA. After identifying aircraft tracers and fingerprints, the impact of the airport activities has been assessed in preliminary transect campaigns. These campaigns covered several locations, both in the vicinity and away from the airport. Results of these campaigns were remarkable. It was observed that the airport's impact is concentrated on the vicinity due to ground airport and aircraft operations. This was in conformity with previous studies. The more interesting observations were the effect of aircraft exhaust on the seashore area as a result of emissions during the approach phase.

Speaking about this, a recent study concluded that areas affected by aircraft exhaust might have been underestimated, reporting high $PM_{2.5}$ levels emitted from jets in the approach path to Los Angeles International Airport (LAX) (Hudda *et al.*, 2014). Also, the other interesting observation is the appearance of aircraft fingerprints in the mountainous areas (e.g. USJ Mansourieh) which triggers many questions regarding the complex interaction between dispersion, wind, and topography which characterizes our study area.

Modelling with ADMS-Airport

ADMS-Airport, one of the 4 dispersion models approved by ICAO, was applied for the first time in the Middle East region in this study using the intermediate approach. This model required a very detailed emissions inventory (EMIT) taking into account operational details for around 63000 aircraft movements for the year 2012, as well as detailed parameters for most of the airport's emission sources. This required a very exhaustive work due to the absence of any previous database for aircraft nor for road traffic near the airport. Most importantly, ADMS-Airport has been validated in the Lebanese context with a correlation coefficient (r) equals to 0.86. Upon gaining confidence through model validation, ADMS, which is an advanced European model, was utilized to assess emissions in the Lebanese area. The emissions for the year 2012 were modelled and results were used to map the spatial variability of NO_2 and VOCs for our study area. Results showed that modelled NO_2 concentrations varied between 38 $\mu g\ m^{-3}$ and 110 $\mu g\ m^{-3}$. These first results allow us to say that Beirut airport contributes to the degradation of air quality not only in its vicinity, but also to that of the Lebanese capital located north of the airport. Highest values were found in the center of the airport (110 $\mu g\ m^{-3}$) and in the urbanized area in the immediate vicinity of the airport (reaching 90 $\mu g\ m^{-3}$). These concentrations decrease gradually away from the airport. Due to wind effects, areas located south of Beirut Airport are minimally affected. An interesting observation was, and which particularly concerns the capital Beirut, that the western part of Beirut seems more affected by pollution from the airport activities. This is explained by aircraft emissions during the landing trajectory over the seashore areas in the western part of Beirut.

Thus, we can say that the measurements and modelling overlapped. Both indicated that the airport impacts air quality in the vicinity and impacts Beirut, to a lesser extent. More importantly, both confirmed that the seashore area is affected by aircraft emissions during the approach phase.

Indoor Measurements

Finally, some of this research has been dedicated to airport indoor pollution. Indoor measurements in this study are the first measurements to assess 47 VOCs inside airports, and basically the first to assess indoor VOCs in Lebanon. This aspect seemed important to identify the pollutants to which employees are exposed daily for 12 to 24 hours a day. Measurements took place inside the maintenance office and at the arrivals hall. In the arrivals hall, measurements showed the presence of heavy alkanes. Under normal conditions of ventilation, concentrations of heavy alkanes ranged from 1 (corresponding to minimum aviation activities) to 52 $\mu g\ m^{-3}$ (rush hour). In an exceptional incident, the percentage of air pumped from the outside (typically set at 20%) was increased to 50%, which lead to the drastic rise of the concentration of heavy alkanes up to an average of 407 $\mu g\ m^{-3}$. This relates to the presence of a direct opening between the apron and the arrivals hall, which renders the arrivals hall directly affected by aircraft emissions. These observations are further evidence that heavy alkanes are special aircraft related emissions. The NO_2 concentration in the arrivals hall varied between 36 and 48 $\mu g\ m^{-3}$ which can signal an alert that the annual mean levels might be close or above the WHO annual guidelines affecting therefore the health of passengers and employees. These high nitrogen dioxide values are probably the reason why airport employees suffer from pulmonary diseases (Yaman, 2001). Moreover, they are mainly the result of the extremely high nitrogen dioxide values in the apron reaching up to 110 $\mu g\ m^{-3}$ as modelled by ADMS for the year 2012 (chapter 9) or measured during the validation campaigns (see chapter 6, section 3).

In brief, all these observations further prove the impact of the airport's activities not only on local air quality, but also on indoor air quality.

Novelty

The novelty of this multidisciplinary thesis (knowledge in the geographical, chemical, and aviation disciplines) lies in several aspects. In fact, it is the first study to assess 50 VOCs from aircraft exhaust emissions during real aircraft operations at different phases of the LTO cycle to identify specific aircraft tracers and fingerprint emissions. Also, it is the first study to track the airport's impact up to 8 km away by measuring 50 VOCs and to prove the impact of landing emissions on air quality. Furthermore, contrary to previous results,

which did not emphasize the impact on airport indoor air, it is the first study to assess 47 VOCs inside an airport building, at different locations, and identify a direct relationship between aircraft number (airport activities) and indoor air.

At the regional level (Middle East), it is the first study to utilize an advanced European model to assess airport emissions in a country with no data.

At the local level (Lebanon), this is the first study to assess VOCs at different locations within and outside Beirut. In addition to this, this the first indoor study in Lebanon to assess VOC concentrations.

Significance and Implications

This study provided an experimental methodology to assess the spatial extent of the impact of an airport's activities on air quality based on tracking specific aircraft tracers (heavy alkanes and heavy aldehydes) which were also identified for the first time in this research. Moreover, the identification of the total fingerprint emissions based on "real data measurements" can provide "real" data for emission factors to be later used in modelling. The identification of the aircraft's impact on the air quality of areas along the landing trajectory of aircraft can hint that similar observations can exist in other countries with a similar situation, and that the impact of airport emissions is not mainly localized in the airport's vicinity. In addition, this research has provided the first emissions inventory for Beirut Airport, which can be utilized in future assessments. After validating ADMS-Airport, such assessments can be used by policy makers in the simulation of mitigation strategies (green taxi, reduction of APU operation hours at RHIA, etc.) and the assessment of health impacts. Finally, this study provided a proof for the impact of outdoor aircraft activities on airport indoor air in RHIA, which can be minimized by providing a barrier between the arrivals hall and the airport's apron.

Study Limitations

Due to the lack of availability of several active samplers in Beirut, it was not possible to take signature samples simultaneously from all the sites. However, we took all the signature samples within one week to limit the and minimize the interference of weather and meteorological parameters. Similarly, for the summer active transect campaign, all the samples were taken within 1 week and during almost the same time interval (13:00-14:30)

corresponding to the rush arrivals traffic in Beirut Airport in order to minimize the difference in the airport's emissions. As for indoor measurements, the comparison between outdoor and indoor VOC levels was based on measurements taken during the same season (fall/winter) corresponding to very similar wind conditions and traffic emissions (same traffic schedules).

On the other hand, the occurrence of sudden technical problems (GC-MS, autosampler), allowed us to exploit the results of only 2 out of 4 conducted signature campaigns and 2 out of 4 transect campaigns.

Regarding ADMS, we have already overcame a big challenge by employing the intermediate scenario; however, this approach doesn't yet treat aircraft plumes as accelerating jets which will be considered in a future study.

Finally, we were also limited by the situation in the country which made it difficult to access several restricted areas whether for collecting data for EMIT or for taking samples during the transect campaigns.

Future Perspectives

After observing the results of this thesis, many questions arise which open the door for several coming studies to answer these questions:

(i) How do the concentrations of pollutants (e.g. VOCs, PM, PAHs, NO_2) vary with aircraft movement along the seashore area? To answer this question, it would be very interesting to simultaneously measure these pollutants along the seashore area versus the number of aircraft counts and identify the temporal variations.

(ii) How do pollutants disperse away from the airport towards the mountains? Are the identified VOC tracers in USJ a result of emission dispersion from the airport located to its southwest by means of the prevailing wind conditions, or is it due to aircraft emissions during the approach phase? How does the interaction between local wind (sea breeze) and topography affect the emissions dispersion? How does the valley breeze affect dispersion? It would be interesting to simultaneously measure VOCs along a transect extending from the airport towards the mountainous area (e.g. USJ) to better understand the complex transport/dispersion phenomena that takes place to the east of the airport due to the special topography surrounding the airport.

(iii) What are the temporal variations of indoor/outdoor VOC concentrations and their relation with aircraft number? It is essential to measure VOC concentrations simultaneously indoors and outdoors versus the temporal variation in aircraft number.

(iv) For ADMS-Airport, a future study will be implemented by using the sophisticated approach of the model (Air File) to model aircraft as jet plumes. This will require very detailed knowledge about aircraft engine specifications and detailed aircraft arrivals and departure trajectories for each single aircraft. Besides this, it is interesting to assess the model's response to changes in wind conditions and to the difference in time scales.

(v) Finally, what are the health impacts of permanent exposures to contaminated air (NO_2) inside the airport and in the apron where employees spend at least 8-12 h? It would be interesting to determine the cumulative occupational exposure of workers to the pollution.

This was an example of some questions we could not answer as part of this doctoral research but that may be new areas for development in the context of research on air quality in Lebanon.

REFERENCES

Adamkiewicz, G., Hsu, H.-H., Vallarino, J., Melly, S.J., Spengler, J.D., Levy, J.I., 2010. Nitrogen dioxide concentrations in neighborhoods adjacent to a commercial airport: a land use regression modeling study. Environ. Health Glob. Access Sci. Source 9, 73. doi:10.1186/1476-069X-9-73

Agilent Technologies, 2016. 5973Network Mass Selective Detector, Hardware Manual [WWW Document]. URL http://www.agilent.com/cs/library/usermanuals/public/73nhw_030751.pdf (accessed 2.15.16).

Ahrens, C.D., 2009. Meteorology Today: An Introduction to Weather, Climate, and the Environment, 9th ed. Brooks Cole, Belmont, Calif.

Ahrens, C.D., Henson, R., 2015. Meteorology Today. Cengage Learning.

AirPACA, 2004. Etude de la qualité de l'air sur l'aéroport « Nice Côte d'âzur » [WWW Document]. URL http://www.airpaca.org/sites/paca/files/publications_import/files/041200_AirPACA_etude_aeroport_Nice_net.pdf (accessed 2.28.16).

Aliyu, A.S., Ramli, A.T., Saleh, M.A., 2015. Assessment of potential human health and environmental impacts of a nuclear power plant (NPP) based on atmospheric dispersion modeling. Atmósfera 28, 13–26. doi:10.1016/S0187-6236(15)72156-9

American Chemistry Council, 2004. n-Alkane Category: decane, undecane, dodecane (CAS Nos. 124-18-5, 1120-21-4, 112-40-3) Voluntary Children's Chemical Evaluation Program (VCCEP) Tier 1 Pilot Submission.

Anderson, B.E., Chen, G., Blake, D.R., 2006. Hydrocarbon emissions from a modern commercial airliner. Atmos. Environ. 40, 3601–3612. doi:10.1016/j.atmosenv.2005.09.072

Ashok, A., Lee, I.H., Arunachalam, S., Waitz, I.A., Yim, S.H.L., Barrett, S.R.H., 2013. Development of a response surface model of aviation's air quality impacts in the United States. Atmos. Environ. 77, 445–452. doi:10.1016/j.atmosenv.2013.05.023

ATAG, 2016. Social and economic benefits of aviation - Air Transport Action Group (ATAG) [WWW Document]. URL http://www.atag.org/our-activities/social-a-economic-benefits-of-aviation/3-social-a-economic-benefits-of-aviation.html (accessed 8.26.16).

ATAG, 2014. Aviation Benefits Beyond Borders.

Atkinson, R., 2003. Kinetics of the gas-phase reactions of OH radicals with alkanes and cycloalkanes. Atmos Chem Phys 3, 2233–2307. doi:10.5194/acp-3-2233-2003

Atkinson, R., 2000. Atmospheric chemistry of VOCs and NOx. Atmos. Environ. 34, 2063–2101. doi:10.1016/S1352-2310(99)00460-4

Atkinson, R., 1986a. Kinetics and mechanisms of the gas-phase reactions of the hydroxyl radical with organic compounds under atmospheric conditions. Chem. Rev. 86, 69–201. doi:10.1021/cr00071a004

Atkinson, R., 1986b. Kinetics and mechanisms of the gas-phase reactions of the hydroxyl radical with organic compounds under atmospheric conditions. Chem. Rev. 86, 69–201. doi:10.1021/cr00071a004

Atkinson, R., Arey, J., 2002. Atmospheric Chemistry of Alkanes. Atmospheric Chemistry of Selected Linear, Branched, and Cyclic C10 Alkane Components of Mineral Spirits (No. California Air Resources Contract No. 97-312).

Atkinson, R., Arey, J., Hoover, S., Preston, K., 2006. ATMOSPHERIC CHEMISTRY OF GASOLINE-RELATED EMISSIONS: FORMATION OF POLLUTANTS OF POTENTIAL CONCERN. Reproductive and Cancer Hazard Assessment Branch Office of Environmental Health Hazard Assessment California Environmental Protection Agency.

Atkinson, R., Aschmann, S.M., 1989. Rate constants for the gas-phase reactions of the OH radical with a series of aromatic hydrocarbons at 296 ± 2 K. Int. J. Chem. Kinet. 21, 355–365. doi:10.1002/kin.550210506

Atkinson, R., Aschmann, S.M., Carter, W.P.L., Winer, A.M., Pitts, J.N., 1982. Kinetics of the reactions of OH radicals with n-alkanes at 299 ± 2 K. Int. J. Chem. Kinet. 14, 781–788. doi:10.1002/kin.550140706

Atkinson, R., Carter, W.P.L., Aschmann, S.M., Winer, A.M., Pitts, J.N., 1984. Kinetics of the reaction of oh radicals with a series of branched alkanes at 297 ± 2 K. Int. J. Chem. Kinet. 16, 469–481. doi:10.1002/kin.550160413

Azzi, M., Johnson, 1992. An introduction to the generic reaction set photochemical smog mechanism, in: Proc. 11th Clean Air Conference. Presented at the 4th Regional IUAPPA Conf, Best, P., Bofinger, N. and Cliff, D., Brisbane, Australia, pp. 451–462.

Badaro-Saliba, N., Adjizian-Gerard, J., Zaarour, R., Abboud, M., Farah, W., Saliba, A.N., Shihadeh, A., 2013. A geostatistical approach for assessing population exposure to

NO_2 in a complex urban area (Beirut, Lebanon). Stoch. Environ. Res. Risk Assess. 28, 467–474. doi:10.1007/s00477-013-0765-3

Barrett, S.R.H., Britter, R.E., Waitz, I.A., 2013. Impact of aircraft plume dynamics on airport local air quality. Atmos. Environ. 74, 247–258. doi:10.1016/j.atmosenv.2013.03.061

BC Air Quality, 2016. Dispersion Modelling [WWW Document]. URL http://www.bcairquality.ca/assessment/dispersion-modelling.html (accessed 8.30.16).

Beyersdorf, A.J., Thornhill, K.L., Winstead, E.L., Ziemba, L.D., Blake, D.R., Timko, M.T., Anderson, B.E., 2012. Power-dependent speciation of volatile organic compounds in aircraft exhaust. Atmos. Environ. 61, 275–282. doi:10.1016/j.atmosenv.2012.07.027

Borbon, A., Fontaine, H., Veillerot, M., Locoge, N., Galloo, J.C., Guillermo, R., 2001. An investigation into the traffic-related fraction of isoprene at an urban location. Atmos. Environ. 35, 3749–3760. doi:10.1016/S1352-2310(01)00170-4

Brasseur, G.P., Cox, R.A., Hauglustaine, D., Isaksen, I., Lelieveld, J., Lister, D.H., Sausen, R., Schumann, U., Wahner, A., Wiesen, P., 1998. European scientific assessment of the atmospheric effects of aircraft emissions. Atmos. Environ. 32, 2329–2418. doi:10.1016/S1352-2310(97)00486-X

Brown, R.H., 2000. Monitoring the ambient environment with diffusive samplers: theory and practical considerations. J. Environ. Monit. 2, 1–9.

C. W. Spicer, M.W.H., 1984. Composition and Photochemical Reactivity of Turbine Engine Exhaust 196.

CAEP, 2008. LAQ Candidate Models Capabilities and Inter-Comparison Study (No. CAEP-8-MODTF-WP05_LAQ_Sample_problem).

CAEP 9, 2013. Committee on Aviation Environmental Protection Ninth Meeting.

California Environmental Protection Agency, 2005. Review of the California Ambient Air Quality Standard For Ozone (No. Volume II of IV Chapters 3-8).

Campbell, G.W., Stedman, J.R., Stevenson, K., 1994. A survey of nitrogen dioxide concentrations in the United Kingdom using diffusion tubes, July–December 1991. Atmos. Environ. 28, 477–486. doi:10.1016/1352-2310(94)90125-2

Campos, V.P., Cruz, L.P.S., Godoi, R.H.M., Godoi, A.F.L., Tavares, T.M., 2010. Development and validation of passive samplers for atmospheric monitoring of SO2, NO2, O3 and H2S in tropical areas. Microchem. J., Brazilian National

Meeting of Analytical Chemistry, 2009 96, 132–138. doi:10.1016/j.microc.2010.02.015

Camredon, M., Aumont, B., 2007. I – L'ozone troposphérique : production/consommation et régimes chimiques [WWW Document]. Httpirevuesinistfrpollution-Atmospherique. URL http://lodel.irevues.inist.fr/pollution-atmospherique/index.php?id=1404&format=print (accessed 4.28.16).

Carruthers, D.J., 2006. Intercomparison of five modelling approaches including ADMS-Airport and EDMS/AERMOD for predicting air quality in the vicinity of London Heathrow Airport.

Carruthers, D.J., McHugh, C., Church, S., Jackson, M., Williams, M., Price, C., Lad, C., 2008. ADMS-AIRPORT: MODEL INTER-COMPARISIONS AND MODEL VALIDATION. CERC, 3 King's Parade, Cambridge CB2 1SJ, UK.

Carruthers, D.J., McHugh, C., Jackson, M., Johnson, K., 2011. Developments in ADMS-Airport to take account of near field dispersion and applications to Heathrow Airport. Int. J. Environ. Pollut. 44, 332. doi:10.1504/IJEP.2011.038434

Carslaw, D.C., Beevers, S.D., Ropkins, K., Bell, M.C., 2006. Detecting and quantifying aircraft and other on-airport contributions to ambient nitrogen oxides in the vicinity of a large international airport. Atmos. Environ. 40, 5424–5434. doi:10.1016/j.atmosenv.2006.04.062

Carslaw, D.C., Ropkins, K., Laxen, D., Moorcroft, S., Marner, B., Williams, M.L., 2008. Near-field commercial aircraft contribution to nitrogen oxides by engine, aircraft type, and airline by individual plume sampling. Environ. Sci. Technol. 42, 1871–1876.

Carvalho, M., 2002. Combustion Technology for a Clean Environment: Selected Papers for the Proceedings of the Third International Conference, Lisbon, Portugal, July 3-6, 1995. CRC Press.

Cavallo, D., Ursini, C.L., Carelli, G., Iavicoli, I., Ciervo, A., Perniconi, B., Rondinone, B., Gismondi, M., Iavicoli, S., 2006. Occupational exposure in airport personnel: characterization and evaluation of genotoxic and oxidative effects. Toxicology 223, 26–35. doi:10.1016/j.tox.2006.03.003

CERC, 2016. CERC > Environmental software > Technical specifications [WWW Document]. URL http://cerc.co.uk/environmental-software/technical-specifications.html (accessed 5.31.16).

CERC, 2015a. ADMS-AIrport User Guide. version 4.0. Cambridge Environmental Research Consultant Ltd, 3 King's Parade. Carmbridge CB2 1SJ.

CERC, 2015b. EMIT: Atmospheric Emissions Inventory Toolkit User Guide. Version 3.4. Cambridge Environmental Research Consultant Ltd, 3 King's Parade. Carmbridge CB2 1SJ.

Chélala, C.Y., 2008. Transport routiers et pollution de l'air en NO2 dans Beyrouth (Liban) Application Du Modele STREET (Ph.D. Thesis). Saint Joseph University-Beirut.

Chin, J.-Y., Batterman, S.A., 2012. VOC composition of current motor vehicle fuels and vapors, and collinearity analyses for receptor modeling. Chemosphere 86, 951–958. doi:10.1016/j.chemosphere.2011.11.017

City of Park Ridge, 2000. Preliminary Study and Analysis of Toxic Air Pollutant Emissions from O'Hare International Airport and the Resulting Health Risks Created by these Toxic Emissions in Surrounding Residential Communities, Volumes I-IV.

Climate Change Science Program and the Subcommittee on Global Change Research, 2003. Chapter 3: Atmospheric Composition, in: Strategic Plan for the U.S. Climate Change Science Program.

Code of Federal Regulations, 2016. Code of Federal Reglations, 40: Chapter 1, Subchapter C, Part 51, Subpart F, 51100, Electronic Code of Federal Regulations.

Committee on Atmospheric Transport and Chemical Transformation in Acid Precipitation, 1983. Acid Deposition: Atmospheric Processes in Eastern North America. Appendex B: Transport and Dispersion Processes. National Academies Press, Washington, D.C.

Conner, T.L., Lonneman, W.A., Seila, R.L., 1995. Transportation-Related Volatile Hydrocarbon Source Profiles Measured in Atlanta. J. Air Waste Manag. Assoc. 45, 383–394. doi:10.1080/10473289.1995.10467370

Dagaut, P., Cathonnet, M., 2006a. The ignition, oxidation, and combustion of kerosene: A review of experimental and kinetic modeling. Prog. Energy Combust. Sci. 32, 48–92. doi:10.1016/j.pecs.2005.10.003

Dagaut, P., Cathonnet, M., 2006b. The ignition, oxidation, and combustion of kerosene: A review of experimental and kinetic modeling. Prog. Energy Combust. Sci. 32, 48–92. doi:10.1016/j.pecs.2005.10.003

Dagaut, P., El Bakali, A., Ristori, A., 2006. The combustion of kerosene: Experimental results and kinetic modelling using 1- to 3-component surrogate model fuels. Fuel 85, 944–956. doi:10.1016/j.fuel.2005.10.008

Daher, N., Saliba, N.A., Shihadeh, A.L., Jaafar, M., Baalbaki, R., Sioutas, C., 2013. Chemical composition of size-resolved particulate matter at near-freeway and urban background sites in the greater Beirut area. Atmos. Environ. 80, 96–106. doi:10.1016/j.atmosenv.2013.08.004

Dakhel, P., Lukachko, S.P., Waitz, I.A., Miake-Lye, R.C., Brown, R.C., 2007. Postcombustion Evolution of Soot Properties in an Aircraft Engine. J. Propuls. Power 23, 942–948. doi:10.2514/1.26738

Delgado-Saborit, J.M., Esteve-Cano, V., 2006. Field Study of Diffusion Collection Rate Coefficients of a No2 Passive Sampler in a Mediterranean Coastal Area. Environ. Monit. Assess. 120, 327–345. doi:10.1007/s10661-005-9065-9

Demirdjian, B., Ferry, D., Suzanne, J., Popovicheva, O.B., Persiantseva, N.M., Shonija, N.K., 2006. Heterogeneities in the Microstructure and Composition of Aircraft Engine Combustor Soot: Impact on the Water Uptake. J. Atmospheric Chem. 56, 83–103. doi:10.1007/s10874-006-9043-9

Dennis Ting, 2009. Reduced and Derated Thrust. Boeing Commercial Airplanes [WWW Document]. URL http://www.theairlinepilots.com/forumarchive/quickref/reducedandderatedthrust.pdf

DfT, 2007. Air Quality Studies for Heathrow: Base Case, Segregated Mode, Mixed Mode and Third Runway Scenarios modelled using ADMS-Airport.

DfT, 2006. Project for the Sustainable Development of Heathow - Report of the Air Quality Technical Panels.

Divaris, K., Vann, W.F., Baker, A.D., Lee, J.Y., 2012. Examining the accuracy of caregivers' assessments of young children's oral health status. J. Am. Dent. Assoc. 1939 143, 1237–1247.

EASA, 2016. Reference Landing and Take-Off (LTO) cycle | European Aviation Environmental Report [WWW Document]. URL https://www.easa.europa.eu/eaer/figures-tables/reference-landing-and-take-lto-cycle (accessed 8.16.16).

EEA, 2016. Nitrogen oxides (NOx) emissions — European Environment Agency [WWW Document]. URL http://www.eea.europa.eu/data-and-maps/indicators/eea-32-nitrogen-oxides-nox-emissions-1 (accessed 5.3.16).

Eickhoff, W., 1998. Emissionen organisch-chemischer Verbindungen aus zivilen Flugzeugtriebwerken. HLfU (Hessische Landesanstalt für Umwelt, Umweltplanung, Arbeits-und Umweltschutz), Heft Nr. 252.

EPA, 2009a. Aircraft Engine Speciated Organic Gases: Speciation of Unburned Organic Gases in Aircraft Exhaust [WWW Document]. URL https://www3.epa.gov/otaq/regs/nonroad/aviation/420r09902.pdf (accessed 2.28.16).

EPA, 2009b. Recommended best practice for quantifying speciated organic gas emissions from aircraft equipped with turbofan, turbojet, and turboprop engines, Version 1.0. ed. Assessment and Standards Division, Office of Transportation and Air Quality, U.S. Environmental Protection Agency, [Washington, D.C.] :

EPA, 1999. Nitrogen Oxides (NOx), Why and How they are Controlled. Office of Air Quality Planning and Standards U.S. Environmental Protection Agency, Research Triangle Park, North Carolina 27711.

EPA, 2006. TANKS Emissions Estimation Software [WWW Document]. URL https://www3.epa.gov/ttnchie1/software/tanks/ (accessed 6.2.16).

European Environment Agency, 2009. EMEP/EEA air pollutant emission inventory guidebook - 2009 — European Environment Agency [WWW Document]. URL http://www.eea.europa.eu/publications/emep-eea-emission-inventory-guidebook-2009 (accessed 6.1.16).

European Environment Agency, 2002. Directive 2002/3/ EC...ozone in ambient air [WWW Document]. URL http://www.eea.europa.eu/policy-documents/directive-2002-3-ec...ozone-in (accessed 2.28.16).

Evans, J.D., 1996. Straightforward statistics for the behavioral sciences. Brooks/Cole Pub. Co., Pacific Grove.

FAA, 2015. Aviation Emissions, Impacts & Mitigation A Primer. Office of Environment and Energy.

FAA, 2014. Aviation Emissions and Air Quality Handbook Version 3.

FAA, 2005. Aviation and Emissions A Primer.

FAA, 2003. Select Reseource Materials and Annotated Bibliography on the Topic of Hazardous Air Pollutants (HAPs) Associated with Aircraft, Airports, and Aviation

[WWW Document]. URL http://www.faa.gov/regulations_policies/policy_guidance/envir_policy/media/HAPs_rpt.pdf (accessed 2.28.16).

Farias, F., ApSimon, H., 2006. Relative contributions from traffic and aircraft NOx emissions to exposure in West London. Environ. Model. Softw., Urban Air Quality ModellingUrban Air Quality Modelling 21, 477–485. doi:10.1016/j.envsoft.2004.07.010

Ferm, M., Svanberg, P.-A., 1998. Cost-efficient techniques for urban- and background measurements of SO2 and NO2. Atmos. Environ. 32, 1377–1381. doi:10.1016/S1352-2310(97)00170-2

Gallego, E., Roca, F.J., Perales, J.F., Guardino, X., 2011. Comparative study of the adsorption performance of an active multi-sorbent bed tube (Carbotrap, Carbopack X, Carboxen 569) and a Radiello® diffusive sampler for the analysis of VOCs. Talanta 85, 662–672. doi:10.1016/j.talanta.2011.04.043

Gallego, E., Roca, F.J., Perales, J.F., Sánchez, G., Esplugas, P., 2012. Characterization and determination of the odorous charge in the indoor air of a waste treatment facility through the evaluation of volatile organic compounds (VOCs) using TD–GC/MS. Waste Manag. 32, 2469–2481. doi:10.1016/j.wasman.2012.07.010

Glasius, M., Funch Carlsen, M., Stroyer Hansen, T., Lohse, C., 1999. Measurements of nitrogen dioxide on Funen using diffusion tubes. Atmos. Environ. 33, 1177–1185. doi:10.1016/S1352-2310(98)00285-4

Gottardini, E., Cristofori, A., Cristofolini, F., Maccherini, S., Ferretti, M., 2008. Ambient levels of nitrogen dioxide (NO2) may reduce pollen viability in Austrian pine (Pinus nigra Arnold) trees — Correlative evidence from a field study. Sci. Total Environ. 402, 299–305. doi:10.1016/j.scitotenv.2008.04.048

Hangartner, M., Nabholz, M., 1998. Calibration of Dispersion Models by Diffusive Samplers.

Heland, J., Schäfer, K., 1998. Determination of major combustion products in aircraft exhausts by FTIR emission spectroscopy. Atmos. Environ. 32, 3067–3072. doi:10.1016/S1352-2310(97)00395-6

Hellén, H., 2006. Sources and Concentrations of Volatile Organic Compounds in Urban Air. University of Helsinki.

Henry, R.C., Lewis, C.W., Collins, J.F., 1994. Vehicle-Related Hydrocarbon Source Compositions from Ambient Data: The GRACE/SAFER Method. Environ. Sci. Technol. 28, 823–832. doi:10.1021/es00054a013

Herndon, S.C., 2012. Measurement of Gaseous HAP Emissions from Idling Aircraft as a Function of Engine and Ambient Conditions. Transportation Research Board.

Herndon, S.C., Rogers, T., Dunlea, E.J., Jayne, J.T., Miake-Lye, R., Knighton, B., 2006. Hydrocarbon Emissions from In-Use Commercial Aircraft during Airport Operations. Environ. Sci. Technol. 40, 4406–4413. doi:10.1021/es051209l

Hildebrandt, M.L., Pokhrel, S., 2002. Climate and Air Quality: A Case Study of PM10 Pollution in Kathmandu, Nepal. ResearchGate 25, 27–35.

Hollender, J., Sandner, F., Möller, M., Dott, W., 2002. Sensitive indoor air monitoring of monoterpenes using different adsorbents and thermal desorption gas chromatography with mass-selective detection. J. Chromatogr. A 962, 175–181. doi:10.1016/S0021-9673(02)00511-3

Hudda, N., Gould, T., Hartin, K., Larson, T.V., Fruin, S.A., 2014. Emissions from an International Airport Increase Particle Number Concentrations 4-fold at 10 km Downwind. Environ. Sci. Technol. 48, 6628–6635. doi:10.1021/es5001566

IATA, 2013. Annual Review.

Iavicoli, I., Carelli, G., Bergamaschi, A., 2006. Exposure evaluation to airborne polycyclic aromatic hydrocarbons in an italian airport. J. Occup. Environ. Med. Am. Coll. Occup. Environ. Med. 48, 815–822. doi:10.1097/01.jom.0000218692.37154.0b

ICAO, 2016. Local Air Quality [WWW Document]. URL http://www.icao.int/environmental-protection/Pages/local-air-quality.aspx (accessed 9.1.16).

ICAO, 2013. ICAO Environmental Report 2013, Aviation and Climate Change.

ICAO, 2011. Airport Air Quality Manual (Doc 9889).

ICAO, 2008a. Annex 16, Vol. II, Aircraft Engine Emissions, third ed.

ICAO, 2008b. Report of the independent experts on the LTTG NOx review and medium and long term technology goals for NOx. International Civil Aviation Organization, Montréal :

ICAO, 2006. Report of the Independent Experts to the Long Term Technology Task Group on the 2006 LTTG NOx Review and the Establishment of Medium and Long Term Technology Goals for NOx.

ICAO, 2005. Annex 16 to the Convention on International Civil Aviation. Environmental Protection. Volume I: Aircraft Noise, 4th ed.

IPCC, 2001. Atmospheric Chemistry and Greenhouse Gases, in: Climate Change 2001.

IPCC, I.P. on C., 2007. Climate Change 2007 - Mitigation of Climate Change: Working Group III contribution to the Fourth Assessment Report of the IPCC. Cambridge University Press.

Jarvis, D.J., Adamkiewicz, G., Heroux, M.-E., Rapp, R., Kelly, F.J., 2010. Nitrogen dioxide. World Health Organization.

Jathar, S.H., Miracolo, M.A., Presto, A.A., Donahue, N.M., Adams, P.J., Robinson, A.L., 2012. Modeling the formation and properties of traditional and non-traditional secondary organic aerosol: problem formulation and application to aircraft exhaust. Atmos Chem Phys 12, 9025–9040. doi:10.5194/acp-12-9025-2012

Jochmann, M.A., Laaks, J., Schmidt, T.C., 2014. Solvent-Free Extraction and Injection Techniques, in: Dettmer-Wilde, K., Engewald, W. (Eds.), Practical Gas Chromatography. Springer Berlin Heidelberg, pp. 371–412.

J.T. Watson and O.D. Sparkman, 2007. Electron Ionization, in: Introduction to Mass Spectrometry: Instrumentation, Applications, and Strategies for Data Interpretation. John Wiley & Sons, Ltd.

Julia, J., 2014. Airborne VOC measurements on board the Zeppelin NT during the PEGASOS campaigns in 2012 deploying the improved Fast-GC-MSD System. Forschungszentrum Jülich.

Jung, K.-H., Artigas, F., Shin, J.Y., 2011. Personal, indoor, and outdoor exposure to VOCs in the immediate vicinity of a local airport. Environ. Monit. Assess. 173, 555–567. doi:10.1007/s10661-010-1404-9

Kärcher, B., 1996. Aircraft-generated aerosols and visible contrails. Geophys. Res. Lett. 23, 1933–1936. doi:10.1029/96GL01853

Kim, B.Y., 2015. Understanding Airport Air Quality and Public Health Studies Related to Airports. Transportation Research Board.

Kim, B.Y., 2012. Guidance for Quantifying the Contribution of Airport Emissions to Local Air Quality. Transportation Research Board.

Kim, B.Y., Fleming, G.G., Lee, J.J., Waitz, I.A., Clarke, J.-P., Balasubramanian, S., Malwitz, A., Klima, K., Locke, M., Holsclaw, C.A., Maurice, L.Q., Gupta, M.L., 2007. System for assessing Aviation's Global Emissions (SAGE), Part 1: Model

description and inventory results. Transp. Res. Part Transp. Environ. 12, 325–346. doi:10.1016/j.trd.2007.03.007

Kim, Y.-H., Kim, K.-H., 2012. Ultimate Detectability of Volatile Organic Compounds: How Much Further Can We Reduce Their Ambient Air Sample Volumes for Analysis? Anal. Chem. 84, 8284–8293. doi:10.1021/ac301792x

KM Chng, 1999. Findings Regarding Source Contribution to Soot Deposition, O'Hare International Airport and Surrounding Communities. Environmental, Inc.

Knighton, W.B., Rogers, T.M., Anderson, B.E., Herndon, S.C., Yelvington, P.E., Miake-Lye, R.C., 2007. Quantification of Aircraft Engine Hydrocarbon Emissions Using Proton Transfer Reaction Mass Spectrometry. J. Propuls. Power 23, 949–958. doi:10.2514/1.22965

Köhler, M.O., Rädel, G., Dessens, O., Shine, K.P., Rogers, H.L., Wild, O., Pyle, J.A., 2008. Impact of perturbations to nitrogen oxide emissions from global aviation. J. Geophys. Res. Atmospheres 113, D11305. doi:10.1029/2007JD009140

Köhler, M.O., Rädel, G., Shine, K.P., Rogers, H.L., Pyle, J.A., 2013. Latitudinal variation of the effect of aviation NOx emissions on atmospheric ozone and methane and related climate metrics. Atmos. Environ. 64, 1–9. doi:10.1016/j.atmosenv.2012.09.013

Koppmann, R., 2008. Volatile Organic Compounds in the Atmosphere. John Wiley & Sons.

Kowang, T.O., Long, C.S., Rasli, A., 2015. Innovation Management and Performance Framework for Research University in Malaysia. Int. Educ. Stud. 8, 32.

Lai, C.H., Chen, K.S., Ho, Y.T., Chou, M.S., 2004. Characteristics of C2–C15 hydrocarbons in the air of urban Kaohsiung, Taiwan. Atmos. Environ. 38, 1997–2011. doi:10.1016/j.atmosenv.2003.11.041

Lee, D.S., Fahey, D.W., Forster, P.M., Newton, P.J., Wit, R.C.N., Lim, L.L., Owen, B., Sausen, R., 2009. Aviation and global climate change in the 21st century. Atmos. Environ. 43, 3520–3537. doi:10.1016/j.atmosenv.2009.04.024

Lee, D.S., Pitari, G., Grewe, V., Gierens, K., Penner, J.E., Petzold, A., Prather, M.J., Schumann, U., Bais, A., Berntsen, T., Iachetti, D., Lim, L.L., Sausen, R., 2010. Transport impacts on atmosphere and climate: Aviation. Atmos. Environ., Transport Impacts on Atmosphere and Climate: The ATTICA Assessment Report 44, 4678–4734. doi:10.1016/j.atmosenv.2009.06.005

Lelievre, C.P., 2009. La qualité de l'air en milieu aéroportuaire : étude sur l'aéroport Paris-Charles-De-Gaulle (phdthesis). Université Paris-Est.

Leuzzi, G., 2002. A SENSITIVITY ANALYSIS OF ADMS-URBAN. ResearchGate.

Levy, J.I., Woody, M., Baek, B.H., Shankar, U., Arunachalam, S., 2012. Current and future particulate-matter-related mortality risks in the United States from aviation emissions during landing and takeoff. Risk Anal. Off. Publ. Soc. Risk Anal. 32, 237–249. doi:10.1111/j.1539-6924.2011.01660.x

Lewis, J.S., Niedzwiecki, R.W., Bahr, D.W., Bullock, S., Cumpsty, N., Dodds, W., DuBois, D., Epstein, A., Freguson, W.W., Fiorento, A., Gorbatko, A.A., Hagen, D.E., Hart, P.J., Hayashi, S., Jamieson, J.B., Kerrebrock, J., Lecht, M., Lowrie, B., Miake-, Lye, R.C., Mortlock, A.K., Moses, C., Renger, K., Sampath, S., Sanborn, J., Simon, B.,, Sorokin, A., Taylor, W., Waitz, I., Wey, C.C., Whitefield, P., Wilson, C.W., Wu, S., 1999. Aircraft Technology and Its Relation to Emissions, in: Aviation and the Global Atmosphere, Special Report of the Intergovernmental Panel on Climate Change. Cambridge University Press, Cambridge (Chapter 7).

Liaud, C., 2014. Développement de méthodes d'échantillonnage rapides et d'analyses différées au laboratoire : détermination de l'évolution temporelle des concentrations des COVs et COSVs et compréhension des processus physico-chimiques en air intérieur (phdthesis). Université de Strasbourg.

Liaud, C., Nguyen, N.T., Nasreddine, R., Le Calvé, S., 2014. Experimental performances study of a transportable GC-PID and two thermo-desorption based methods coupled to FID and MS detection to assess BTEX exposure at sub-ppb level in air. Talanta 127, 33–42. doi:10.1016/j.talanta.2014.04.001

Lieuwen, T.C., Yang, V., 2013. Gas Turbine Emissions. Cambridge University Press.

Lin, S., Munsie, J.P., Herdt-Losavio, M., Hwang, S.A., Civerolo, K., McGarry, K., Gentile, T., 2008. Residential proximity to large airports and potential health impacts in New York State. Int. Arch. Occup. Environ. Health 81, 797–804. doi:10.1007/s00420-007-0265-1

Liu, Y., Shao, M., Fu, L., Lu, S., Zeng, L., Tang, D., 2008. Source profiles of volatile organic compounds (VOCs) measured in China: Part I. Atmos. Environ., PRIDE-PRD 2004 Campaign : Program of Regional Integrated Experiments on Air Quality over Pearl River Delta of China 42, 6247–6260. doi:10.1016/j.atmosenv.2008.01.070

Liyasova, M., Li, B., Schopfer, L.M., Nachon, F., Masson, P., Furlong, C.E., Lockridge, O., 2011. Exposure to tri-o-cresyl phosphate detected in jet airplane passengers. Toxicol. Appl. Pharmacol. 256, 337–347. doi:10.1016/j.taap.2011.06.016

Longhurst, J.W.S., Raper, D.W., Conlan, D.E., 1996. Local and regional air quality impacts of airport operations. Environmentalist 16, 83–90. doi:10.1007/BF01325099

Macintosh, A., Wallace, L., 2009. International aviation emissions to 2025: Can emissions be stabilised without restricting demand? Energy Policy 37, 264–273. doi:10.1016/j.enpol.2008.08.029

Mahashabde, A., Wolfe, P., Ashok, A., Dorbian, C., He, Q., Fan, A., Lukachko, S., Mozdzanowska, A., Wollersheim, C., Barrett, S.R.H., Locke, M., Waitz, I.A., 2011. Assessing the environmental impacts of aircraft noise and emissions. Prog. Aerosp. Sci. 47, 15–52. doi:10.1016/j.paerosci.2010.04.003

Marchand, C., Bulliot, B., Le Calvé, S., Mirabel, P., 2006. Aldehyde measurements in indoor environments in Strasbourg (France). Atmos. Environ. 40, 1336–1345. doi:10.1016/j.atmosenv.2005.10.027

Masiol, M., Harrison, R.M., 2014. Aircraft engine exhaust emissions and other airport-related contributions to ambient air pollution: A review. Atmos. Environ. 95, 409–455. doi:10.1016/j.atmosenv.2014.05.070

Matysik, S., Ramadan, A.B., Schlink, U., 2010. Spatial and temporal variation of outdoor and indoor exposure of volatile organic compounds in Greater Cairo. Atmospheric Pollut. Res. 1, 94–101. doi:10.5094/APR.2010.012

McGulley, Frick and Gilman, 1995. Final Report: Air Quality Survey, Seattle- Tacoma International Airport. Port of Seattle, WA.

Moussiopoulos, N., Sahm, P., Karatzas, K., Papalexiou, S., Karagiannidis, A., 1997. Assessing the impact of the New Athens airport to urban air quality with contemporary air pollution models. Atmos. Environ. 31, 1497–1511. doi:10.1016/S1352-2310(96)00283-X

Myhre, G., Shine, K.P., Rädel, G., Gauss, M., Isaksen, I.S.A., Tang, Q., Prather, M.J., Williams, J.E., van Velthoven, P., Dessens, O., Koffi, B., Szopa, S., Hoor, P., Grewe, V., Borken-Kleefeld, J., Berntsen, T.K., Fuglestvedt, J.S., 2011. Radiative forcing due to changes in ozone and methane caused by the transport sector. Atmos. Environ. 45, 387–394. doi:10.1016/j.atmosenv.2010.10.001

Nakhle, M.M., Annesi-Maesano, I., Ziade, N., Abboud, M., Farah, W., 2013. Impact of air pollution on health in Beirut- BAPHE (Beirut AirPollution and Health Effects) protocol and results, in: ResearchGate. Presented at the Environment and Health.

Namieśnik, J., Zabiegała, B., Kot-Wasik, A., Partyka, M., Wasik, A., 2004. Passive sampling and/or extraction techniques in environmental analysis: a review. Anal. Bioanal. Chem. 381, 279–301. doi:10.1007/s00216-004-2830-8

National Research Council (U.S.), 2002. For greener skies : reducing environmental impacts of aviation / Committee on Aeronautics Research and Technology for Environmental Compatibility, Aeronautics and Space Engineering Board, Division on Engineering and Physical Sciences, National Research Council. - Version details. National Academies Press, Washington, D.C.

Nikoleris, T., Gupta, G., Kistler, M., 2011. Detailed estimation of fuel consumption and emissions during aircraft taxi operations at Dallas/Fort Worth International Airport. Transp. Res. Part Transp. Environ. 16, 302–308. doi:10.1016/j.trd.2011.01.007

Norton, T., 2014. Aircraft Greenhouse Gas Emissions during the Landing and Takeoff Cycle at Bay Area Airports. Masters Proj.

Nullet, D., 2016. Local Winds [WWW Document]. URL https://laulima.hawaii.edu/access/content/group/2c084cc1-8f08-442b-80e8-ed89faa22c33/book/chapter_4/localw.htm (accessed 5.10.16).

Olsen, S.C., Brasseur, G.P., Wuebbles, D.J., Barrett, S.R.H., Dang, H., Eastham, S.D., Jacobson, M.Z., Khodayari, A., Selkirk, H., Sokolov, A., Unger, N., 2013. Comparison of model estimates of the effects of aviation emissions on atmospheric ozone and methane. Geophys. Res. Lett. 40, 6004–6009. doi:10.1002/2013GL057660

Palmes, E.D., GUNNISON, A.F., DiMATTIO, J., TOMCZYK, C., 1976. Personal sampler for nitrogen dioxide. Am. Ind. Hyg. Assoc. J.

Palmes, E.D., Lindenboom, R.H., 1979. Ohm's law, Fick's law, and diffusion samplers for gases. Anal. Chem. 51, 2400–2401. doi:10.1021/ac50050a026

Parra, M.A., Elustondo, D., Bermejo, R., Santamaría, J.M., 2008. Quantification of indoor and outdoor volatile organic compounds (VOCs) in pubs and cafés in Pamplona, Spain. Atmos. Environ. 42, 6647–6654. doi:10.1016/j.atmosenv.2008.04.026

Peace, H., Maughan, J., Owen, B., Raper, D., 2006. Identifying the contribution of different airport related sources to local urban air quality. Environ. Model. Softw.,

Urban Air Quality ModellingUrban Air Quality Modelling 21, 532–538. doi:10.1016/j.envsoft.2004.07.014

Penner, J.E., 1999. Aviation and the Global Atmosphere: A Special Report of the Intergovernmental Panel on Climate Change. Cambridge University Press.

Pisano, J.T., McKendry, I., Steyn, D.G., Hastie, D.R., 1997. Vertical Nitrogen Dioxide and Ozone Concentrations Measured from a Tethered Balloon in the Lower Fraser Valley.

Pison, I., Menut, L., 2004. Quantification of the impact of aircraft traffic emissions on tropospheric ozone over Paris area. Atmos. Environ. 38, 971–983. doi:10.1016/j.atmosenv.2003.10.056

Pitari, G., Mancini, E., Bregman, A., 2002. Climate forcing of subsonic aviation: Indirect role of sulfate particles via heterogeneous chemistry. Geophys. Res. Lett. 29, 2057. doi:10.1029/2002GL015705

Pleil, J.D., Smith, L.B., Zelnick, S.D., 2000. Personal exposure to JP-8 jet fuel vapors and exhaust at air force bases. Environ. Health Perspect. 108, 183–192.

Ramírez, N., Cuadras, A., Rovira, E., Borrull, F., Marcé, R.M., 2010. Comparative study of solvent extraction and thermal desorption methods for determining a wide range of volatile organic compounds in ambient air. Talanta 82, 719–727. doi:10.1016/j.talanta.2010.05.038

Ratliff, G., Sequeira, C., 2009. Aircraft Impacts on Local and Regional Air Quality in the United States. PARTNER Report 15 Final Report (Report No. PARTNER-COE-2009-002).

Rava, M., Verlato, G., Bono, R., Ponzio, M., Sartori, S., Blengio, G., Kuenzli, N., Heinrich, J., Götschi, T., de Marco, R., 2007. A predictive model for the home outdoor exposure to nitrogen dioxide. Sci. Total Environ. 384, 163–170. doi:10.1016/j.scitotenv.2007.06.014

Rehwagen, M., Schlink, U., Herbarth, O., 2003. Seasonal cycle of VOCs in apartments. Indoor Air 13, 283–291.

RIDEM, 2008. Characterization of Ambient Air Toxics in Neighborhoods Abutting T.F. Green Airport and Comparison Sites: Final Report. Rhode Island Department of Environmental Management.

Ritchie, G., Still, K., III, J.R., Bekkedal, M., Bobb, A., Arfsten, D., 2003a. Biological And Health Effects Of Exposure To Kerosene-Based Jet Fuels And Performance

Additives. J. Toxicol. Environ. Health Part B 6, 357–451. doi:10.1080/10937400306473

Ritchie, G., Still, K., Rossi, J., Bekkedal, M., Bobb, A., Arfsten, D., 2003b. Biological and health effects of exposure to kerosene-based jet fuels and performance additives. J. Toxicol. Environ. Health B Crit. Rev. 6, 357–451. doi:10.1080/10937400306473

Ritchie, G.D., Still, K.R., Alexander, W.K., Nordholm, A.F., Wilson, C.L., Rossi, J., Mattie, D.R., 2001. A review of the neurotoxicity risk of selected hydrocarbon fuels. J. Toxicol. Environ. Health B Crit. Rev. 4, 223–312. doi:10.1080/10937400118874

Salameh, T., Afif, C., Sauvage, S., Borbon, A., Locoge, N., 2014. Speciation of non-methane hydrocarbons (NMHCs) from anthropogenic sources in Beirut, Lebanon. Environ. Sci. Pollut. Res. 21, 10867–10877. doi:10.1007/s11356-014-2978-5

Saltzman, B.E., 1954. Colorimetric Microdetermination of Nitrogen Dioxide in Atmosphere. Anal. Chem. 26, 1949–1955. doi:10.1021/ac60096a025

Schindler, B.K., Weiss, T., Schütze, A., Koslitz, S., Broding, H.C., Bünger, J., Brüning, T., 2013. Occupational exposure of air crews to tricresyl phosphate isomers and organophosphate flame retardants after fume events. Arch. Toxicol. 87, 645–648. doi:10.1007/s00204-012-0978-0

Schürmann, G., Schäfer, K., Jahn, C., Hoffmann, H., Bauerfeind, M., Fleuti, E., Rappenglück, B., 2007a. The impact of NOx, CO and VOC emissions on the air quality of Zurich airport. Atmos. Environ. 41, 103–118. doi:10.1016/j.atmosenv.2006.07.030

Schürmann, G., Schäfer, K., Jahn, C., Hoffmann, H., Bauerfeind, M., Fleuti, E., Rappenglück, B., 2007b. The impact of NOx, CO and VOC emissions on the air quality of Zurich airport. Atmos. Environ. 41, 103–118. doi:10.1016/j.atmosenv.2006.07.030

Schürmann, G., Schäfer, K., Jahn, C., Hoffmann, H., Bauerfeind, M., Fleuti, E., Rappenglück, B., 2007c. The impact of NOx, CO and VOC emissions on the air quality of Zurich airport. Atmos. Environ. 41, 103–118. doi:10.1016/j.atmosenv.2006.07.030

Seinfeld, J.H., 1995. CHEMISTRY OF OZONE IN THE URBAN AND REGIONAL ATMOSPHERE, in: Progress and Problems in Atmospheric Chemistry. WORLD SCIENTIFIC, pp. 34–57.

Semadeni, M., 1994. Hydroxyl radical reactions with volatile organic compounds under simulated tropospheric conditions (theses). Diss. Naturwiss. ETH Zürich, Nr. 10809, 1994. Ref.: R. Schwarzenbach ; Korref.: J. A. Kerr ; Korref.: H. van den Berg.

Serevicien, V., Baltrėnas, P., Baltrėnaitė, E., Marčiulaitienė, E., Paliulis, D., 2014. Investigation of NO2 Behaviour in the Temperate Continental Climate Road Environment. Water. Air. Soil Pollut. 225. doi:10.1007/s11270-014-2173-9

Shrivastava, A., Gupta, V.B., 2011. Methods for the determination of limit of detection and limit of quantitation of the analytical methods. Chron. Young Sci. 2, 21. doi:10.4103/2229-5186.79345

Sigma-Aldrich, 2016. Passive (Diffusive) Sampling Overview [WWW Document]. Sigma-Aldrich. URL http://www.sigmaaldrich.com/analytical-chromatography/air-monitoring/passive-sampling.html (accessed 2.13.16).

Simone, N.W., Stettler, M.E.J., Barrett, S.R.H., 2013. Rapid estimation of global civil aviation emissions with uncertainty quantification. Transp. Res. Part Transp. Environ. 25, 33–41. doi:10.1016/j.trd.2013.07.001

Simpson, J.E., 1994. Sea Breeze and Local Winds. Cambridge University Press.

Slemr, F., Giehl, H., Habram, M., Slemr, J., Schlager, H., Schulte, P., Haschberger, P., Lindermeir, E., Döpelheuer, A., Plohr, M., 2001. In-flight measurement of aircraft CO and nonmethane hydrocarbon emission indices. J. Geophys. Res. Atmospheres 106, 7485–7494. doi:10.1029/2000JD900580

Slemr, F., Giehl, H., Slemr, J., Busen, R., Schulte, P., Haschberger, P., 1998. In-flight measurement of aircraft non-methane hydrocarbon emission indices. Geophys. Res. Lett. 25, 321–324. doi:10.1029/97GL03784

Sneddon, J., Masuram, S., Richert, J.C., 2007. Gas Chromatography-Mass Spectrometry-Basic Principles, Instrumentation and Selected Applications for Detection of Organic Compounds. Anal. Lett. 40, 1003–1012. doi:10.1080/00032710701300648

Solomon, S., Qin, D., Manning, M., Chen, Z., 2007. Climate Change 2007: The Physical Science Basis: Contribution of Working Group I to the Fourth Assessment Report of the Intergovernmental Panel on Climate Change. Cambridge University Press.

Spicer, C.W., Holdren, M.W., Lyon, T.F., Riggin, R.M., 1984. Composition and Photochemical Reactivity of Turbine Engine Exhaust.

Spicer, C.W., Holdren, M.W., Riggin, R.M., Lyon, T.F., 1994. Chemical composition and photochemical reactivity of exhaust from aircraft turbine engines. Ann. Geophys. 12, 944–955. doi:10.1007/s00585-994-0944-0

Spicer, C.W., Holdren, M.W., Smith, D.L., Hughes, D.P., Smith, M.D., 1992a. Chemical Composition of Exhaust From Aircraft Turbine Engines. J. Eng. Gas Turbines Power 114, 111. doi:10.1115/1.2906292

Spicer, C.W., Holdren, M.W., Smith, D.L., Hughes, D.P., Smith, M.D., 1992b. Chemical Composition of Exhaust From Aircraft Turbine Engines. J. Eng. Gas Turbines Power 114, 111–117. doi:10.1115/1.2906292

Stull, R.B. (Ed.), 1988. An Introduction to Boundary Layer Meteorology. Springer Netherlands, Dordrecht.

Tesseraux, I., 2004. Risk factors of jet fuel combustion products. Toxicol. Lett. 149, 295–300. doi:10.1016/j.toxlet.2003.12.040

Tsague, L., Tsogo, J., Tamo, T., 2006. Prediction of the production of nitrogen oxide (NOx) in turbojet engines, Technical note. Atmospheric Environment 40, 5727–5733.

Tsakas, M.P., Siskos, P.A., 2011. Indoor Air Quality in the Control Tower of Athens International Airport, Greece. Indoor Built Environ. 20, 284–289. doi:10.1177/1420326X10381108

Tunnicliffe, W.S., O'Hickey, S.P., Fletcher, T.J., Miles, J.F., Burge, P.S., Ayres, J.G., 1999. Pulmonary function and respiratory symptoms in a population of airport workers. Occup. Environ. Med. 56, 118–123.

Turner, D.B., Schulze, R.H., 1996. Practical Guide to Atmospheric Dispersion Modeling. Trinity Consultants, Dallas : Pitsburgh.

Unique, 2005. Aircraft APU Emissions at Zurich Airport.

Unique, 2004. Aircraft NOx-Emissions within the Operational LTO Cycle. Unique (Flughafen Zürich AG), P.O. Box, CH-8058 Zuric, In cooperation with Swiss Flight Data Monitoring, CH-8058 Zurich.

United Nations, U.N.E.C. for, 2007. Environmental Indicators and Indicator-based Assessment Reports: Eastern Europe, Caucasus and Central Asia. United Nations Publications.

UNWTO, 2015. TourismHighlightsReport, UnitedNationsWorldTourismOrga- nization, Spain.

UNWTO, 2013. TourismHighlightsReport, UnitedNationsWorldTourismOrga- nization, Spain.

U.S. Environment Protection Agency, TO-14A, 1999. Compendium Method TO-14A Determination Of Volatile Organic Compounds (VOCs) In Ambient Air Using Specially Prepared Canisters With Subsequent Analysis By Gas Chromatography [WWW Document]. URL http://www3.epa.gov/ttnamti1/files/ambient/airtox/to-14ar.pdf (accessed 2.14.16).

U.S. Environmental Protection Agency, 1999. Compendium Method TO-17 - Compendium of Methods for the Determination of Toxic Organic Compounds in Ambient Air. Determination of Volatile Organic Compounds in Ambient Air Using Active Sampling Onto Sorbent Tubes [WWW Document]. URL https://www3.epa.gov/ttnamti1/files/ambient/airtox/to-17r.pdf (accessed 3.8.16).

US EPA, 2016. Health | Nitrogen Dioxide | US EPA [WWW Document]. URL https://www3.epa.gov/airquality/nitrogenoxides/health.html (accessed 8.16.16).

Venkatram, A., Karamchandani, P., Pai, P., Goldstein, R., 1994. The development and application of a simplified ozone modeling system (SOMS). Atmos. Environ. 28, 3665–3678. doi:10.1016/1352-2310(94)00190-V

Villanueva, F., Tapia, A., Amo-Salas, M., Notario, A., Cabañas, B., Martínez, E., 2015. Levels and sources of volatile organic compounds including carbonyls in indoor air of homes of Puertollano, the most industrialized city in central Iberian Peninsula. Estimation of health risk. Int. J. Hyg. Environ. Health 218, 522–534. doi:10.1016/j.ijheh.2015.05.004

Volden, J., Thomassen, Y., Greibrokk, T., Thorud, S., Molander, P., 2005. Stability of workroom air volatile organic compounds on solid adsorbents for thermal desorption gas chromatography. Anal. Chim. Acta 530, 263–271. doi:10.1016/j.aca.2004.09.019

Waked, A., Afif, C., 2012. Emissions of air pollutants from road transport in Lebanon and other countries in the Middle East region. Atmos. Environ. 61, 446–452. doi:10.1016/j.atmosenv.2012.07.064

Wang, C., Yang, X., Guan, J., Gao, K., Li, Z., 2014. Volatile organic compounds in aircraft cabin: Measurements and correlations between compounds. Build. Environ. 78, 89–94. doi:10.1016/j.buildenv.2014.04.016

Wang, J., Jin, L., Gao, J., Shi, J., Zhao, Y., Liu, S., Jin, T., Bai, Z., Wu, C.-Y., 2013. Investigation of speciated VOC in gasoline vehicular exhaust under ECE and

EUDC test cycles. Sci. Total Environ. 445–446, 110–116. doi:10.1016/j.scitotenv.2012.12.044

Westerdahl, D., Fruin, S.A., Fine, P.L., Sioutas, C., 2008. The Los Angeles International Airport as a source of ultrafine particles and other pollutants to nearby communities. Atmos. Environ. 42, 3143–3155. doi:10.1016/j.atmosenv.2007.09.006

WHO, 2005. WHO Air quality guidelines for particulate matter, ozone, nitrogen dioxide and sulfur dioxide - global update 2005 [WWW Document]. WHO. URL http://www.who.int/phe/health_topics/outdoorair/outdoorair_aqg/en/ (accessed 5.4.16).

Wilkerson, J.T., Jacobson, M.Z., Malwitz, A., Balasubramanian, S., Wayson, R., Fleming, G., Naiman, A.D., Lele, S.K., 2010. Analysis of emission data from global commercial aviation: 2004 and 2006. Atmos Chem Phys 10, 6391–6408. doi:10.5194/acp-10-6391-2010

Witten, M.L., Zeiger, E., Ritchie, G.D., 2011. Jet Fuel Toxicology. CRC Press.

Wood, E., 2008. Aircraft and Airport-related Hazardous Air Pollutants: Research Needs and Analysis. Transportation Research Board.

Woolfenden, E., 2010a. Sorbent-based sampling methods for volatile and semi-volatile organic compounds in air. Part 2. Sorbent selection and other aspects of optimizing air monitoring methods. J. Chromatogr. A, Extraction Techniques 1217, 2685–2694. doi:10.1016/j.chroma.2010.01.015

Woolfenden, E., 2010b. Sorbent-based sampling methods for volatile and semi-volatile organic compounds in air. J. Chromatogr. A 1217, 2674–2684. doi:10.1016/j.chroma.2009.12.042

Yaman, S.H., 2001. Aircraft and vehicle induced emissions at the Beirut International Airport a characterization and exposure assessment - by Sarah Hassan Yaman (Thesis).

Yelvington, P.E., Herndon, S.C., Wormhoudt, J.C., Jayne, J.T., Miake-Lye, R.C., Knighton, W.B., Wey, C., 2007. Chemical Speciation of Hydrocarbon Emissions from a Commercial Aircraft Engine. J. Propuls. Power 23, 912–918. doi:10.2514/1.23520

Yim, S.H.L., Stettler, M.E.J., Barrett, S.R.H., 2013. Air quality and public health impacts of UK airports. Part II: Impacts and policy assessment. Atmos. Environ. 67, 184–192. doi:10.1016/j.atmosenv.2012.10.017

Yu, C.H., Morandi, M.T., Weisel, C.P., 2008. Passive dosimeters for nitrogen dioxide in personal/indoor air sampling: A review. J. Expo. Sci. Environ. Epidemiol. 18, 441–451. doi:10.1038/jes.2008.22

Yu, K.N., Cheung, Y.P., Cheung, T., Henry, R.C., 2004. Identifying the impact of large urban airports on local air quality by nonparametric regression. Atmos. Environ. 38, 4501–4507. doi:10.1016/j.atmosenv.2004.05.034

Zeldovich, Y., 1946. The Oxidation of Nitrogen in Combustion and Explosions. Acta Physicochim. 21, 577–628.

Zhu, Y., Fanning, E., Yu, R.C., Zhang, Q., Froines, J.R., 2011. Aircraft emissions and local air quality impacts from takeoff activities at a large International Airport. Atmos. Environ. 45, 6526–6533. doi:10.1016/j.atmosenv.2011.08.062

ANNEXES

Annex 4-1: Certificates of VOC concentrations in the standard bottles

AIR LIQUIDE
FRANCE INDUSTRIE

AIR LIQUIDE

CNRS - LMSPC - UMR 7515 - ECPM
MME JEANMAIRE
25, RUE BECQUEREL

67087 STRASBOURG CEDEX 2

N° de Commande: L 12207/MERMAID/SL

Agence AL : Est
Code Produit : SD190040252

Référence AL : 27339172-10
Produit / Emb.: KON4M/ 11 L Loué(s)
Centre logistique : FR79/DE

Mélange CRYSTAL

CERTIFICAT

N°: 9366753001

PAGE 1 /3

Composants	Teneur demandée	Résultat	Incertitude * ± % rel.
ACETYLENE	100	(100 ± 20) Mol-ppb	20
ETHYLENE	100	(100 ± 20) Mol-ppb	20
ETHANE	100	(103 ± 21) Mol-ppb	20
PROPYLENE	100	(99 ± 20) Mol-ppb	20
PROPANE	100	(101 ± 20) Mol-ppb	20
BUTADIENE-1.3	100	(100 ± 20) Mol-ppb	20
BUTENE 1	100	(100 ± 20) Mol-ppb	20
BUTENE-2 CIS	100	(101 ± 20) Mol-ppb	20
BUTENE-2 TRANS	100	(101 ± 20) Mol-ppb	20

*intervalle de confiance : 95% (2 incertitudes-type)

N° bouteille : 177

Volume bouteille : 11 L Loué(s)

Raccord : C

Pression à 15°C : 150 Bar

T° stockage-utilisation : -10 à 50 °C

Pression mini d´utilisation : 10 Bar

Date limite d'utilisation: 31.05.2014

Date d'autorisation : 31.05.2013

Il s'agit d'un certificat réalisé par ordinateur, qui est valable sans signature.

Air Liquide GPM Europe
Rue Gay Lussac, F-77292 MITRY-MORY
Certification combinée n° SM / 2008 / 31169 a

Visa
LACHAUD

AIR LIQUIDE
FRANCE INDUSTRIE

AIR LIQUIDE

CNRS - LMSPC - UMR 7515 - ECPM
MME JEANMAIRE
25, RUE BECQUEREL

67087 STRASBOURG CEDEX 2

N° de Commande: L 12207/MERMAID/SL

Agence AL : Est
Code Produit : SD190040252

Référence AL : 27339172-10
Produit / Emb.: KON4M/ 11 L Loué(s)
Centre logistique : FR79/DE

Mélange CRYSTAL

CERTIFICAT

N°: 9366753001

PAGE 2 /3

Composants	Teneur demandée	Résultat	Incertitude * ± % rel.
ISOBUTANE	100	(101 ± 20) Mol-ppb	20
N-BUTANE	100	(101 ± 20) Mol-ppb	20
ISOPRENE	100	(99 ± 20) Mol-ppb	20
PENTENE-1	100	(99 ± 20) Mol-ppb	20
CIS-2-PENTENE	100	(99 ± 20) Mol-ppb	20
TRANS-2-PENTENE	100	(100 ± 20) Mol-ppb	20
ISOPENTANE	100	(100 ± 20) Mol-ppb	20
PENTANE	100	(100 ± 20) Mol-ppb	20
HEXENE-1	100	(100 ± 20) Mol-ppb	20

*intervalle de confiance : 95% (2 incertitudes-type)

N° bouteille :
177

Volume bouteille :
11 L Loué(s)

Raccord :
C

Pression à 15°C :
150 Bar

T° stockage-utilisation :
-10 à 50 °C

Pression mini d'utilisation :
10 Bar

Date limite d'utilisation:
31.05.2014

Date d'autorisation :
31.05.2013

Il s'agit d'un certificat réalisé par ordinateur, qui est valable sans signature.

Air Liquide GPM Europe
Rue Gay Lussac, F-77292 MITRY-MORY
Certification combinée n° SM / 2008 / 31169 a

Visa
LACHAUD

Certificate of Analysis

DESCRIPTION : **ASTM D3710 QUANTITATIVE CALIBRATION MIX**

CATALOG # : **506435** **MFG DATE :** **6/3/2013**

LOT # : **LC00830** **EXP DATE :** **6/2016**

COMPONENT (1)	CAS#	SUPELCO LOT#	%PURITY (2)	WEIGHT% (3) THEORETICAL	WEIGHT% (3) ANALYTICAL
n-Butylbenzene	104-51-8	LB09309	98.7	3.50	3.52
n-Decane	124-18-5	LB06072	99.7	3.50	3.50
n-Dodecane	112-40-3	LB00874	99.3	3.50	3.49
n-Heptane	142-82-5	LB05152	99.5	10.50	10.47
n-Hexane	110-54-3	LA90410	99.3	5.80	5.77
n-Octane	111-65-9	LA94647	99.4	5.80	5.81
n-Pentadecane	629-62-9	LA98455	99.9	2.30	2.31
n-Pentane	109-66-0	LA81290	99.5	8.10	8.14
n-Propylbenzene	103-65-1	LA92696	99.8	4.70	4.67
n-Tetradecane	629-59-4	LA99306	99.7	2.30	2.31
n-Tridecane	629-50-5	LB09034	99.3	2.30	2.26
p-Xylene	106-42-3	LB04801	99.9	14.00	14.03
Toluene	108-88-3	LA90411	99.9	11.60	11.60
2-Methylbutane	78-78-4	LB09104	99.1	10.50	10.48
2-Methylpentane	107-83-5	LA93816	99.9	5.80	5.83
2,4-Dimethylpentane	108-08-7	LB09031	99.8	5.80	5.78

(1) Components are in alphabetical order.

(2) Determined by GC-FID unless otherwise noted.

(3) Weight percent of component in solution (+/- 0.05%).
Components less than 98% pure are corrected for impurities.
Certified weights are not applicable to ampuls stored after opening, even if resealed.

*** For a complete understanding of the nature and hazards of this chemical standard mixture;
and for information on possible component reactions and their products;
Refer to an MSDS document for each of the individual components,
in addition to the information on the MSDS provided.

Duane Funk

Duane Funk
Quality Manager

SUPELCO
Solutions within.
595 North Harrison Road
Bellefonte, PA 16823-0048 USA
Phone (814) 359-3441

Annex 7-1: Generic Reaction Set (GRS) used in ADMS-Airport

The Generic Reaction Set (GRS) Chemistry scheme (Azzi and Johnson, 1992) is a semi-empirical photo chemical model that reduces the complicated series of chemical reactions involving NO, NO_2, O_3 and many hydrocarbons to just the following seven reactions:

1. Radical production from photo-oxidation of ROC
   $ROC + hv \rightarrow RP + ROC$
2. Oxidation of nitric oxide by radicals
   $RP + NO \rightarrow NO_2$
3. Photolysis of nitrogen dioxide to nitric oxide
   $NO_2 + hv \rightarrow NO + O_3$
4. Nitric oxide-ozone titration reaction
   $NO + O_3 \rightarrow NO_2$
5. Radical pool sink through recombination to stable products
   $RP + RP \rightarrow RP$
6. Sink for nitrogen dioxide to stable gaseous nitrates
   $RP + NO_2 \rightarrow SGN$
7. Sink for nitrogen dioxide to stable non-gaseous nitrates
   $RP + NO_2 \rightarrow SNGN$

where ROC are the reactive organic compounds, RP is the radical pool, SGN is the stable gaseous nitrogen product, SNGN is the stable non-gaseous nitrogen product, and hv is the ultraviolet- radiation. Reactions (3) and (4) represent exact chemical reactions that happen very quickly, while the rest of the reactions are only approximate representations of their chemical counterparts.

Annex 8-1: Spatial and source details for several source groups used in EMIT for Beirut Airport

Table 1: Spatial details for aircraft taxiing, arrival, take-off, and climb-out groups

Source Group	Source Name	Depth (m)	Elevation (m)	X_1	Y_1	X_2	Y_2	X_3	Y_3	X_4	Y_4
Arrival	Approach (3000-1500 ft)	540	730	123378	228170	123446	228239	123465	228223	123395	228151
	Approach (1500 ft-)	460	230	123446	228239	123378	228170	126663	212123	126761	212143
	Landing roll	3.5	1.75	126687	212128	126736	212139	127313	209482	127264	209471
Taxi	Taxi-in (4 sources)	3.5	1.75	127281	209430	127310	209474	128058	210037	128010	210053
	Taxi-out (5 sources)	3.5	1.75	127936	209724	127950	209772	128928	210370	128900	210330
Take-off	Take-off	3.5	1.75	127523	208085	127481	208113	128930	210278	128971	210250
Climb-out	Climb-out	900	450	127562	208047	127439	208149	126037	206613	126149	206496

Coordinates are given in metric units (Lambert projection).

Table 2: Source details for aircraft taxiing, aircraft take-off, and aircraft climb groups.

Source Group	Source Name	Field Name	
		Thrust (%)	TIM (min)
Aircraft Arrival	Approach (3000-1500 ft)	30	2.5
	Approach (1500 ft-touchdown)	30	2.5
	Landing roll	30	0.6
Aircraft Taxi	Taxi-in	7	4
	Taxi-out	7	6
Take-off	Take-off	100	0.7
Climb-out	**Climb-out**	85	2

Table 3: Spatial details for APU group

Source Group	Source Name	Depth (m)	Elevation (m)	X_1	Y_1	X_2	Y_2	X_3	Y_3	X_4	Y_4
Aircraft APU	Aircraft APU	12	6	127800	210282	127814	209879	128118	209792	128427	210215

Coordinates are given in metric units (Lambert projection).

Table 4: Source details for aircraft GSE group

Source Group	Source Name	Depth (m)	Elevation (m)	X_1	Y_1	X_2	Y_2	X_3	Y_3	X_4	Y_4
Aircraft GSE	All GSE	2	1	127857	210293	127857	209903	128102	209827	128344	210184

Coordinates are given in metric units (Lambert projection).

Table 5: Vertex details for airside vehicles (GSE)

Source Group	Source Name	Road width (m)	Speed (km/h)	Vertices*				Traffic/day		
				X_1	Y_1	X_2	Y_2	Motor-cycles	Light Vehicles	Heavy Vehicles
Airside Traffic	Ramp 1,7	100	30	128246	210055	128099	209825	0	5400	6
Airside Traffic	Ramp 16,7	60	30	127854	209904	128139	209813	0	5088	6
Airside Traffic	Ramp 18,24	100	30	127857	210289	127853	209836	0	4968	6

*Coordinates are given in metric units (Lambert projection).

Table 6: Road sources surrounding the airport

Source Group	Source Name	Road width (m)	Speed (km/h)	Vertices*				Traffic		
				X_1	Y_1	X_2	Y_2	Motorcycles	Light Vehicles	Heavy Vehicles
Surrounding Roads	Airport Entrance	30.6	60	128117	210564	128233	211007	803.068	29229.88	430.914

*Coordinates are given in metric units (Lambert projection).

UNIVERSITÉ DE STRASBOURG

EDSC
Ecole Doctorale des
Sciences Chimiques

Tharwat MOKALLED

The Impact of Beirut - Rafic Hariri International Airport's Activities on the Air Quality of Beirut & its Suburbs: Measurements & Modelling of VOCs and NO_2

Résumé

Cette thèse étudie l'impact de l'Aéroport international de Beyrouth sur la qualité de l'air de Beyrouth et ses banlieues par mesures et modélisation des COVs et NO_2. Il s'agit de la première étude qui identifie les signatures des émissions (COVs) issues des avions sous opération réelle. Grâce aux signatures détectées lors de 4 campagnes réalisées, nous constatons que l'aéroport a un impact sur la qualité de l'air de son voisinage, la zone côtière (trajectoire d'atterrissage), et les zones montagneuses. Ces résultats sont confirmés *via* le modèle ADMS-Airport, utilisé pour la première fois au Moyen-Orient et validé pour les conditions libanaises (r = 0.86). Par ailleurs, les concentrations de 47 COVs ont été mesurées pour la première fois à l'intérieur d'un bâtiment de l'aéroport. Les teneurs en COVs qui sont corrélées au nombre d'avions sont en dessous des valeurs seuils sauf pour l'acroléine alors que la celle de NO_2 peut constituer un danger pour la santé.

Mots-clés: Aéroport, Composés Organiques Volatils, Dioxyde d'azote, Métrologie, Air ambiant, Air intérieur, Inventaire des emissions, Modélisation de dispersion atmosphérique des aéroports (ADMS).

Abstract

This work mainly investigated the impact of Beirut Airport on the air quality of Beirut and its suburbs *via* both measurements and modeling of VOCs and NO_2. This is the first study to determine VOC signatures of exhaust emissions from aircraft under real operation. Using these signatures, the impact of the airport activities was tracked in 4 transect campaigns, where it was found that the airport impacts air quality not only in its vicinity, but also on the seashore (landing jet trajectory) and in mountainous areas. These results were confirmed *via* modeling with ADMS-Airport, implemented for the first time in the Middle East, after being validated in the Lebanese conditions (r = 0.86). As a secondary goal, and for the first time, 47 VOCs were assessed inside an airport building. Measured VOC levels did not present any risks except for acrolein. In the arrivals hall, NO_2 levels indicated a health hazard; while a direct relationship was found between aircraft number and VOC concentrations.

Keywords: Airport, Volatile Organic Compounds, Nitrogen dioxide, Meteorology, Ambient air, Indoor air, Emissions inventory, Atmospheric Dispersion Modelling System (ADMS)-Airport.